

# WILCOX SANDSTONE RESERVOIRS IN THE DEEP SUBSURFACE ALONG THE TEXAS GULF COAST:

## Their Potential for Production of Geopressured Geothermal Energy

### DISCLAIMER

D. G. Bebout  
B. R. Weise  
A. R. Gregory  
M. B. Edwards

This report was prepared as an account of work sponsored by an agency of the United States Government. Neither the United States Government nor any agency thereof, nor any of their employees, makes any warranty, express or implied, or assumes any legal liability or responsibility for the accuracy, completeness, or usefulness of any information, apparatus, product, or process disclosed, or represents that its use would not infringe privately owned rights. Reference herein to any specific commercial product, process, or service by trade name, trademark, manufacturer, or otherwise does not necessarily constitute or imply its endorsement, recommendation, or favoring by the United States Government or any agency thereof. The views and opinions of authors expressed herein do not necessarily state or reflect those of the United States Government or any agency thereof.

Assisted by A. D. Allie, D. A. Budd, V. J. Gavenda,  
B. W. Hainey, H. S. Hamlin, J. H. Han, J. C. Herwig,  
A. S. Lawal, J. L. Lockley, S. D. Mann, J. S. Posey,  
and M. S. Ritchie

RECEIVED  
5-5-83  
RECEIVED  
5-5-83  
**NOTICE**  
**PORTIONS OF THIS REPORT ARE ILLEGIBLE.**  
It has been reproduced from the best  
available copy to permit the broadest  
possible availability.

Funded by the  
U.S. Department of Energy  
Division of Geothermal Energy  
Under Contract No. DE-AS05-76ET28461  
(formerly EY-76-S-05-4891)

Bureau of Economic Geology  
W. L. Fisher, Director  
The University of Texas at Austin  
Austin, Texas 78712



DISTRIBUTION OF THIS DOCUMENT IS UNLIMITED

1982



## **DISCLAIMER**

**This report was prepared as an account of work sponsored by an agency of the United States Government. Neither the United States Government nor any agency Thereof, nor any of their employees, makes any warranty, express or implied, or assumes any legal liability or responsibility for the accuracy, completeness, or usefulness of any information, apparatus, product, or process disclosed, or represents that its use would not infringe privately owned rights. Reference herein to any specific commercial product, process, or service by trade name, trademark, manufacturer, or otherwise does not necessarily constitute or imply its endorsement, recommendation, or favoring by the United States Government or any agency thereof. The views and opinions of authors expressed herein do not necessarily state or reflect those of the United States Government or any agency thereof.**

## **DISCLAIMER**

**Portions of this document may be illegible in electronic image products. Images are produced from the best available original document.**

## CONTENTS

Abstract .....	1
Introduction .....	2
Regional setting .....	3
Stratigraphic sections .....	6
Lower Wilcox sandstone distribution .....	8
Upper Wilcox sandstone distribution .....	10
Formation fluid pressure .....	13
Formation temperature used to delineate geothermal fairways .....	15
Formation porosity and permeability .....	18
Zapata Fairway .....	24
Duval Fairway .....	33
Live Oak Fairway .....	43
De Witt Fairway .....	57
<i>Depositional and structural style</i> .....	57
<i>Formation pressures and temperatures</i> .....	58
<i>Porosity and permeability</i> .....	59
<i>Formation water salinity</i> .....	59
<i>Cuero fault block</i> .....	60
Colorado Fairway .....	89
<i>Depositional and structural style</i> .....	89
<i>Formation and fluid properties</i> .....	89
<i>Eagle Lake fault block</i> .....	89
Harris Fairway .....	103
Summary and conclusions .....	114
Acknowledgments .....	115
References .....	116
Appendix A: Metric conversion factors .....	117
Appendix B: Well names and locations .....	117

*Figures*

1. Tertiary formations, Gulf Coast of Texas .....	2
2. Wilcox geothermal corridor .....	2
3. Depositional/structural style of the Tertiary section along the Texas Gulf Coast .....	3
4. Wilcox geothermal fairways and lines of regional cross sections .....	4
5. Regional dip section .....	5
6. Structural configuration on top of the Wilcox Group .....	6
7. Faults in the Wilcox Group .....	7
8. Total thickness of the Wilcox Group .....	8
9. Well log control and location of sections .....	9
10. Electric log showing division of the Wilcox Group into the sandstone-rich lower and upper parts .....	10
11. Stratigraphic dip section 1 .....	in pocket
12. Stratigraphic dip section 2 .....	in pocket
13. Stratigraphic dip section 3 .....	in pocket
14. Stratigraphic dip section 4 .....	in pocket
15. Stratigraphic dip section 5 .....	in pocket
16. Stratigraphic dip section 6 .....	in pocket
17. Stratigraphic dip section 7 .....	in pocket
18. Stratigraphic dip section 8 .....	in pocket
19. Stratigraphic dip section 9 .....	in pocket
20. Stratigraphic dip section 10 .....	in pocket
21. Stratigraphic dip section 11 .....	in pocket
22. Stratigraphic dip section 12 .....	in pocket

23. Stratigraphic dip section 13 .....	in pocket
24. Stratigraphic dip section 14 .....	in pocket
25. Stratigraphic dip section 15 .....	in pocket
26. Stratigraphic dip section 16 .....	in pocket
27. Stratigraphic dip section 17 .....	in pocket
28. Stratigraphic dip section 18 .....	in pocket
29. Stratigraphic dip section 19 .....	in pocket
30. Stratigraphic dip section 20 .....	in pocket
31. Stratigraphic dip section 21 .....	in pocket
32. Stratigraphic strike section A .....	in pocket
33. Stratigraphic strike section B .....	in pocket
34. Net-sandstone map, lower Wilcox Group .....	11
35. Net-sandstone map, upper Wilcox Group .....	12
36. Stratigraphic strike section of the upper Wilcox, Lower Texas Gulf Coast .....	14
37. Depth to the operational top of geopressure along the Wilcox geothermal corridor, Texas Gulf Coast .....	16
38. Operational top of geopressure determined from shale resistivity and transit times for a well in De Witt County .....	17
39. Shale resistivity ratio curve for De Witt County .....	18
40. Net-sandstone distribution in the lower Wilcox with the 200° and 300° F isotherms at the top of the lower Wilcox .....	19
41. Net-sandstone distribution in the upper Wilcox with the 200° and 300° F isotherms at the top of the upper Wilcox .....	20
42. Temperatures and geothermal gradients for the Harris Fairway area .....	21
43. Temperatures and geothermal gradients for the De Witt Fairway area .....	22
44. Temperatures and geothermal gradients for parts of Live Oak, McMullen, Duval, Webb, and Zapata Counties .....	23
45. Well control, faults at the top of the Wilcox, and area of prospective reservoir sandstones, Zapata Fairway .....	25
46. Well control and lines of stratigraphic and structural sections, Zapata Fairway .....	25
47. Structural dip section A-A', southern part of the Zapata Fairway .....	26
48. Structural dip section C-C', central part of the Zapata Fairway .....	27
49. Structural dip section E-E', northern part of the Zapata Fairway .....	28
50. Bottom-hole shut-in pressures plotted as a function of depth for Zapata County .....	29
51. Operational top of geopressure and geopressure gradients from shale resistivity data for a well in Zapata County .....	30
52. Temperatures and geothermal gradients for Zapata Fairway .....	31
53. Salinity versus depth calculated from electric logs of five wells in Zapata County .....	32
54. Well control, faults at the top of the Wilcox, and area of prospective reservoirs, Duval Fairway .....	34
55. Well control and lines of stratigraphic and structural sections, Duval Fairway .....	35
56. Structural dip section A-A', Duval Fairway .....	36
57. Bottom-hole shut-in pressures plotted as a function of depth for Duval County .....	38
58. Operational top of geopressure and geopressure gradients from shale resistivity data for a well in Duval County .....	39
59. Operational top of geopressure and geopressure gradients from shale resistivity data for a well on section A-A', Duval County .....	40
60. Temperatures and geothermal gradients for Duval County .....	41
61. Salinity versus depth calculated from electric logs of five wells in Duval County .....	42
62. Well control, faults at the top of the Wilcox, and area of prospective sandstones, Live Oak Fairway .....	44
63. Well control and lines of stratigraphic and structural sections, Live Oak Fairway and area to the northeast .....	45
64. Structural dip section A-A', southern part of the Live Oak Fairway .....	46
65. Structural dip section B-B', central part of the Live Oak Fairway .....	46
66. Structural dip section C-C', northern part of the Live Oak Fairway .....	47
67. Stratigraphic dip section A-A', southern part of the Live Oak Fairway .....	48
68. Stratigraphic dip section B-B', central part of the Live Oak Fairway .....	49
69. Stratigraphic dip section C-C', northern part of the Live Oak Fairway .....	50
70. Bottom-hole shut-in pressures plotted as a function of depth for 26 wells in Live Oak County .....	51

71. Parameter plots showing variation of formation and fluid properties along section A-A', Live Oak County.....	52
72. Operational top of geopressure and geopressure gradients from shale resistivity data for a well on section A-A', Live Oak County .....	53
73. Temperatures and geothermal gradients for Live Oak Fairway.....	54
74. Temperatures and geothermal gradients for fairway areas including parts of Live Oak, McMullen, Duval, Webb, and Zapata Counties .....	55
75. Salinity versus depth calculated from electric logs of six wells in Live Oak County .....	56
76. Porosity versus depth for six wells in Live Oak County .....	56
77. Location of wells and lines of section, De Witt Fairway .....	57
78. Stratigraphic dip section D-D', De Witt Fairway .....	58
79. Net sandstone between the top of the Wilcox and the D1 marker, De Witt Fairway .....	59
80. a. Structure on top of the D4 marker, De Witt Fairway .....	60
b. Index cross section showing mapping horizon in figure 80a .....	61
81. Structural dip section A-A', De Witt Fairway .....	62
82. Structural dip section B-B', De Witt Fairway.....	63
83. Structural dip section C-C', De Witt Fairway.....	64
84. Structural dip section D-D', De Witt Fairway .....	65
85. Structural dip section E-E', De Witt Fairway.....	66
86. Structural dip section F-F', De Witt Fairway .....	67
87. Stratigraphic strike section M-M', De Witt Fairway .....	68
88. Bottom-hole shut-in pressure versus depth for the De Witt County area .....	69
89. Parameter plots showing shale resistivity, temperature, porosity, and salinity profiles and variation of operational top of geopressure and geopressure gradients along cross section D-D', De Witt County .....	70
90. Operational top of geopressure and geopressure gradients from shale resistivity data for an updip well on cross section D-D', De Witt County .....	71
91. Operational top of geopressure and geopressure gradients from shale resistivity data for downdip well Kilroy No. 1 Mueller on cross section D-D', De Witt County.....	72
92. Operational top of geopressure and geopressure gradients from shale resistivity data for downdip well Texaco No. 1 Angerstein on cross section D-D', De Witt County .....	73
93. Temperatures and geothermal gradients for the De Witt Fairway area .....	74
94. Temperatures and geothermal gradients for wells located on four fairway cross sections, De Witt County .....	75
95. Porosity versus permeability for Atlantic No. 1 Schorre well on cross section D-D', De Witt County .....	76
96. Porosity versus permeability for Atlantic No. 1 Kerlick well on cross section B-B', De Witt County .....	77
97. Porosity versus permeability for Atlantic No. 1-A Newsom well in De Witt County .....	78
98. Porosity and permeability versus depth for Atlantic No. 1 Schorre well on section D-D', De Witt County .....	79
99. Porosity versus depth for six wells in De Witt County .....	80
100. Generalized salinity trends as a function of depth in De Witt County .....	81
101. Salinity versus depth calculated from electric logs of 11 wells in De Witt County .....	82
102. Calculated salinity profile for Atlantic No. 1 Schorre well on section D-D', De Witt County .....	83
103. Structure, well control, lines of section, and location of the Cuero fault block .....	84
104. Stratigraphic dip section A-A', Cuero fault block.....	85
105. Stratigraphic strike section B-B', Cuero fault block .....	85
106. Net sandstone in correlation unit B, Cuero fault block .....	86
107. Net sandstone in correlation unit C, Cuero fault block .....	86
108. Net sandstone in correlation unit D, Cuero fault block .....	87
109. Net sandstone in correlation unit E, Cuero fault block .....	87
110. Net sandstone in correlation unit F, Cuero fault block .....	88
111. Net sandstone in correlation unit G, Cuero fault block .....	88
112. Location of wells and lines of section, Colorado Fairway.....	90
113. Stratigraphic dip section B-B', Colorado Fairway .....	91
114. a. Structural map, Colorado Fairway.....	92
b. Index section, Colorado Fairway .....	93
115. Structural dip section A-A', Colorado Fairway .....	93

116. Structural dip section B-B', Colorado Fairway .....	94
117. Structural dip section C-C', Colorado Fairway .....	95
118. Shale resistivity versus depth for the Union No. A-1 Thomas well on cross section M-M', Colorado County .....	96
119. Structural strike section M-M', Colorado Fairway .....	97
120. Temperatures and geothermal gradients for 48 wells in Colorado County .....	98
121. Eagle Lake fault block, Colorado Fairway .....	99
122. Stratigraphic strike section M-M', Colorado Fairway .....	100
123. Porosity versus permeability for the Union No. A-1 Thomas well on cross section M-M', Colorado County .....	101
124. Calculated salinity profile for the Union No. A-1 Thomas well on cross section M-M', Colorado County .....	102
125. Location of wells and lines of section, Harris Fairway .....	103
126. Stratigraphic dip section D-D', Harris Fairway .....	104
127. Structural dip section D-D', Harris Fairway .....	105
128. Structural dip section E-E', Harris Fairway .....	106
129. Structural dip section H-H', Harris Fairway .....	107
130. Bottom-hole shut-in pressures plotted as a function of depth for 23 wells in Harris County area .....	108
131. Shale resistivity versus depth for a nongeopressured well on cross section H-H', San Jacinto County .....	109
132. Operational top of geopressure and geopressure gradients from shale resistivity data for a well on cross section D-D', Waller County .....	110
133. Temperatures and geothermal gradients for Harris Fairway .....	111
134. Temperatures and geothermal gradients for wells on three fairway cross sections, Harris County .....	112
135. Salinity versus depth calculated from electric logs of 14 wells in Harris Fairway .....	113

### *Tables*

1. Correlation of stratigraphic markers in the Zapata, Duval, and Live Oak Fairways .....	24
2. Sidewall-core data from two wells in Zapata County .....	24
3. Diamond-core data from five Duval County wells .....	33
4. Summary of the physical characteristics of the six Wilcox geopressured geothermal fairways .....	114

## ABSTRACT

Regional studies of the lower Eocene Wilcox Group in Texas were conducted to assess the potential for producing heat energy and solution methane from geopressured fluids in the deep-subsurface growth-faulted zone. However, in addition to assembling the necessary data for the geopressured geothermal project, funded by the U.S. Department of Energy, this study has provided regional information of significance to exploration for other resources such as lignite, uranium, oil, and gas. Because the focus of this study was on the geopressured section, emphasis was placed on correlating and mapping those sandstones and shales occurring deeper than about 10,000 ft.

The Wilcox and Midway Groups comprise the oldest thick sandstone/shale sequence of the Tertiary of the Gulf Coast. The Wilcox crops out in a band 10 to 20 mi wide located 100 to 200 mi inland from the present-day coastline. The Wilcox sandstones and shales in the outcrop and updip shallow subsurface were deposited primarily in fluvial environments; downdip in the deep subsurface, on the other hand, the Wilcox sediments were deposited in large deltaic systems, some of which were reworked into barrier-bar and strandplain systems. Growth faults developed within the deltaic systems, where they prograded basinward beyond the older, stable Lower Cretaceous shelf margin onto the less stable basinal muds. Continued displacement along these faults during burial resulted in (1) entrapment of pore fluids within isolated sandstone and shale sequences and (2) buildup of pore pressure greater than hydrostatic pressure and development of geopressure.

Regional electric log correlation markers made possible the subdivision of the Wilcox into lower, middle, and upper parts. The net-sandstone map of the lower Wilcox indicates a dominantly lobate pattern northeast from De Witt County to the Sabine River. Fisher and McGowen (1967) interpreted the lower Wilcox in that area to have been deposited in a high-constructive delta system, which they named the Rockdale Delta System. To the south, the lower Wilcox net-sandstone map indicates a narrow, elongate trend; Fisher and McGowen interpreted these sediments to have been deposited in strandplain and barrier-bar systems and named them the San Marcos Strandplain and Cotulla Barrier-Bar Systems.

The dominantly shale section of the middle Wilcox was deposited as a result of a marine transgression over the lower Wilcox. Thus, the shale is an offshore equivalent both of middle Wilcox sandstones far updip and of sandstones of the lower part of the upper Wilcox.

The net-sandstone map of the upper Wilcox indicates abrupt thickening along the Lower and Middle Texas Gulf Coast, resulting from deposition contemporaneous with faulting in major deltaic systems. In contrast, along the Upper Texas Gulf Coast, abrupt downdip thickening does not occur, and these strata are not extensively growth faulted.

Information on subsurface pressures and pressure gradients was obtained from (1) bottom-hole shut-in pressure data from drill-stem tests, (2) shale resistivity data from electric logs, (3) mud weights from well log headings, and (4) shale transit times from sonic logs. The top of geopressure was picked at approximately the depth where a pressure gradient of 0.7 psi per foot occurs. This depth is considered the "operational" top of geopressure because it is somewhat higher pressure than the 0.465 psi per foot hydrostatic pressure gradient. The zone where pressure gradients are between 0.465 and 0.7 psi per foot is transitional and difficult to identify consistently. The resulting map indicates that the top of geopressure occurs between depths of 8,000 and 13,000 ft along the Wilcox trend; in general, the top of geopressure is deeper in high-sandstone areas and shallower in high-shale areas.

Formation temperatures, corrected to equilibrium values, were determined throughout the Wilcox trend to permit calculation of the amount of methane dissolved in the water. Knowledge of subsurface temperature is also essential in studying diagenesis of sandstone, dewatering of shale, and maturation of organic material and generation of hydrocarbons.

As a result of this regional study of the Wilcox Group, six geothermal fairways were identified—Zapata, Duval, Live Oak, De Witt, Colorado, and Harris. Thick sandstone units with formation temperatures greater than 300°F occur in all fairways; however, high porosity and permeability occur in only the De Witt Fairway (Cuero area), making it the only one having high potential for geopressured geothermal energy production.

## INTRODUCTION

This regional study of the distribution of sandstone within the Wilcox Group (fig. 1) is part of a much broader investigation that will assess the potential for producing geothermal energy from the deep subsurface geopressured zone of onshore Tertiary strata along the Texas Gulf Coast (Dorfman and Deller, 1975, 1976). The objective of the study is to identify areas along the Wilcox trend in Texas most favorable for testing this potential resource. Criteria used to identify geopressured geothermal reservoirs containing resources suitable for electric power generation included a reservoir volume of 3 mi<sup>3</sup>, fluid temperature greater than 300°F, pressure gradient of at least 0.7 psi per foot, and permeability of more than 20 md (Bebout and others, 1976a).

SYSTEM	SERIES	GROUP/FORMATION
Quaternary	Recent Pleistocene	Undifferentiated Houston
	Pliocene	Goliad
	Miocene	Fleming
		Anahuac
	?	?
Tertiary	Oligocene	Frio Vicksburg
		Jackson
	Eocene	Claiborne
		Wilcox
		Midway

Figure 1. Tertiary formations, Gulf Coast of Texas. The Wilcox Group, the study interval of this geothermal report, is shown by the diagonal pattern; the geothermal potential of the Frio and Vicksburg Formations, shown by the dot pattern, has been reviewed in other Bureau of Economic Geology reports (Bebout and others, 1975a, 1975b, 1976a, 1978b; Loucks, 1978).

Reports summarizing similar regional assessments of the Frio Formation and describing a prospective test-well site have been published by the Bureau of Economic Geology, The University of Texas at Austin (Bebout and others, 1975a, 1975b, 1976a, and 1978b). The geothermal potential of the Vicksburg Formation was summarized by Loucks (1978).

The Wilcox and Midway Groups, lower Eocene, constitute the oldest thick sandstone/shale sequence within the Gulf Coast Tertiary System. Wilcox sandstones and shales crop out in a 10- to 20-mi-wide band that is subparallel to and 100 to

200 mi inland from the present-day coastline (fig. 2). From the outcrop, the Wilcox dips coastward into the subsurface, forming one of at least eight thick wedges of Tertiary sandstone/shale in this area (Hardin and Hardin, 1961). Sediments within the updip part of the wedges were deposited primarily by fluvial processes. Downdip, sediments were transported across the Wilcox fluvial plain and were deposited in huge deltaic systems; some deltaic sediments were reworked and transported along shore by marine processes and then redeposited on barrier bars and strandplains. A basic understanding of the environmental setting of the Wilcox was developed by Fisher and McGowen (1967) and Fisher (1969), following earlier studies by Culbertson (1940), Echols and Malkin (1948), and Hargis (1962).

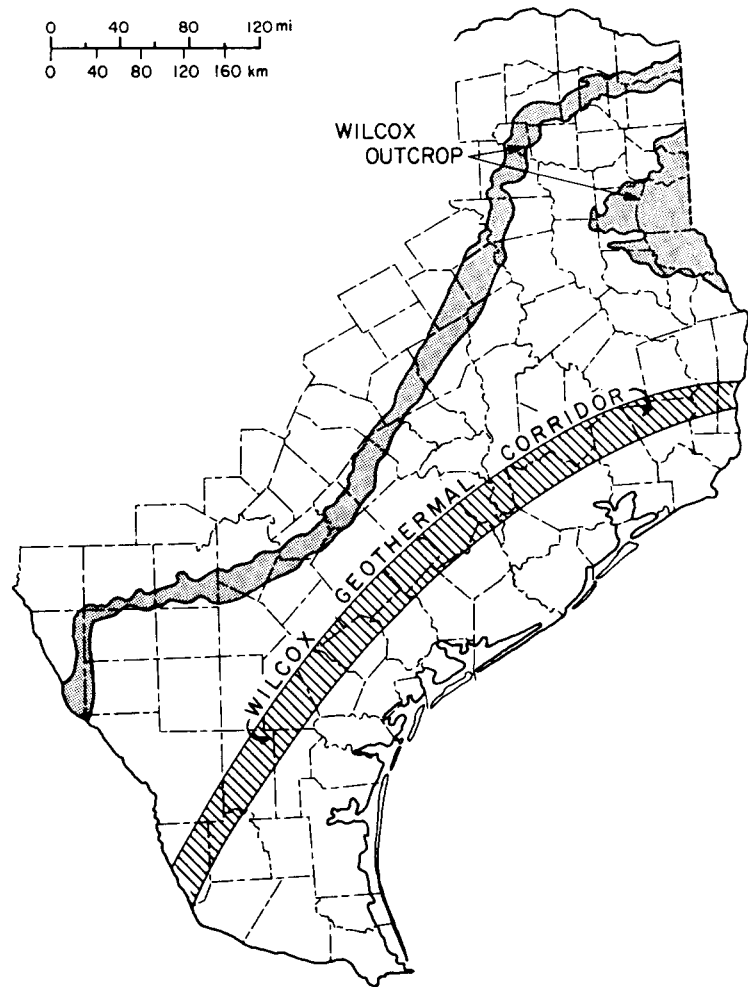


Figure 2. Wilcox geothermal corridor. The corridor occurs where Wilcox sandstones are present in the deep subsurface under conditions of high temperature and pressure.

Growth faults developed near the shorelines of several of the larger delta lobes, where thick wedges of sand and mud were deposited on unconsolidated offshore mud of the previous sediment wedge (fig. 3). Subsidence and displacement along these faults during burial isolated thick sandstone and shale sequences. Isolation of the sandstone units prevented updip escape of pore fluids during subsequent compaction resulting from loading. Vertical escape of pore fluids was prevented by low vertical permeability of superposed shales. Limited fluid circulation within these growth-faulted blocks caused the downward increase in pressure gradient from a normal hydrostatic pressure gradient of 0.465 psi per foot to between 0.7 and 1.0 psi per foot. The increased porosity and water content of sediments, caused by the buildup in fluid pressure and consequent reduction in overburden pressure, reduces the thermal conductivity and increases the geothermal

gradient. Gradients in the hydropressured zones range from  $1.5^{\circ}$  to  $2.0^{\circ}$ F per 100 ft and from  $2.0^{\circ}$  to more than  $3.0^{\circ}$ F per 100 ft in the geopressured zones. The faulted, downdip section of the Wilcox Group, which exhibits a high pressure gradient and temperatures exceeding  $300^{\circ}$  F, constitutes the Wilcox geothermal corridor (fig. 2). Along this corridor, six geothermal fairways were outlined (fig. 4) on the basis of sandstone distribution and isotherm maps.

## REGIONAL SETTING

The Wilcox Group is composed of a thick wedge of sandstone and shale that crops out several hundred feet above sea level at its updip limit. More than 100 mi downdip, the Wilcox is 10,000 ft below sea level (figs. 5 and 6). Regional dip averages 100 ft per mile. Where Wilcox deltas prograded gulfward of the underlying Lower

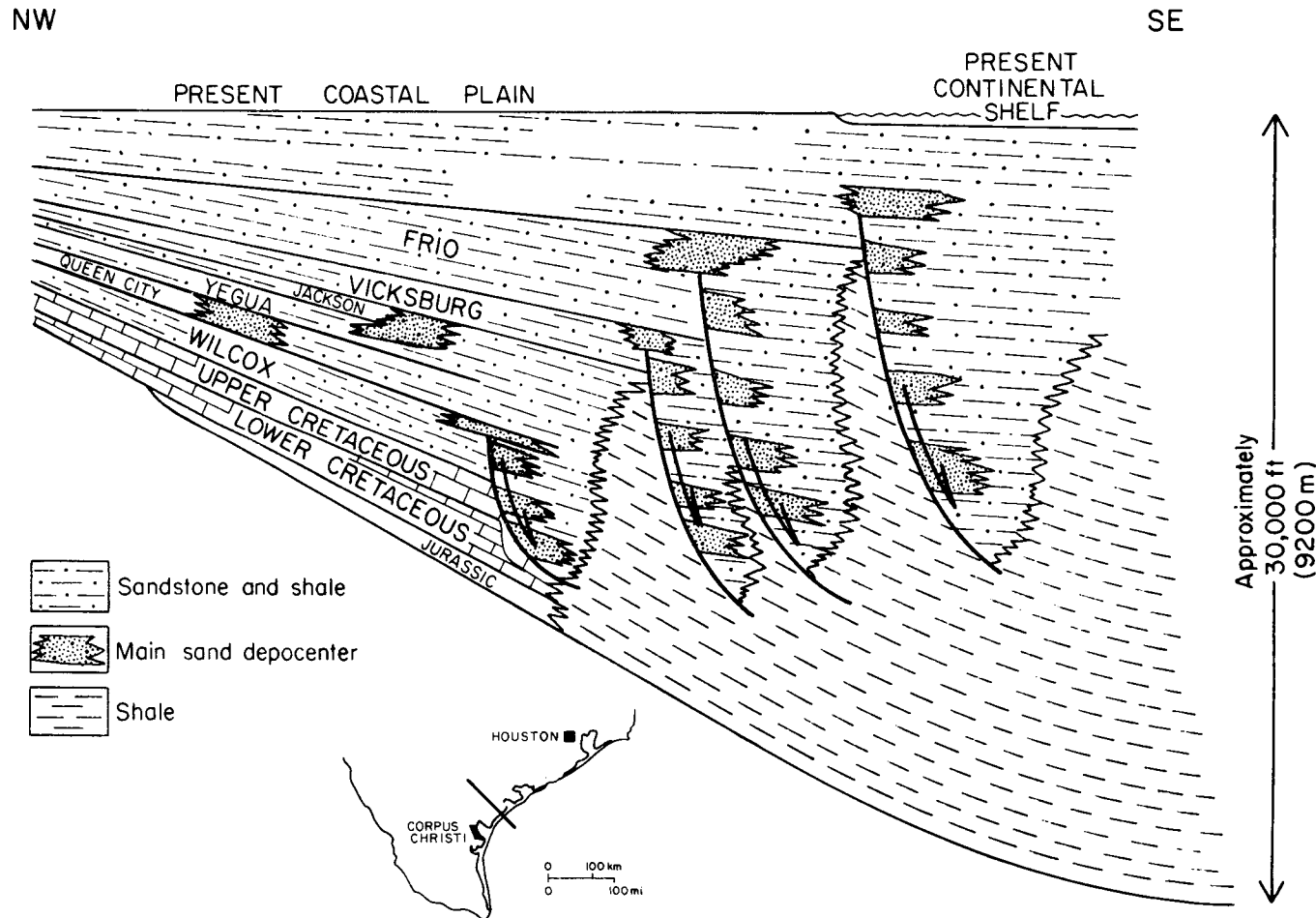


Figure 3. Depositional/structural style of the Tertiary section along the Texas Gulf Coast. Geopressured geothermal reservoirs occur downdip of major growth faults where deltaic sandstones were hydrologically isolated from surrounding rocks.

Cretaceous Stuart City shelf margin (Edwards and Sligo Formations), growth faults developed in a band 20 mi wide (fig. 7), indicating that the gulfward edge of the shelf controlled the location of the Wilcox growth faults. Sandstones and shales of the Wilcox thicken abruptly downdip of the Stuart City shelf margin (fig. 5, wells 7 and 8). The zone of steeper (more closely spaced) contours on the structure and thickness maps (figs. 6 and 8) coincides with the location of the best developed growth faults.

The base of the Wilcox Group is transitional with the underlying marine Midway Group. The upper part of the Midway is believed by many to be a prodelta marine facies of the lowermost Wilcox

fluvial and deltaic facies (Culbertson, 1940; Echols and Malkin, 1948; Johnston, 1977; Townsend, 1954). In agreement with the stratigraphic boundaries defined by Culbertson (1940), Echols and Malkin (1948), Murray (1955), and Fisher (1969), the top of the Wilcox Group is placed at the top of the Carrizo Sandstone.

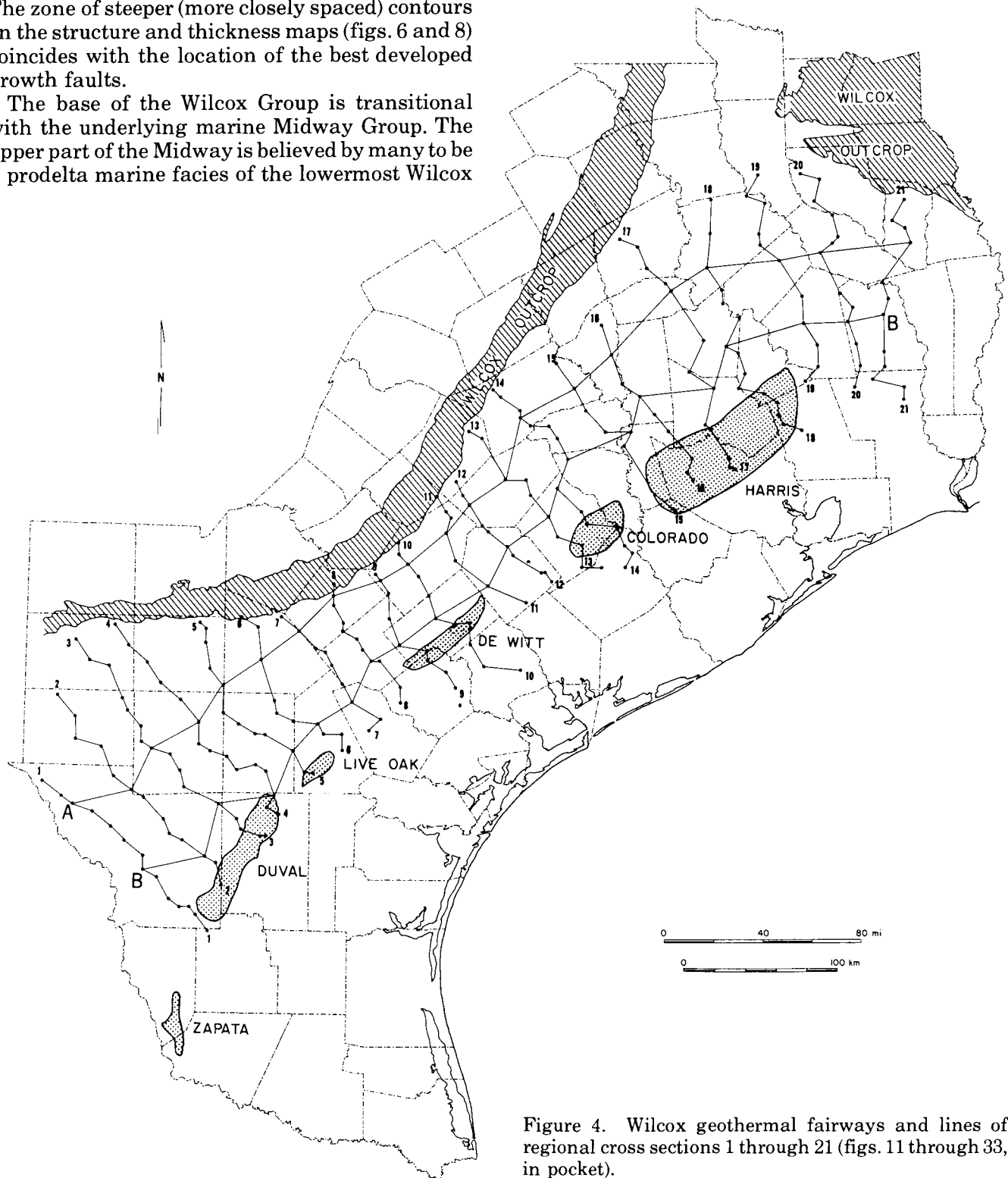


Figure 4. Wilcox geothermal fairways and lines of regional cross sections 1 through 21 (figs. 11 through 33, in pocket).

C

C

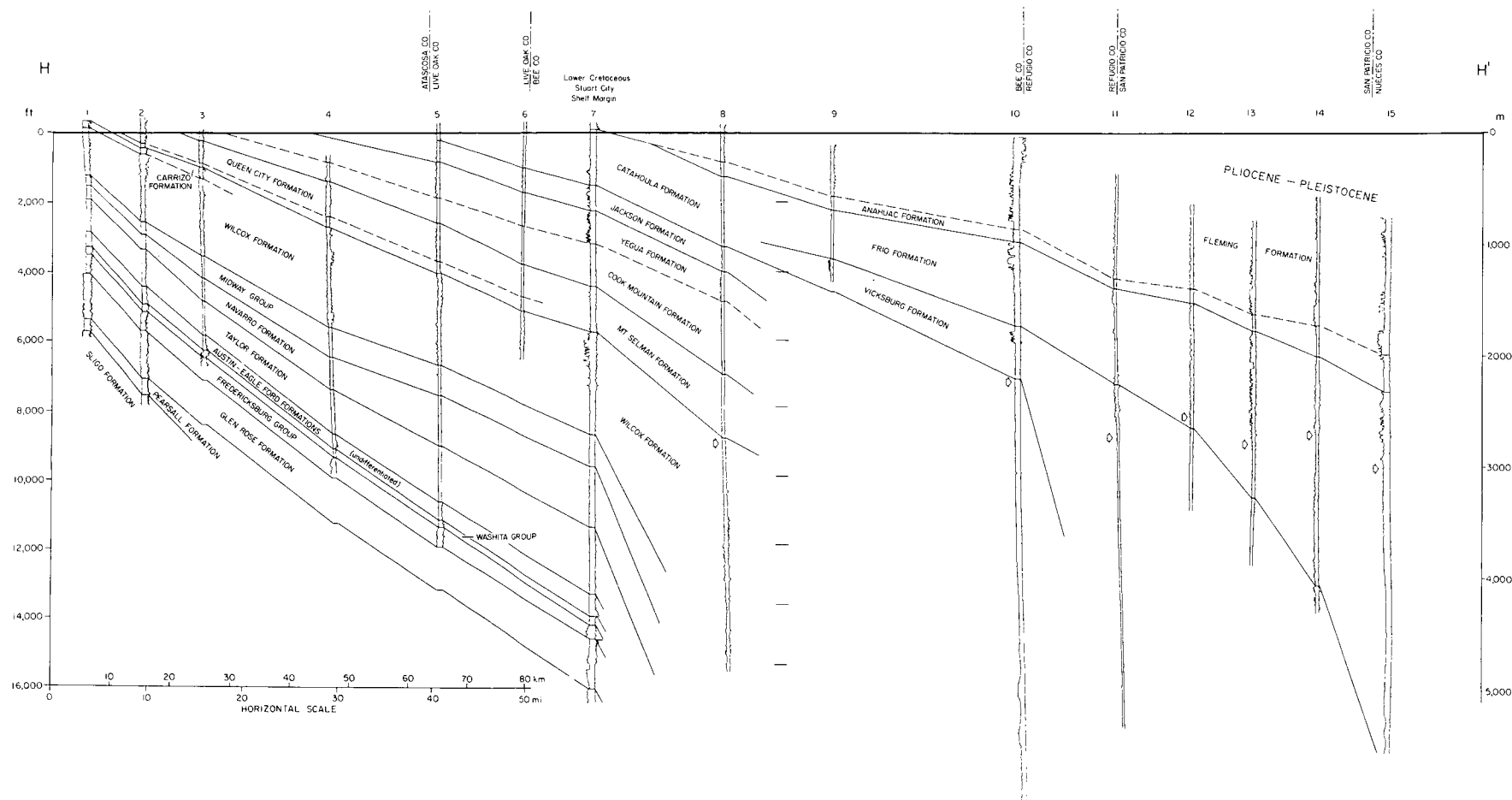


Figure 5. Regional dip section (see Bebout and others, 1976b, p. 4, for line of section H-H'). The Wilcox Group thickens abruptly just downdip of the Lower Cretaceous Stuart City shelf margin by means of a complex system of growth faults.

## STRATIGRAPHIC SECTIONS

Twenty-one regional stratigraphic dip sections, spaced 15 to 20 mi apart, were constructed using electric logs from wells along the Texas Gulf Coast (fig. 9). On each well log, the top of the Wilcox and two regional markers have been identified (fig. 10); these markers were selected through the detailed correlations of closely spaced wells in the fairway areas discussed later in this report. The markers were then projected onto the regional cross sections and extended throughout the Wilcox trend. The lower regional marker corresponds to the top of the lower Wilcox Group of Fisher and McGowen (1967). The upper regional marker is at

the base of the upper Wilcox as delineated by Fisher and McGowen, except in South Texas, where their stratigraphic interpretations have been modified (Zapata, Duval, and Live Oak Fairways, this report; Edwards, 1981). Maps showing the regional distribution of sandstone in

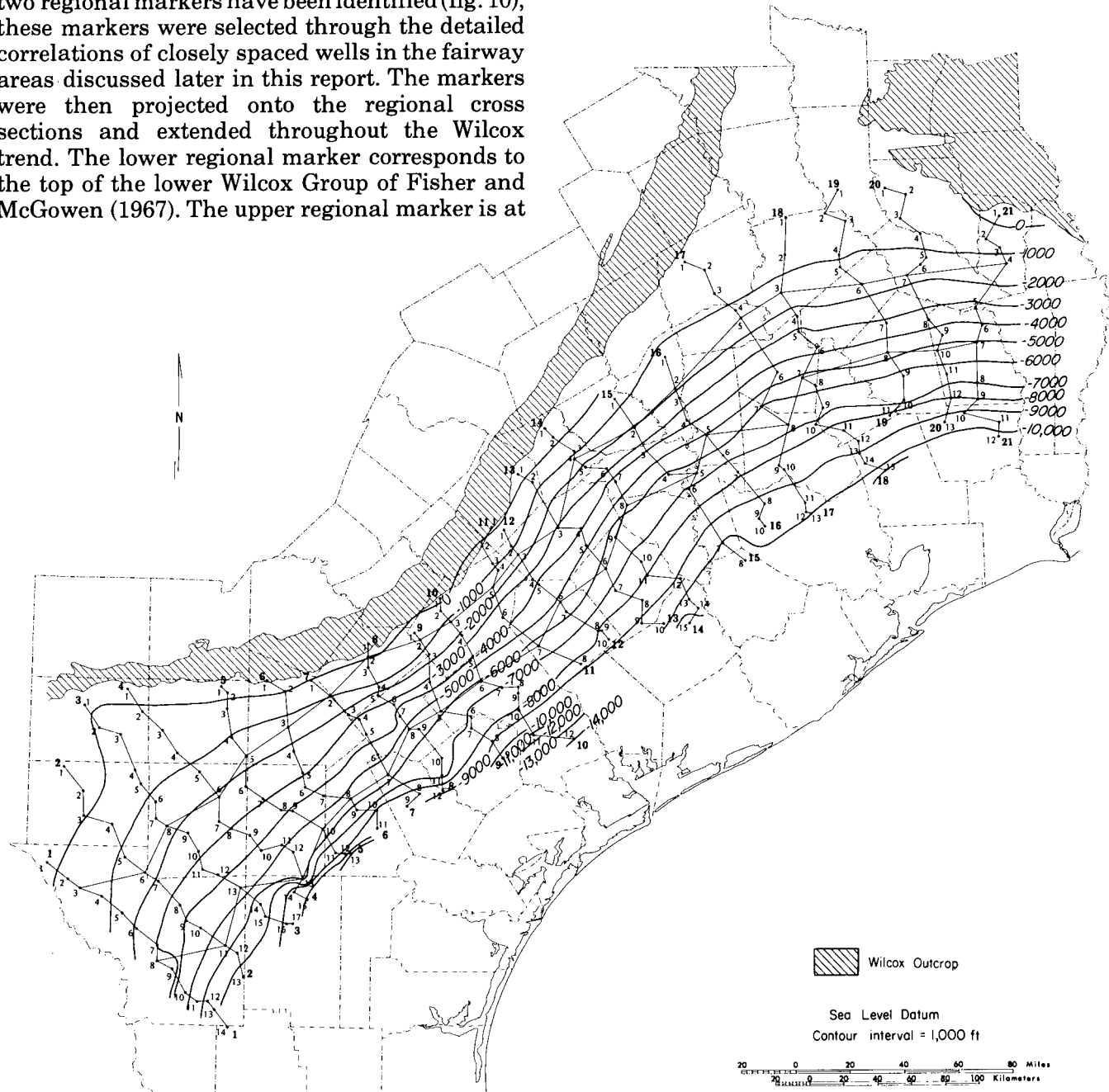


Figure 6. Structural configuration on top of the Wilcox Group.

the lower and upper Wilcox have been constructed by Fisher and McGowen (1967) and Fisher (1969), respectively.

Each of the dip sections (figs. 11 through 31, in pocket) includes 10 to 15 wells. The sections extend from near the outcrop to the downdip limit of Wilcox sandstones or well control. Strike sections (figs. 32 and 33, in pocket) were constructed to ensure correlation among dip sections. Datum for the sections is the top of the Wilcox Group. Growth faults present at the downdip end of the sections have been omitted so as not to obscure well-to-well correlation of sandstones.

The shallowest depth at which the pressure gradient is 0.7 psi per foot is marked by the black arrow on stratigraphic sections (figs. 11 through 33). This pressure gradient occurs well beneath the base of the updip part of the Wilcox, whereas downdip, within the zone of growth faulting, the

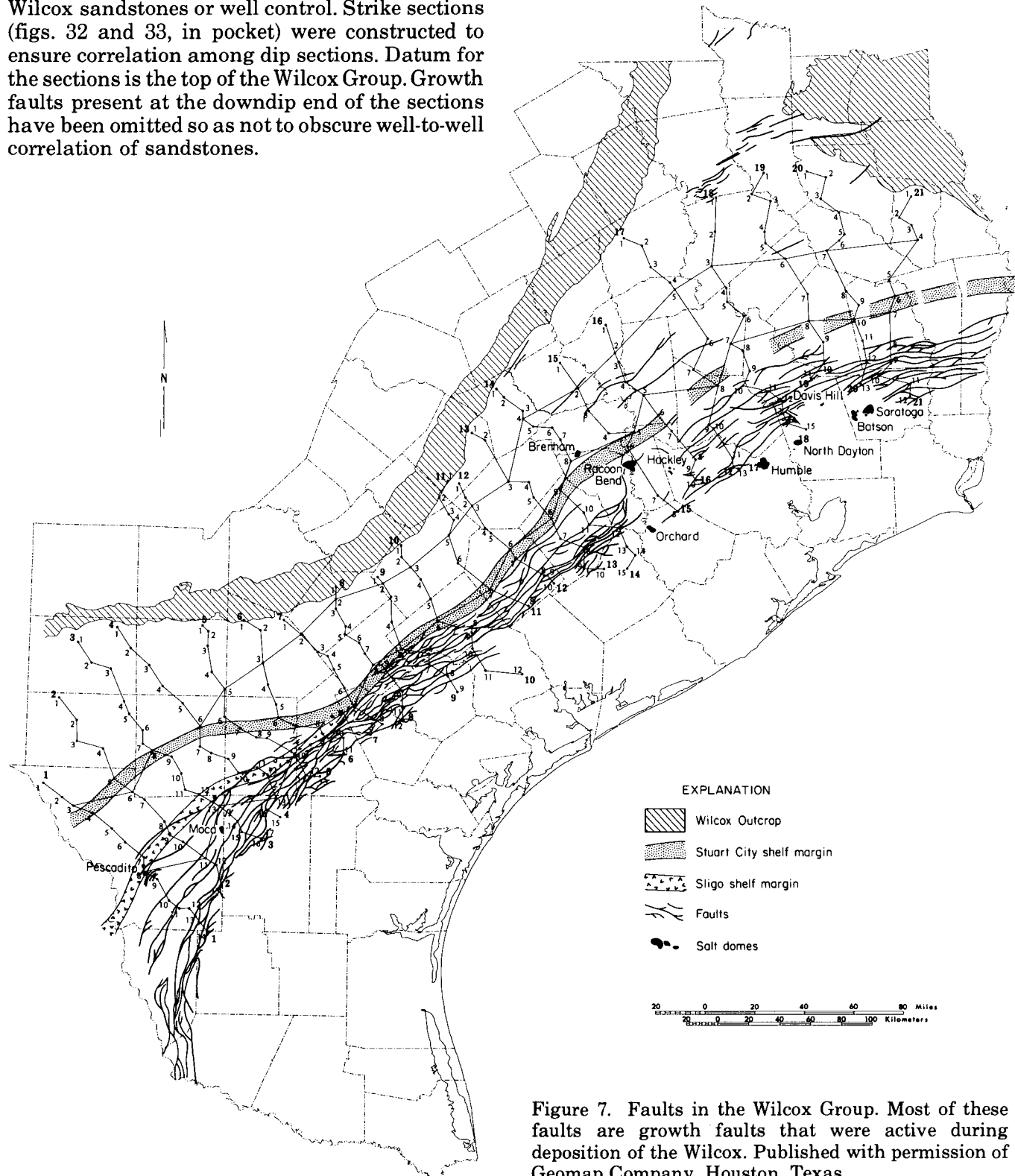


Figure 7. Faults in the Wilcox Group. Most of these faults are growth faults that were active during deposition of the Wilcox. Published with permission of Geomap Company, Houston, Texas.

0.7-psi-per-foot gradient generally occurs within the upper part of the Wilcox Group. A subsurface fluid temperature of 300°F is also indicated on the cross sections.

## LOWER WILCOX SANDSTONE DISTRIBUTION

The net-sandstone map of the lower Wilcox (fig. 34) is based on control provided by wells used in this investigation and by maps previously prepared by the Bureau of Economic Geology as part of an extensive study of the lower Wilcox (Fisher and McGowen, 1967). These maps show

that areas of maximum net sandstone trend subparallel to the modern Gulf Coast. The sandstone trends are broad (up to 80 mi wide) and lobate along the Upper and Middle Texas Gulf Coast and narrow (approximately 20 mi wide) and elongate along the Lower Texas Gulf Coast.

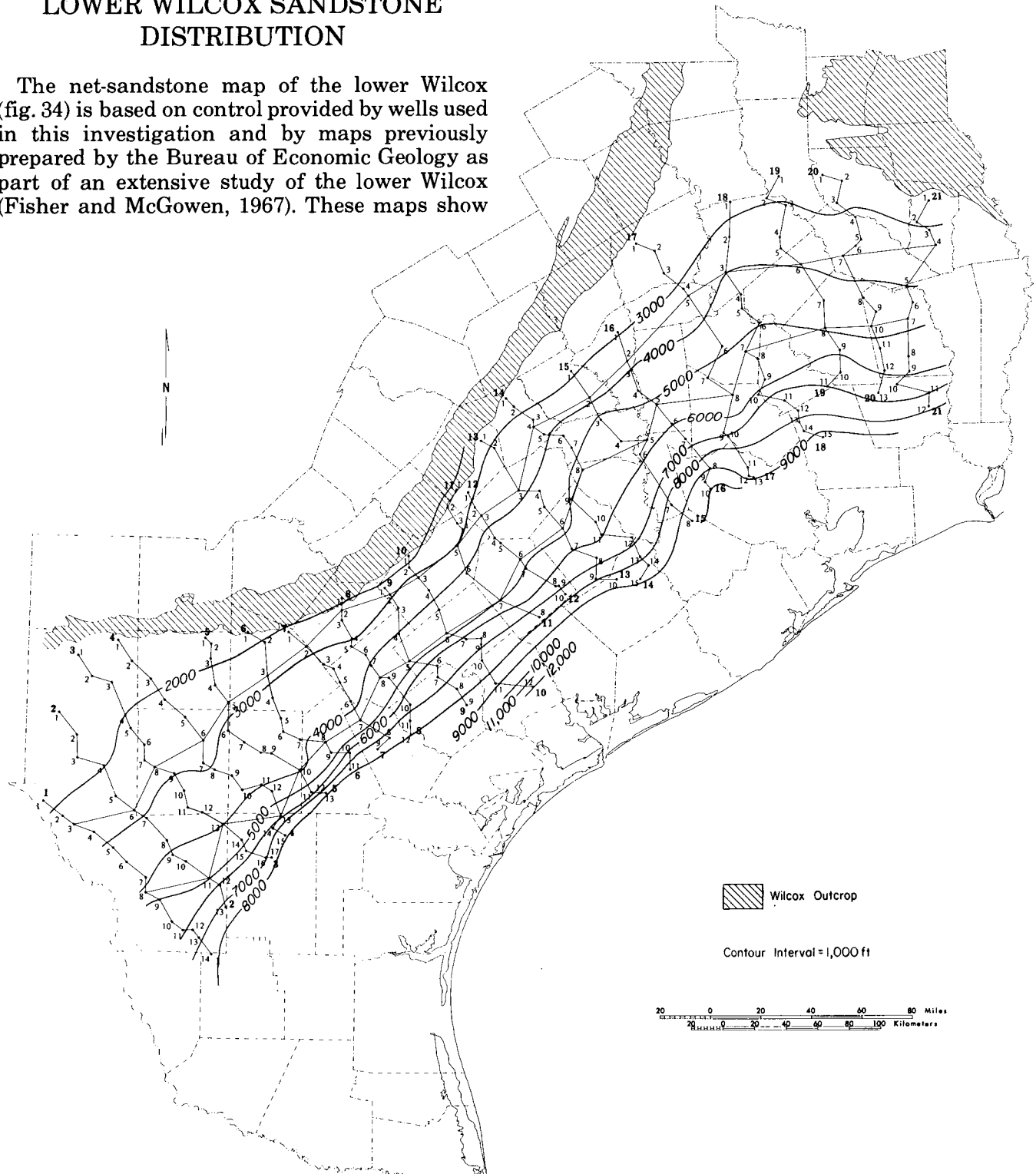


Figure 8. Total thickness of the Wilcox Group.

Net-sandstone values range from more than 2,000 ft to the north to slightly more than 400 ft to the south.

Along the northern two-thirds of the Wilcox trend, net sandstone exhibits a lobate pattern from De Witt County to the south to Sabine County to the north (fig. 34). Fisher and McGowen (1967) interpreted these patterns to be those of a high-constructive delta system (the Rockdale Delta System). The southernmost delta lobe, named the

Guadalupe Delta by Fisher and McGowen, was subsequently cut by a large erosional feature, the Yoakum Channel (Hoyt, 1959). Fisher and McGowen suggested that the Yoakum Channel is a submarine canyon that was scoured by density currents of reworked deltaic sediments that flowed

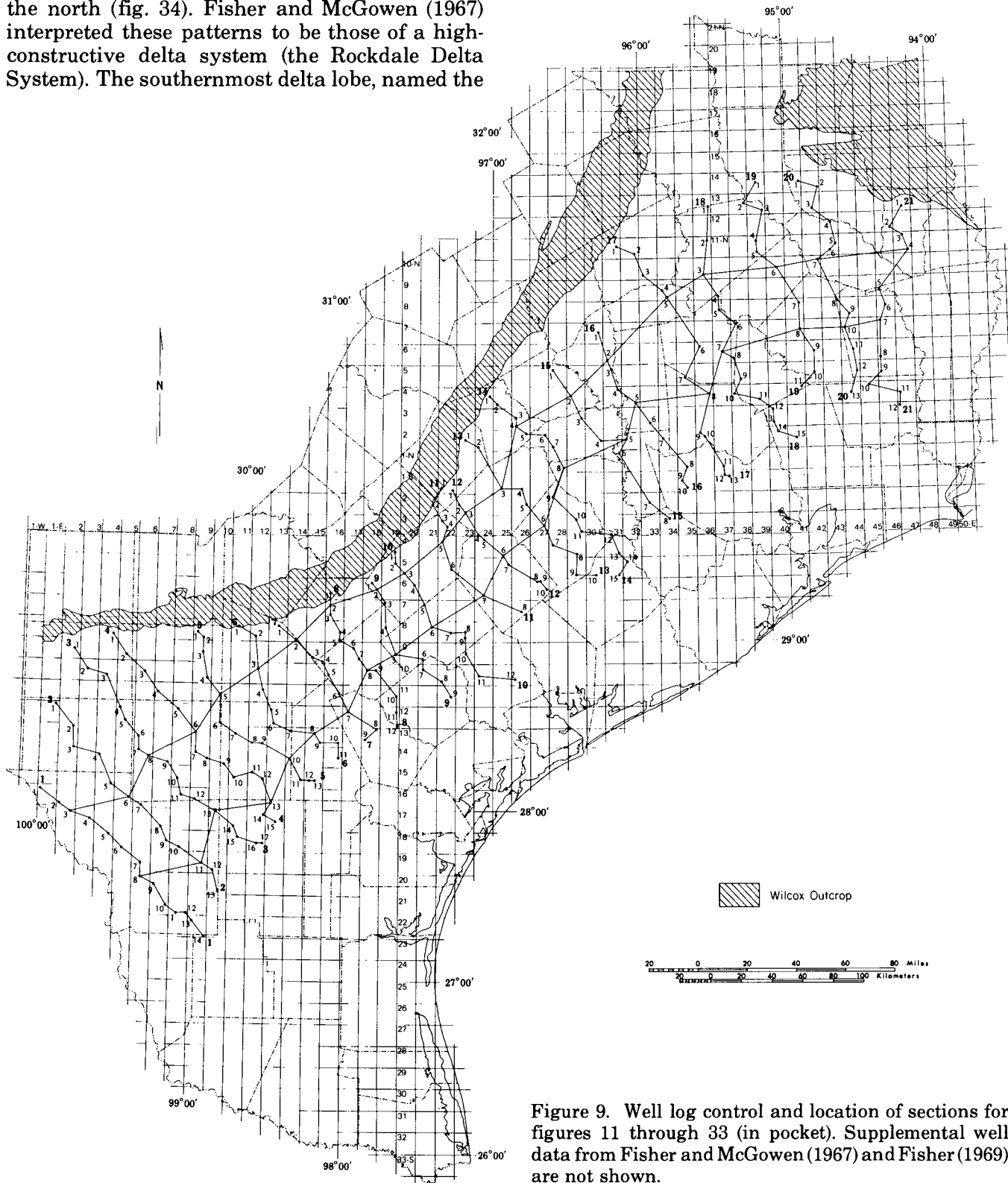


Figure 9. Well log control and location of sections for figures 11 through 33 (in pocket). Supplemental well data from Fisher and McGowen (1967) and Fisher (1969) are not shown.

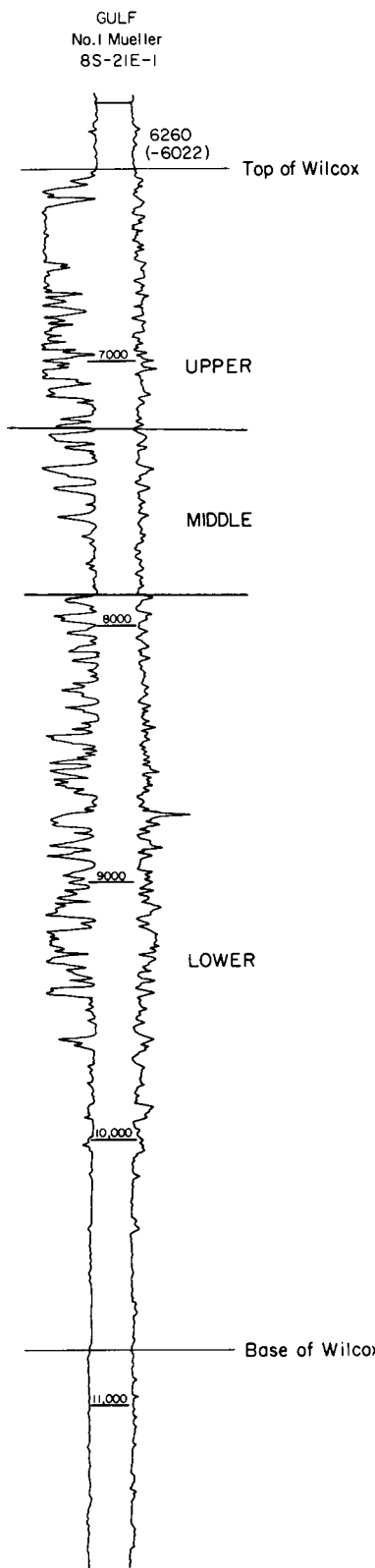


Figure 10. Electric log showing division of the Wilcox Group into the sandstone-rich lower and upper parts, each of which represents a major progradational cycle, separated by middle Wilcox shales deposited during a marine transgression. This log is from well number 6 in dip section 10, shown in figure 20 (in pocket).

down slope. In the axis of the channel, the entire lower Wilcox sandstone section was removed and replaced by a dominantly shale section (figs. 32 and 33, in pocket).

South of De Witt County, the lower Wilcox exhibits a narrow, elongate net-sandstone trend that contrasts with the broad lobate trend to the north. Fisher and McGowen (1967) suggested that this strike-dominated trend was deposited within strandplain and barrier-bar depositional systems. The trend was named the San Marcos Strandplain and Cotulla Barrier-Bar Systems.

This geothermal assessment emphasizes the most downdip Wilcox sandstone units where reservoirs exist with potential for production of 300°F geothermal water. The sandstone lobes of the lower Wilcox along the Middle and Upper Texas Gulf Coast coincide closely with those mapped by Fisher and McGowen (1967).

## UPPER WILCOX SANDSTONE DISTRIBUTION

The upper Wilcox along the Lower Texas Gulf Coast consists of sandstone and shale and, in the updip areas, thickens gradually from the outcrop toward the Gulf of Mexico (fig. 35). Downdip, across a distance of about 10 to 15 mi, the upper Wilcox abruptly thickens as a result of deposition contemporaneous with faulting. Along the Middle and Upper Texas Gulf Coast, however, upper Wilcox strata are not extensively growth faulted, and abrupt downdip thickening of the sedimentary section does not occur in the area of well control. Thus, net sandstone in the downdip parts of the upper Wilcox is thickest in the Lower to Middle Texas Gulf Coast (fig. 35). In the Lower Texas Gulf Coast, this linear trend was referred to as the "shelf-edge sand facies of the lower Wilcox South Texas Shelf System" by Fisher and McGowen (1967). However, this important gas trend consists of upper, rather than lower, Wilcox deposits that have been growth faulted to great depths (Edwards, 1980a, 1981).

The upper Wilcox growth-fault zone is about 10 to 15 mi wide, and dip sections transect many faults. Just updip of the fault zone, the top of the Wilcox is generally at a depth of about 6,000 ft. In this updip part, the upper Wilcox ranges in thickness from 1,400 ft in the north to 1,900 ft in the south. Across the fault zone, the top of the Wilcox occurs at depths as great as 9,000 to 12,000 ft. Downdip, total thickness for the upper Wilcox cannot be determined because of the lack of sufficiently deep wells, but correlation of selected

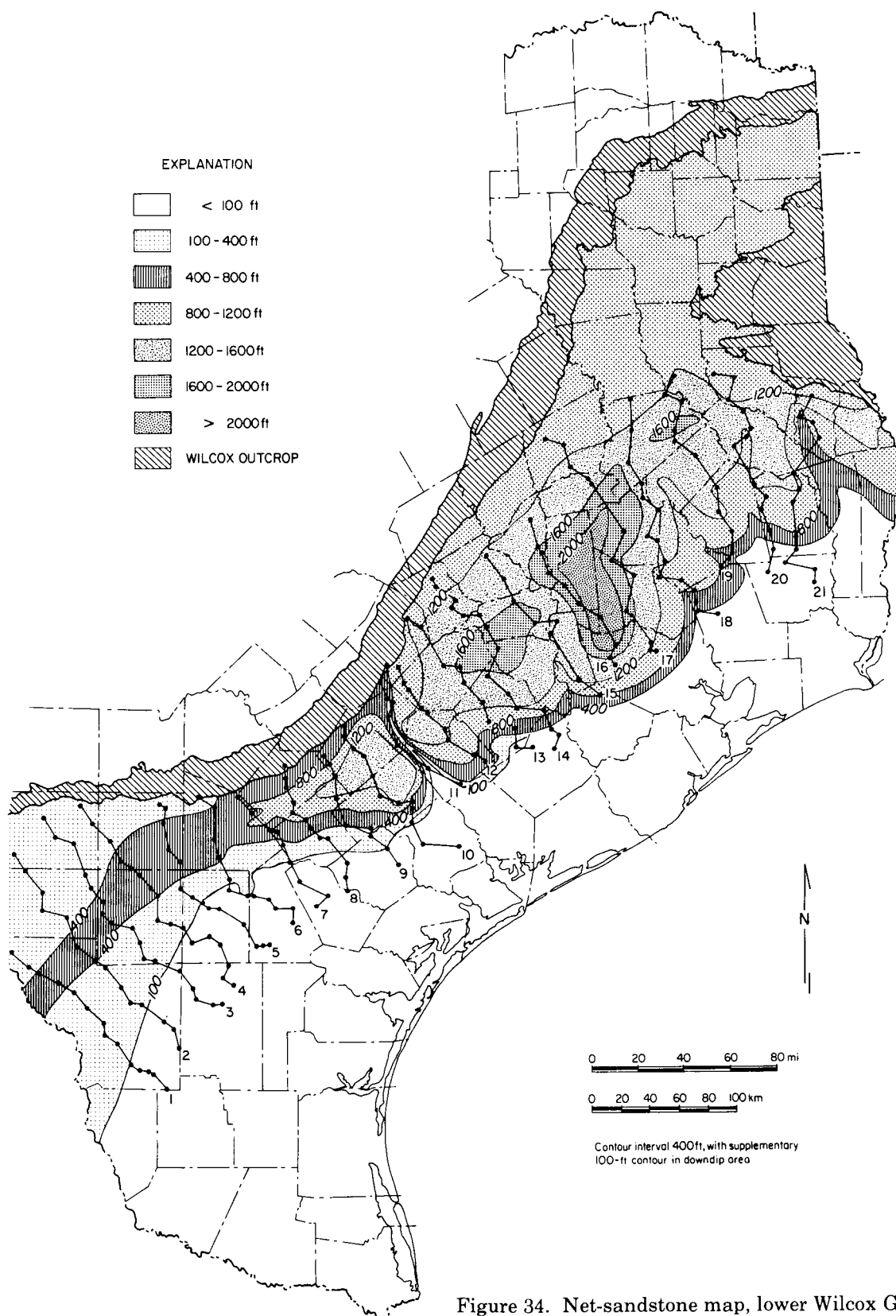


Figure 34. Net-sandstone map, lower Wilcox Group.

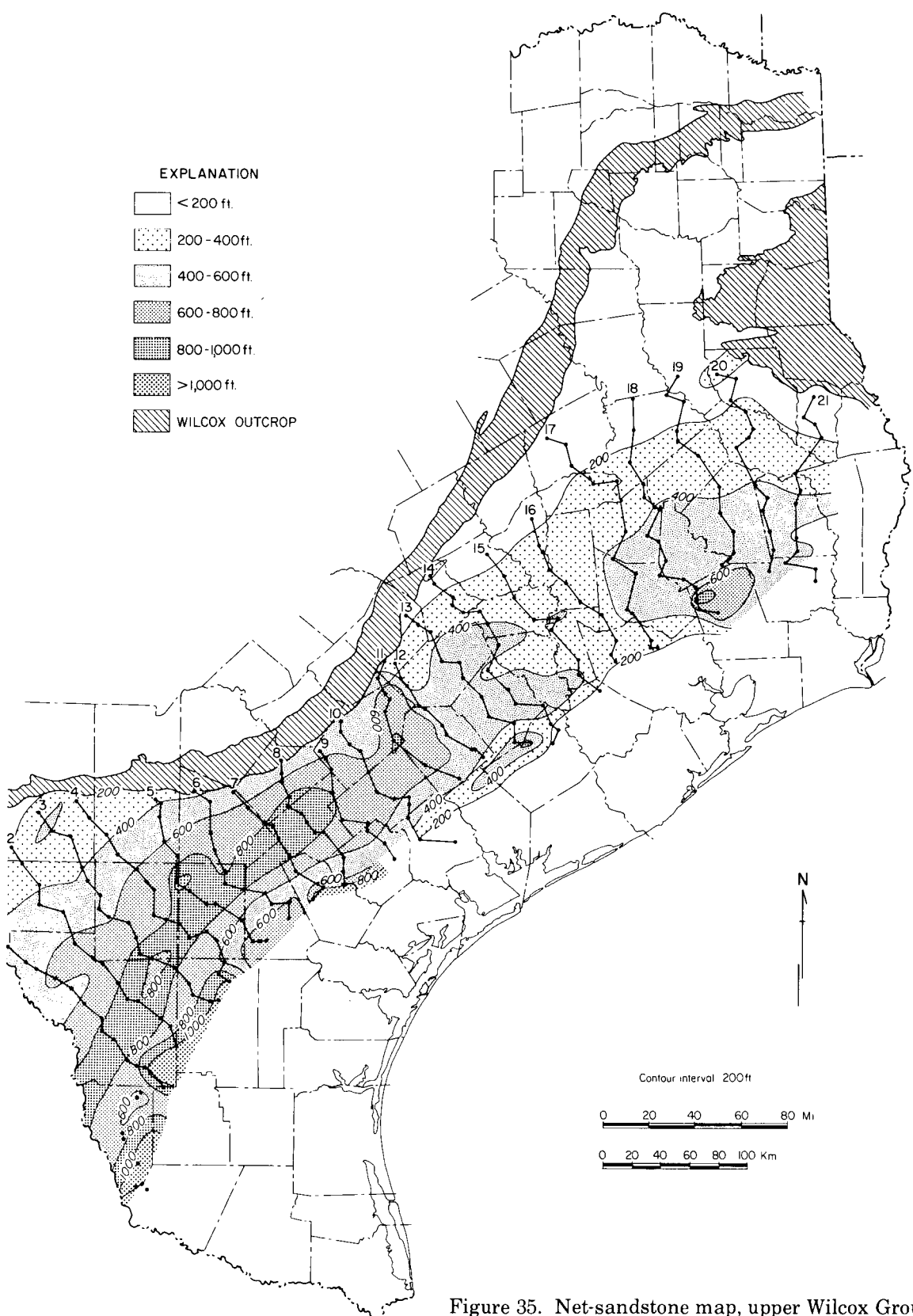


Figure 35. Net-sandstone map, upper Wilcox Group.

intervals of the upper part of the Wilcox indicates expansion of the section by a factor ranging from about 6 to 10. The deepest downdip wells penetrate 6,000 ft of upper Wilcox strata.

A stratigraphic strike section from Zapata to Karnes Counties relates the sandstone-bearing intervals of the three fairways in South Texas (fig. 36). The section shows that the high-sandstone areas of the fairways extend 13 to 60 mi along strike, and that the prospective sandstones present in the fairways developed at different times and do not correlate. Thus, the oldest sandstones, situated in the lower part of the upper Wilcox, occur in the Duval Fairway below marker Du3. The intermediate sandstones, situated in the middle part of the upper Wilcox, occur in the Zapata Fairway between markers Z2 and Z3. The youngest sandstones, at the top of the upper Wilcox, occur in the Live Oak Fairway above marker L2.

Along strike to the northeast in Karnes County, the upper Wilcox is commonly developed as a massive sandstone, exhibiting only minor, thin shale intervals. Detailed correlation within this sandstone sequence is therefore impossible. Sandstone and shale intervals in the upper Wilcox of South Texas are comparatively easy to correlate. Downdip, across the growth-fault zone, shales gradually become dominant, and sandstones increase in thickness but decrease in percent of total section (Edwards, 1980b). Detailed examination of logs from both sides of major growth faults shows that the sandstone/shale ratio is not appreciably altered by the growth faults, even where the thickness is increased by a factor of 2 or more.

The geographic restriction of sandstone depocenters along strike suggests that the dispersal system was not strike oriented on a regional scale. In updip areas, log patterns generally show blocky patterns exhibiting sudden lateral changes, and the sediments are interpreted as having been deposited in distributary channels. In contrast, sediments in downdip areas that show upward-coarsening trends are interpreted as having been deposited as delta-front and distributary-mouth bar facies (Edwards, 1980b, 1981).

## FORMATION FLUID PRESSURE

Subsurface fluid pressure is important in determining (1) the ability of a reservoir to produce fluids at the surface without pumping and (2) the solubility of methane in formation waters. In the hydropressed zone, which extends downward

from the water table, formation fluids are under hydrostatic pressure only; thus, pumping is required to bring fluids to the surface. In the deeper subsurface, where permeability barriers occur, confined formation fluids may support some of the weight of the overlying rocks. These formation fluids are considered to be geopressed, and fluid pressure gradients are greater than 0.465 psi per foot. The higher the pressure gradient is, the greater the production potential will be, although other factors also influence production. A pressure gradient of approximately 0.7 psi per foot or greater is considered necessary to make a geopressed geothermal reservoir viable. This pressure gradient has been referred to as the "operational" top of geopressure (Bebout and others, 1975a, 1975b, 1976a, and 1978b), as it may have greater practical importance than the conventional top of geopressure.

Four sources of information from which pressures and pressure gradients can be determined are currently available; however, accuracy of predicting pressures is variable. The information sources are: (1) bottom-hole shut-in pressure (BHSIP) data from drill-stem tests (DST), (2) shale resistivity data from induction logs, (3) mud weights from well log headings, and (4) shale transit time data from sonic logs. It is important to note that these data are based on different characteristics of the formation, and therefore may not produce similar results when used to determine pressure.

Bottom-hole shut-in pressure data from drill-stem tests were obtained from completion cards for producing wells. Because only one or two pressure measurements were made for each well, it was necessary to combine information from numerous wells in an area to determine the average pressure gradient. A least-squares regression line through the BHSIP data plotted against depth was used to estimate pressure gradients at any depth within the area of interest (for example, see the discussions of the Live Oak Fairway).

Pressure gradients were determined in this study primarily by calculating fluid pressure from induction logs (fig. 37). Detection and evaluation of geopressed formations using the short-normal curve or amplified short-normal resistivity curve (Hottmann and Johnson, 1965) rely on the observation that, under conditions of normal compaction, shale resistivity ( $R_{sh}$ ) increases with depth as the porosity and water content of shales decrease. Resistivities of geopressed shale depart from the normal trend, and lower values of  $R_{sh}$  are recorded because of the increased porosity and water content of the geopressed shales. The amount of divergence of  $R_{sh}$  from the established

normal compaction trend is a measure of the pore-fluid pressure in the shale and adjacent sandstone. The normal procedure for detecting geopressures involves a semilog plot with  $R_{sh}$  plotted on the logarithmic scale and depth plotted on the linear scale (fig. 38). Shale with higher than normal resistivity (caprock) is sometimes observed above the operational top of geopressure. The caprock occurs in the transition zone between hydropressed and strongly geopressed conditions and may be sharp and definitive or gradual and equivocal.

Divergence of  $R_{sh}$  from the normal compaction trend is related to the observed pressure gradient in adjacent sandstone formations. The ratio  $R_{sh}$  (normal)/ $R_{sh}$  (observed) was plotted against pressure gradient for Eocene formations (fig. 39) in De Witt County. Geopressure profiles for individual wells in the area can be constructed using this curve.

Resistivity values were derived only from shales greater than 30 ft thick; silty, calcareous, and washed-out shales were avoided. Resistivity data for shales at depths less than 4,000 to 5,000 ft were disregarded because these shallow formations contain fresh water having high resistivity values that cannot be used to establish the compaction trend; the presence of gas-cut mud or mud containing additives to combat lost circulation also contributes to spurious resistivity data. Other discontinuities observed in the trend line may be caused by an abrupt change in lithology (such as from normal shales to bentonitic shales), difference in the geologic age with consequent changes in shale properties, major changes in borehole size, and possibly the presence of dispersed free gas. Shales located near salt masses were avoided because their low resistivity (high salinity) may falsely indicate higher than normal pressure.

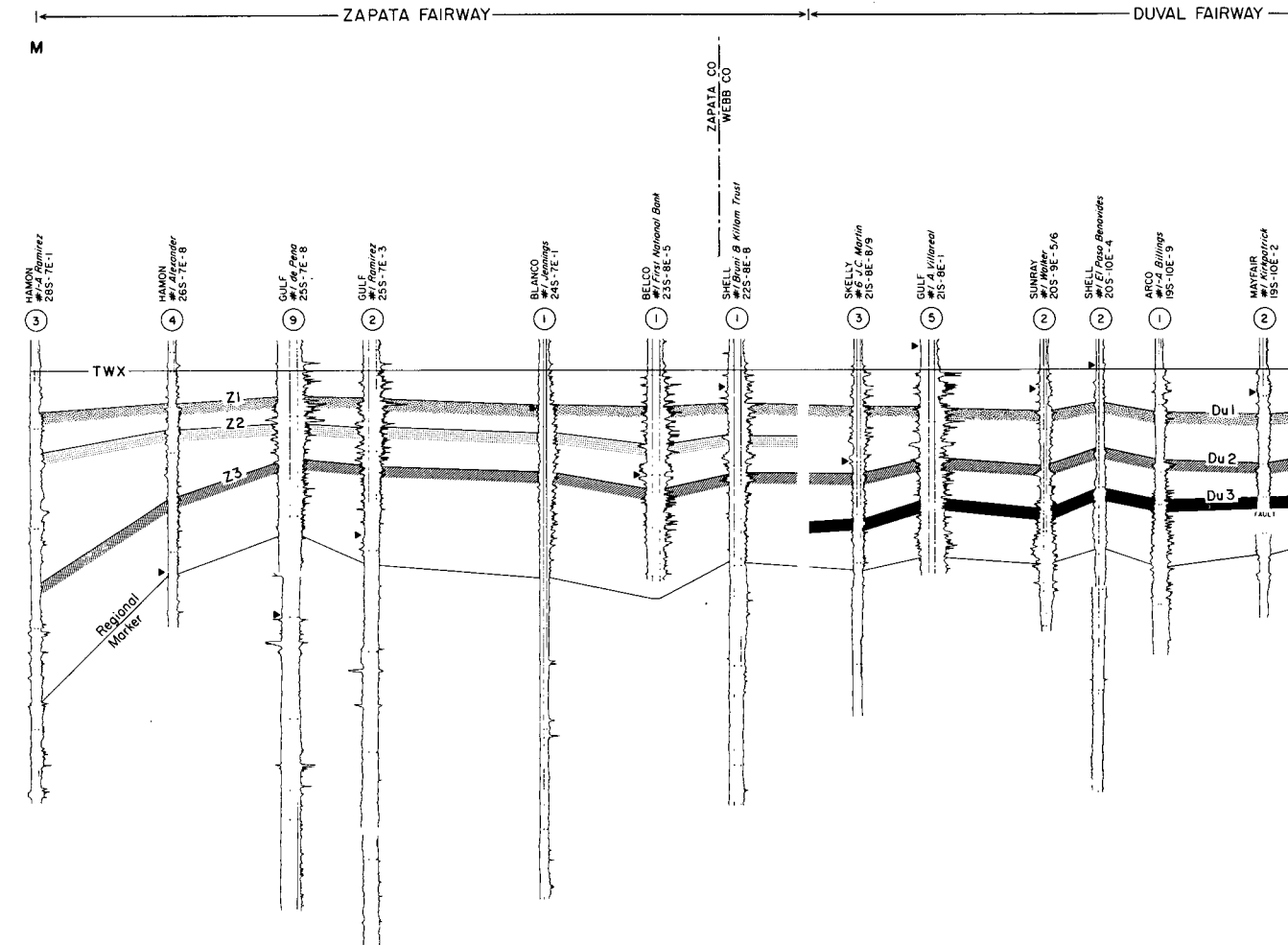


Figure 36. Stratigraphic strike section of the upper Wilcox, Lower Texas Gulf Coast. Principal correlation markers used within and between the three South Texas fairways are shown.

Mud weight versus depth recorded on shale resistivity plots (fig. 38) provided a first approximation of the operational top of the geopressured zone. Although some recorded mud weights may be inaccurate and misleading for determining geopressure tops, a mud weight of 12.6 to 13.6 lb per gallon was used to approximate the operational top of geopressure, especially if the quality of well log data was questionable. Depth to top of geopressure could then be determined by an interpretive process that included evaluating the other sources of information listed above. Using mud weights from well logs is not recommended for quantitative evaluation of geopressure.

In fresh-water zones, sonic logs are considered more reliable than electric logs for locating and evaluating geopressures. By plotting shale transit time versus depth on semilog paper (fig. 38), the normal compaction curve (NCC) was established, and the geopressure top was located at the depth

where shale transit time departs from the normal trend. Usually there was good correlation between top of geopressure determined from shale resistivity and from shale interval-transit times. As figure 38 shows, however, operational top of geopressure determined from the transit time plot is about 600 ft above that determined from shale resistivity; this illustrates the divergence of results that can be obtained from empirical relationships based on measurements of different properties of the same stratigraphic section.

## FORMATION TEMPERATURE USED TO DELINEATE GEOTHERMAL FAIRWAYS

Formation temperature data corrected to equilibrium values have been used in this study

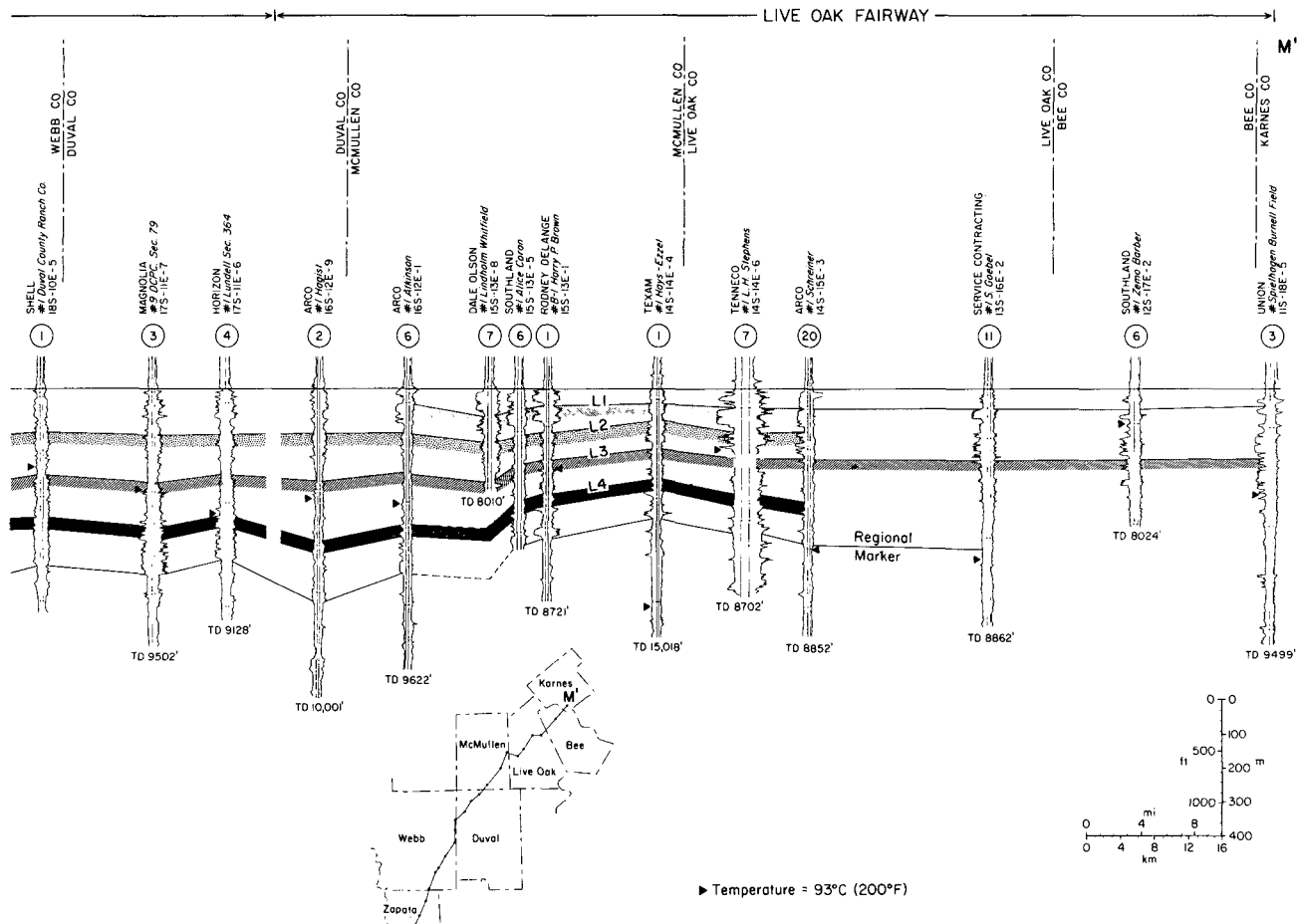


Figure 36 (continued)

primarily to delineate areas where thick sandstone reservoirs have temperatures greater than 300°F. Knowledge of the formation fluid temperatures is also essential in calculating the amount of methane in solution in the water and in studying the diagenesis of the sandstone, shale, and organic material at depth (Burst, 1959, 1969; Dow, 1978). Thus, temperature greatly affects factors that control porosity, permeability, and elastic properties of prospective reservoir rocks.

The depth at which subsurface temperatures reach 300°F is indicated on all wells on the stratigraphic sections (figs. 11 through 33). Geothermal fairways were identified by plotting the 300°F isotherm on the net-sandstone maps of

lower and upper Wilcox (figs. 40 and 41). Wilcox sandstone reservoirs having fluid temperatures higher than 300°F are shown gulfward of this isotherm. Six fairways — Harris, Colorado, De Witt, Live Oak, Duval, and Zapata — were outlined in this manner (fig. 4).

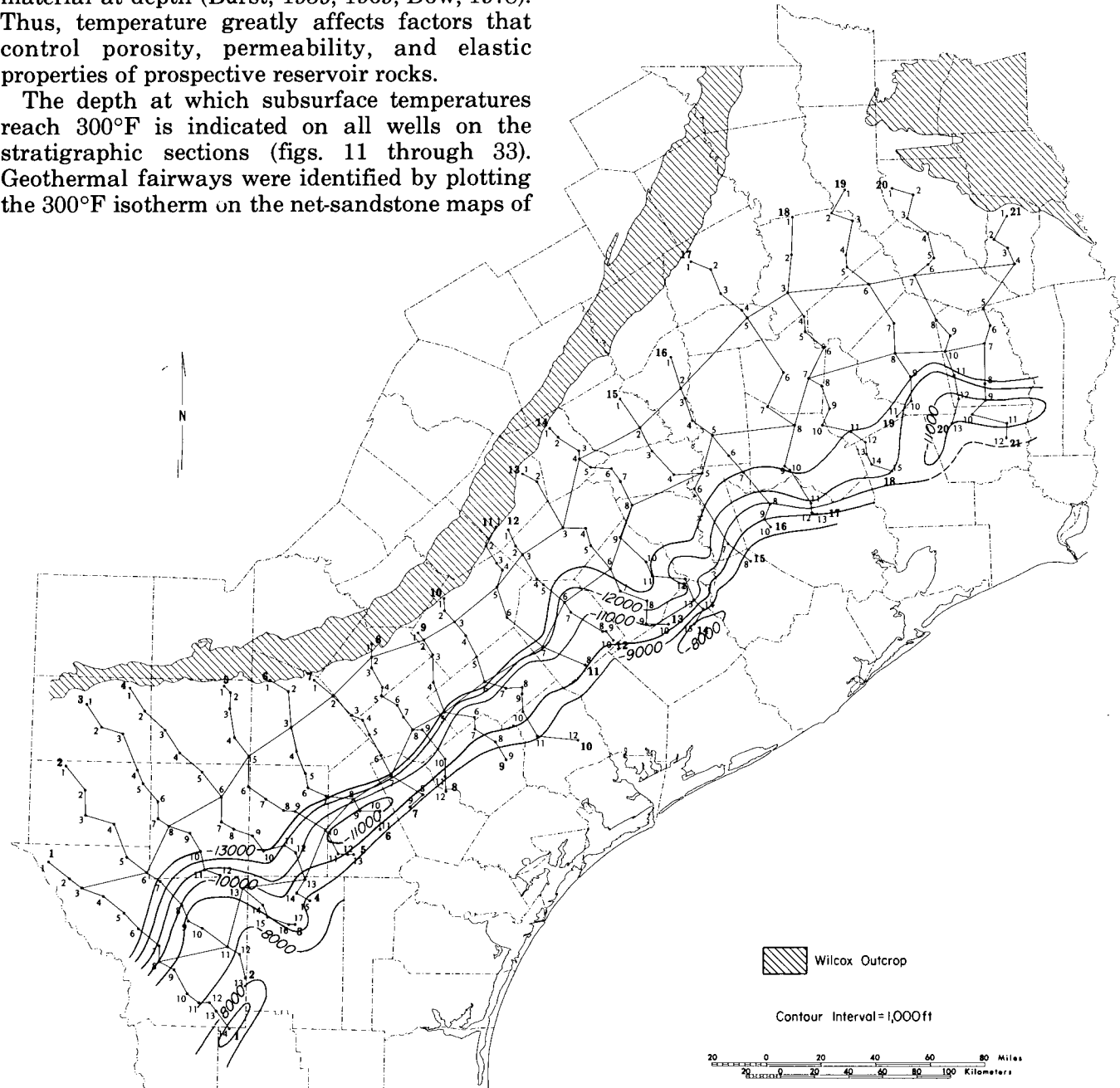


Figure 37. Depth to the operational top of geopressure along the Wilcox geothermal corridor, Texas Gulf Coast. These depths were determined primarily on the basis of shale resistivity ( $R_{sh}$ ) versus depth plots.

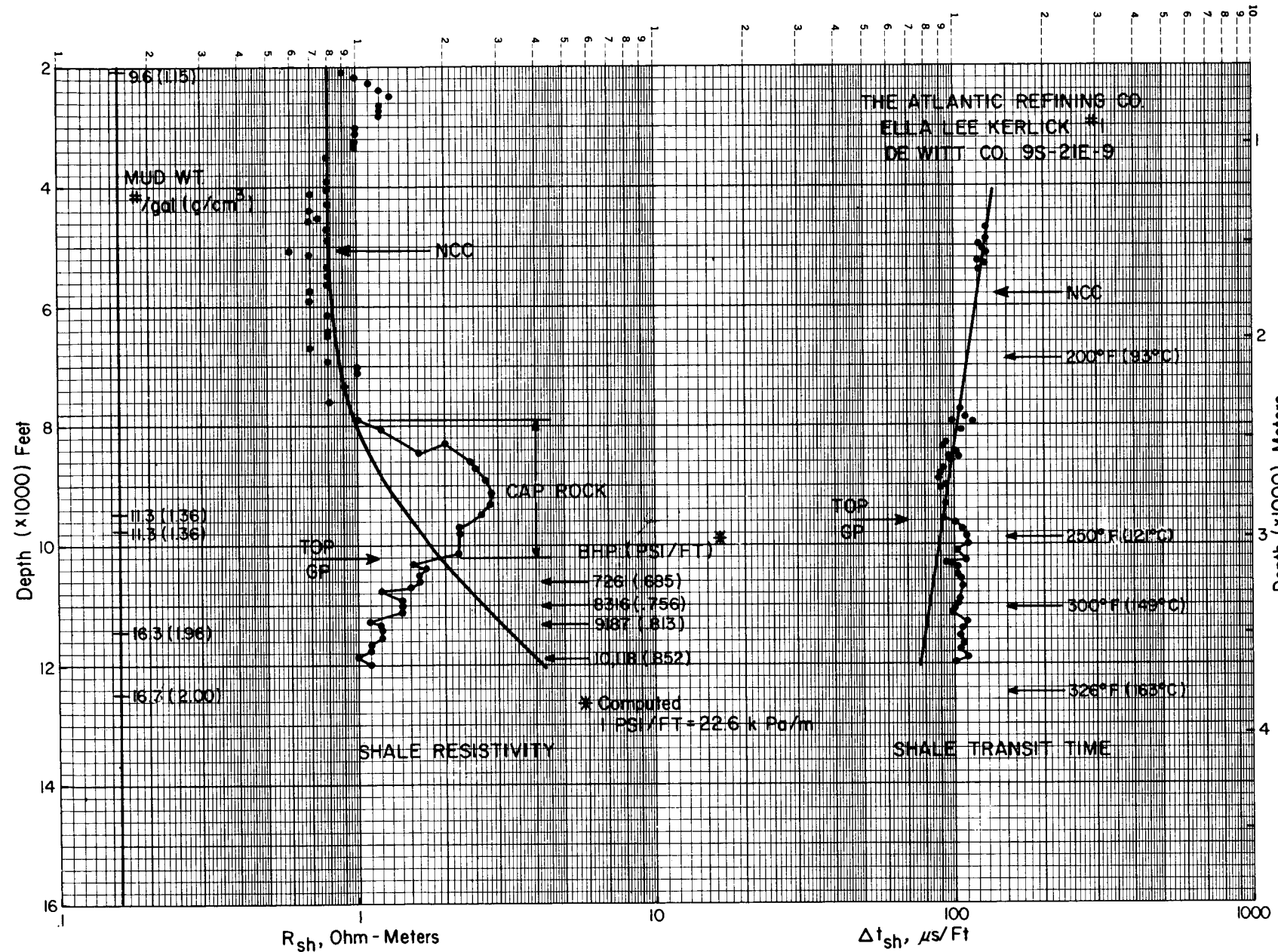


Figure 38. Operational top of geopressure determined from shale resistivity and transit times for a well in De Witt County.

Plots of temperature versus depth for wells in these fairways illustrate the presence of three geothermal gradients that change slope as a function of depth. These gradients are referred to as shallow, medium, and deep (figs. 42 through 44). In addition, gradients increase, and higher temperatures occur at shallower depths toward the southwest along the Wilcox trend.

Temperature data used to obtain gradients for this report were taken from well logs and corrected to approximate thermal equilibrium by the empirical relation developed by Kehle (1971).

$$T_E = T_L - 8.819 \times 10^{-12} D^3 - 2.143 \times 10^{-8} D^2 + 4.375 \times 10^{-3} D - 1.018 \quad (1)$$

where  $T_E$  = equilibrium temperature ( $^{\circ}$ F)

$T_L$  = bottom-hole temperature from well logs ( $^{\circ}$ F) and

$D$  = depth (ft).

## FORMATION POROSITY AND PERMEABILITY

Porosity and permeability values from whole-core analyses were used when core data were

available. Porosity ( $\phi$ ) was also computed from the formation resistivity factor ( $F$ ) and the cementation factor ( $m$ ), using the empirical equation developed by Archie (1942).

$$F = \phi^{-m} \quad (2)$$

where  $m = 1.8$  for sandstones.

Formation factor is defined as a ratio of resistivities that can be obtained from induction and SP well logs. It is assumed that

$$R_o = R_t \text{, and} \\ F = R_o/R_w \quad (3)$$

where  $R_o = R_t$  = resistivity of rock that is 100-percent saturated with formation water of resistivity  $R_w$ , determined from the deep induction log (ohm-meters), and

$R_w$  = resistivity of formation water at given temperature and salinity, determined from the SP log (ohm-meters).

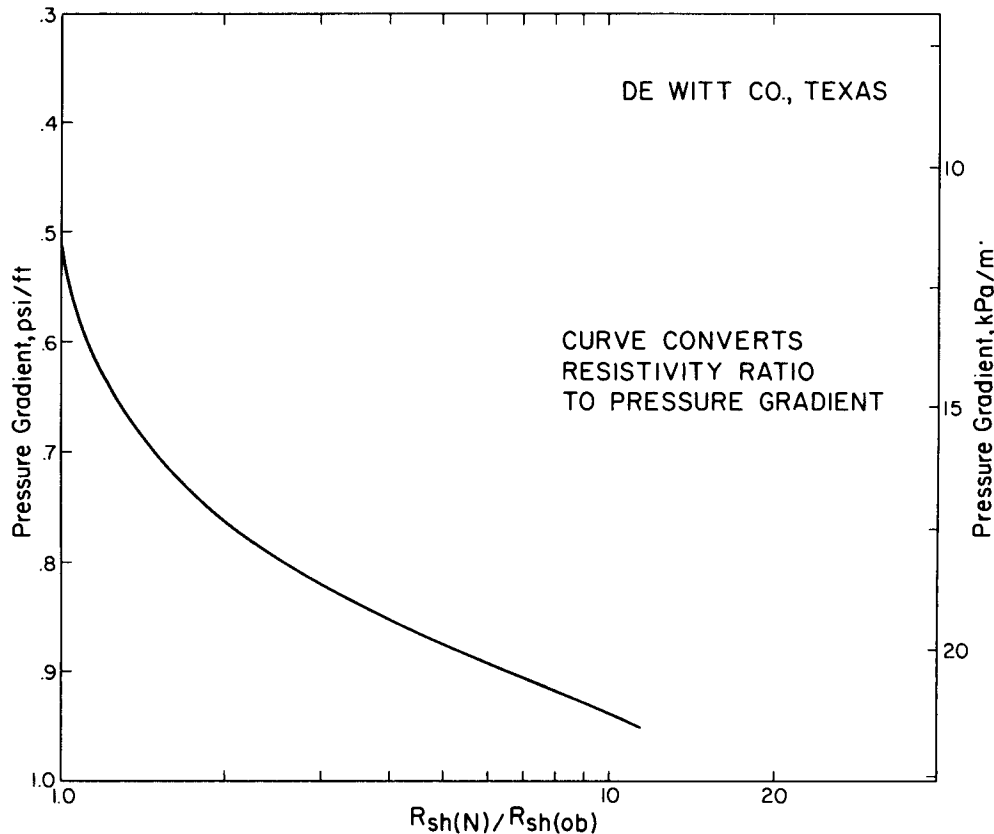


Figure 39. Shale resistivity ratio curve for De Witt County.

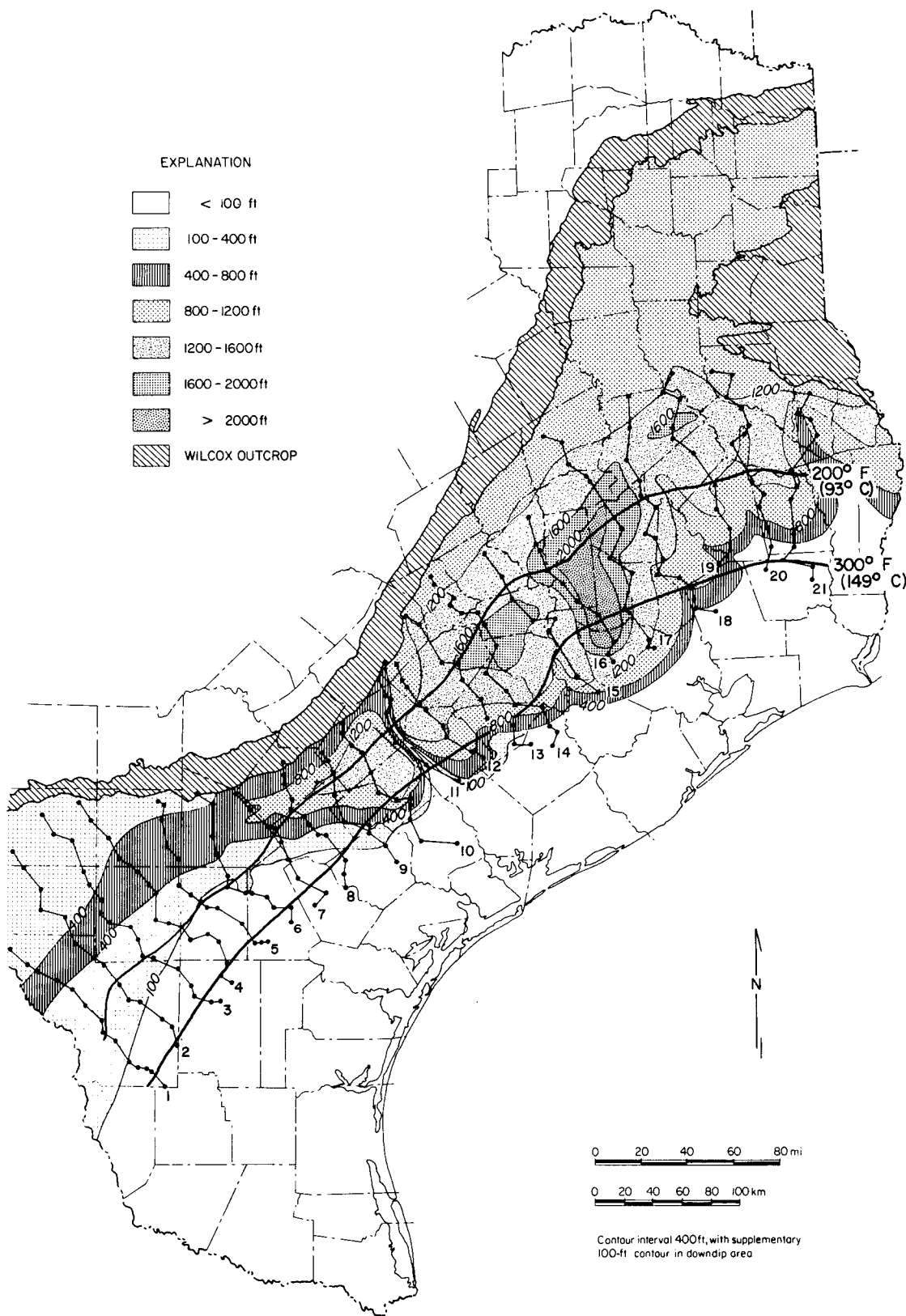


Figure 40. Net-sandstone distribution in the lower Wilcox with the 200° and 300°F isotherms at the top of the lower Wilcox.

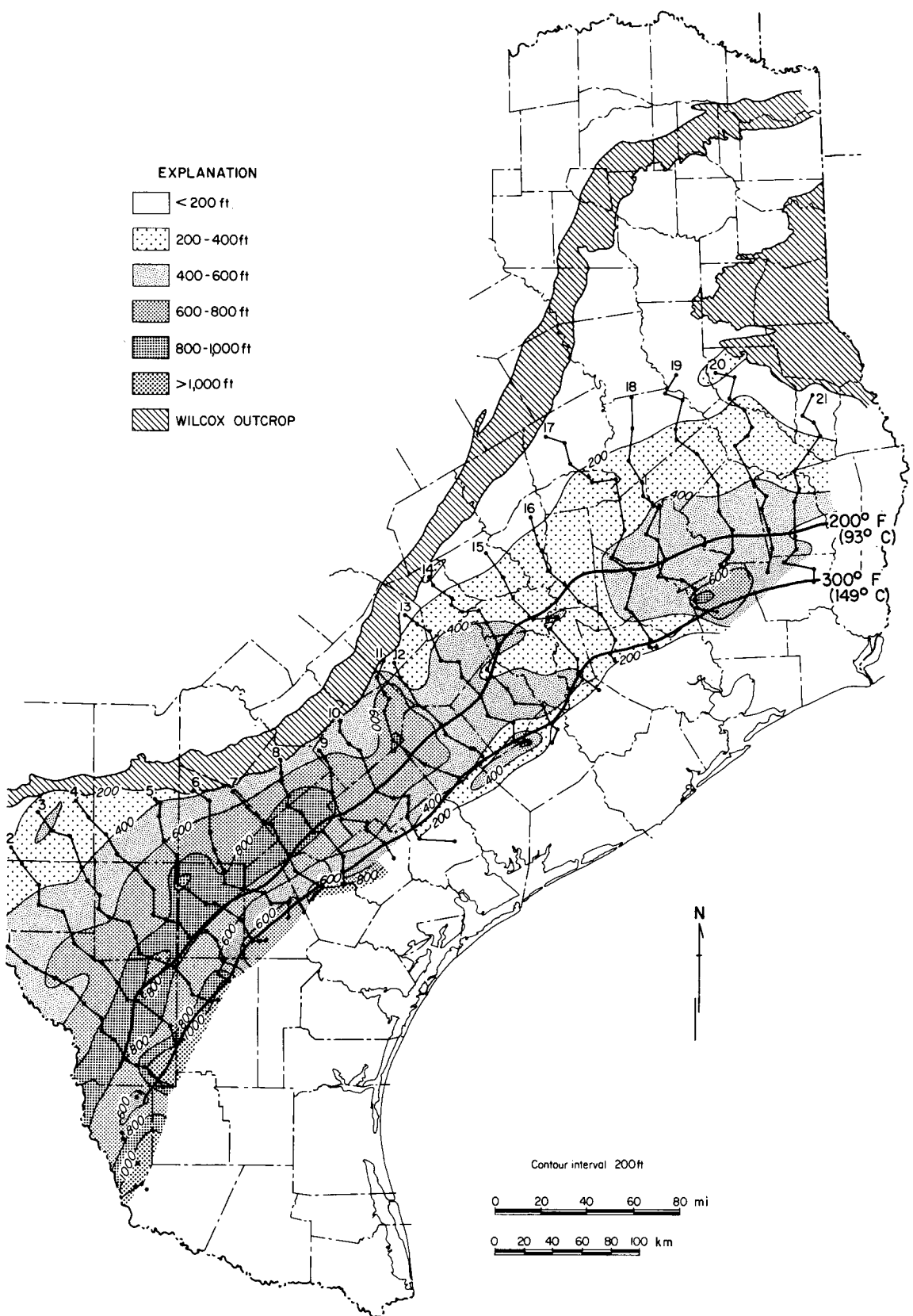


Figure 41. Net-sandstone distribution in the upper Wilcox with the 200° and 300°F isotherms at the top of the upper Wilcox.

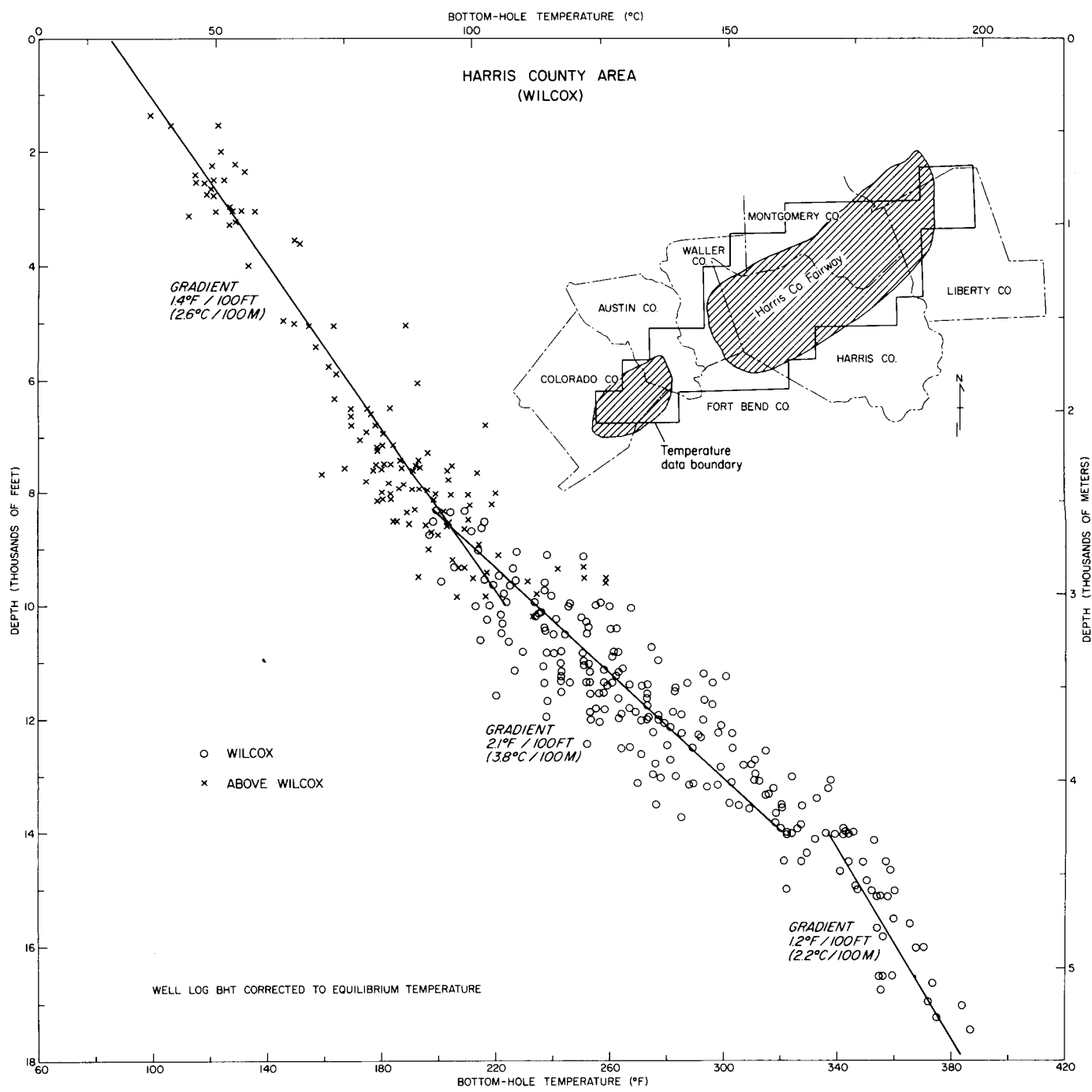


Figure 42. Temperatures and geothermal gradients for the Harris Fairway area.

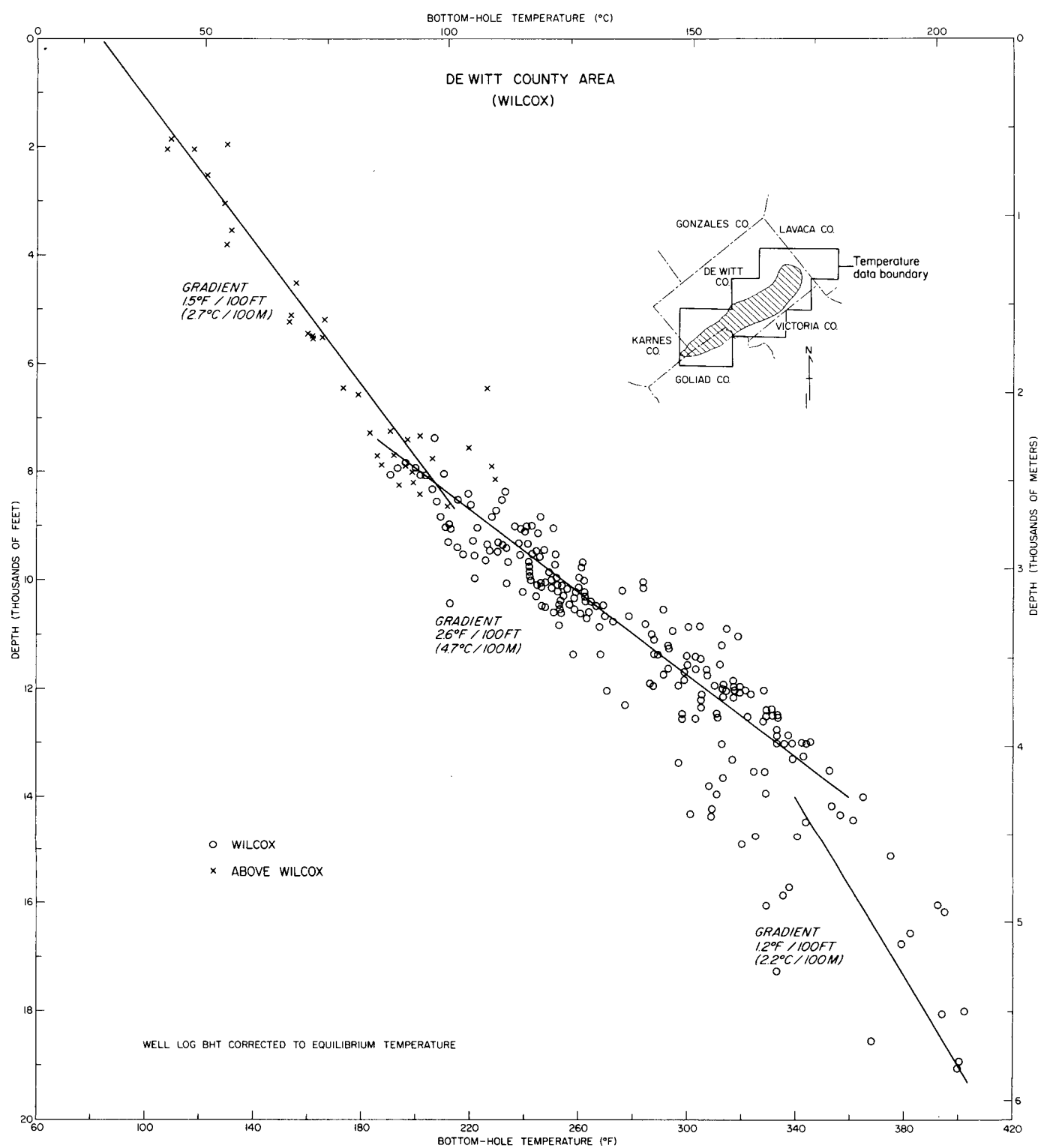


Figure 43. Temperatures and geothermal gradients for the De Witt Fairway area.

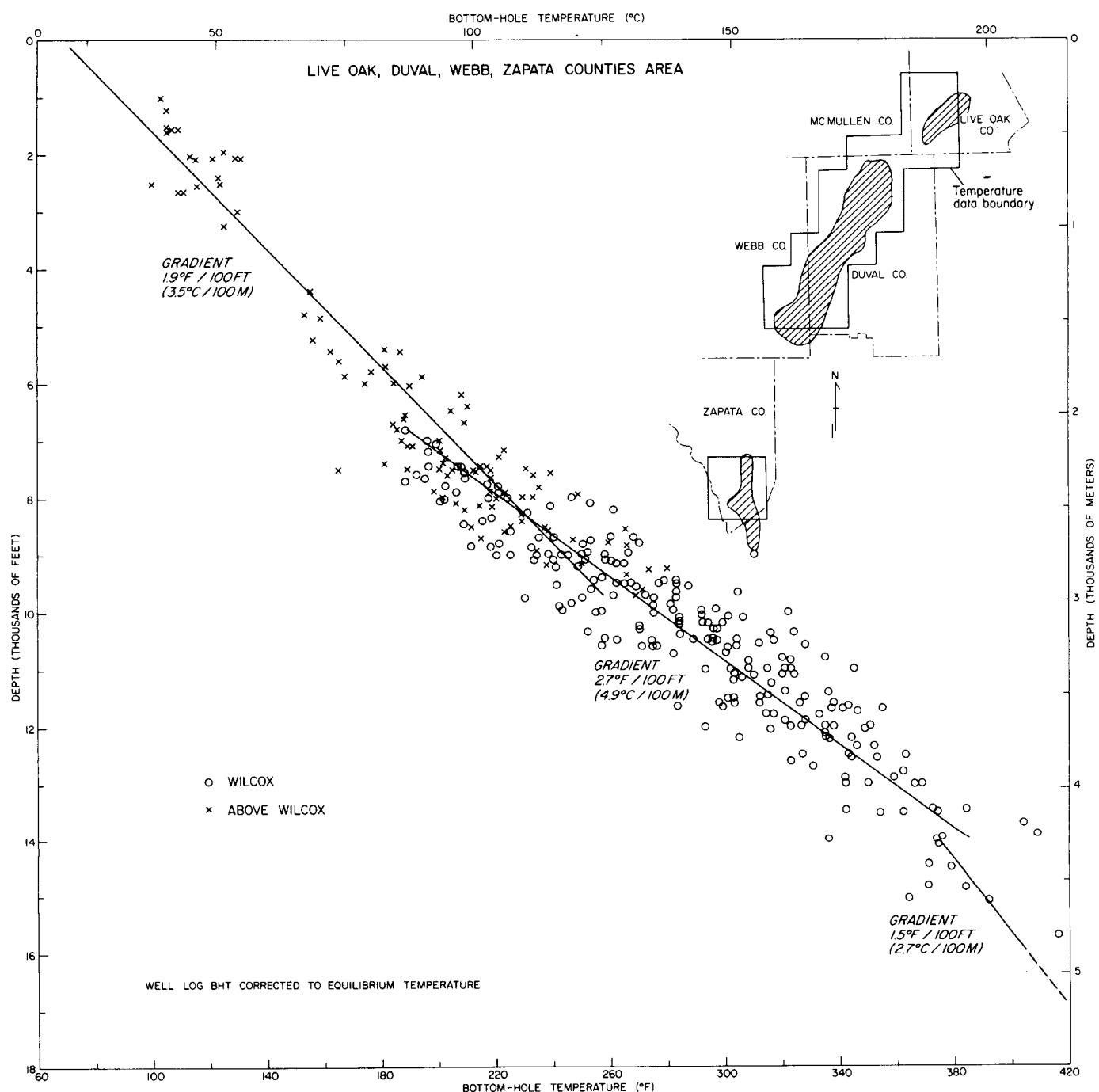


Figure 44. Temperatures and geothermal gradients for parts of Live Oak, McMullen, Duval, Webb, and Zapata Counties.

## ZAPATA FAIRWAY

The Zapata Fairway, elongated north to south, is located primarily in Zapata County but also extends to the south into Starr County (figs. 45 and 46). The fairway is approximately 27 mi long and 6 mi wide and has an area of 110 mi<sup>2</sup>. It was delineated as an area of possible geopressured geothermal reservoirs during regional study of the Wilcox Group along the Texas Gulf Coast (Bebout and others, 1978a). Selection of this study area was based on the presence of considerable thicknesses of sandstone having fluid temperatures higher than 300°F. The sandstones of the Zapata Fairway are of the upper Wilcox Group and are part of a general, gradually upward-coarsening sequence about 2,000 ft thick.

This sequence was subdivided and correlated in the fairway area using numerous markers; only five markers are shown in this report (figs. 47 through 49). Most of the markers are in sections having many alternating layers of sandstone and shale, and some appear to be persistent over large areas. The two principal markers, which have been correlated throughout the Texas Gulf Coast, are the top and the base of the upper Wilcox (fig. 36). Three additional markers are shown: (1) marker Z1 occurs at the top of the main sandstone-bearing interval and below an uppermost shale-rich interval (fig. 47); (2) marker Z2 is above the sandstone units in the middle part of the upper Wilcox, these units being the prime targets of this geothermal study; and (3) marker Z3 occurs below the main sandstone-bearing part of the upper Wilcox. Correlation of these markers with markers in the Duval and Live Oak Fairways is shown in table 1.

The most prospective reservoirs of the Zapata Fairway are two distinct sandstone bodies occurring immediately below marker Z2. These sandstones range from about 280 to 620 ft thick and occur at depths of 7,800 to 10,150 ft. Wells farthest downdip show that these sandstone bodies grade into shale toward the east.

The Zapata Fairway is located on the growth-faulted upper Wilcox shelf edge, which includes two or three major growth faults with displacements of up to 3,000 ft at the level of the Z2 marker and at least 10 smaller faults. The zone of growth faulting is more than 13 mi wide. Sedimentary units in the upper part of the Wilcox increase in thickness by a factor of 3 from west to east because of faulting contemporaneous with sedimentation.

The top of geopressure, defined as the depth at which the pressure gradient exceeds the hydrostatic pressure gradient of 0.465 psi per foot,

occurs at an average depth of 6,000 ft in Zapata County (fig. 50). However, some reservoirs as deep as 10,700 ft are not geopressured. The gradient of 0.7 psi per foot occurs at an average depth of 9,000 ft. Maximum pressure gradients of about 0.85 psi per foot, determined from bottom-hole shut-in pressures measured during drill-stem tests, occur in a few reservoirs below 10,000 ft (fig. 50). Maximum gradients of up to 0.96 psi per foot are indicated by geopressure profiles computed for individual wells (fig. 51).

Temperatures of 200° and 300°F occur at average depths of 7,000 and 11,400 ft, respectively (fig. 52). A geothermal gradient of 1.59°F per 100 ft is common down to 8,000 ft, and 2.1°F per 100 ft is common at greater depths.

Salinity of shallow reservoir waters varies widely from 10,000 to 75,000 ppm NaCl. Upper Wilcox sandstones in Zapata County have water salinities that range from 17,000 to 60,000 and average 40,000 ppm NaCl, on the basis of computations from electric logs of five wells (fig. 53).

Few core analyses are available for Zapata County, but sidewall-core data for limited depth intervals in two wells are listed in table 2. These limited data suggest that porosity and permeability are very low.

Table 1. Correlation of stratigraphic markers in the Zapata, Duval, and Live Oak Fairways.

UPPER WILCOX MARKERS	ZAPATA FAIRWAY	DUVAL FAIRWAY	LIVE OAK FAIRWAY
	TOP OF WILCOX		"Slick Sand"
Z1		Du1	L1 "Luling Sand"
Z2		Du2	L2 "Mackhank" - "Massive"
Z3		Du3	L3
			L4
BASE OF UPPER WILCOX (REGIONAL MARKER)			

Table 2. Sidewall-core data from two wells in Zapata County.

DEPTH (ft)	PERMEABILITY (md)	POROSITY (%)
9,153 to 9,558	0 to 2.9 (avg. 0.5)	17 to 21 (avg. 18.0)
10,027 to 10,634	0 to 6.6 (avg. 2.0)	18 to 22 (avg. 20.0)
10,498 to 10,499	8 to 19	18 to 20

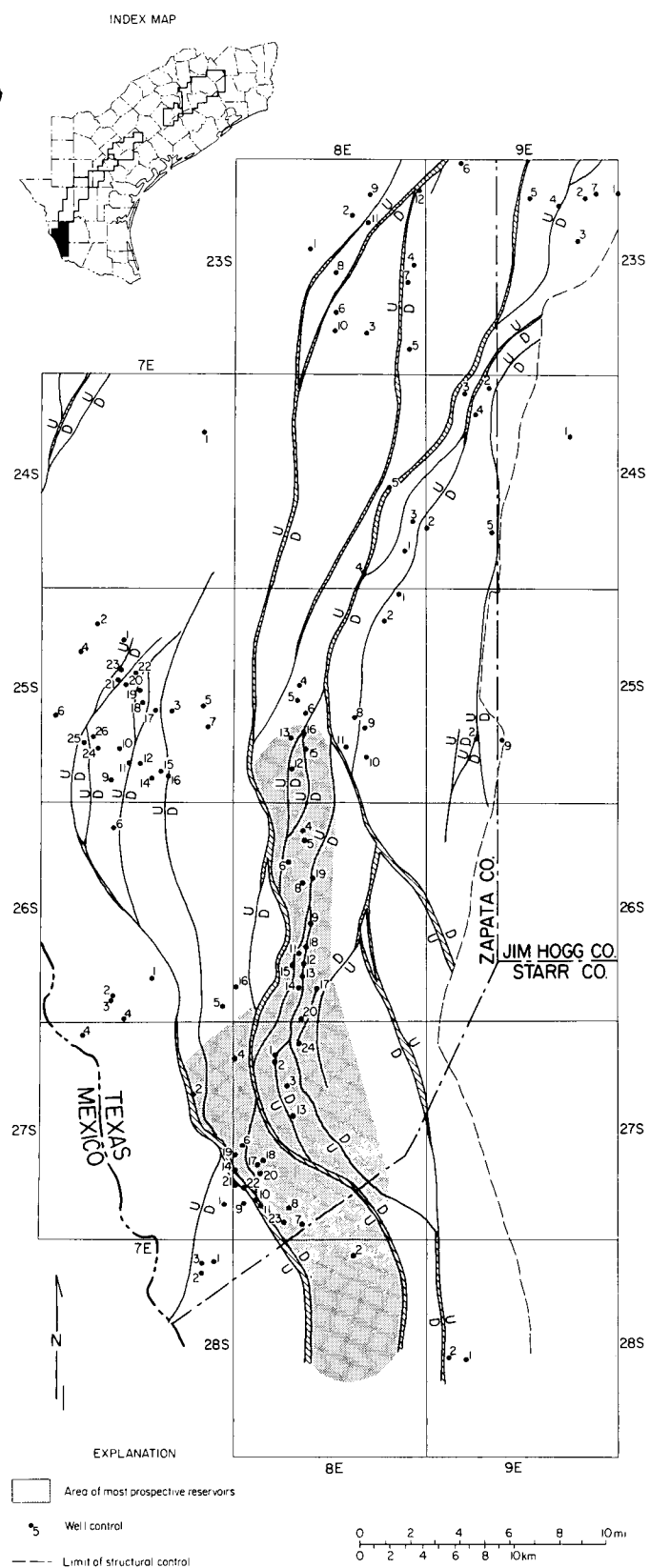


Figure 45. Well control, faults at the top of the Wilcox, and area of prospective reservoir sandstones, Zapata Fairway.

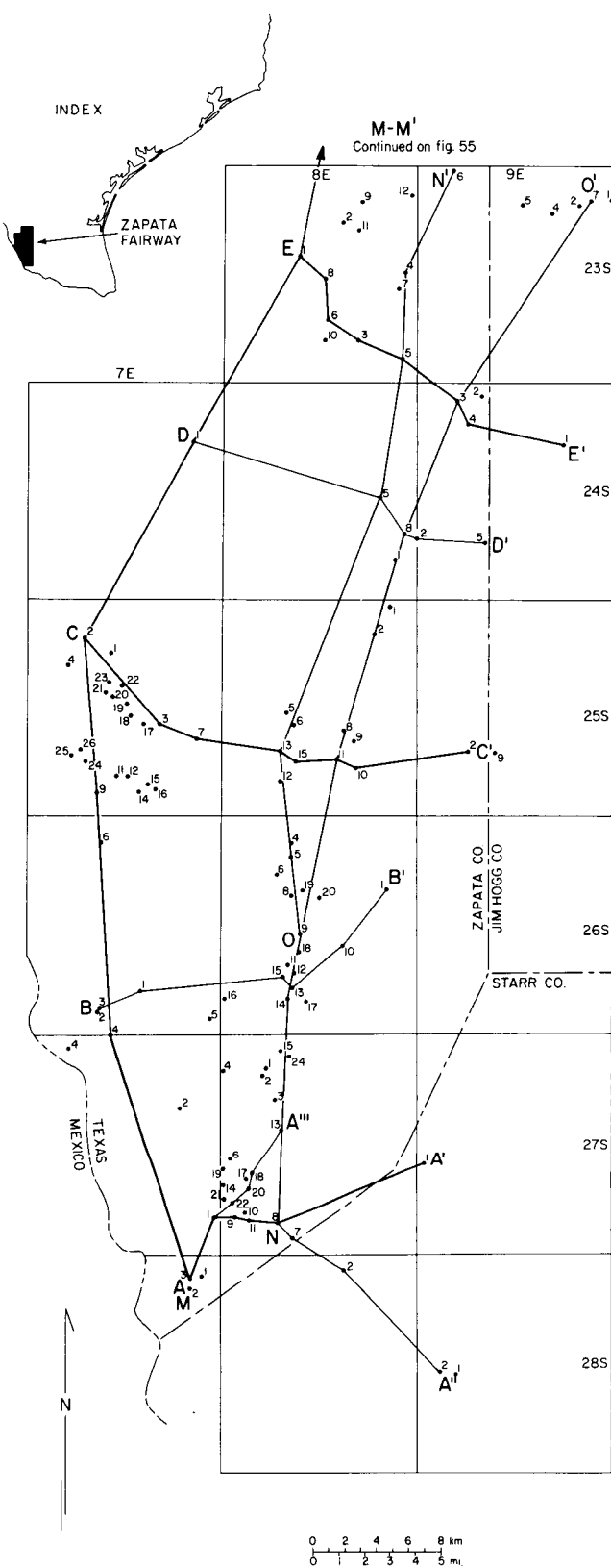


Figure 46. Well control and lines of stratigraphic and structural sections, Zapata Fairway. Heavy lines indicate the sections included in this report.

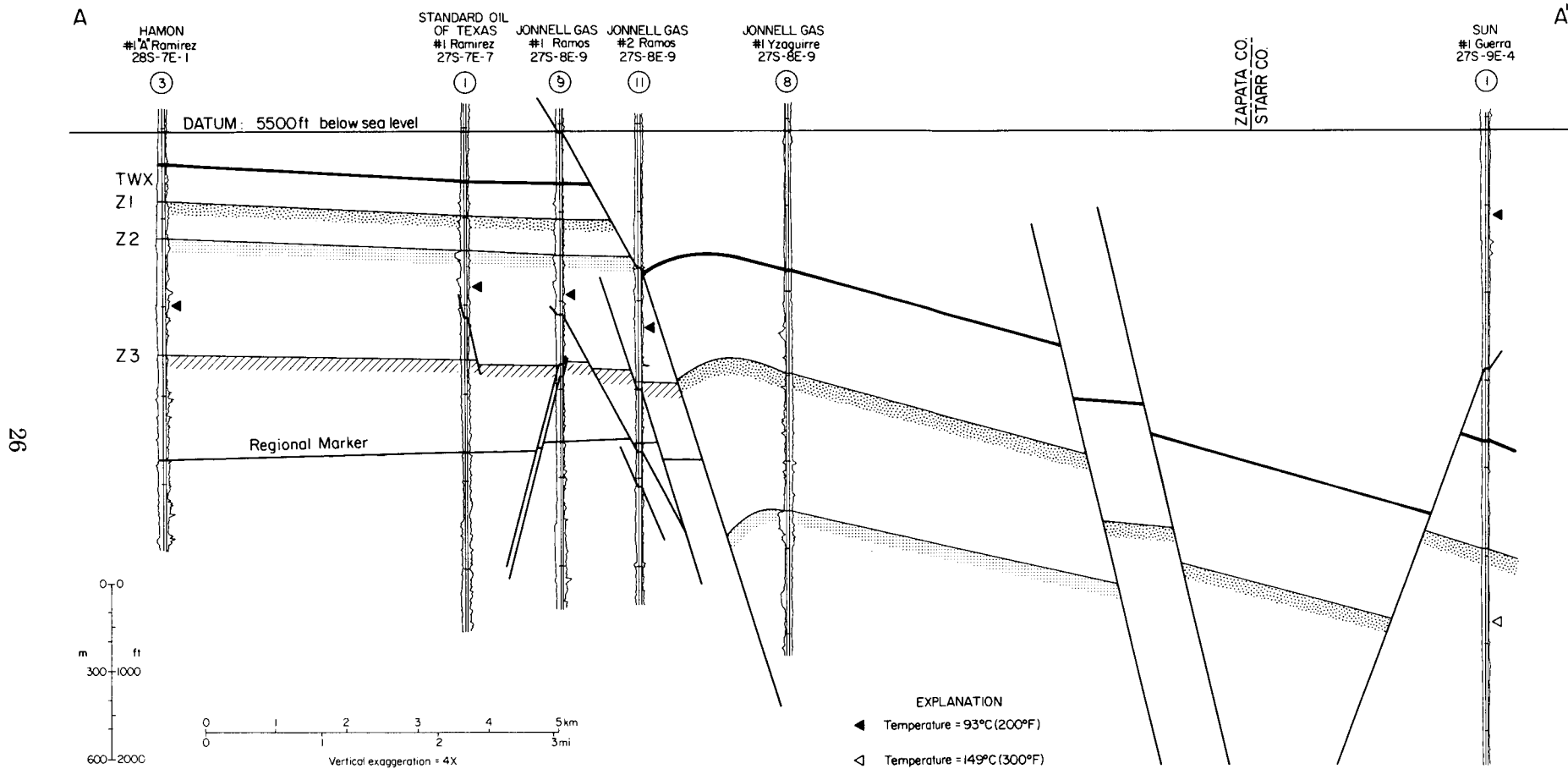


Figure 47. Structural dip section A-A', southern part of the Zapata Fairway.

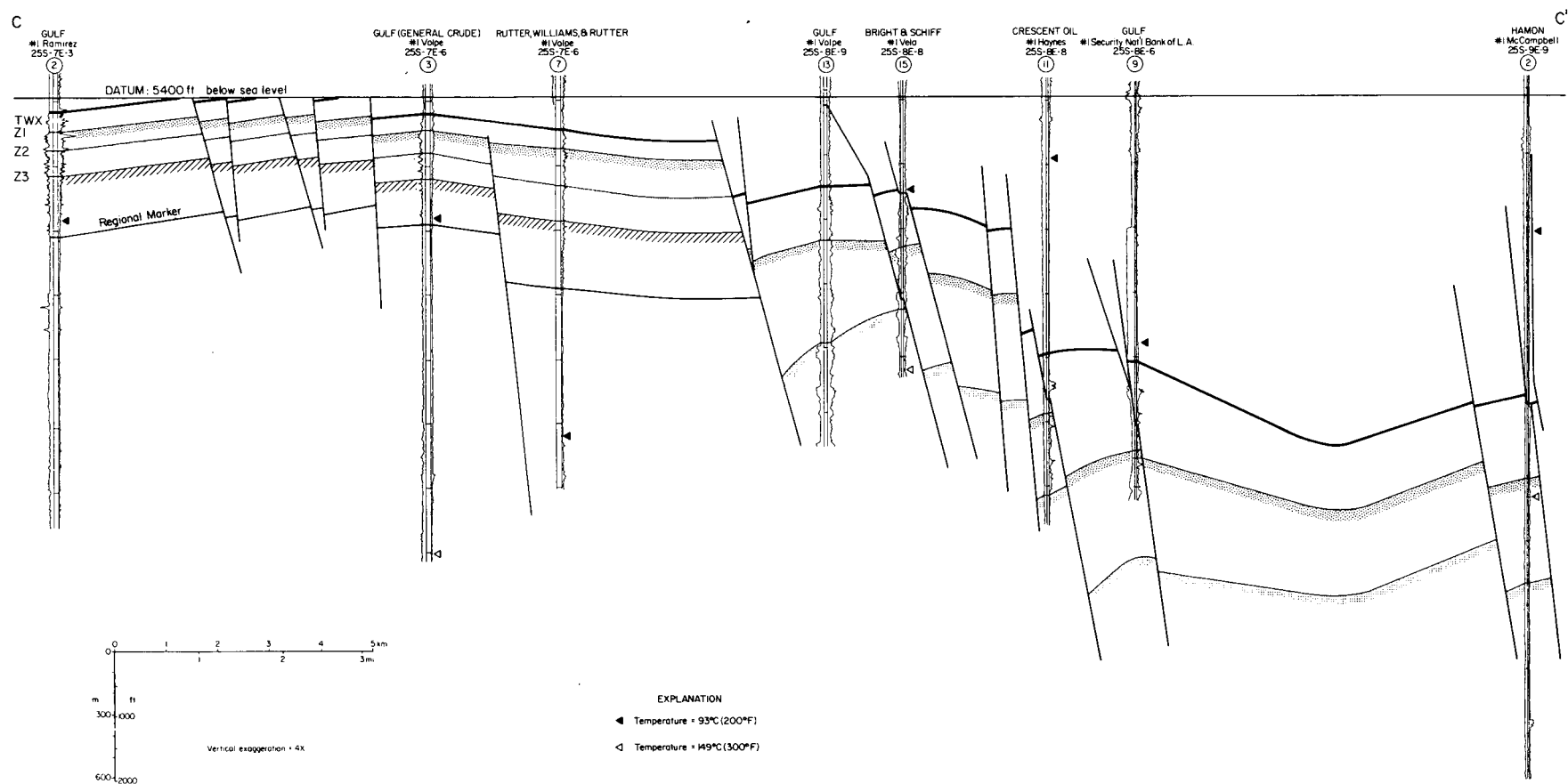


Figure 48. Structural dip section C-C', central part of the Zapata Fairway.

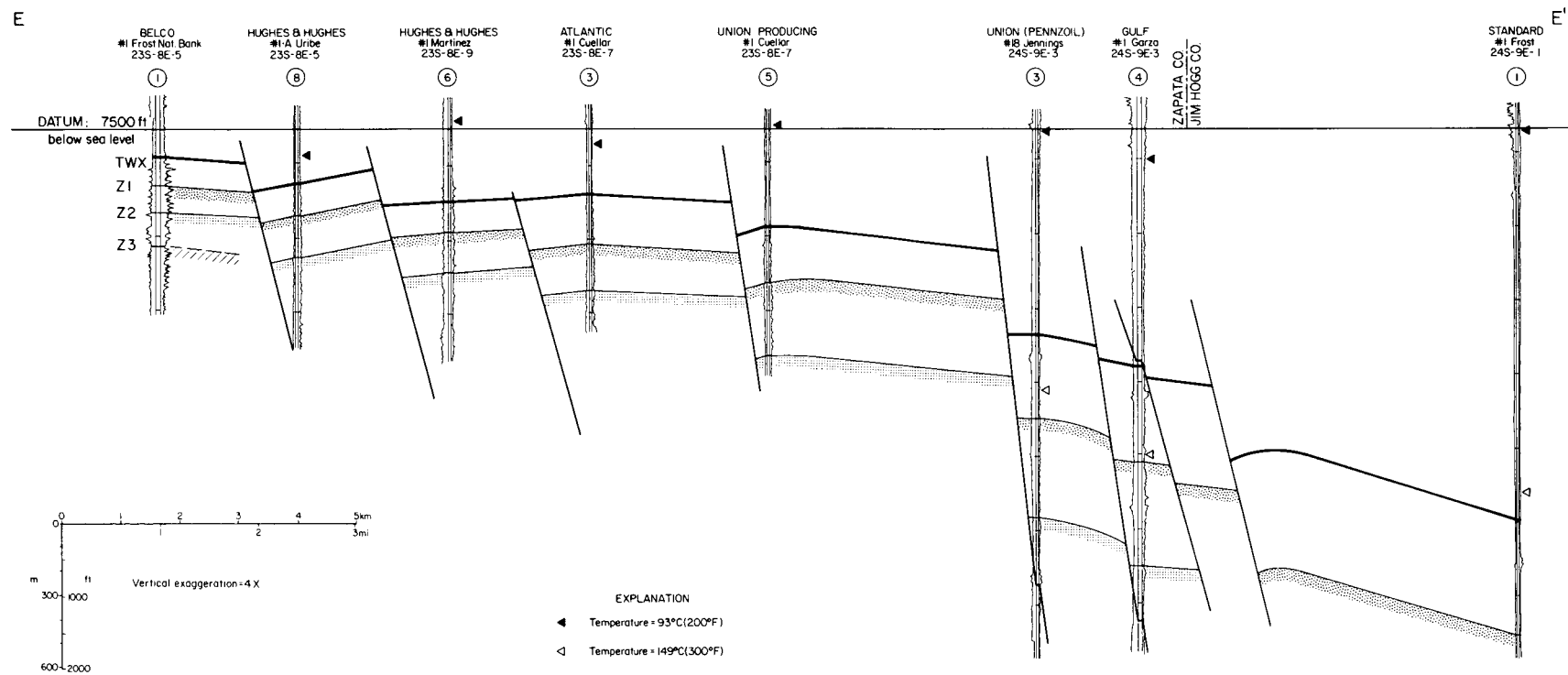


Figure 49. Structural dip section E-E', northern part of the Zapata Fairway.

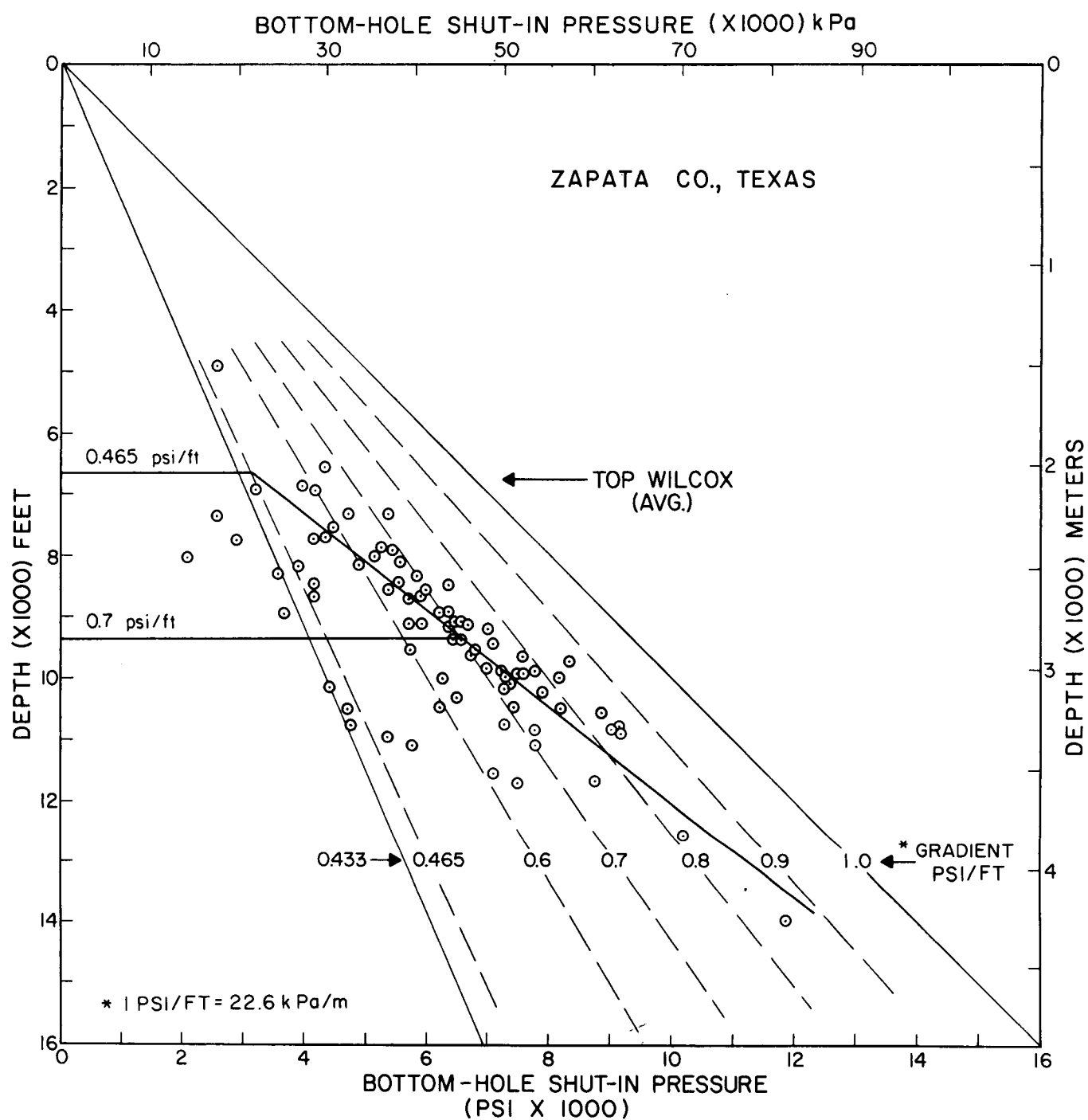


Figure 50. Bottom-hole shut-in pressures plotted as a function of depth for Zapata County.

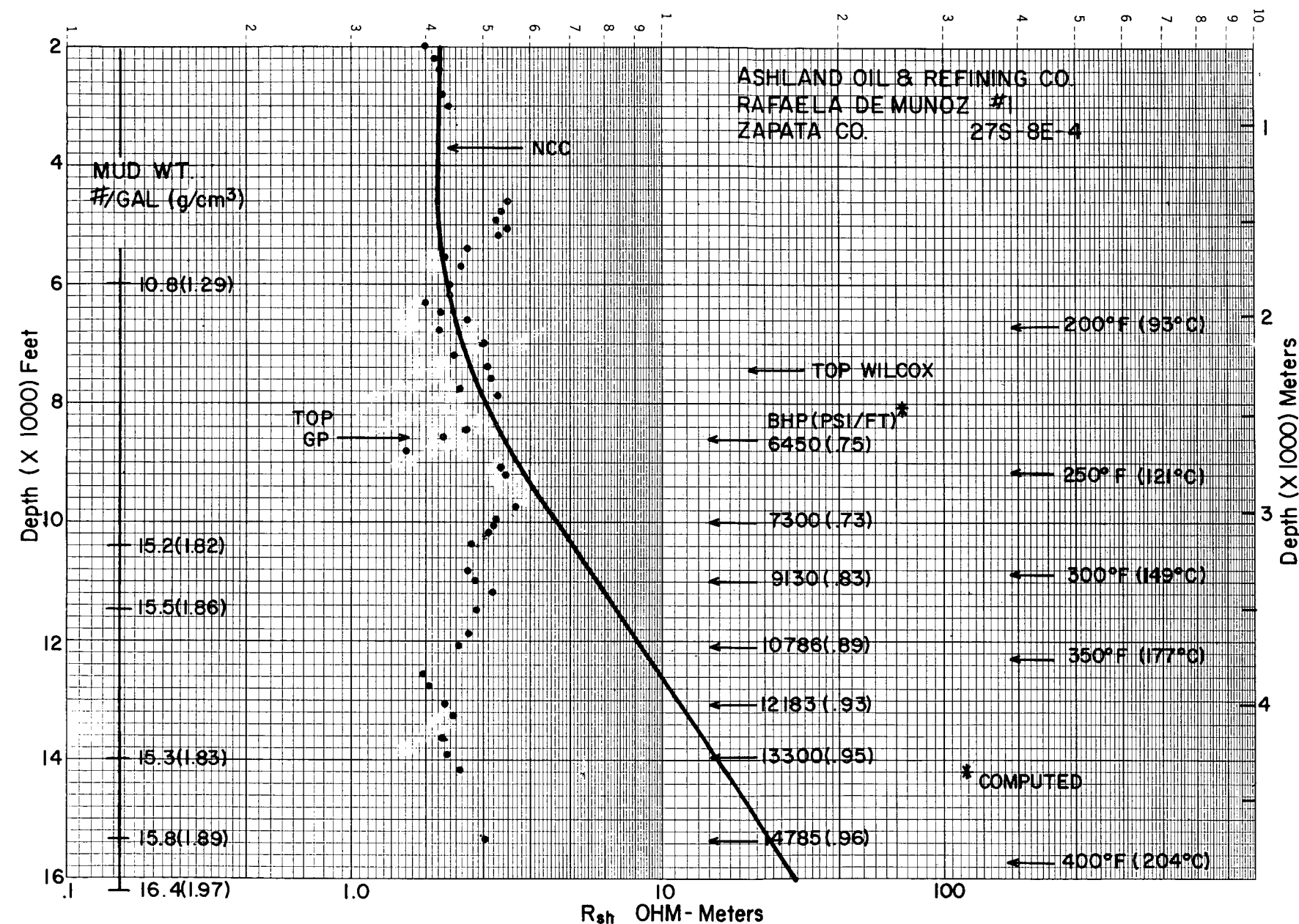


Figure 51. Operational top of geopressure and geopressure gradients from shale resistivity data for a well in Zapata County.

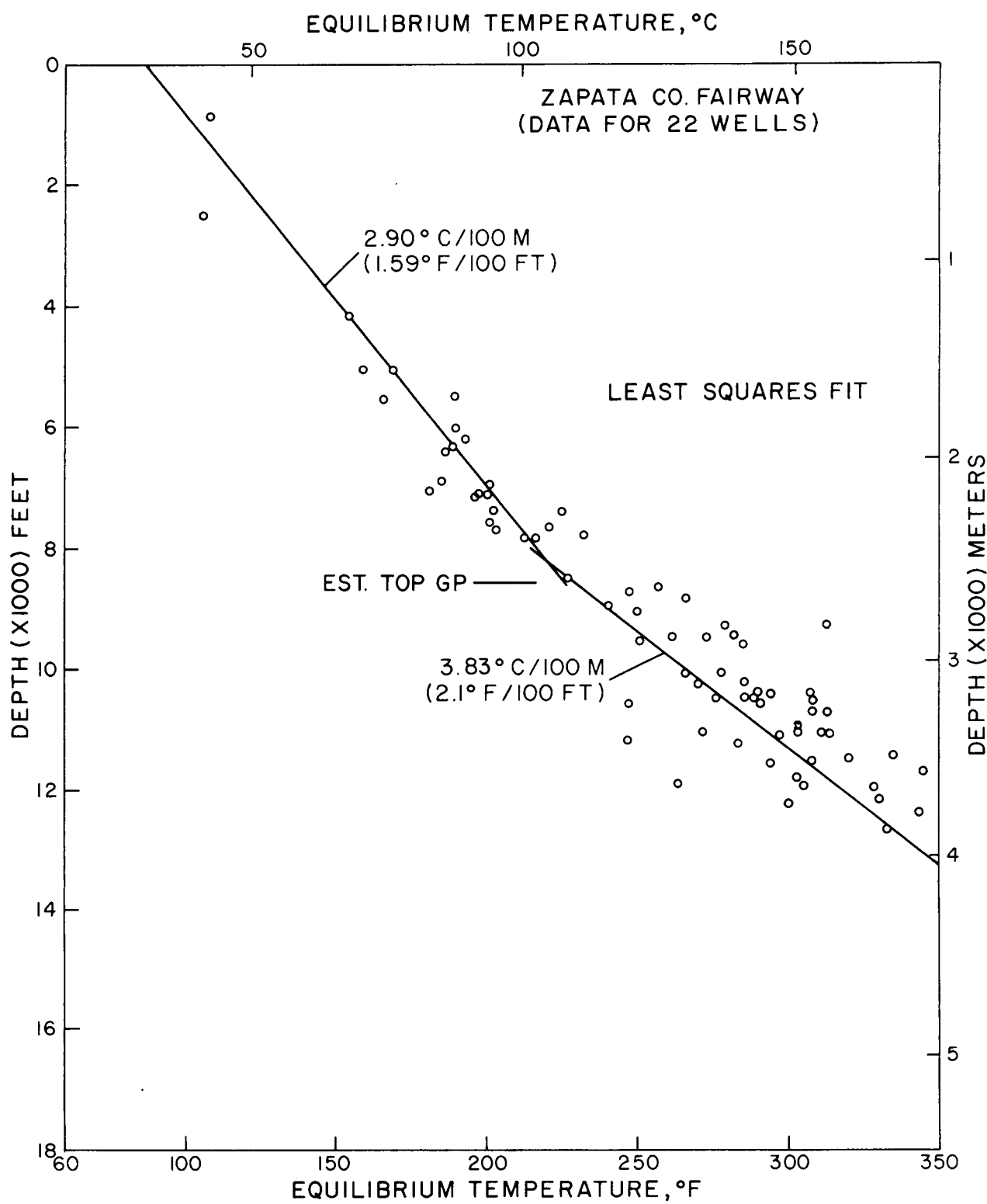


Figure 52. Temperatures and geothermal gradients for Zapata Fairway.

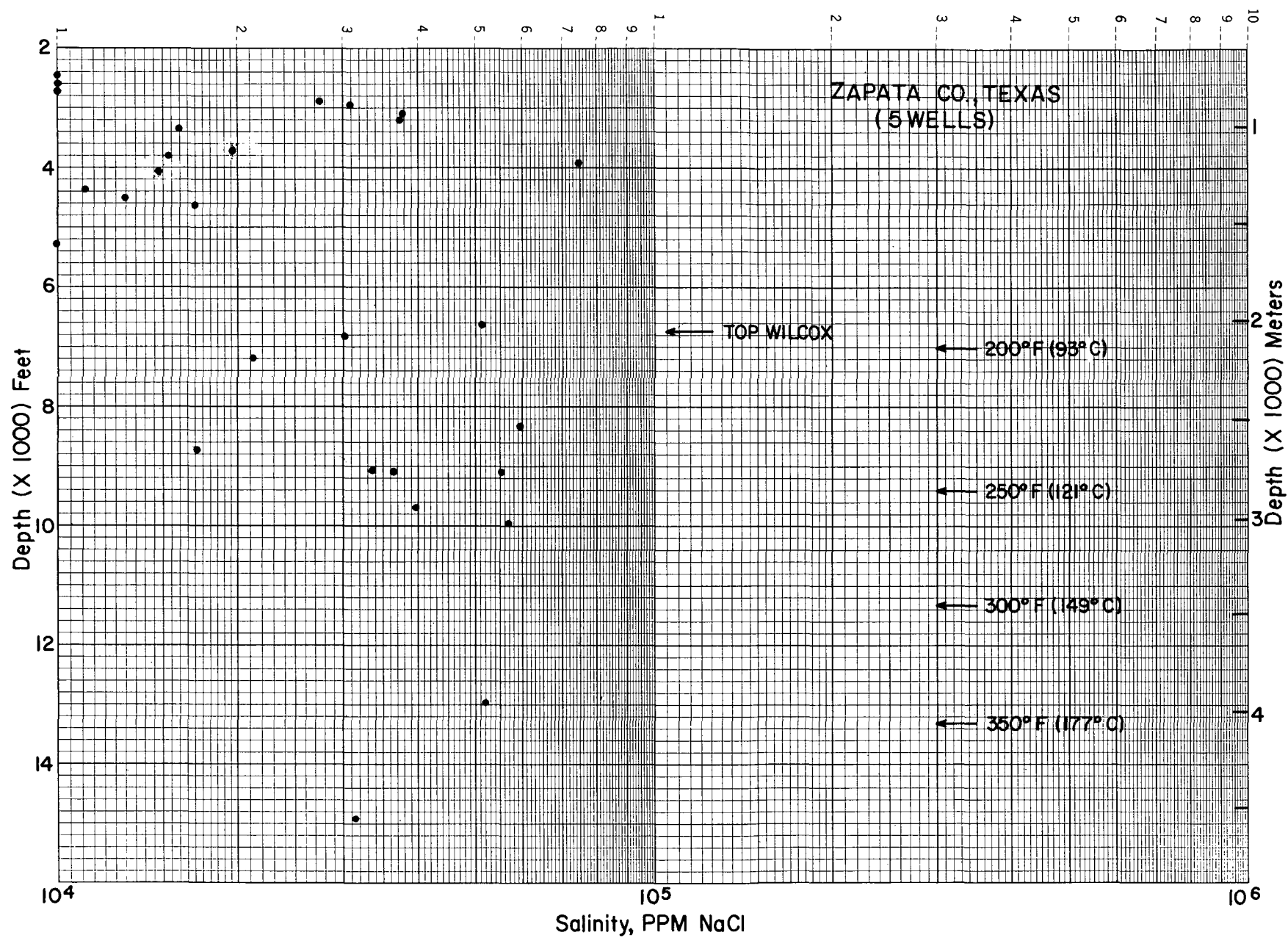


Figure 53. Salinity versus depth calculated from electric logs of five wells in Zapata County.

## DUVAL FAIRWAY

The Duval Fairway trends southwest through Duval and Webb Counties and also extends south into Jim Hogg County and north into McMullen County (figs. 54 and 55). This fairway, which is approximately 60 mi long and 9 mi wide, was originally designated as two separate fairways (Duval and Webb) in previous studies (Beabout and others, 1978a). During the present study, these two areas were observed to contain one continuous stratigraphic unit of geopressured Wilcox sandstones with fluid temperatures greater than 300°F.

In the Duval Fairway area, prospective thick sandstones occur in the lower part of the upper Wilcox; shallower sandstones are relatively thin. The Rosita and Seven Sisters gas fields are located along this trend. In updip areas, the upper Wilcox is about 2,000 ft thick. Downdip it thickens to at least 6,000 ft. In the fairway area, the upper Wilcox was subdivided and correlated with three markers (Du1, Du2, Du3), in addition to the top and base of the upper Wilcox (fig. 56). Equivalent markers in the Zapata and Live Oak Fairways are shown in table 1.

The main sandstone-bearing interval occurs beneath the Du3 marker. This interval extends downward to the regional marker at the base of the upper Wilcox and contains very massive sandstones over a large part of the updip area of the fairway. Downdip, the sandstones are separated by thick shale sequences and are arranged into upward-coarsening sequences.

The prospective sandstone interval of the Duval Fairway occurs in the Rosita Field area below marker Du2 at a depth of about 11,000 ft and continues down to at least 15,000 ft. Sandstones whose total thickness is at least 600 ft in this fairway contain fluids with temperatures greater than 300°F. Wells farthest downdip do not show significant thinning of sandstone bodies.

The elongate trend of the Duval Fairway approximately coincides with the belt of linear to arcuate growth faults that developed along the upper Wilcox shelf edge contemporaneous with deposition (fig. 54). This hinge zone includes five to

seven faults with displacement of as much as 2,000 to 3,000 ft at the level of the Du2 and Du3 markers. Given present well control, the growth-faulted zone appears to be 11 to 14 mi wide, but the downdip limit of the fairway is poorly outlined. The upper Wilcox increases in thickness across the growth-faulted zone by a factor of approximately 6. Lack of adequate well control in the Duval Fairway limits fairway evaluation.

The top of geopressure, defined as the depth at which the pressure gradient exceeds 0.465 psi per foot, occurs at an average depth of 8,600 ft in Duval County (fig. 57). The gradient of 0.7 psi per foot occurs at an average depth of 10,000 ft. Gradients reach 0.9 psi per foot at 11,800 ft. Operational top of geopressure determined from shale resistivity plots for two wells in Duval County occurs between depths of 8,150 and 9,800 ft (figs. 58 and 59).

In Duval County, the geothermal gradient is 1.6°F per 100 ft above a depth of 8,000 ft (fig. 60). At greater depths, the gradient increases to 3.1°F per 100 ft in the geopressured zone. The average gradient in the fairway is 2.7°F per 100 ft (fig. 44). A temperature of 300°F occurs at an average depth of 10,750 ft.

Salinities of formation waters range from 10,000 to 55,000 ppm NaCl. These values were calculated from water resistivities derived from the SP logs for five wells in Duval County (fig. 61).

Porosity and permeability data from five wells in Duval County are listed in table 3. These data suggest that porosity and permeability in the fairway are too low for production of geopressured geothermal resources.

Table 3. Diamond-core data from five Duval County wells.

DEPTH (ft)	PERMEABILITY (md [avg.])	POROSITY (% [avg.])
9,500 to 9,530	253	23.5
10,524 to 10,542	2	15
11,362 to 11,368	5 to 44	8 to 14
11,853 to 12,033	0.17	6.8
12,133 to 12,333	0.29	12.6
13,800 to 14,000	0.1	12.0

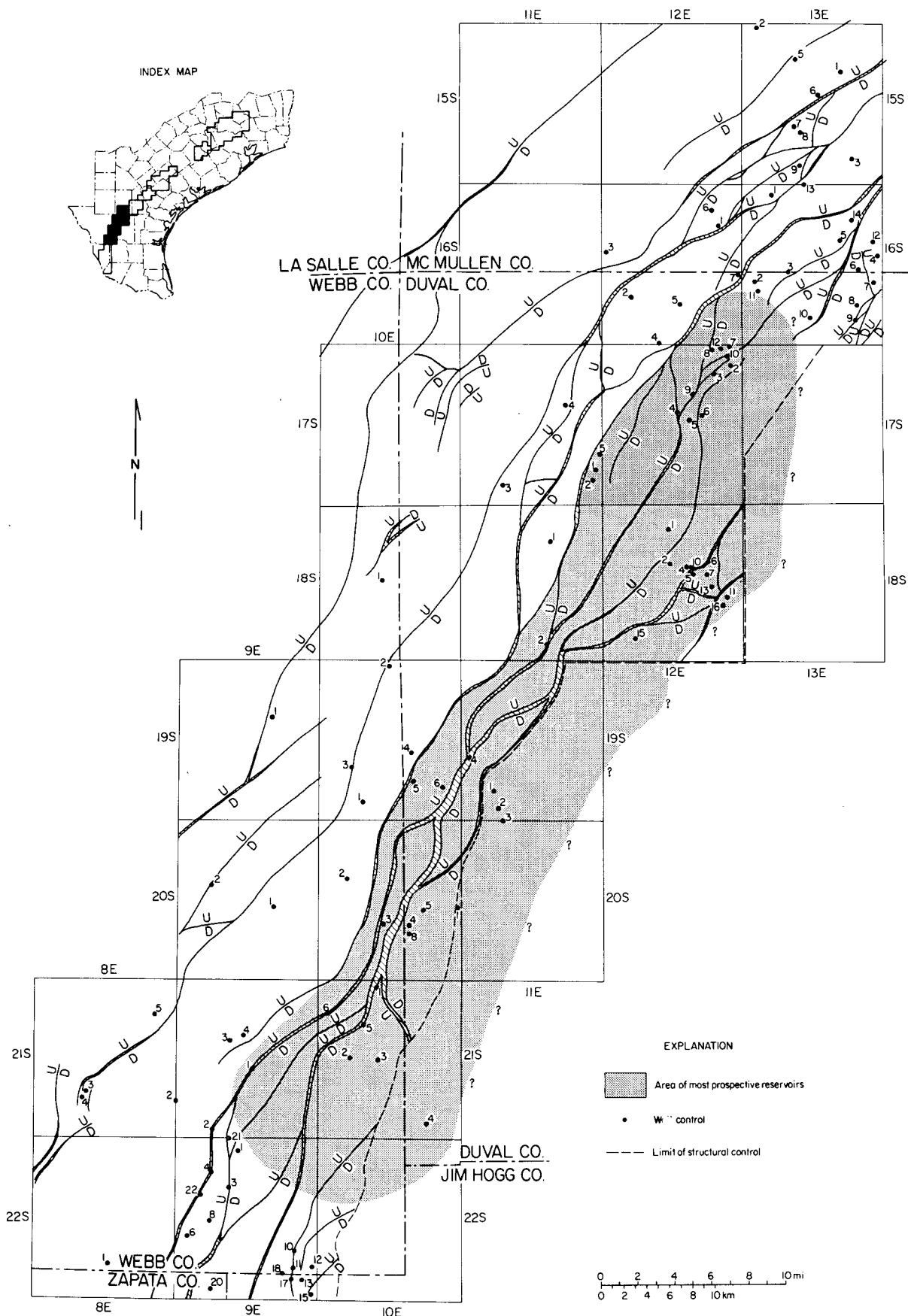


Figure 54. Well control, faults at the top of the Wilcox, and area of prospective reservoirs, Duval Fairway.

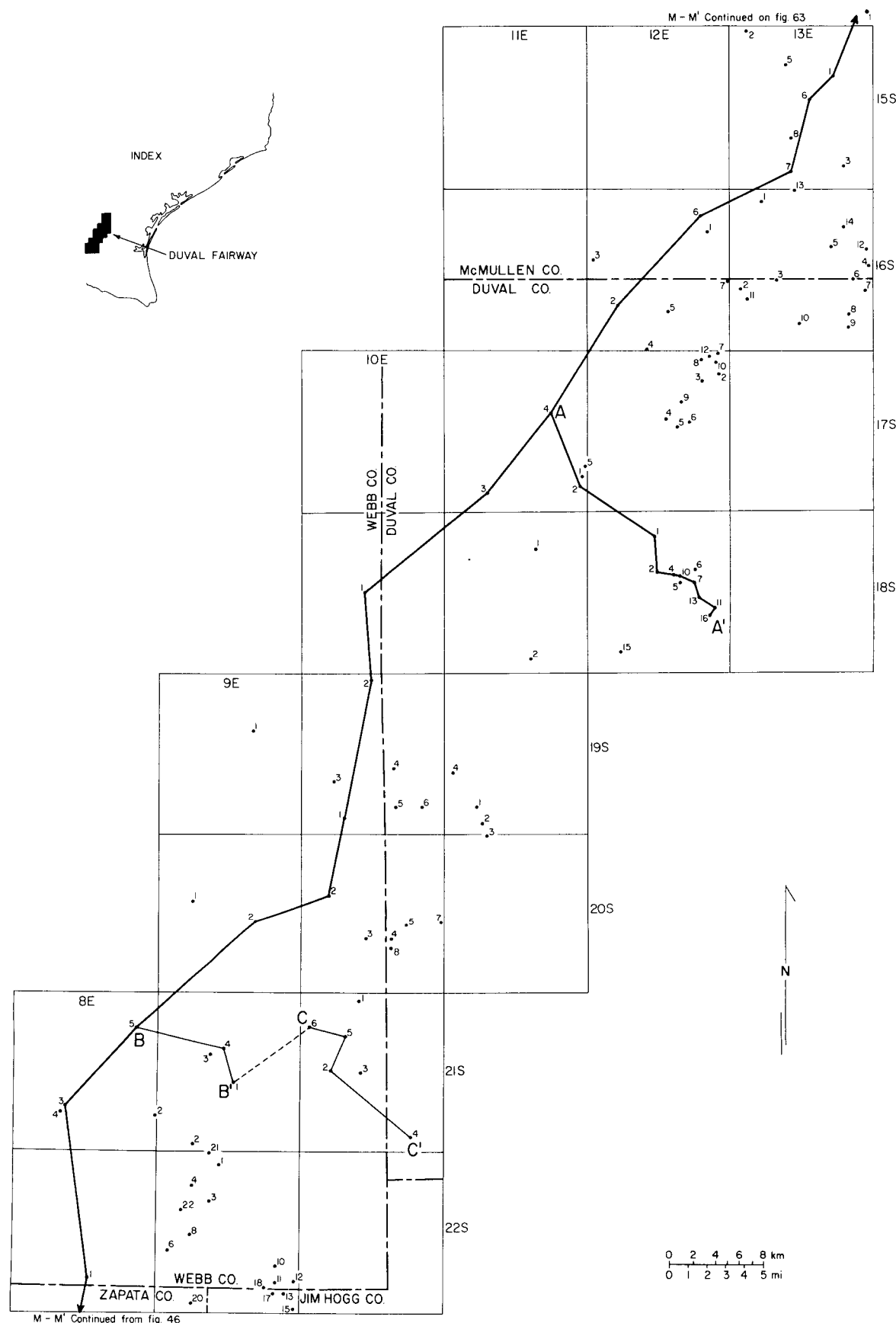


Figure 55. Well control and lines of stratigraphic and structural sections, Duval Fairway. Heavy lines indicate the sections included in this report.

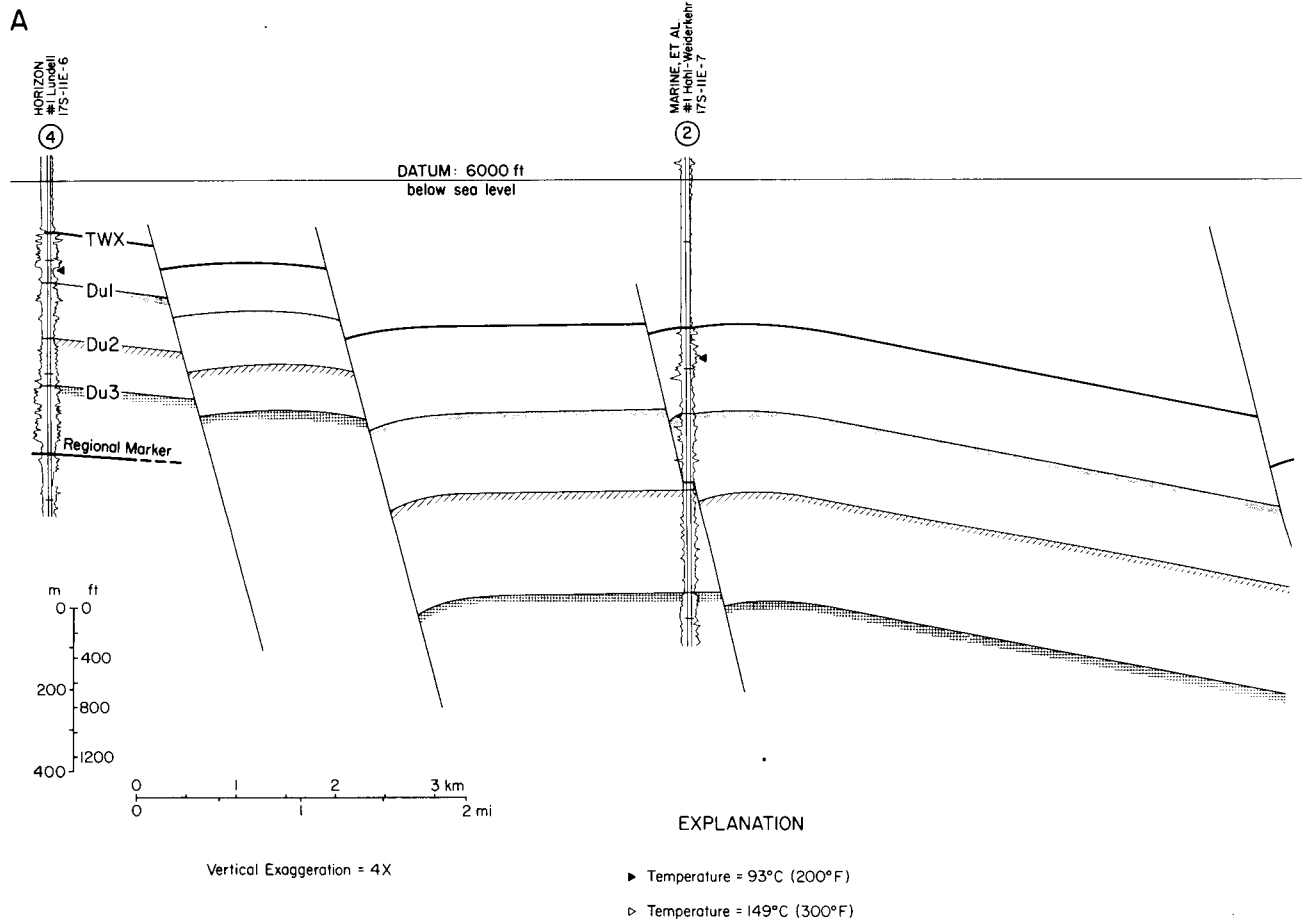


Figure 56. Structural dip section A-A', Duval Fairway.

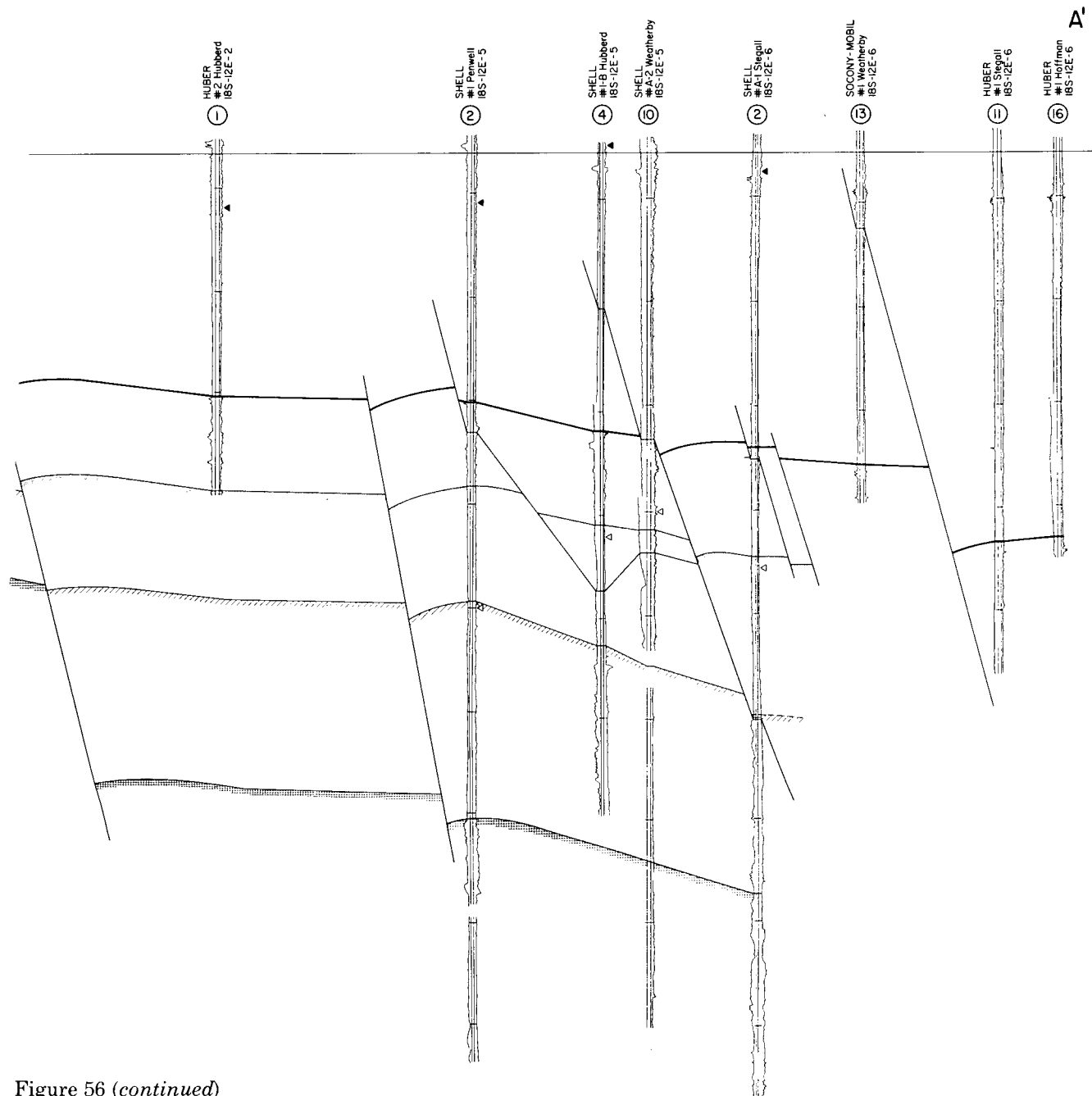


Figure 56 (continued)

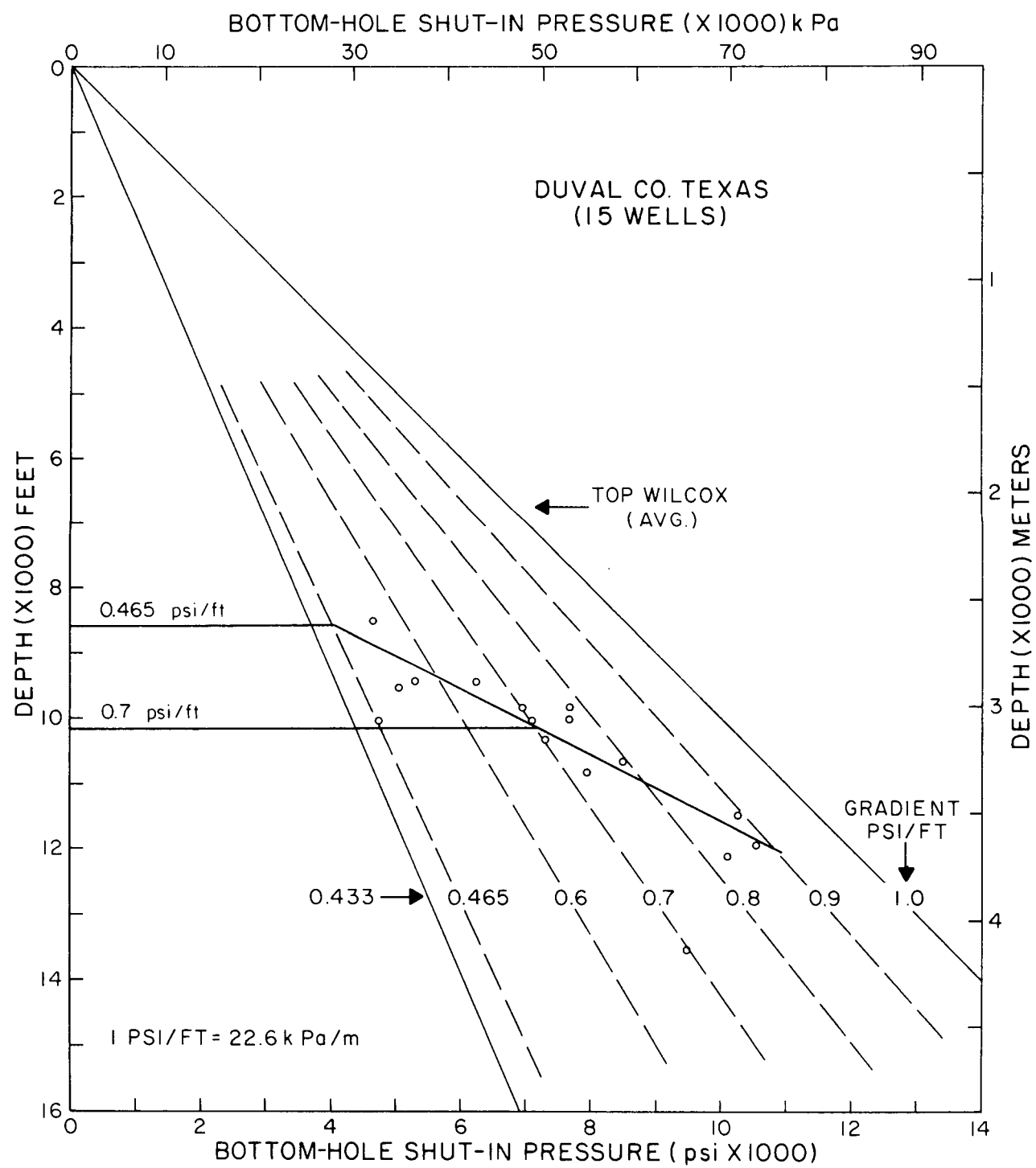


Figure 57. Bottom-hole shut-in pressures plotted as a function of depth for Duval County.

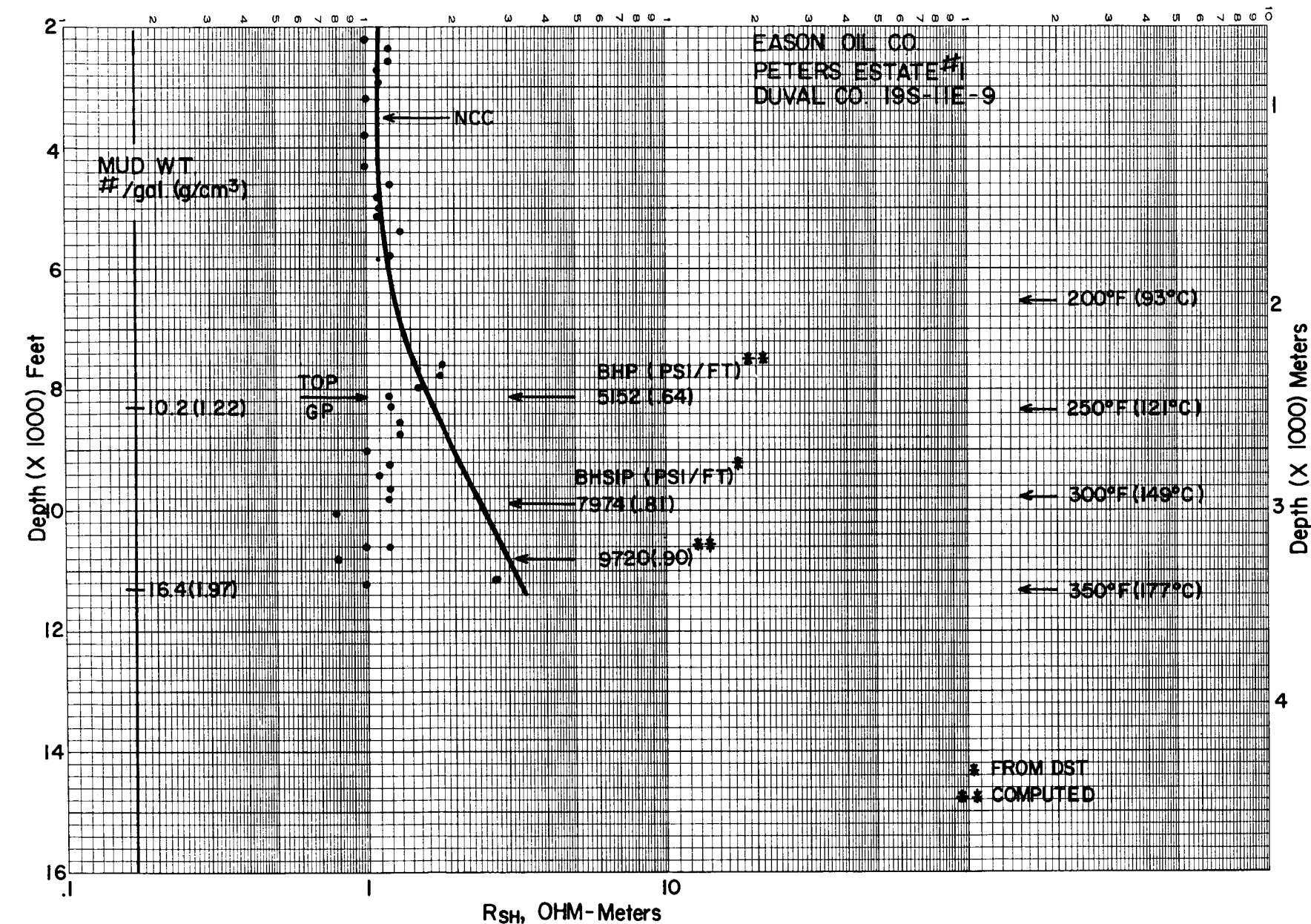


Figure 58. Operational top of geopressure and geopressure gradients from shale resistivity data for a well in Duval County.

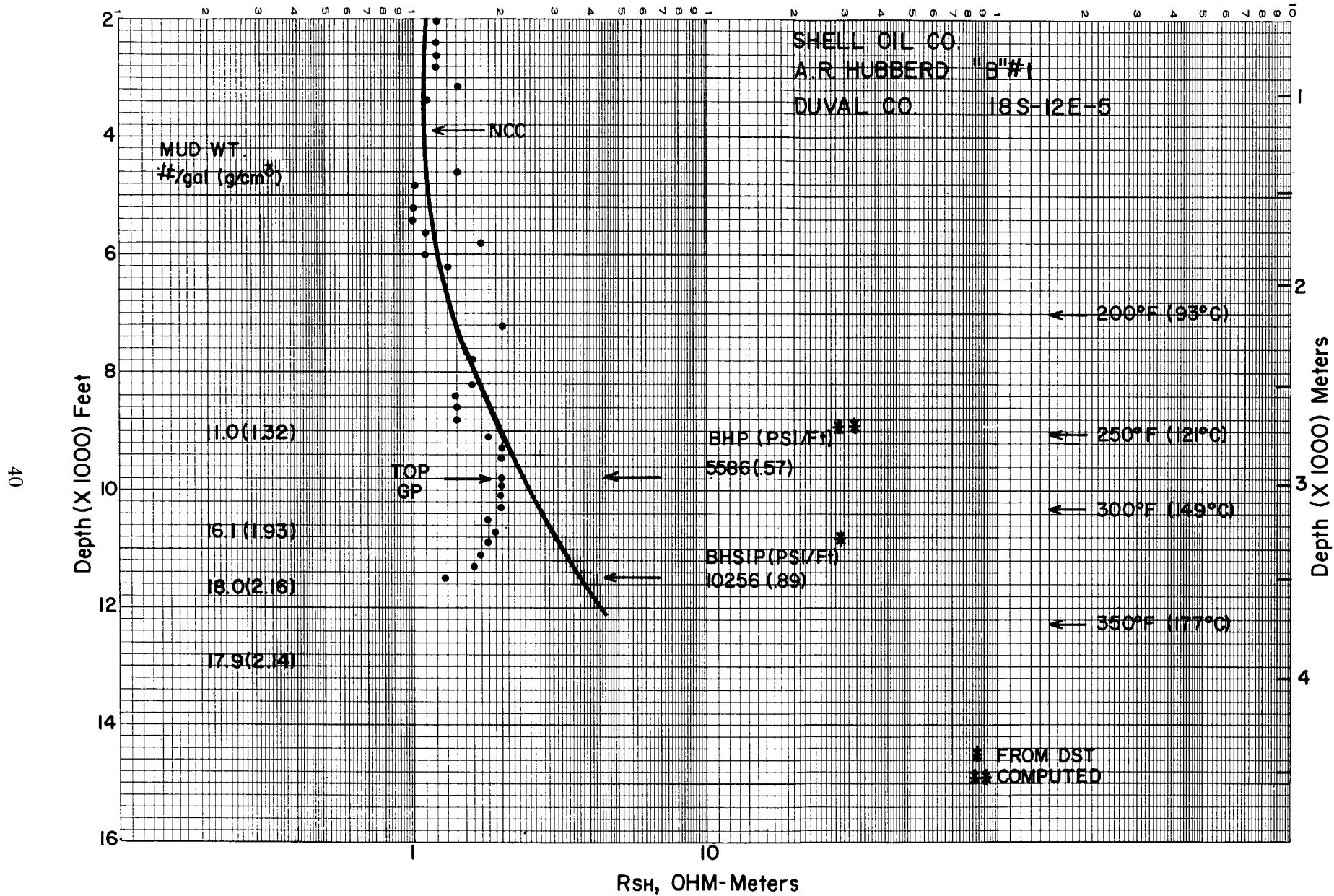


Figure 59. Operational top of geopressure and geopressure gradients from shale resistivity data for a well on section A-A' (fig. 56), Duval County.

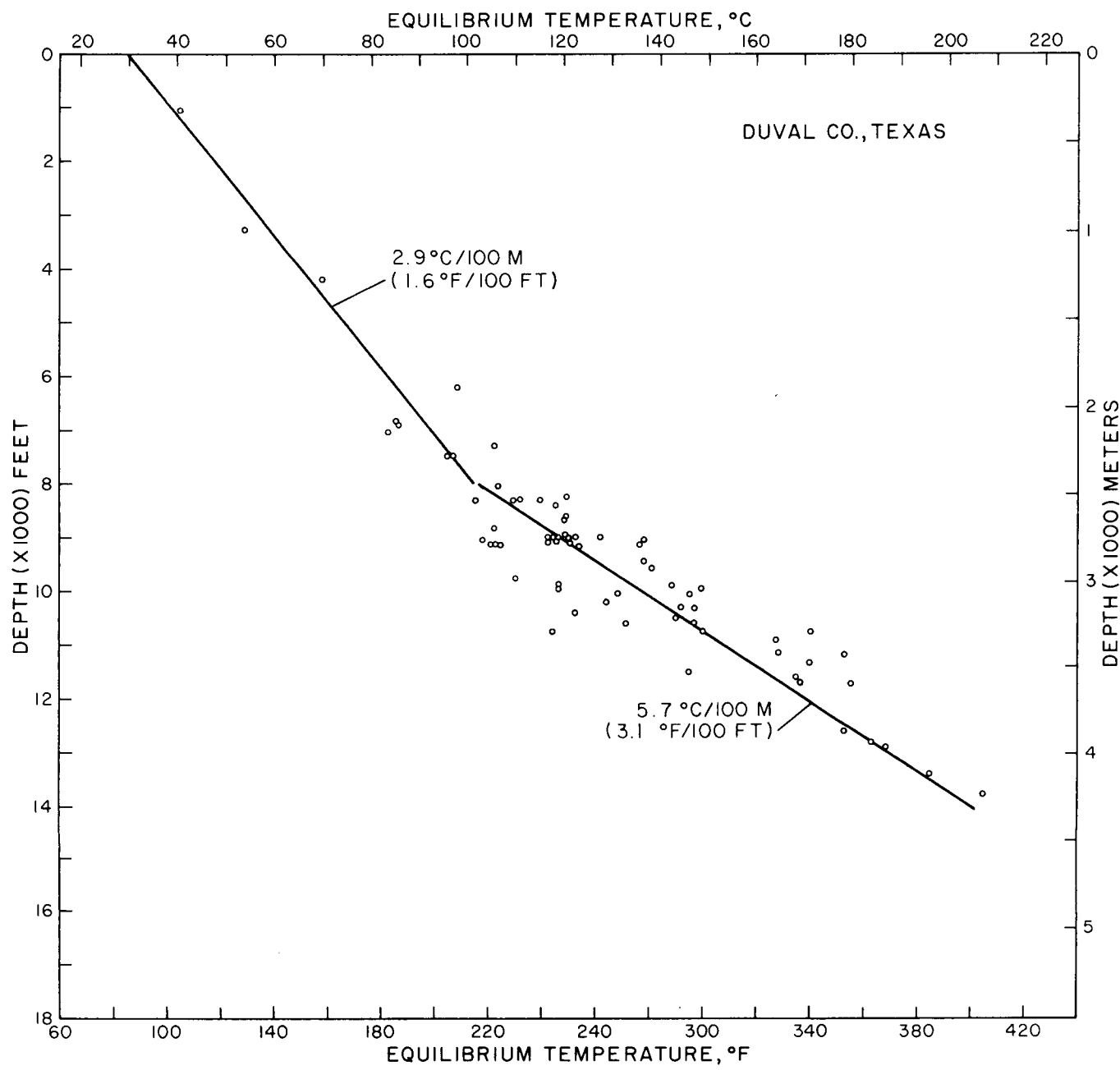


Figure 60. Temperatures and geothermal gradients for Duval County.

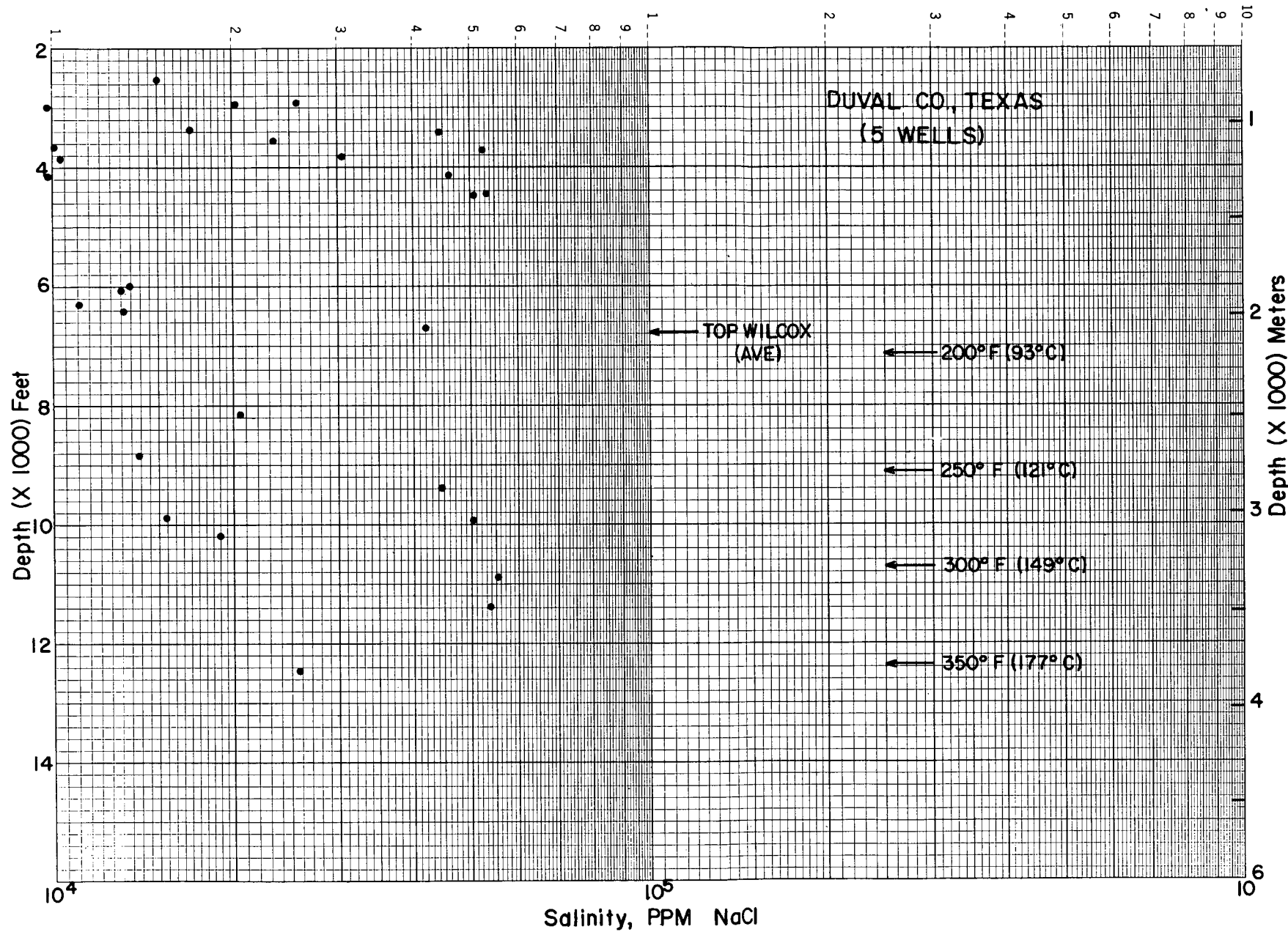


Figure 61. Salinity versus depth calculated from electric logs of five wells in Duval County.

## LIVE OAK FAIRWAY

The Live Oak Fairway is entirely within Live Oak County (figs. 62 and 63) and is approximately 13 mi long and 6 mi wide. The total area is approximately 70 mi<sup>2</sup>. This fairway was delineated in earlier studies (Bebout and others, 1978a) on the basis of thick, laterally extensive, geopressured sandstones having fluid temperatures greater than 300°F.

Prospective sandstones in the fairway occur in the upper Wilcox. Updip toward the northwest, the upper Wilcox is about 1,300 ft thick; downdip, where only the uppermost part of the upper Wilcox has been penetrated, it is at least 3,000 ft thick (figs. 64 through 66). Major fields producing hydrocarbons from the upper Wilcox in this area include the Tom Lyne Field updip and the Katz-Slick Field downdip.

In the Live Oak Fairway, four markers were used to subdivide the upper Wilcox; two of the markers (L1 and L2) are near the top of the Wilcox and were correlated throughout the fairway, and two lower markers (L3 and L4) were identified only in updip wells. Additional markers are the top of the Wilcox and base of the upper Wilcox regional markers. Equivalent markers in the Zapata and Duval Fairways and locally recognized names are shown in table 1.

The prospective reservoirs in the Live Oak Fairway are sandstones between the top of the Wilcox and the L2 marker (figs. 67 through 69). Most of the sandstone units exhibit complex upward-coarsening sequences. These sandstones become increasingly shaly in downdip areas (figs. 67 through 69; Edwards, 1980b). The L2 sandstone is 300 ft thick in the northwest and has not been penetrated in downdip areas. Beneath marker L4 is another section of thick, upward-coarsening sandstone and shale sequences.

In the downdip parts of the Live Oak Fairway, the prospective sandstone-bearing interval begins at the top of the Wilcox at approximately 9,200 to 10,600 ft, and extends downward at least 4,000 ft and possibly as much as 8,000 ft. However, only the upper part of this interval, which contains 600 ft of net sandstone, has been penetrated.

Growth faults in the Live Oak Fairway (fig. 62) probably developed at the margin of a rapidly prograding delta (Edwards, 1981). The growth-faulted zone has a total known width of about 16 mi, but faulting in downdip areas is not well understood, although the largest faults occur in the central and downdip areas. Approximately

nine faults are present across the growth-fault zone in this fairway. From northwest to southeast across the growth-fault zone, the upper part of the Wilcox (the "Slick" sands) increases in thickness from 140 to 1,400 ft, indicating an unusually large growth factor of 10 (figs. 67 through 69).

The top of geopressure occurs from 7,000 to 8,000 ft, on the basis of bottom-hole shut-in pressures from drill-stem tests for 26 wells in Live Oak County (fig. 70). A gradient of 0.7 psi per foot occurs at an average depth of 9,950 ft. The maximum pressure gradient observed was 0.78 psi per foot at 10,450 ft.

Shale resistivity plots demonstrate that updip wells on cross section A-A' were not geopressured (fig. 71). Tops of isopiestic gradient surfaces along cross section A-A' show that only the two wells farthest downdip penetrate highly geopressured zones; the detailed shale resistivity plot (fig. 72) shows that the top of geopressure occurs at a depth of 9,000 ft in the well farthest downdip.

The geothermal gradient shallower than 8,990 ft in the Live Oak Fairway (fig. 73) is 1.9°F per 100 ft. At greater depths, in the geopressured zone, the gradient increases to 3.2°F per 100 ft, higher than the average gradient of 2.7°F per 100 ft for the larger fairway area including parts of Live Oak, McMullen, Duval, Webb, and Zapata Counties (fig. 74). Temperature versus depth plots and isothermal surfaces of 200°F, 250°F, and 300°F are shown for control wells in cross section A-A' (fig. 71).

Salinities of formation waters in the six wells on cross section A-A' increase to a maximum value of about 150,000 ppm NaCl (figs. 71 and 75) at depths of 4,400 and 9,400 ft. Limited data showing low salinities between depths of 4,400 and 7,800 ft are of doubtful quality. Below 7,800 ft, salinities decrease to an average value of about 38,000 ppm NaCl at a depth of 11,000 ft.

Porosities computed from formation resistivity factors for six wells on cross section A-A' (figs. 71 and 76) decrease from about 35 percent at 3,000 ft to about 10 percent at 11,000 ft. Limited diamond-core data from two wells in Live Oak County show an average porosity of 21 percent and permeability of 20 md in the sandstone interval from 7,982 to 8,000 ft. From 10,470 to 10,480 ft, the porosity and permeability average 16 percent and 8 md, respectively. Sidewall cores from depths of 10,000 to 12,000 ft indicate porosity ranging from 17 to 24 percent and permeability ranging from 5 to 40 md. These values indicate generally poor reservoir quality relative to other fairways.

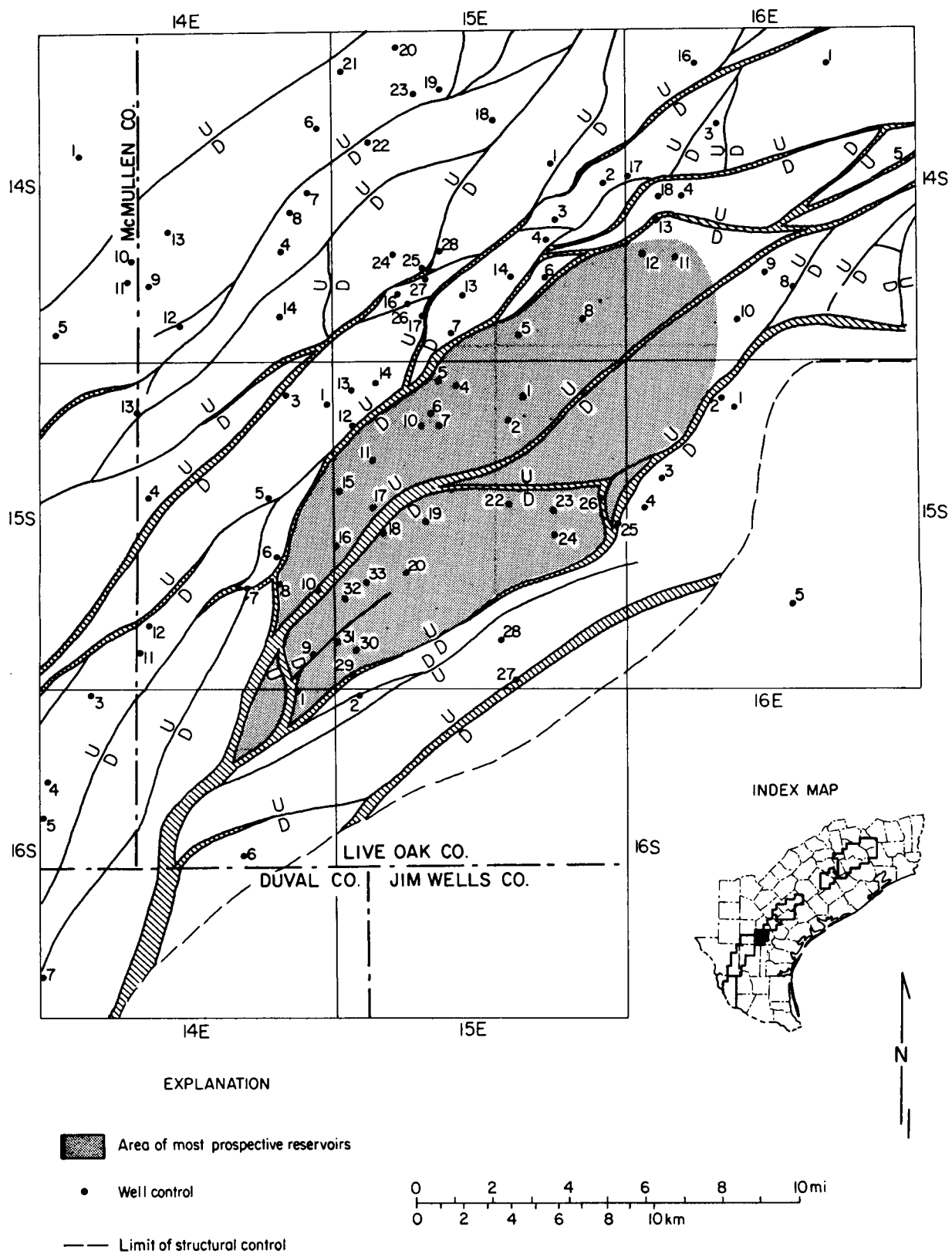


Figure 62. Well control, faults at the top of the Wilcox, and area of prospective sandstones, Live Oak Fairway.

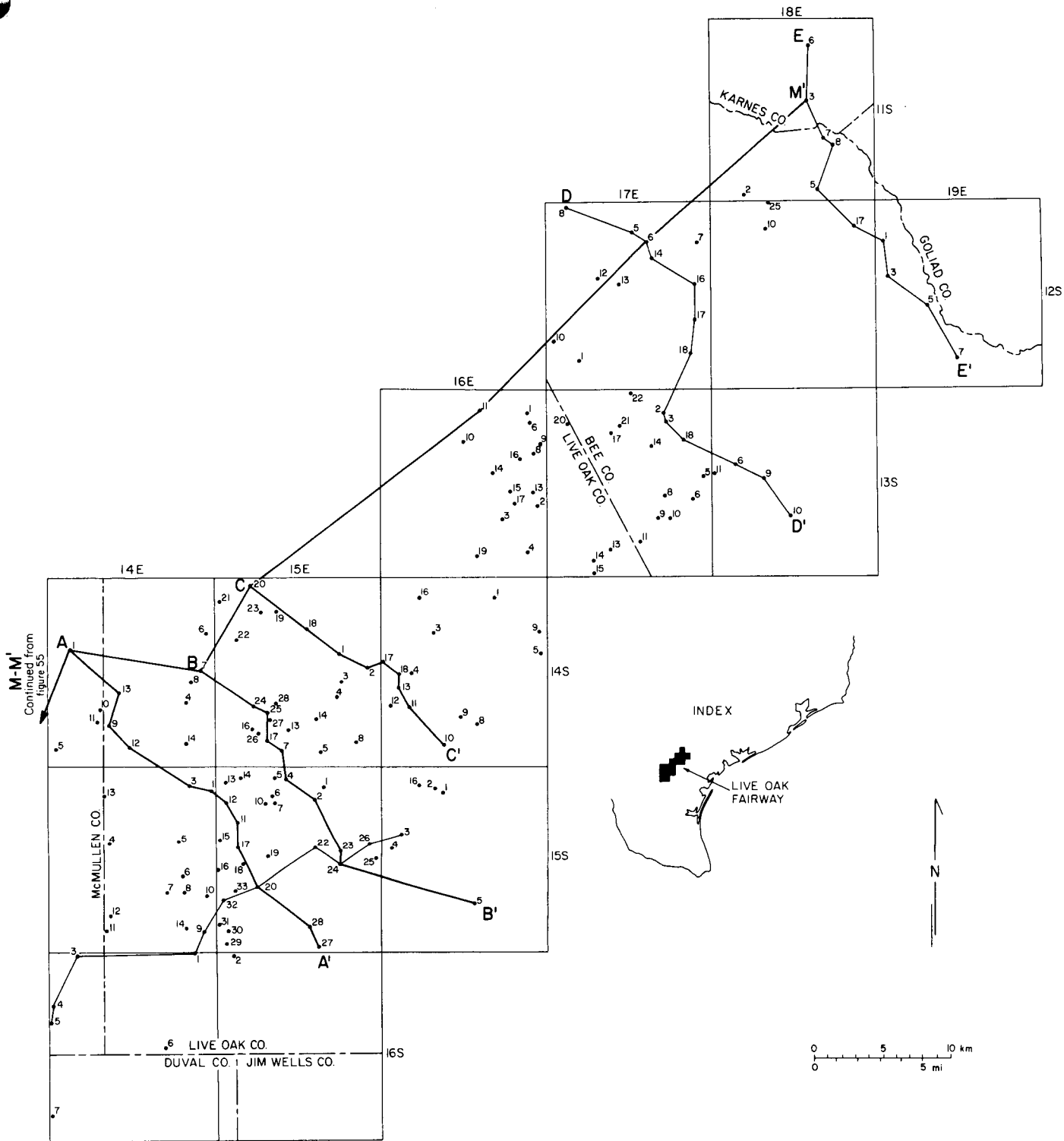


Figure 63. Well control and lines of stratigraphic and structural sections, Live Oak Fairway and area to the northeast. Heavy lines indicate the sections included in this report.

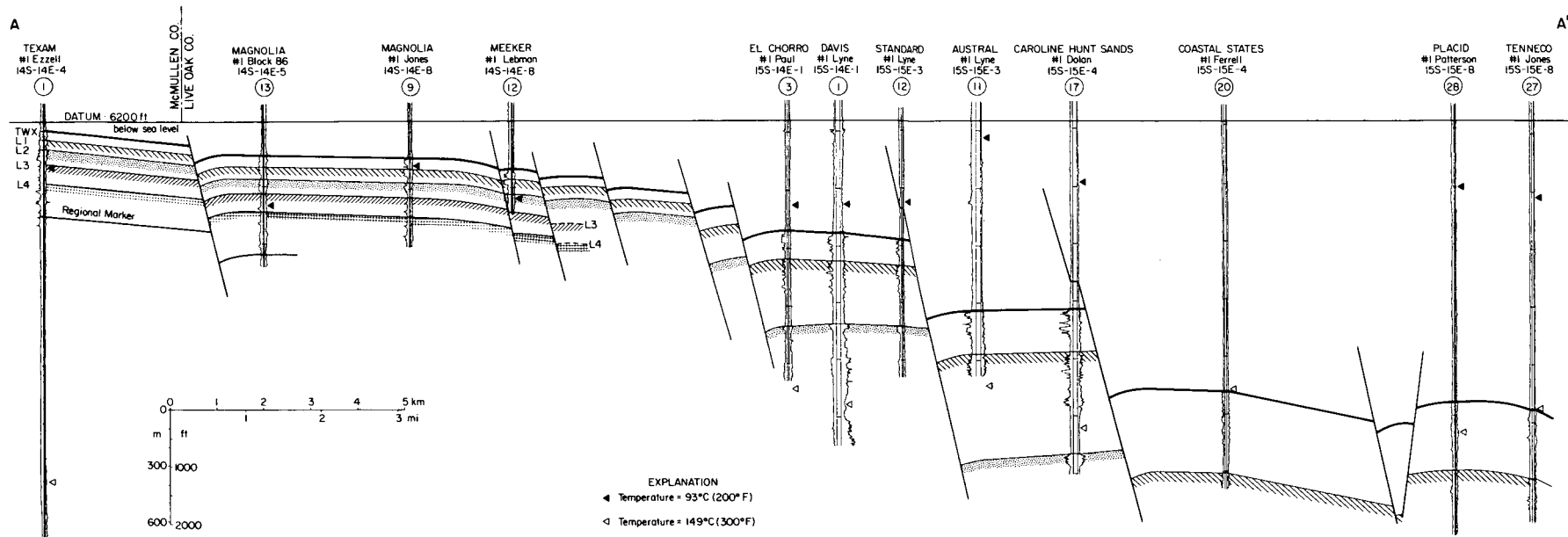


Figure 64. Structural dip section A-A', southern part of the Live Oak Fairway.

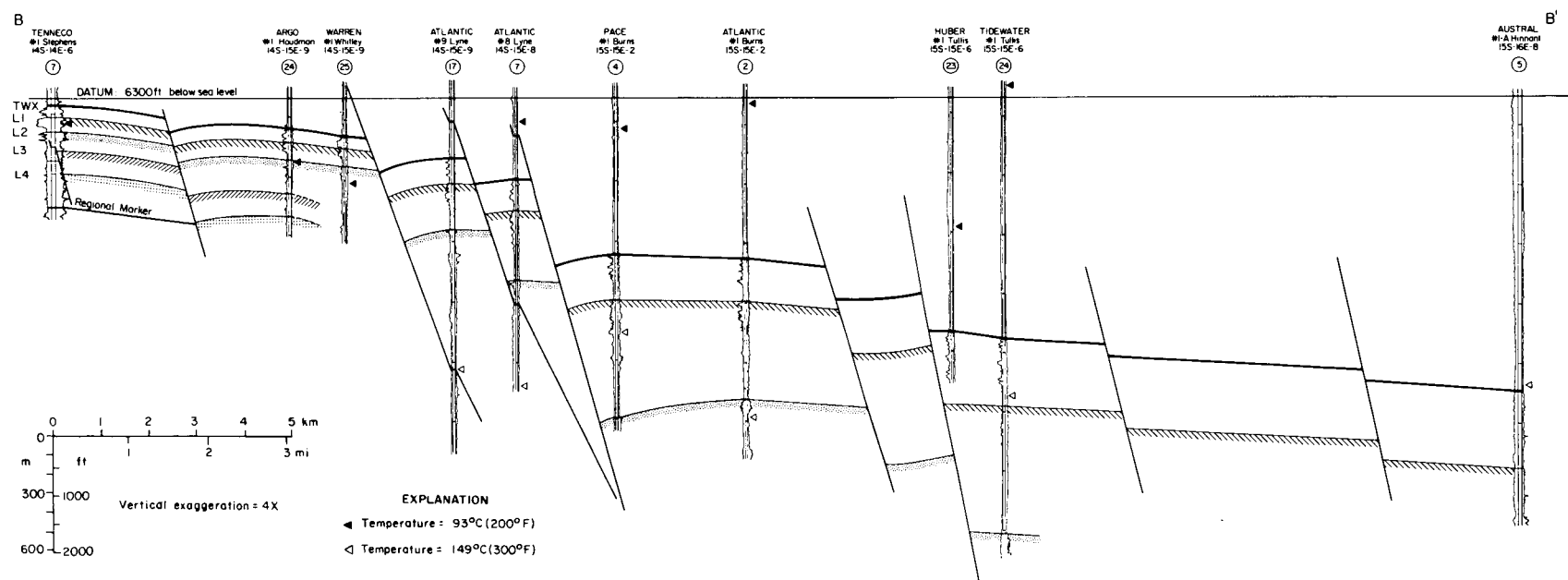


Figure 65. Structural dip section B-B', central part of the Live Oak Fairway.

C

C'

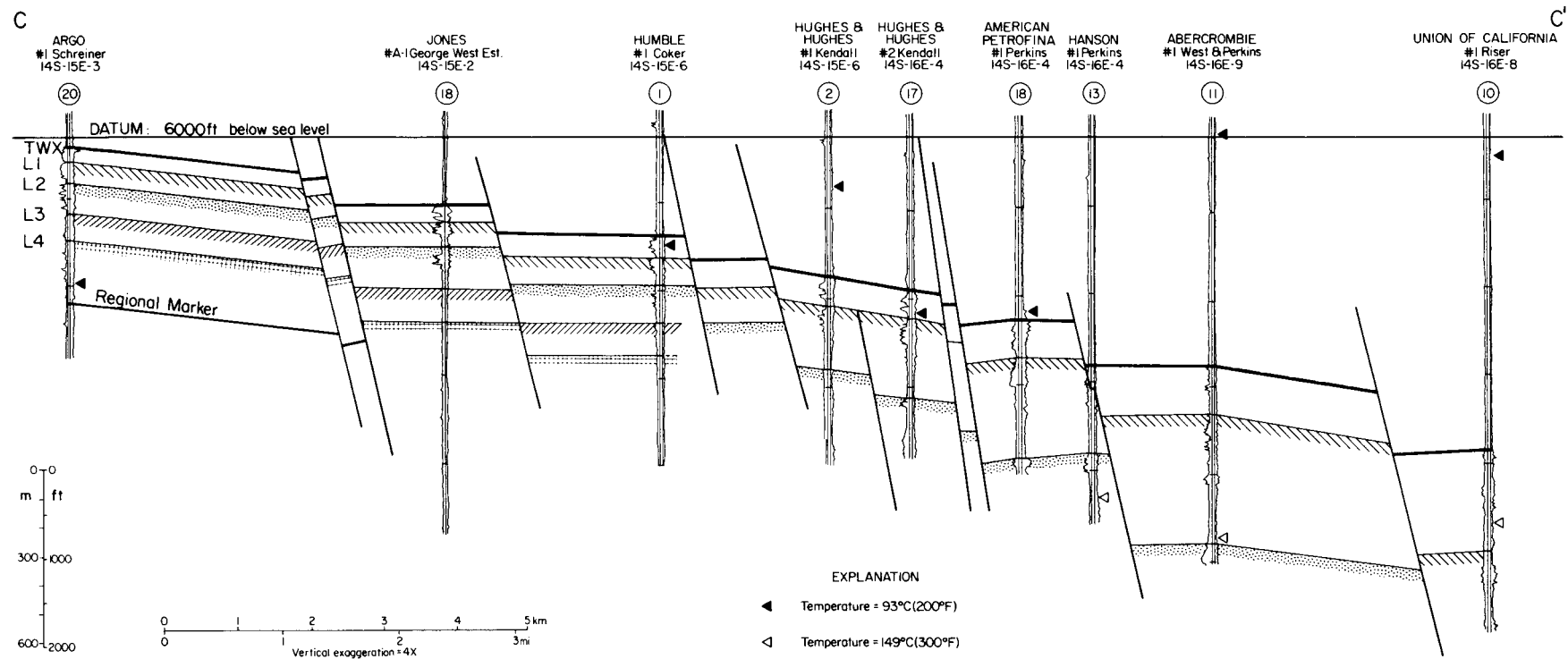


Figure 66. Structural dip section C-C', northern part of the Live Oak Fairway.

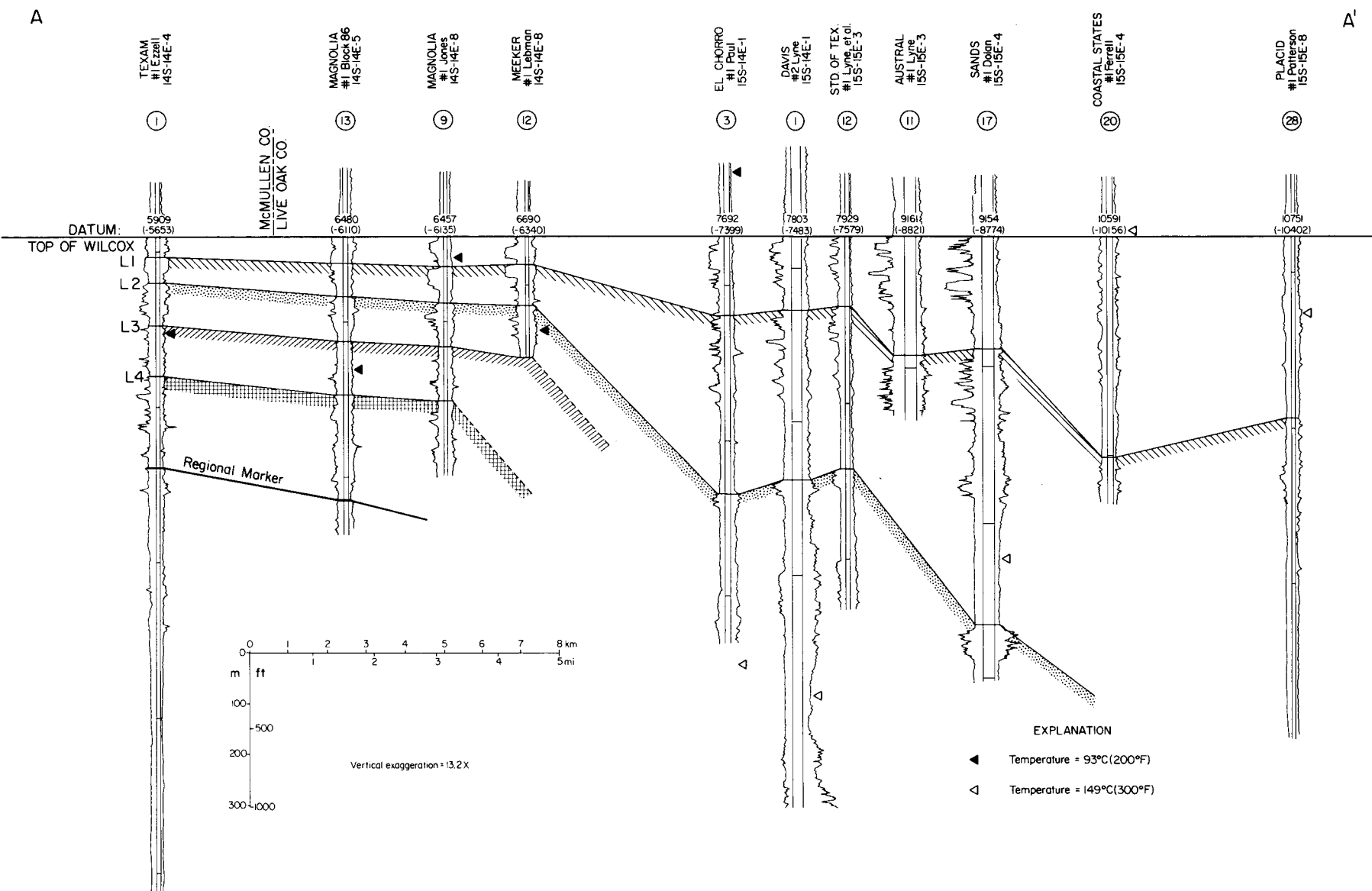


Figure 67. Stratigraphic dip section A-A', southern part of the Live Oak Fairway. Growth faults are eliminated to better show correlation between wells.

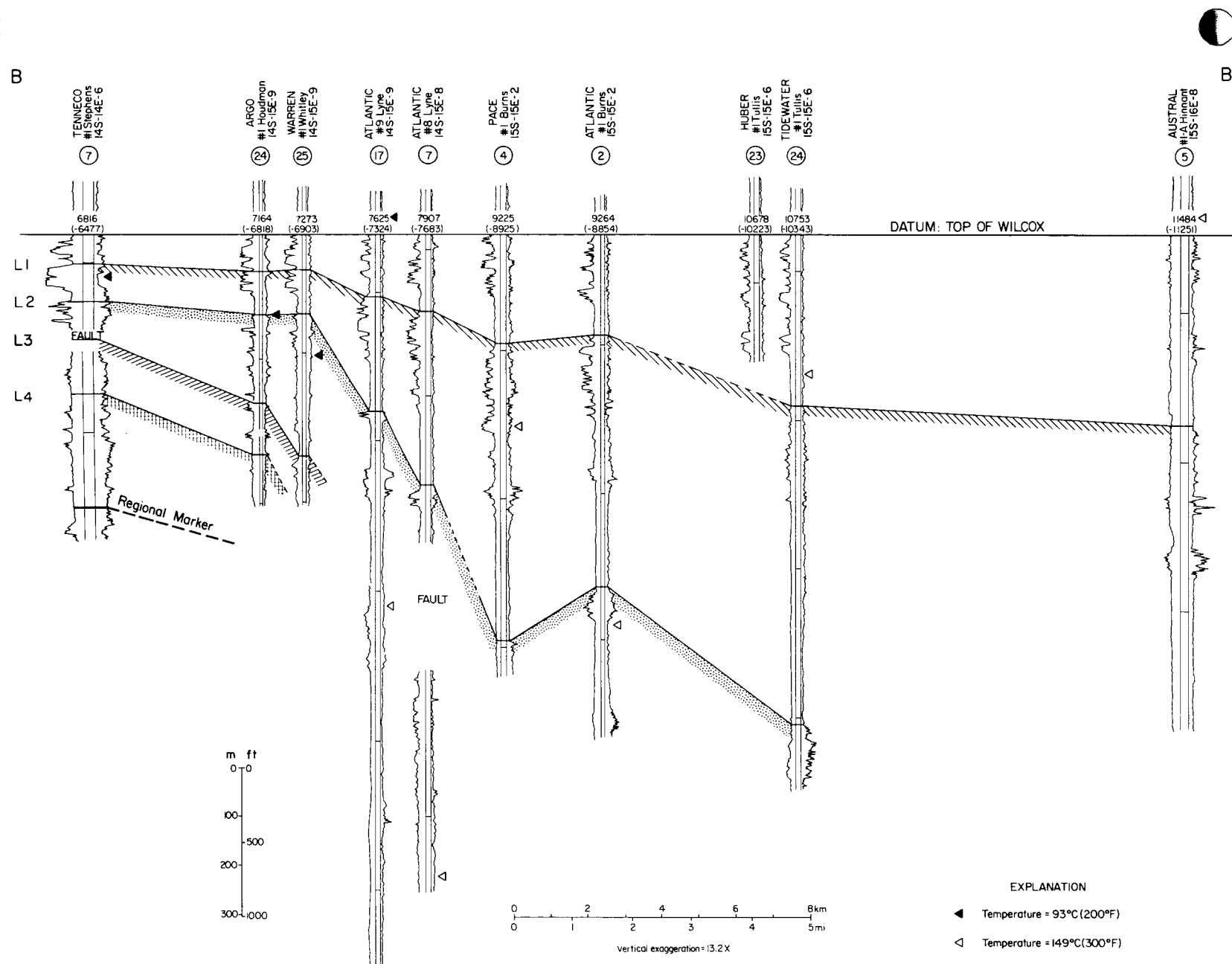


Figure 68. Stratigraphic dip section B-B', central part of the Live Oak Fairway.

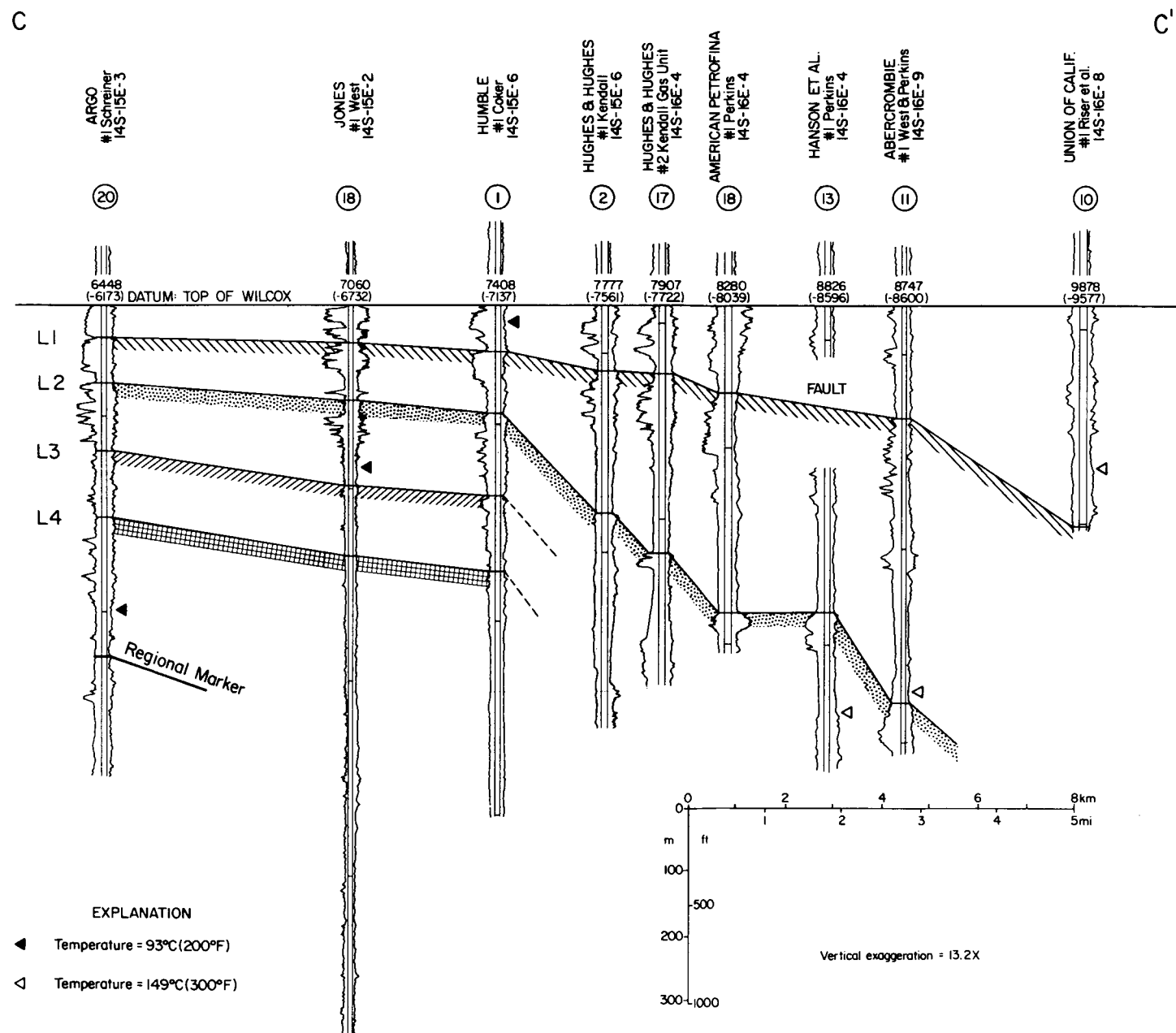


Figure 69. Stratigraphic dip section C-C', northern part of the Live Oak Fairway.

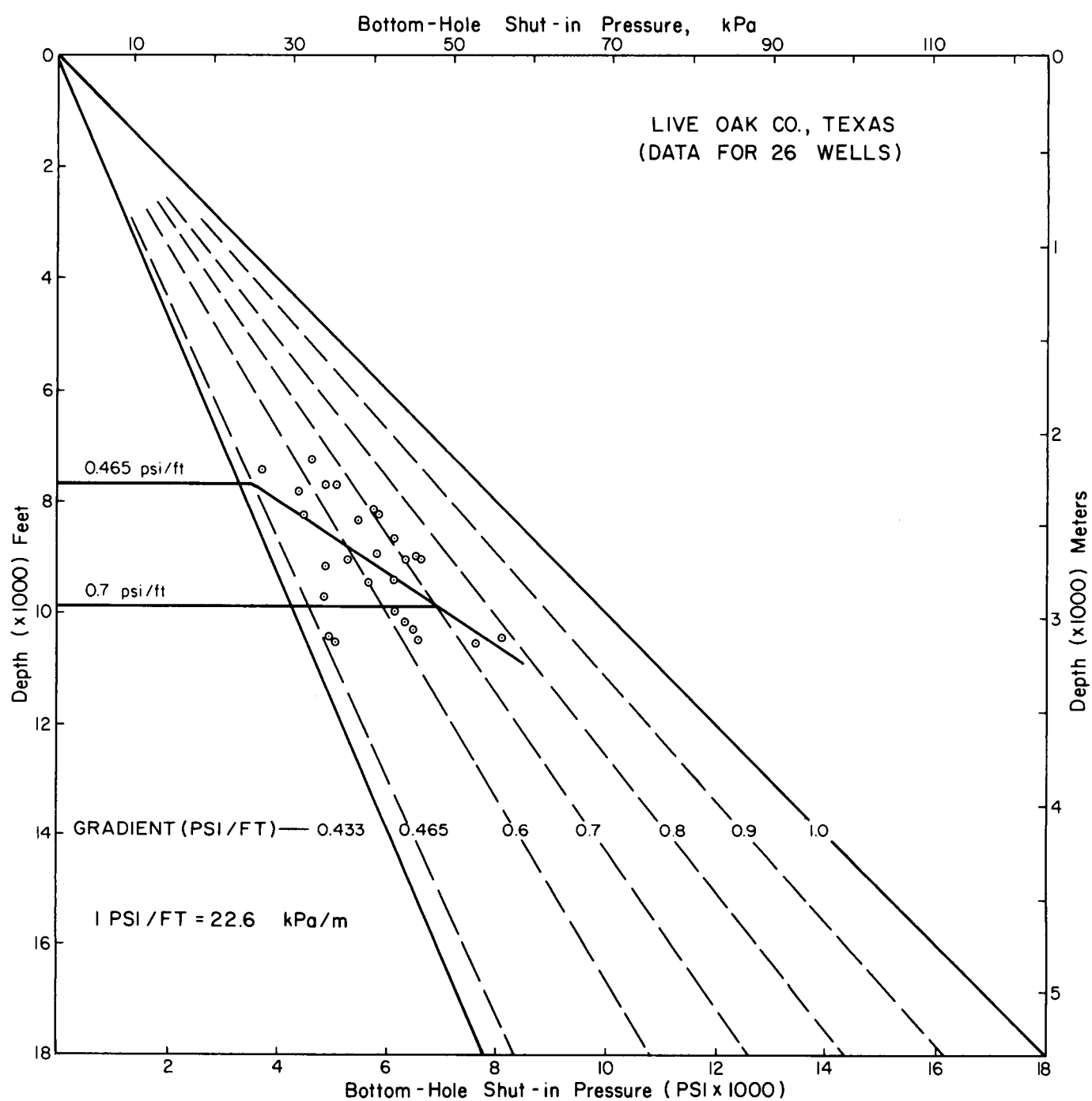


Figure 70. Bottom-hole shut-in pressures plotted as a function of depth for 26 wells in Live Oak County.

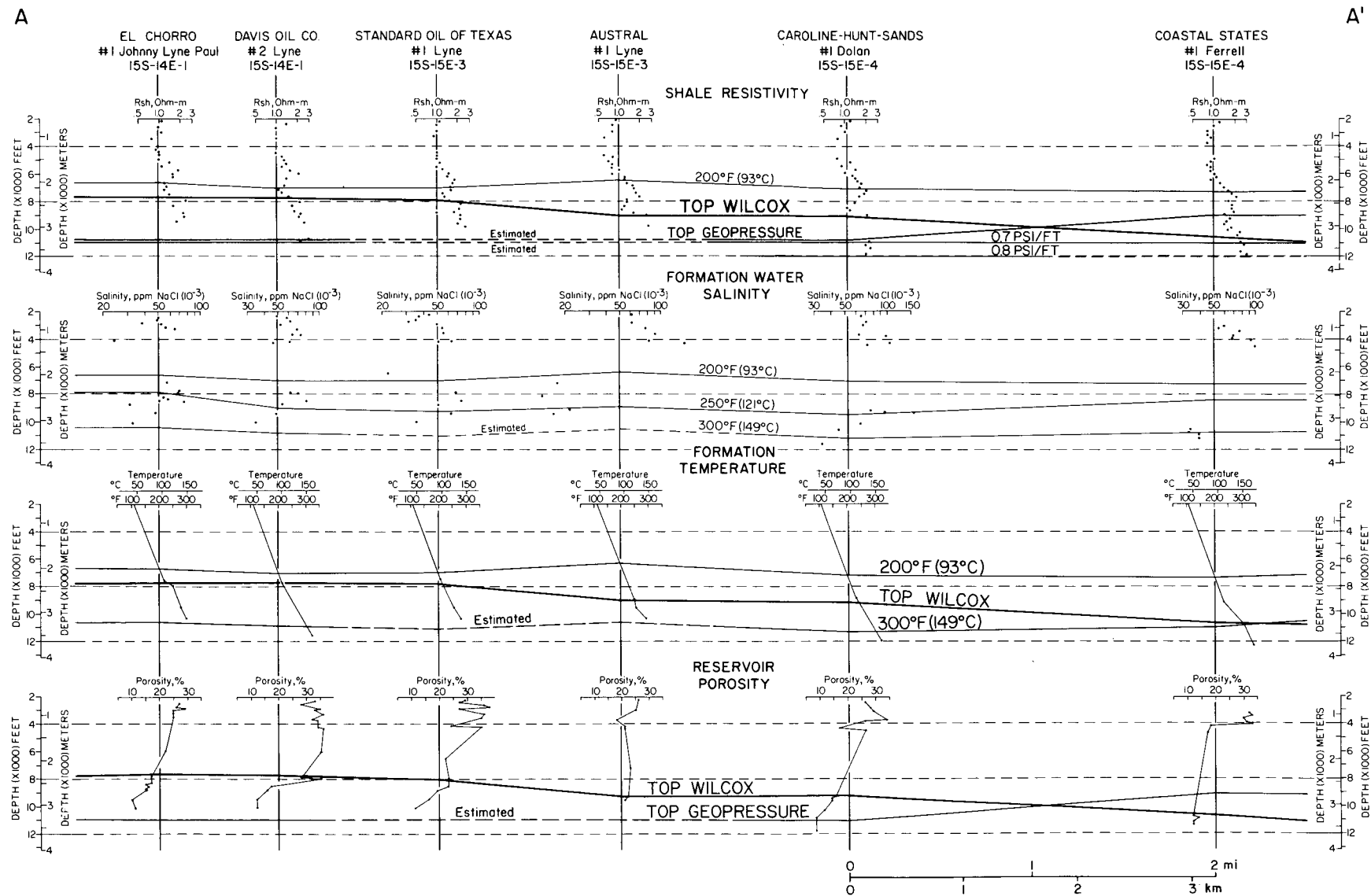


Figure 71. Parameter plots showing variation of formation and fluid properties along section A-A', Live Oak County.

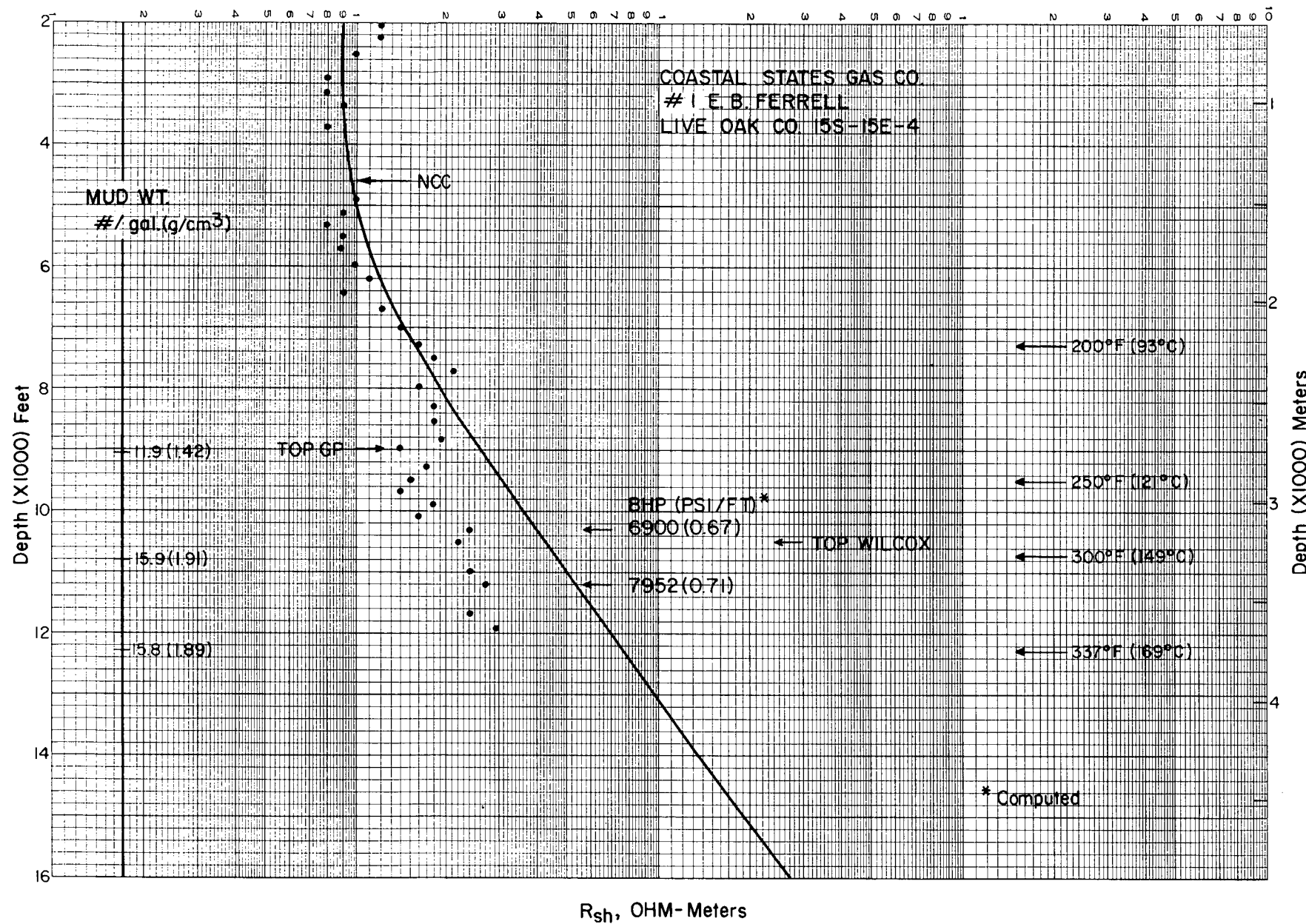


Figure 72. Operational top of geopressure and geopressure gradients from shale resistivity data for a well on section A-A', Live Oak County.

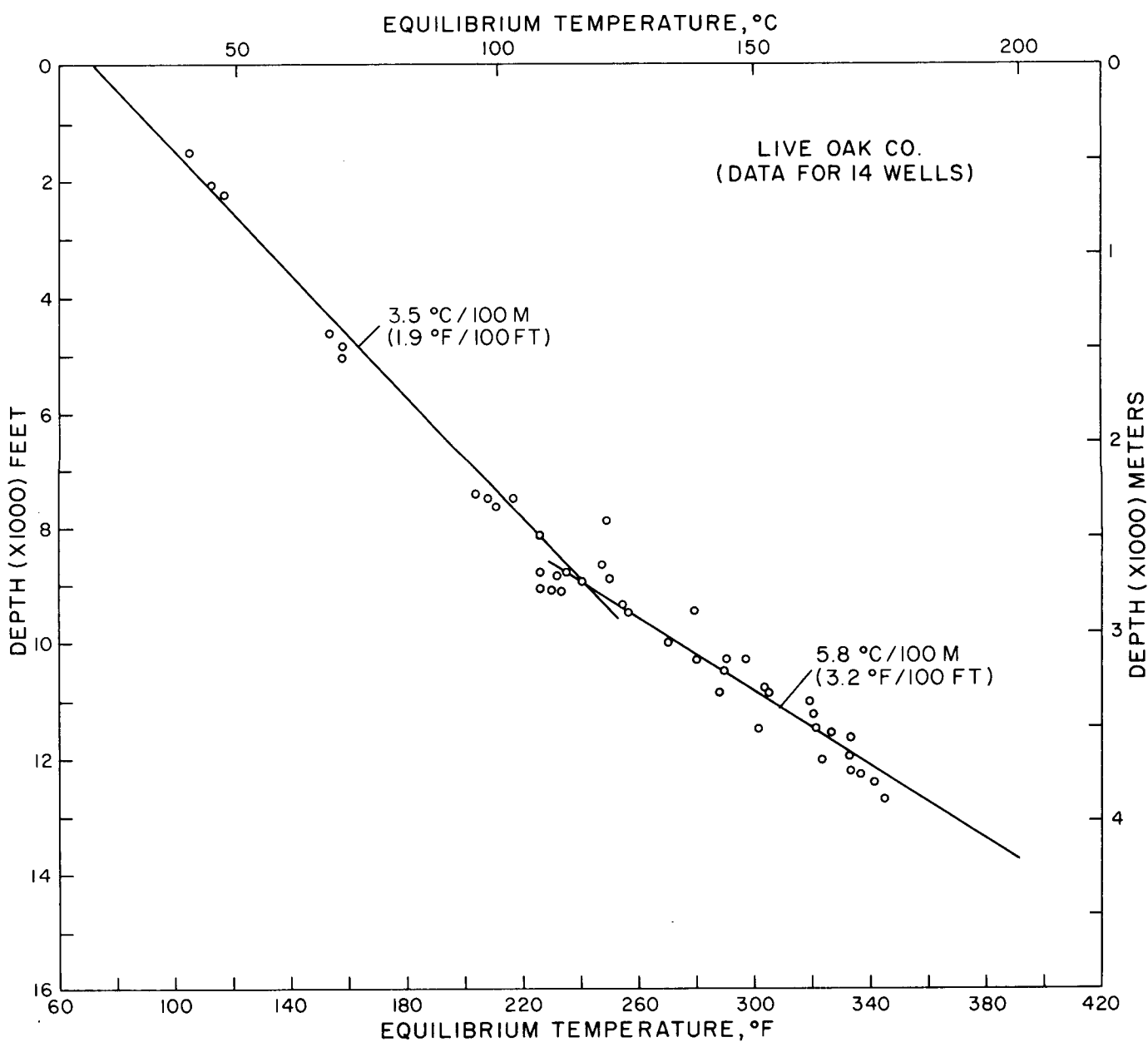


Figure 73. Temperatures and geothermal gradients for Live Oak Fairway.

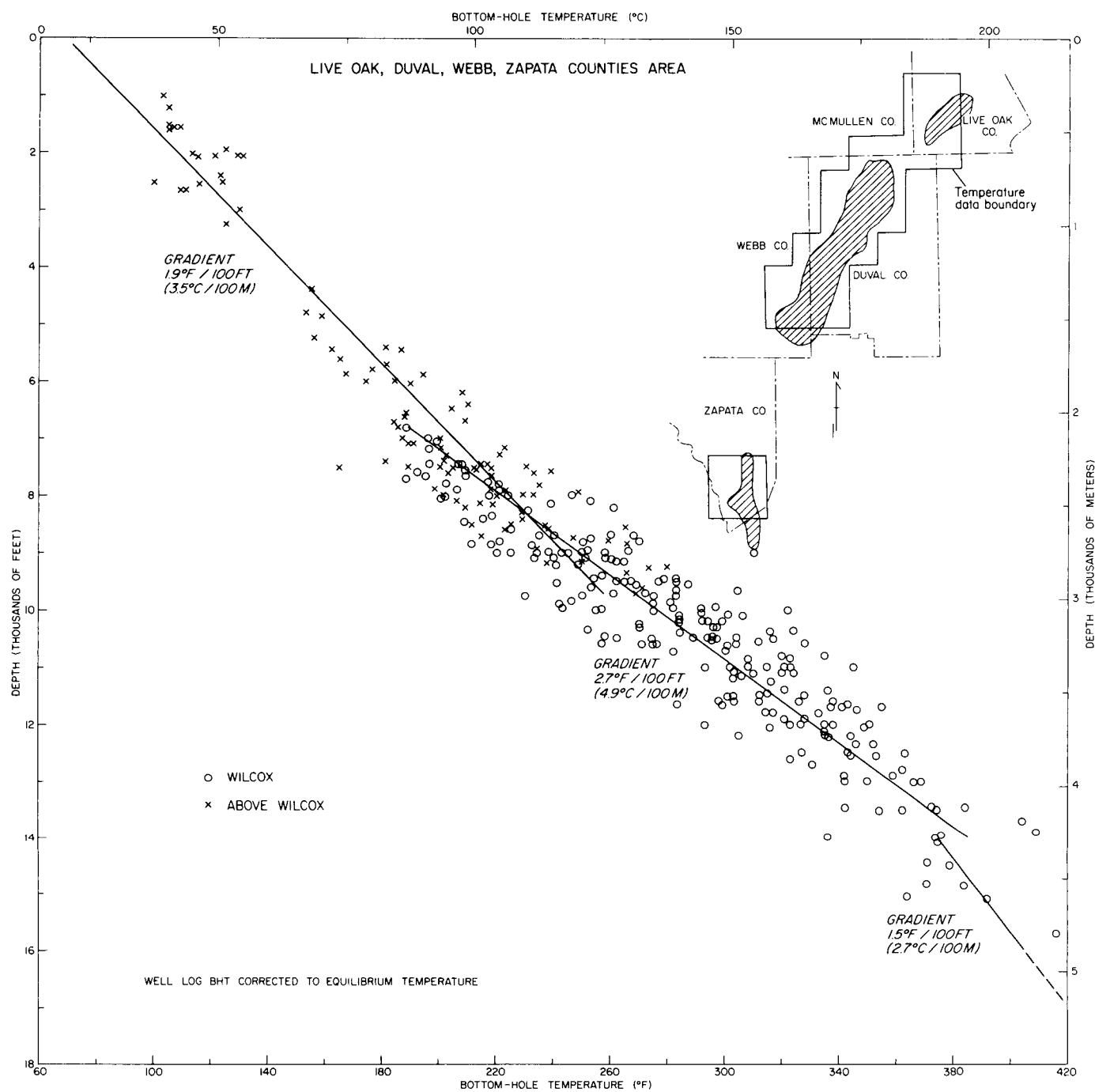


Figure 74. Temperatures and geothermal gradients for fairway areas including parts of Live Oak, McMullen, Duval, Webb, and Zapata Counties.

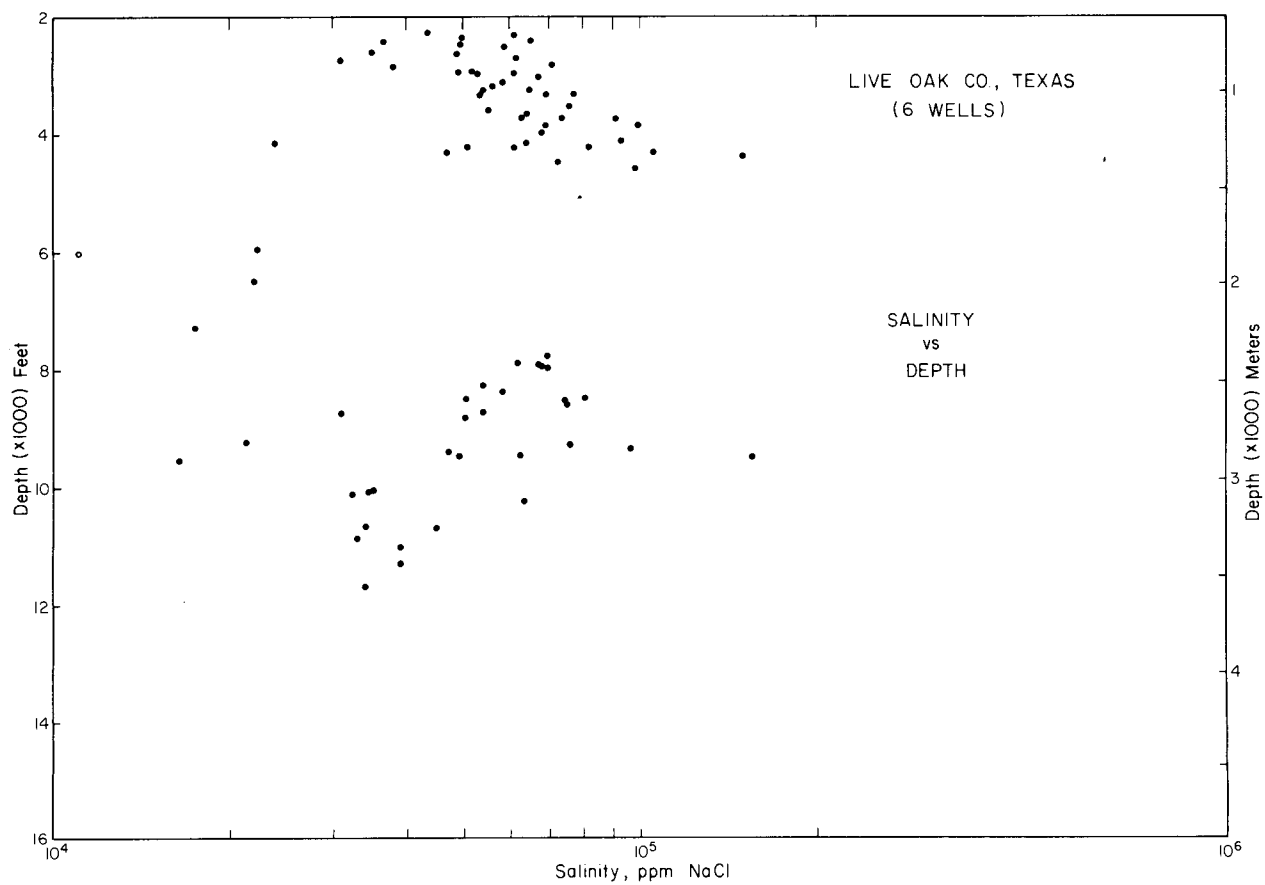


Figure 75. Salinity versus depth calculated from electric logs of six wells in Live Oak County.

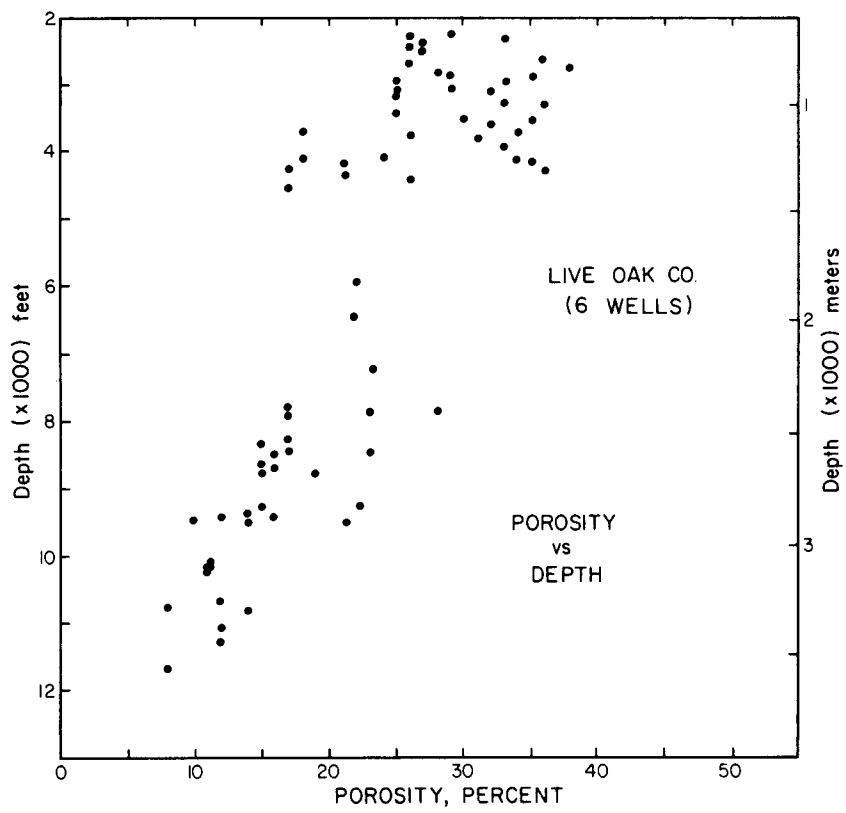


Figure 76. Porosity versus depth for six wells in Live Oak County. Porosities were calculated from well logs.

# DE WITT FAIRWAY

## *Depositional and Structural Style*

The De Witt Fairway, located in southeastern De Witt County (fig. 77), is 40 mi long northeast to southwest and 6 mi wide. It was first recognized with widely spaced well control on the regional cross sections. Detailed study of the De Witt Fairway is based on analysis of all available electric logs from wells that penetrate the lower Wilcox (fig. 77). Five stratigraphic dip sections and one stratigraphic strike section established the correlation grid into which all well logs were correlated; only stratigraphic section D-D' is included in this report (fig. 78). Closely spaced wells in the fairway can be correlated confidently with electric logs, primarily by means of resistivity markers within the shale and siltstone sections.

Several of these markers have been extended across the entire fairway and are the basis for subdividing the formation into five units in the De Witt Fairway. Two of these markers (D1 and D2) are regional markers used to informally subdivide the Wilcox into lower, middle, and upper. These markers have been extended throughout the Wilcox trend in Texas, as indicated on the regional cross sections (figs. 11 through 33, in pocket). The other markers pertain only to the De Witt Fairway and do not correspond to those used in the other fairways described in this report. These markers do, however, provide a basis for subdividing the formation into thinner map units, which are more useful in delineating sandstone and shale trends and interpreting general depositional environments. Potential geopressured geothermal sandstone reservoirs occur beneath the D4 marker.

The Wilcox Group in the De Witt Fairway can be divided vertically into three main parts (fig. 78).

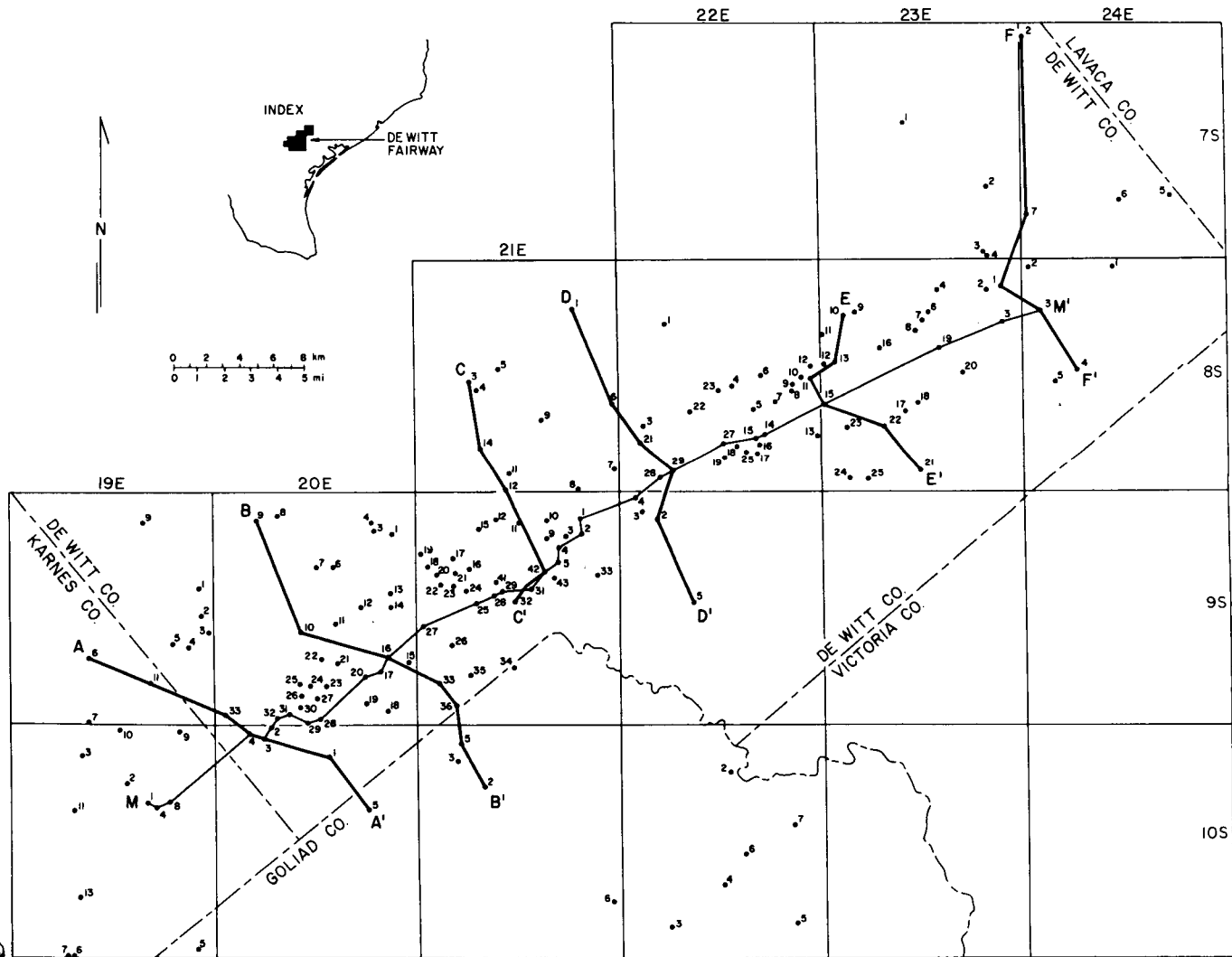


Figure 77. Location of wells and lines of section, De Witt Fairway.

The lower part, beneath the D2 marker, is characterized by high sandstone content that is highly variable laterally as a result of rapid facies changes. The middle part, between the D2 and D1 markers, consists predominantly of shale and thin sandstone units that are generally strike aligned, are persistent over a large area, and provide excellent correlation markers. The upper part, above the D1 marker, is mainly massive sandstone, which, when mapped, shows that sandstone trends are dip oriented (fig. 79); detailed correlations are possible only in the thin sandstones and shale of the lower part.

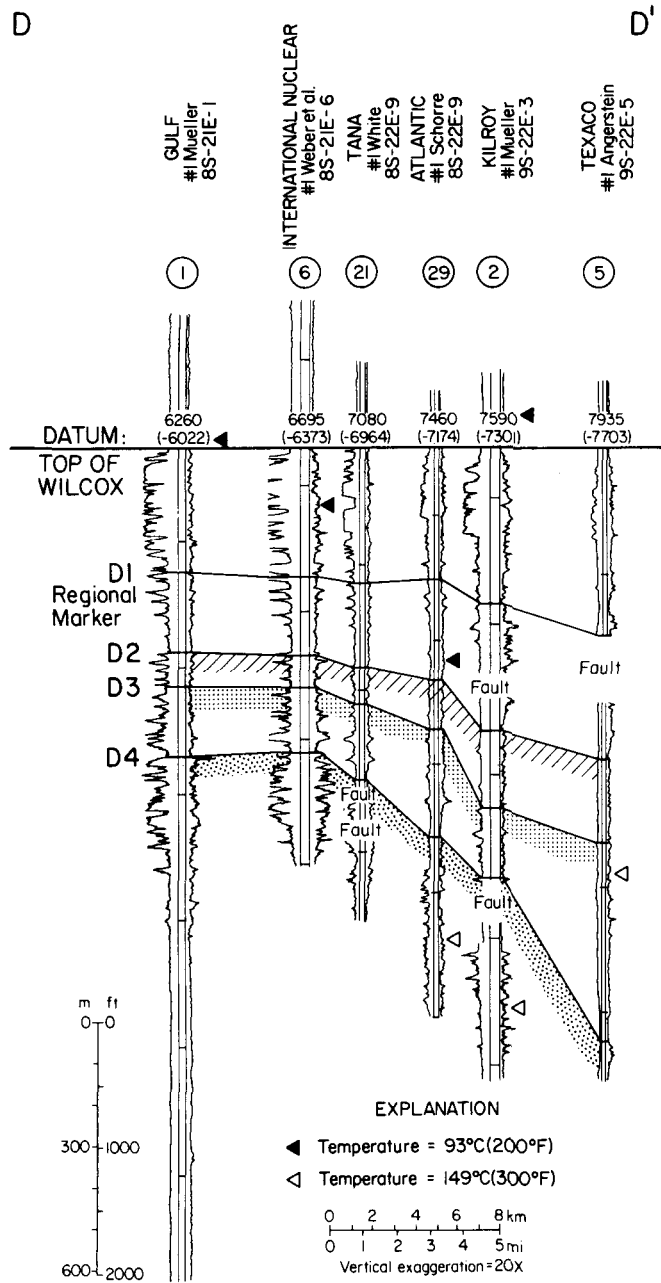


Figure 78. Stratigraphic dip section D-D', De Witt Fairway.

The depositional/structural style of the Gulf Coast Basin is controlled by growth faults that formed contemporaneously with deposition. The De Witt Fairway is located in the complexly growth-faulted part of the Wilcox trend (figs. 7, 80a and b) just downdip of the Lower Cretaceous Stuart City carbonate shelf edge. The faults trend northwest parallel to the carbonate shelf edge and to the strike of the Wilcox. Displacement across the faults ranges from tens of feet to several hundred feet (figs. 81 through 87), but, in general, fault displacement and section thickening is greatest in the lower part of the Wilcox beneath the D3 marker.

Local thickening of the sandstone and shale section updip into the bounding growth fault, although characteristic of growth faults, is not commonly documented because of a lack of well control close to the faults. In the De Witt Fairway, thickening is particularly well documented on line E-E' (fig. 85) where the section thickens between markers D1 and D3 updip from well 15 to well 11. Regional thickening of the sections on the downdip side of growth faults is common and is illustrated on all of the dip cross sections (figs. 81 through 86).

#### Formation Pressures and Temperatures

Below a depth of 10,000 ft, most of the gas- and oil-producing reservoirs in the Wilcox are geopressedured, and the pressure gradient increases with depth. Bottom-hole shut-in pressures from drill-stem tests in the De Witt County area (fig. 88) clearly show that most geopressedured formations first occur between depths of 9,000 and 10,000 ft; generally, pressure gradients increase with depth to a maximum of about 0.85 psi per foot. Top of geopressure determined from shale resistivity data occurs from 9,550 to 10,500 ft along structural cross section D-D' (fig. 89). Depth to the isopiestic gradient of 0.8 psi per foot decreases sharply from 12,000 ft in the updip wells (fig. 90) to 10,850 ft in the Kilroy No. 1 Mueller (fig. 91) and 11,750 ft in the Texaco No. 1 Angerstein (fig. 92).

The geothermal gradient in the upper Wilcox at depths of 7,400 to 14,000 ft is about 2.6°F per 100 ft; a gradient of 1.2°F per 100 ft occurs in the lower Wilcox at depths of 14,000 to 19,000 ft. Shallow formations above the Wilcox at depths of 0 to 8,500 ft have a geothermal gradient of about 1.5°F per 100 ft. A temperature of 300°F is attained at a depth of 11,700 ft (fig. 93); updip of the fairway, this temperature occurs at greater depth (13,000 ft) and downdip, at shallower depth (approximately 11,000 ft).

Geothermal gradients in the control wells in the De Witt Fairway sections show only slight variations (fig. 94). For wells in sections B-B', C-C', D-D', and E-E', the average gradient is 1.7°F per 100 ft in the Wilcox at depths of 0 to 11,000 ft and is 2.4°F per 100 ft at depths of 11,000 to 14,100 ft. Temperature profiles (fig. 89) correspond to data points for section D-D' (fig. 94).

### *Porosity and Permeability*

Diamond-core data for three wells in the Wilcox geopressured sandstones in the De Witt Fairway area (figs. 95 through 97) show that porosities range from 5 to 23 percent and permeabilities range from less than 2.1 to more than 100 md. Most of the core data are for the depth interval of 10,680 to 12,080 ft. Permeabilities for the Atlantic No. 1 Schorre well (fig. 98) range from less than 0.1 to more than 200 md in the depth interval of 10,800 to 11,800 ft. There is an approximate linear decrease in porosity as depth increases for the six control wells in section D-D' (figs. 89 and 99). The anomalous increase in porosity at a depth of about 11,000 ft coincides with the top of the lower Wilcox Group. This porosity increase occurs in the

prospective reservoir section containing proximal deltaic facies (distributary-mouth bar and distributary channel).

### *Formation Water Salinity*

Salinity of formation waters was derived from formation water resistivity ( $R_w$ ) obtained from the spontaneous potential (SP) log, following the algorithm developed by Bateman and Konen (1977). Estimation of the equivalent sodium chloride concentration (salinity) from  $R_w$  at any formation temperature ( $T_f$ ) is made from the relation

$$\text{ppm (NaCl)} = y^{1.05} \quad (4)$$

where  $y = 3 \times 10^5 / [R_w(T_f + 7) - 1]$ .

Salinity as a function of depth in the De Witt Fairway area can be divided into four generalized trends (figs. 100 and 101): (1) salinity increases at

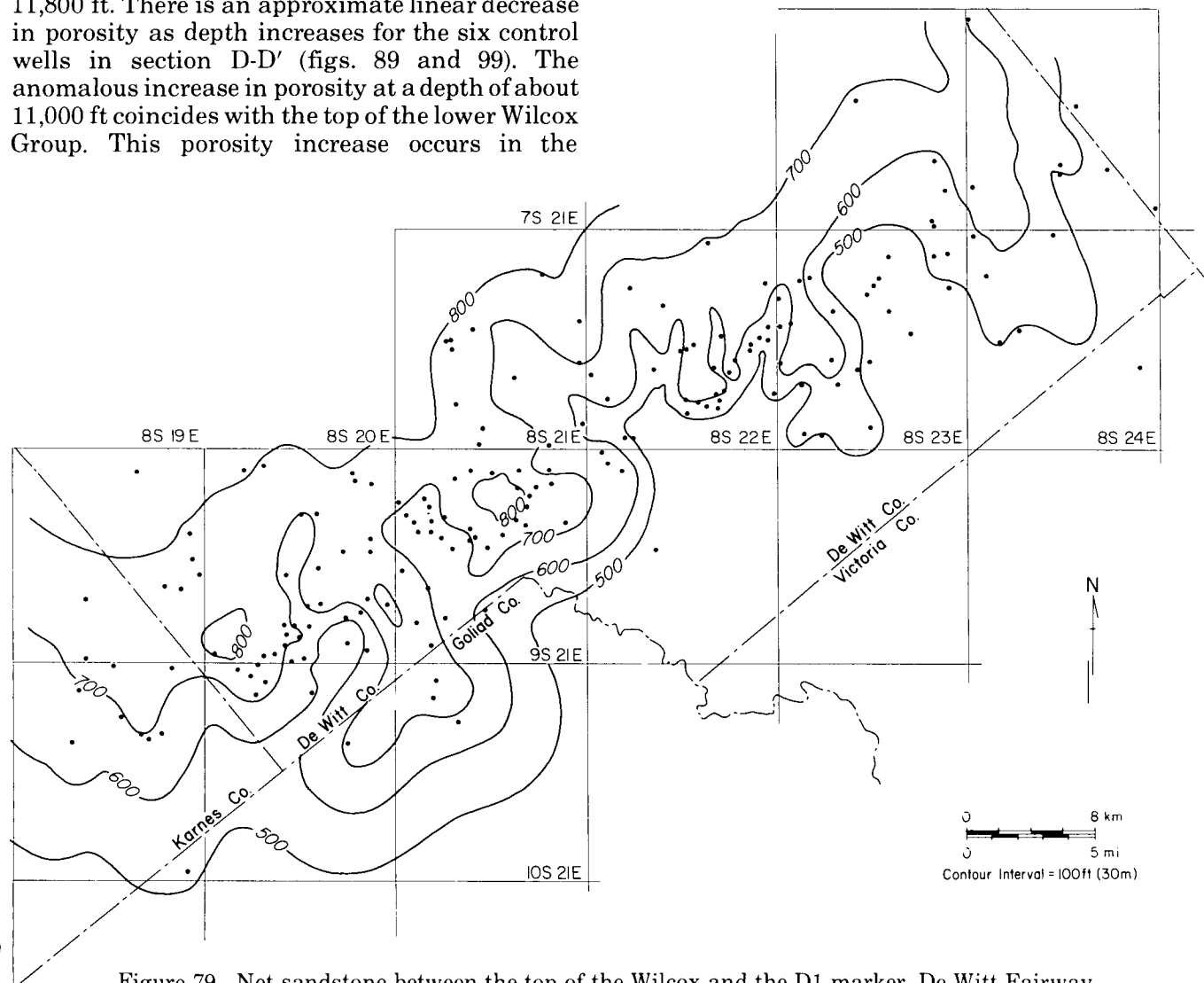


Figure 79. Net sandstone between the top of the Wilcox and the D1 marker, De Witt Fairway.

shallow depths of 2,000 to 6,000 ft; (2) from about 5,900 to 8,200 ft, salinities are high, having reasonably constant average values of more than 100,000 ppm NaCl; (3) below 8,200 ft and extending to the operational top of geopressure as determined from shale resistivity data, salinities decrease to about 40,000 ppm; and (4) in the deep geopressured zones, salinity oscillates between higher and lower values for different sandstones. Most of these trends are recognizable in salinity plots for the Atlantic No. 1 Schorre well (fig. 102) and on the D-D' cross section (fig. 89).

No salinities from chemical analyses of water samples were available for use in this report.

### Cuero Fault Block

The Cuero fault block is located in the northeast part of De Witt Fairway (fig. 103). The growth fault

defining the northwest (updip) side of the block is displaced approximately 700 ft at the top of the reservoir section (D4 marker); the fault at the southeast (downdip) side is displaced approximately 400 ft at the same marker. The width of the Cuero fault block between these two faults varies from 1.7 to 2.0 mi. The length of the fault block is approximately 15 mi.

More than 550 ft of sandstone occurs in the lower Wilcox section beneath marker D4 in the Atlantic No. 1 Schorre well located at the southwest end of the Cuero fault block. Individual sandstone beds range in thickness from 5 to 40 ft, but composites of several beds occur near the top of many correlation units (labeled "B" through "H," figs. 104 and 105), grading from shale at the base to sandstone at the top. Each unit is interpreted to represent an upward-coarsening sequence. Sedimentary structures in whole cores from several of the sandstones in the Schorre well (sandstone units B,

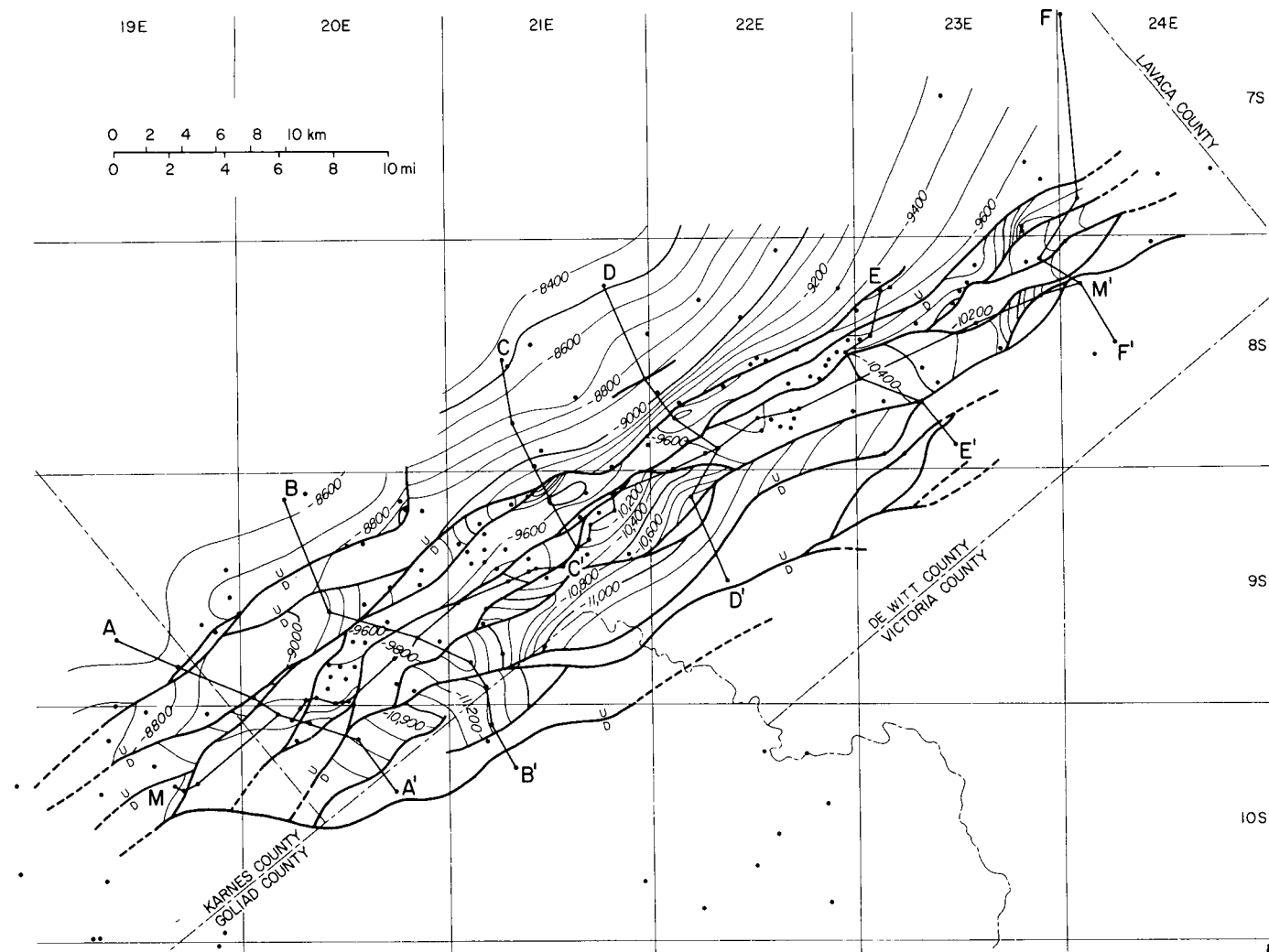


Figure 80a. Structure on top of the D4 marker, De Witt Fairway.

C, and F) indicate that they were deposited in a variety of deltaic environments. Furthermore, the deeper sandstones were deposited on the distal parts of the delta front and on the delta-front slope; the intermediate sandstones were deposited in interdistributary bays and crevasse splays; and the upper sandstones were deposited in interdistributary bays, distributary channels, distributary-mouth bars, and marshes. Thus, more distal deltaic environments are represented in the lower sandstones, and more proximal deltaic environments are indicated in the upper units. The electric log of this section, obtained from the Schorre well, shows thin, high-resistivity sandstones in the lower part and thick, low-resistivity sandstones near the top, also indicating the upward transition from distal to proximal deltaic facies.

Net-sandstone maps (figs. 106 through 111) of correlation units B through G are based on the detailed correlations of wells within the fault block. Because these correlations cannot be

extended beyond the bounding faults, the maps are considerably limited in areal extent in dip direction, and the entire facies tract is not represented. However, these maps show that dip-aligned sandstone patterns, interpreted as representing the distributary-channel facies, shift from the northeast in the lower correlation units to the southwest in the upper units. Thus, the lower Wilcox section in the Atlantic No. 1 Schorre well is represented by more distal delta-front facies lower in the section, and by proximal distributary-channel and marsh facies at the top of the section as a result of the shift of the distributaries to the southwest.

The top of the sandstone-rich lower Wilcox section below marker D4 varies in depth from 10,490 to 10,660 ft below sea level. The operational top of geopressure occurs at approximately 10,000 ft in the Cuero fault block, and subsurface fluid temperatures of 300°F have been measured within the lower Wilcox section below the D4 marker.

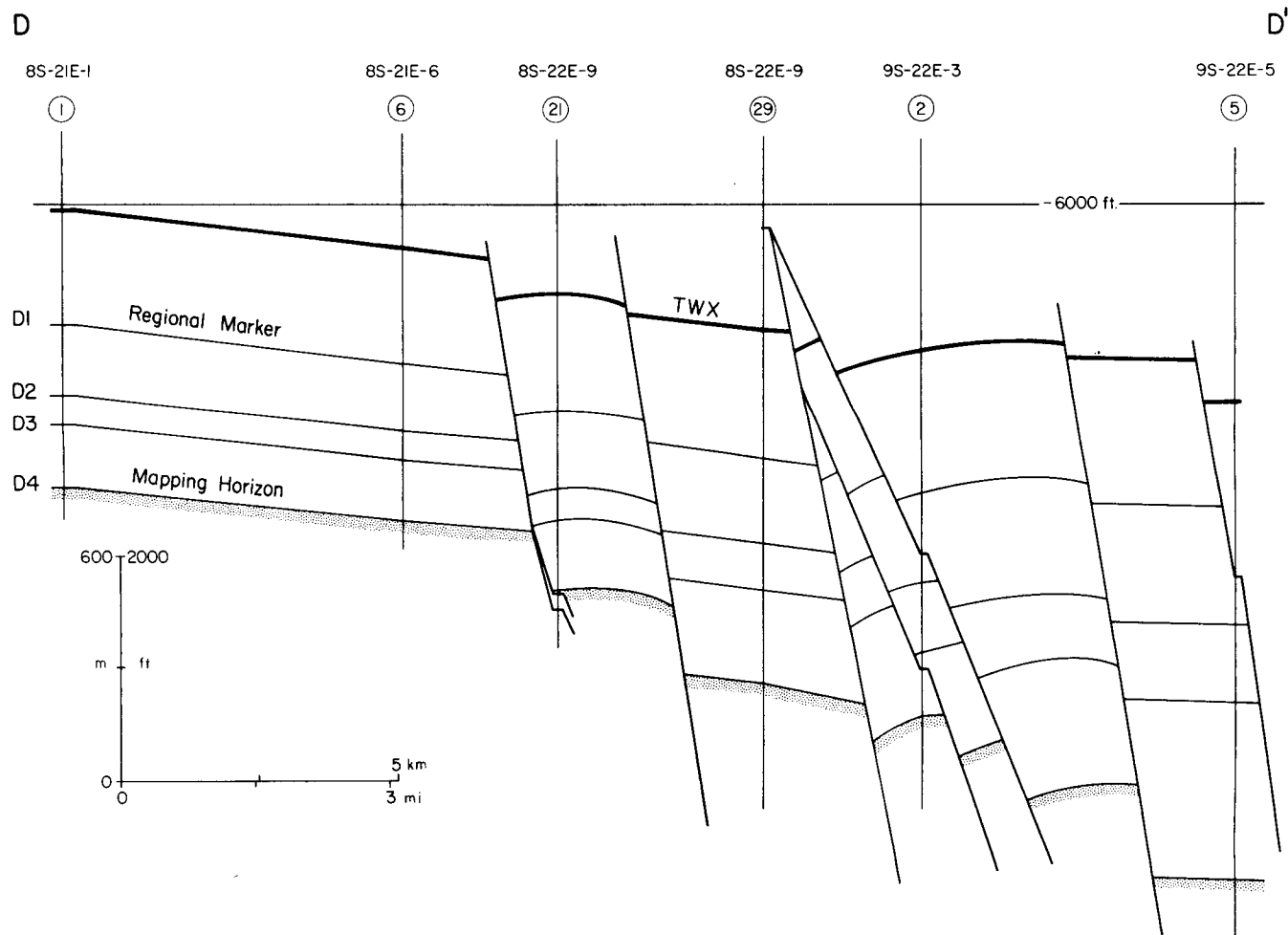


Figure 80b. Index cross section showing mapping horizon in figure 80a.

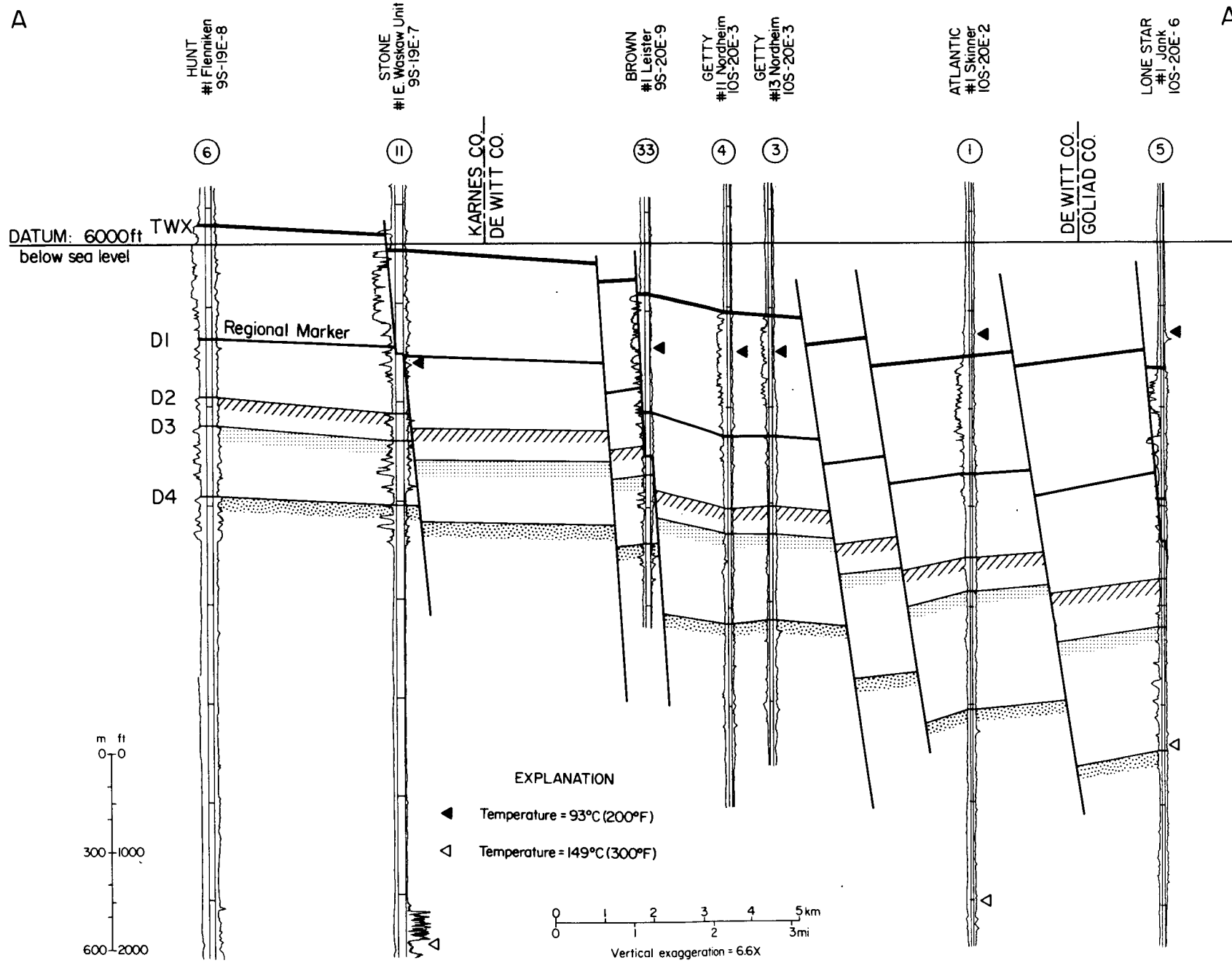


Figure 81. Structural dip section A-A', De Witt Fairway.

C

C

B B'

UNION TEXAS #1 Warwas 9S-20E-3 (9)

MONSANTO & ADA #1 Roberts 9S-20E-5 (10)

MONSANTO #1 Estrella 9S-20E-7 (16)

ATLANTIC #1 Kerlick 9S-21E-9 (38)

LONE STAR #1 Gips 9S-21E-9 (36)

LONE STAR #1 Emma Haynes Est. 10S-21E-3 (6)

HUMBLE #1 Mary A. Meyer 10S-21E-2/3 (2)

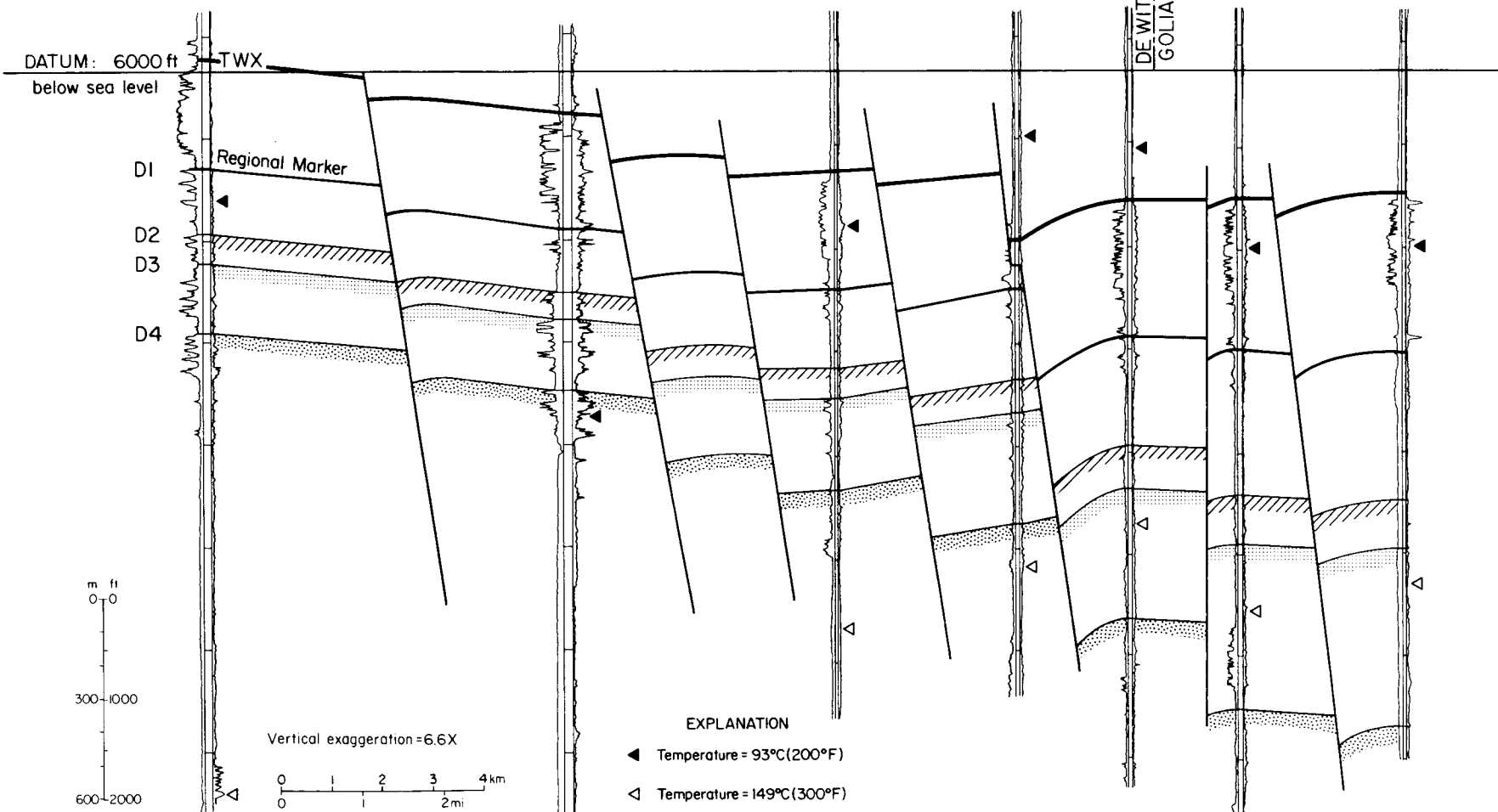


Figure 82. Structural dip section B-B', De Witt Fairway.

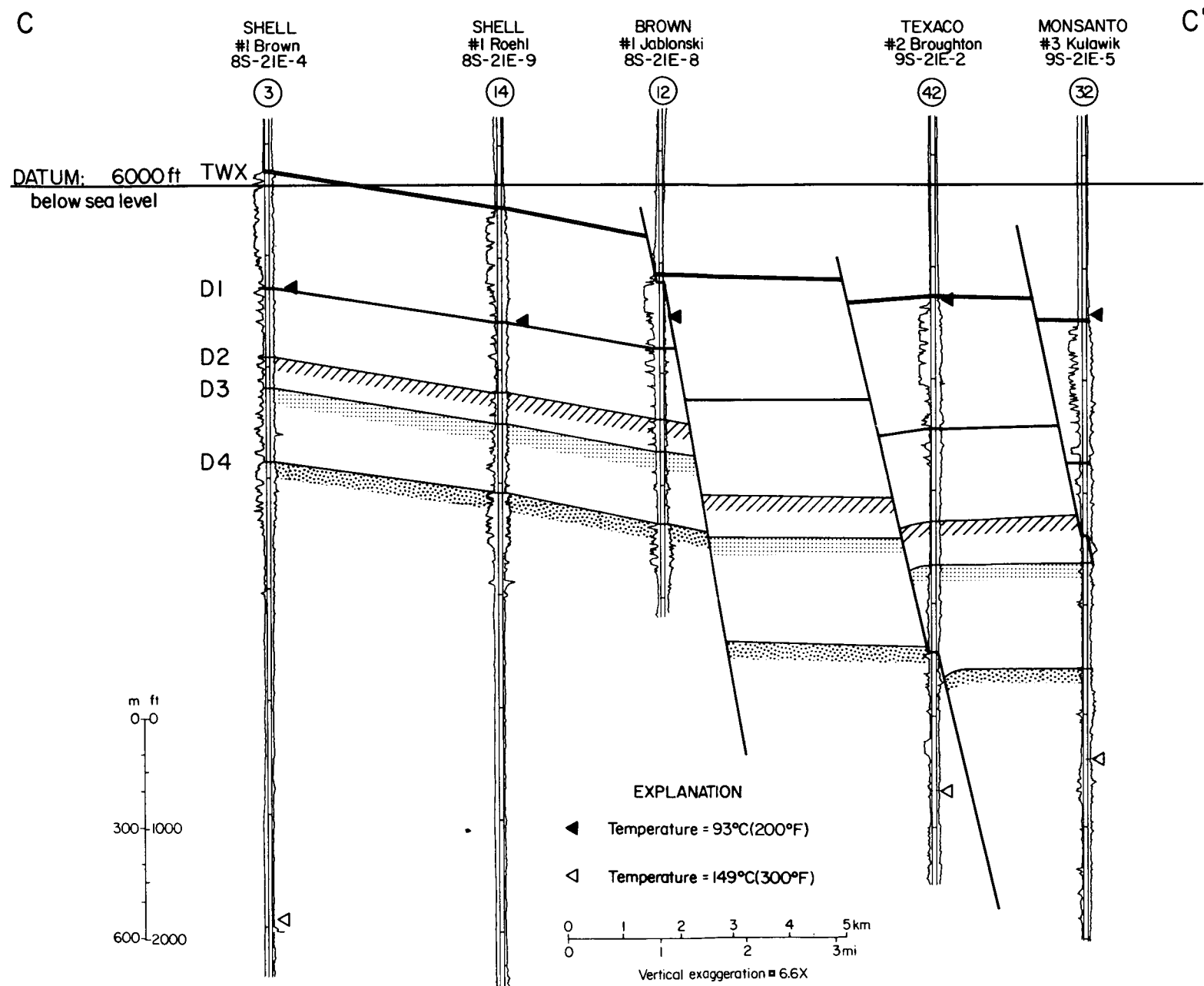


Figure 83. Structural dip section C-C', De Witt Fairway.

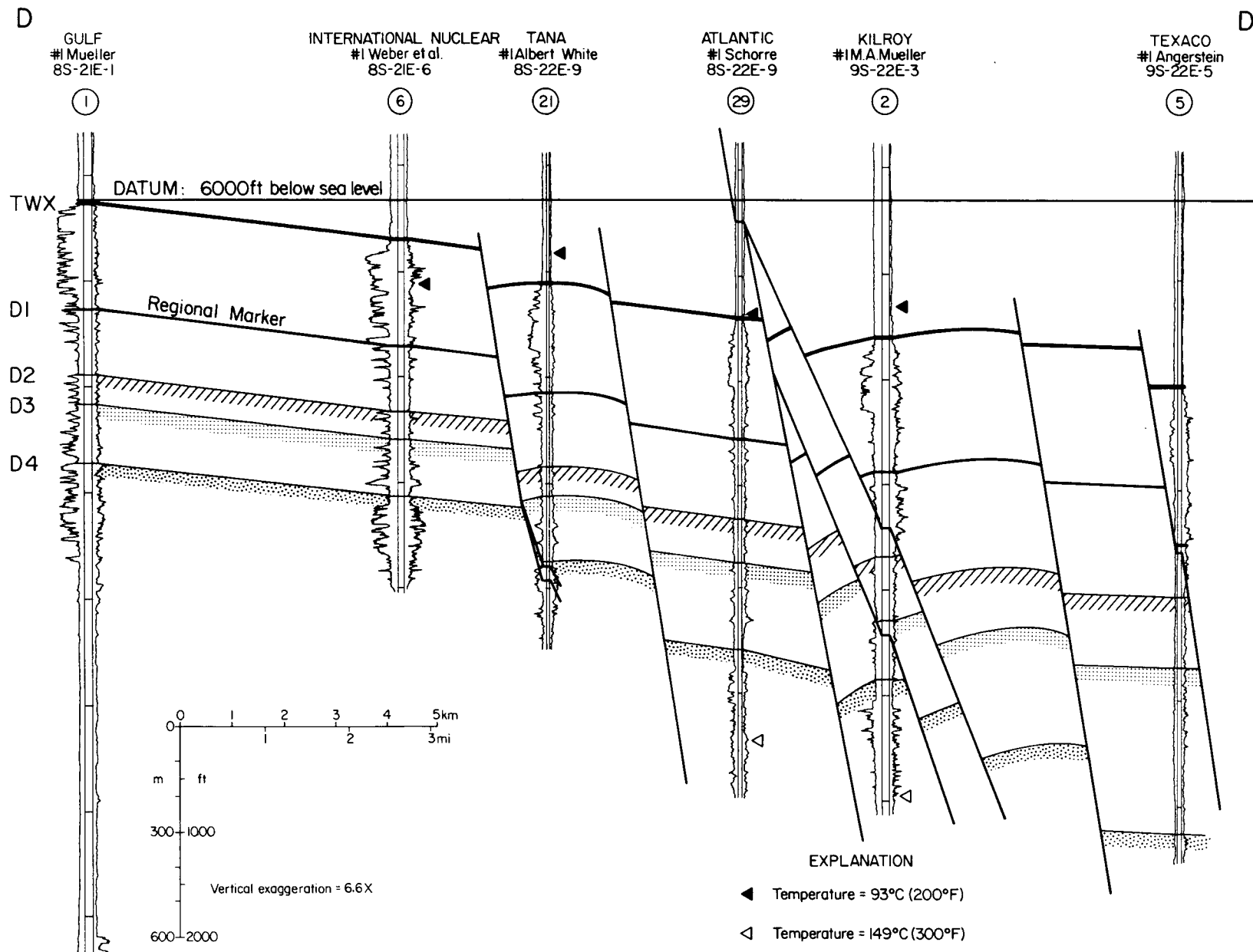


Figure 84. Structural dip section D-D', De Witt Fairway.

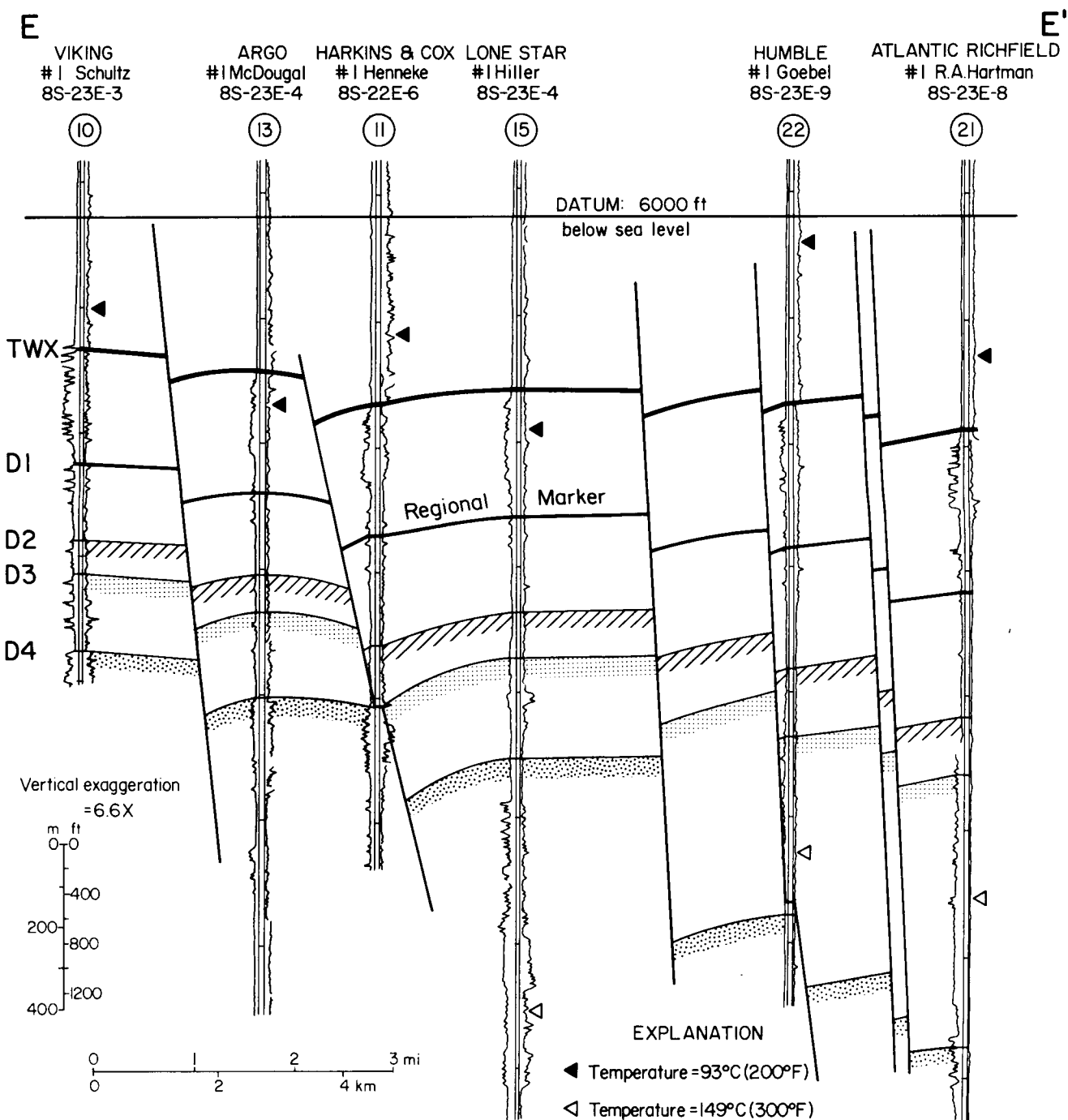


Figure 85. Structural dip section E-E', De Witt Fairway.

F

F'

MOBIL  
#1 Hagen Gas Unit  
7S-24E-3

HUMBLE  
#1 Kunetka  
7S-24E-9

ATLANTIC  
#1 Sidney Daniels  
8S-23E-1

LONE STAR  
#A-1 Friar  
8S-24E-3

HUMBLE  
#1 Pridgen  
8S-24E-4

(2)

(7)

(1)

(3)

(4)

DATUM: 6000ft below sea level

TWX

D1

Regional Marker

D2

D3

D4

67

0 1 2 3 4 5 km

m

ft

300 1000  
600 2000

Vertical exaggeration = 6.6X

## EXPLANATION

◀ Temperature = 93°C (200°F)

▷ Temperature = 149°C (300°F)

Figure 86. Structural dip section F-F', De Witt Fairway.

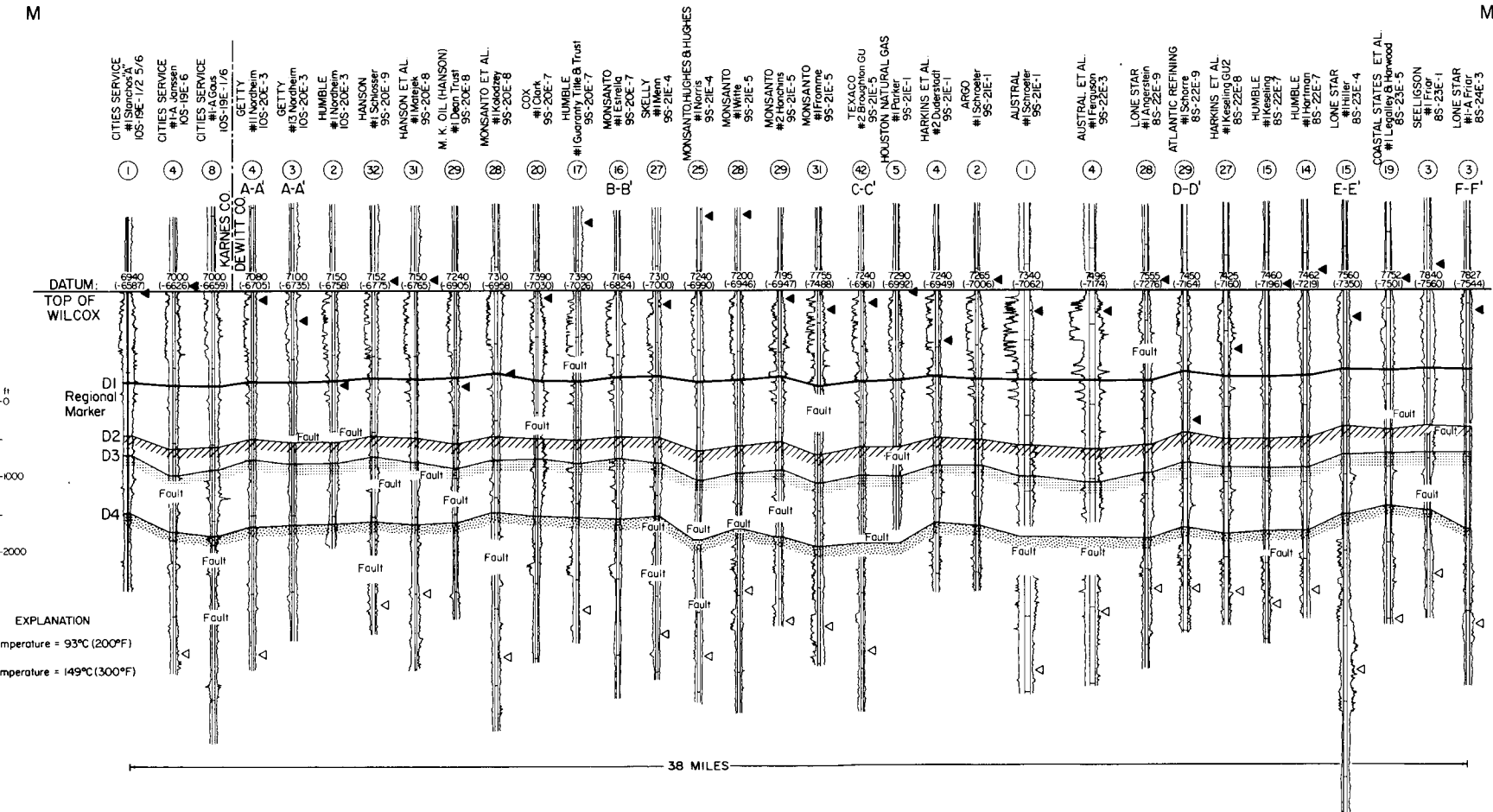


Figure 87. Stratigraphic strike section M-M', De Witt Fairway.

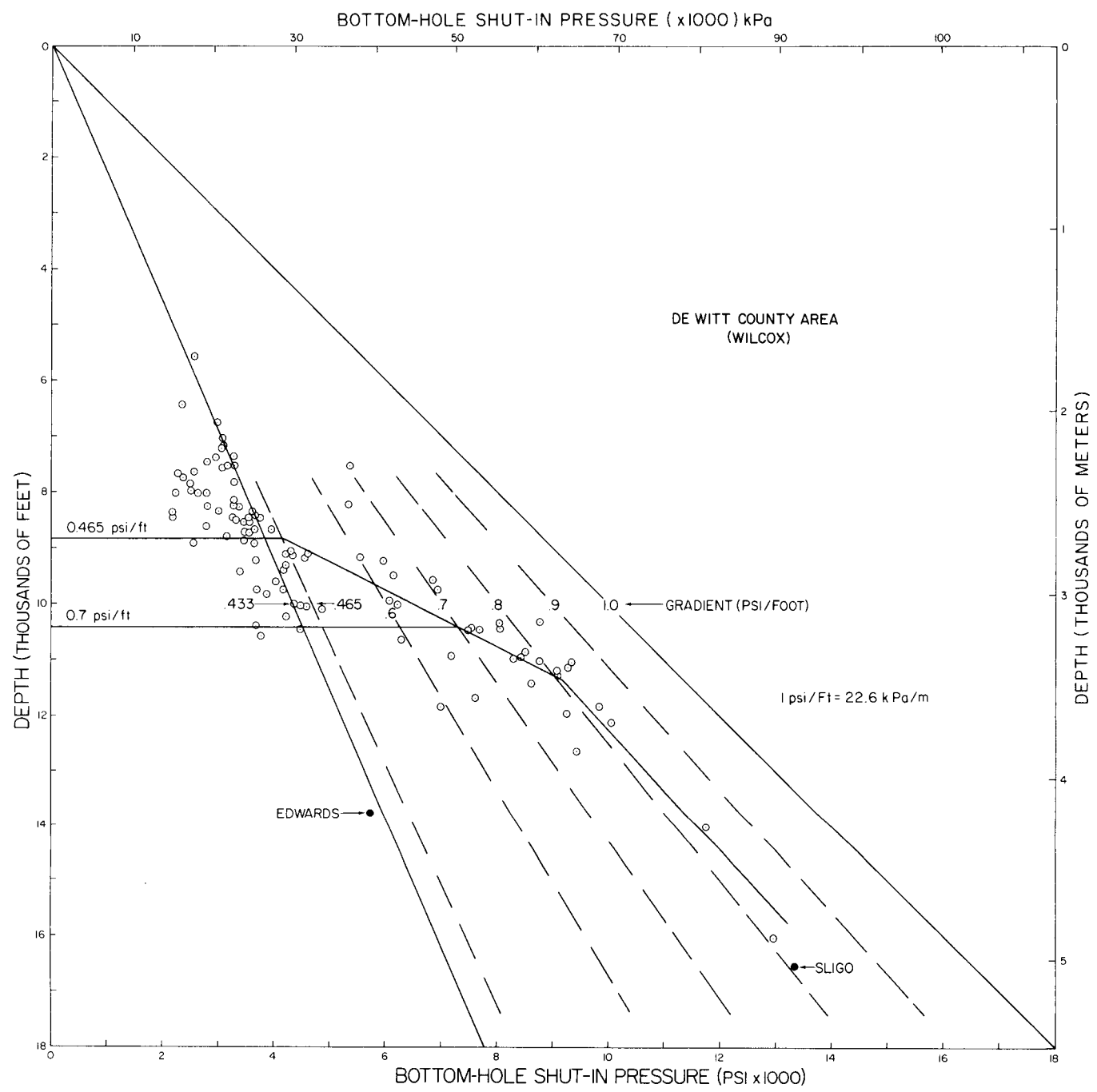


Figure 88. Bottom-hole shut-in pressure versus depth for the De Witt County area.

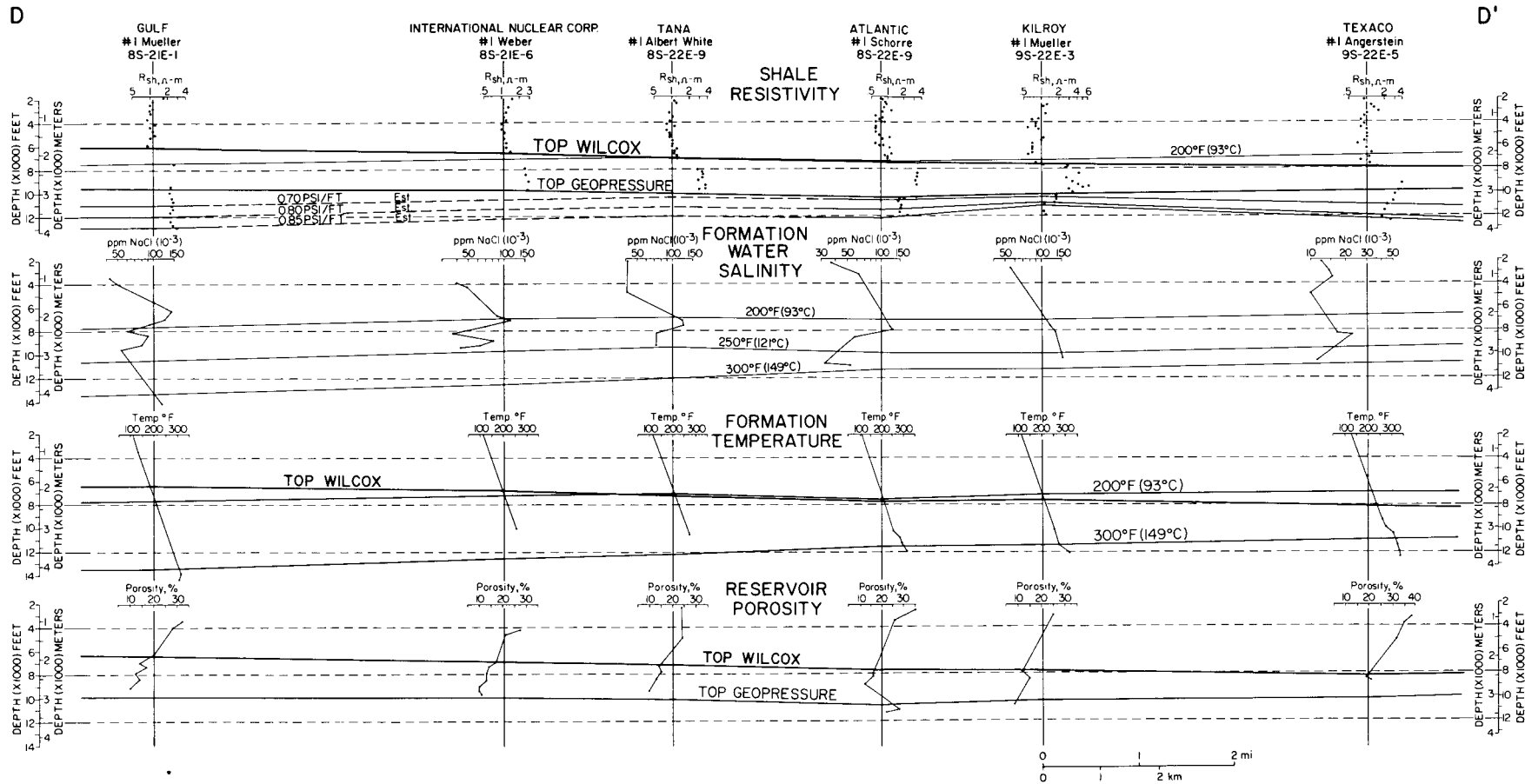


Figure 89. Parameter plots showing shale resistivity, temperature, porosity, and salinity profiles and variation of operational top of geopressure and geopressure gradients along cross section D-D', De Witt County.

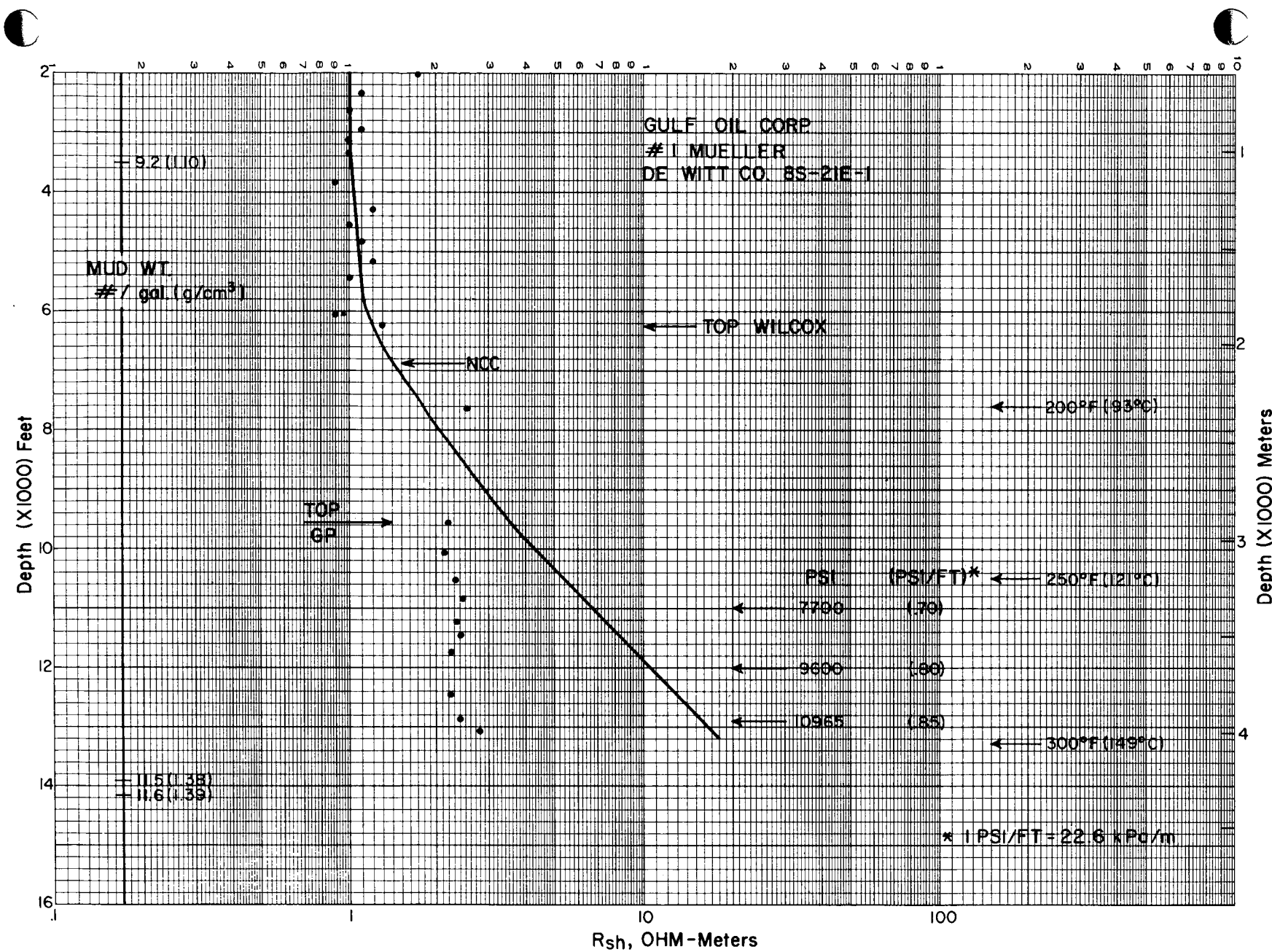


Figure 90. Operational top of geopressure and geopressure gradients from shale resistivity data for an updip well on cross section D-D', De Witt County.

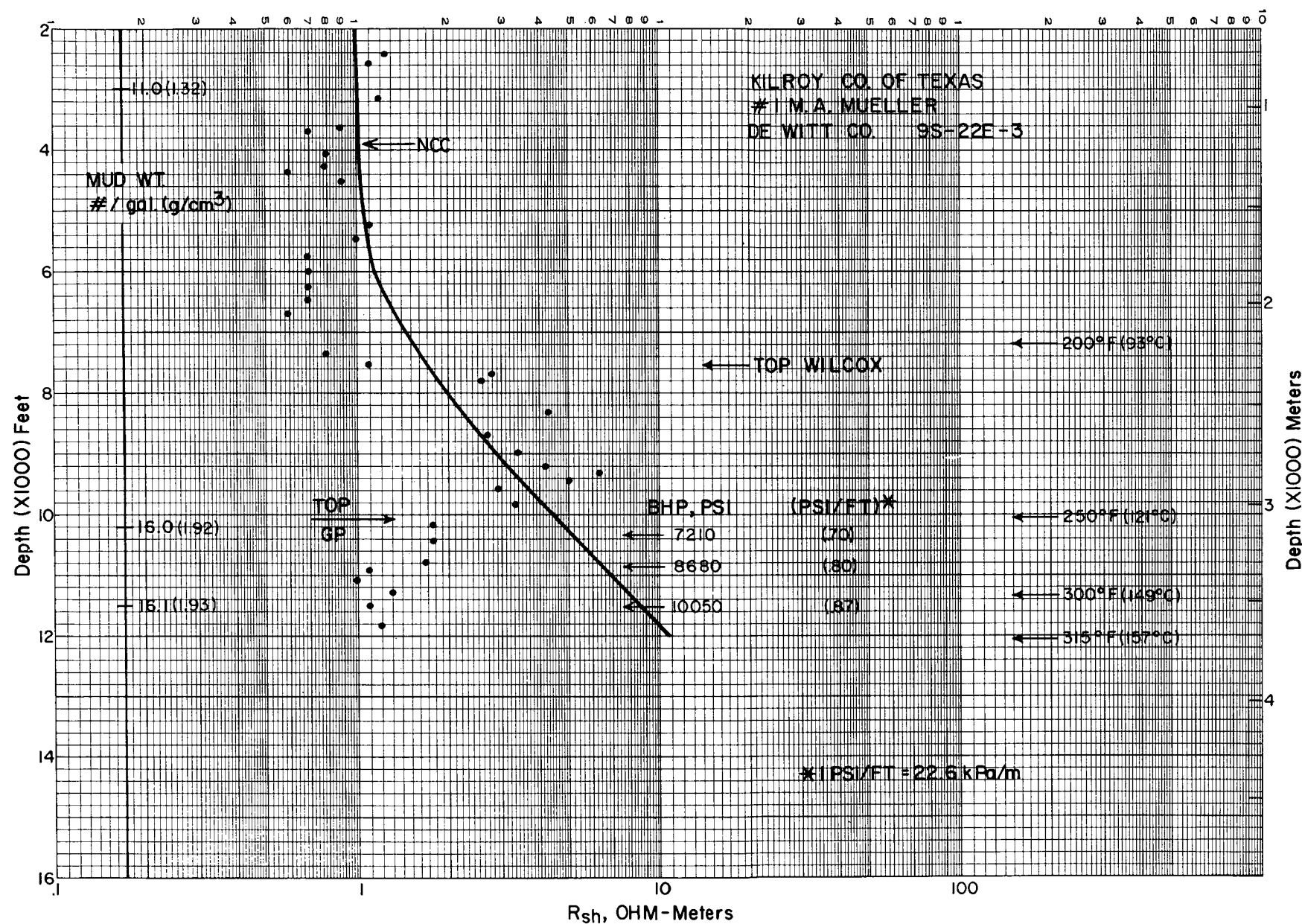


Figure 91. Operational top of geopressure and geopressure gradients from shale resistivity data for downdip well Kilkroy No. 1 Mueller on cross section D-D', De Witt County.

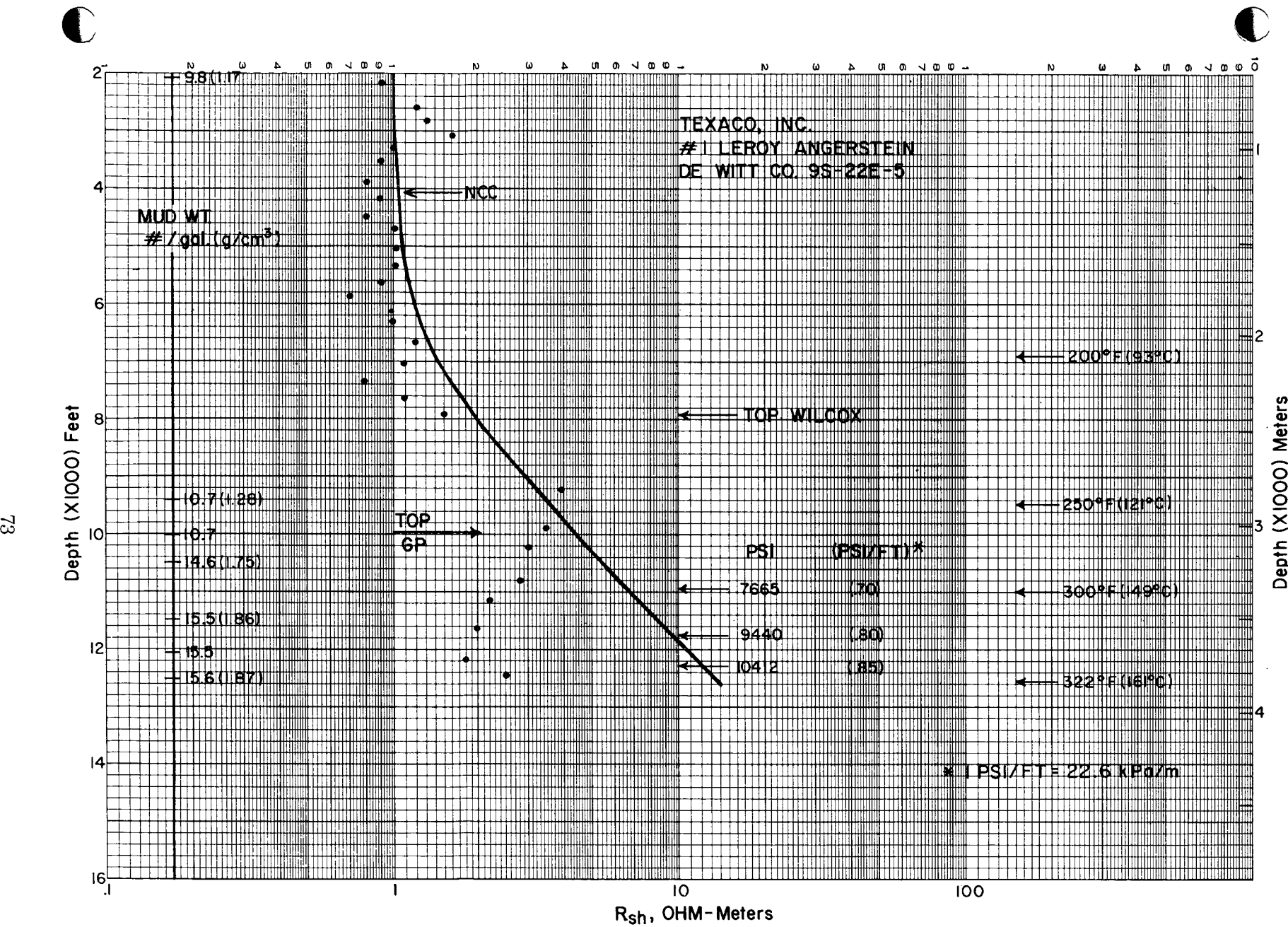


Figure 92. Operational top of geopressure and geopressure gradients from shale resistivity data for downdip well Texaco No. 1 Angerstein on cross section D-D', De Witt County.

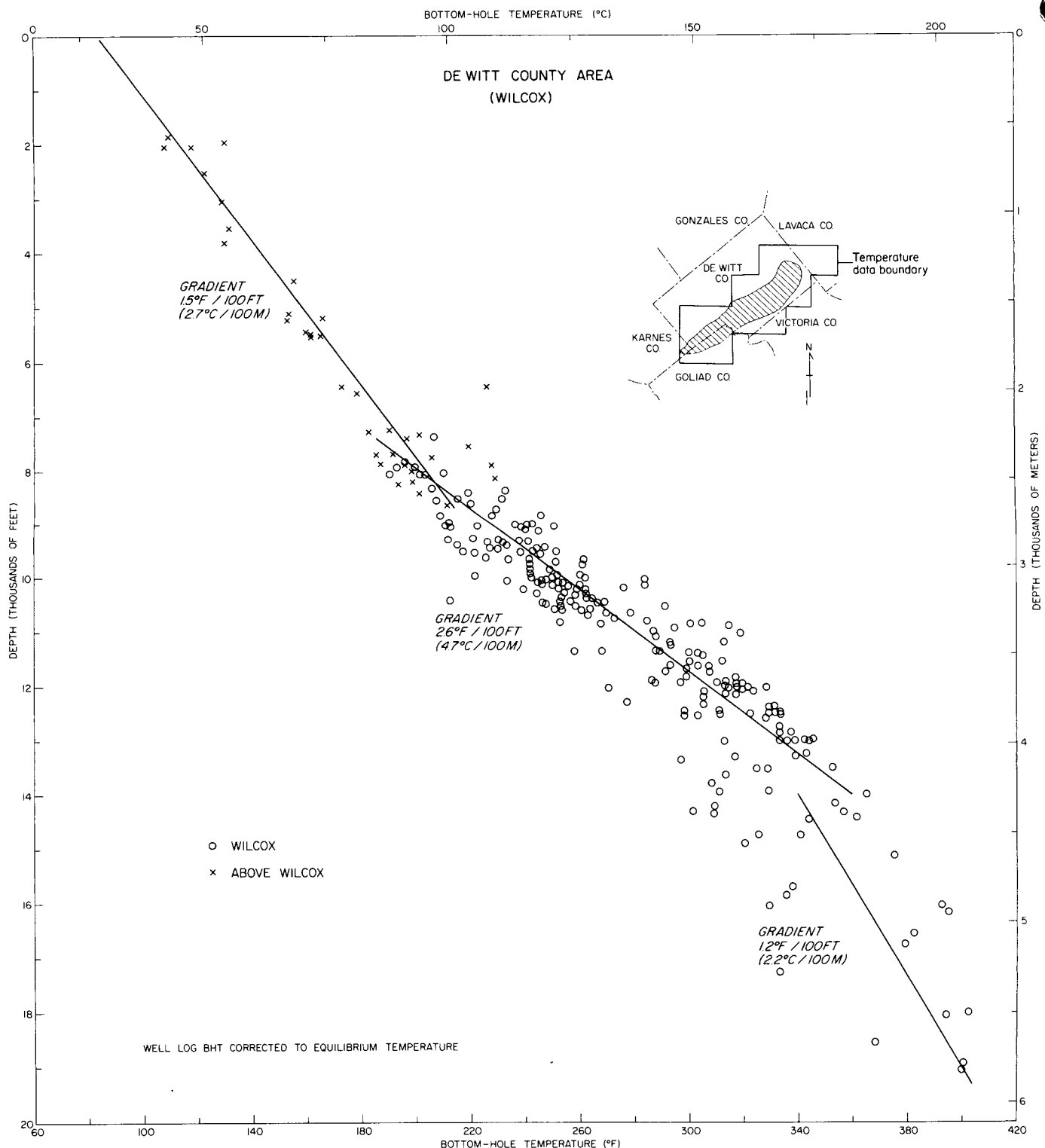
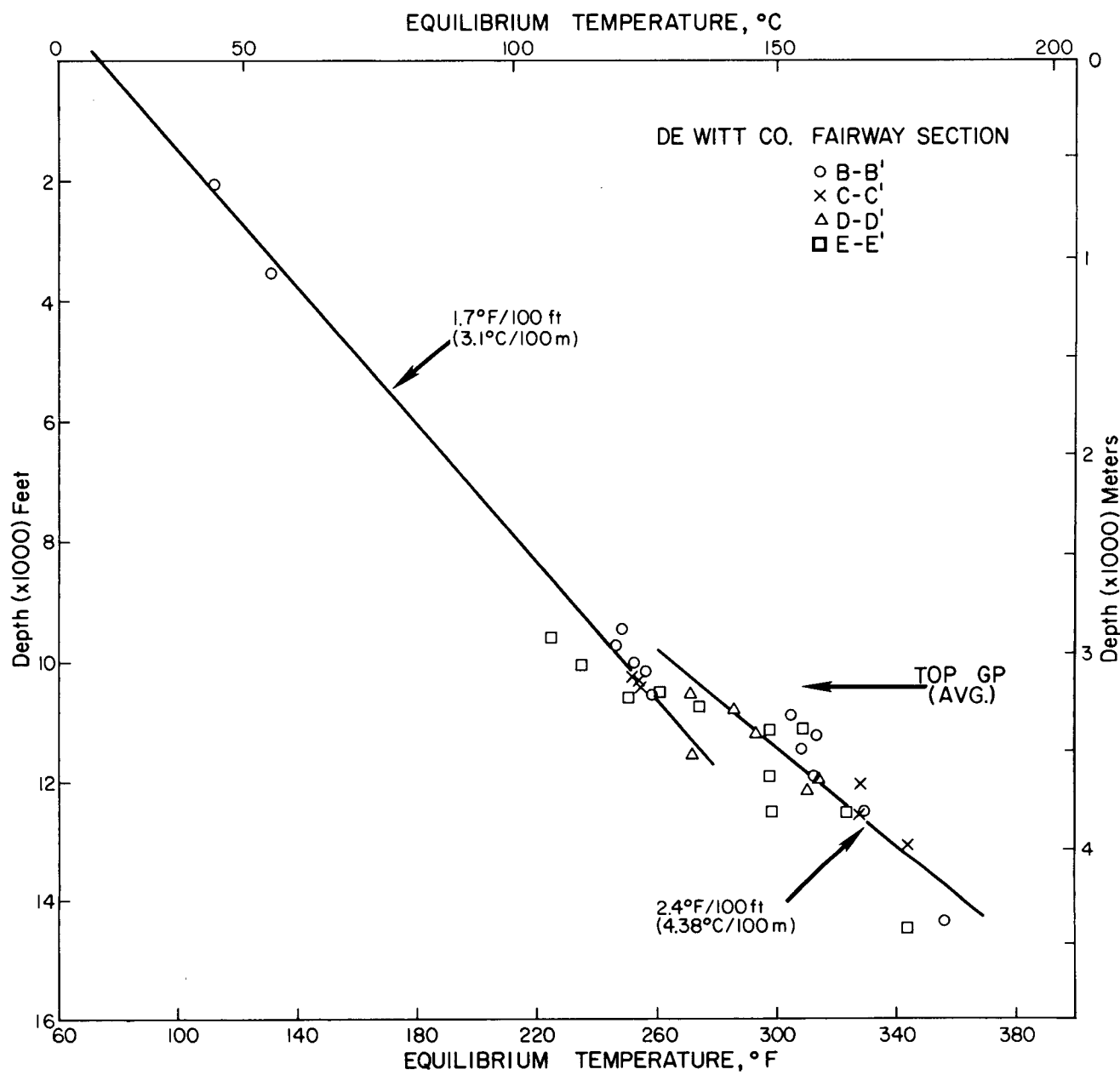


Figure 93. Temperatures and geothermal gradients for the De Witt Fairway area.



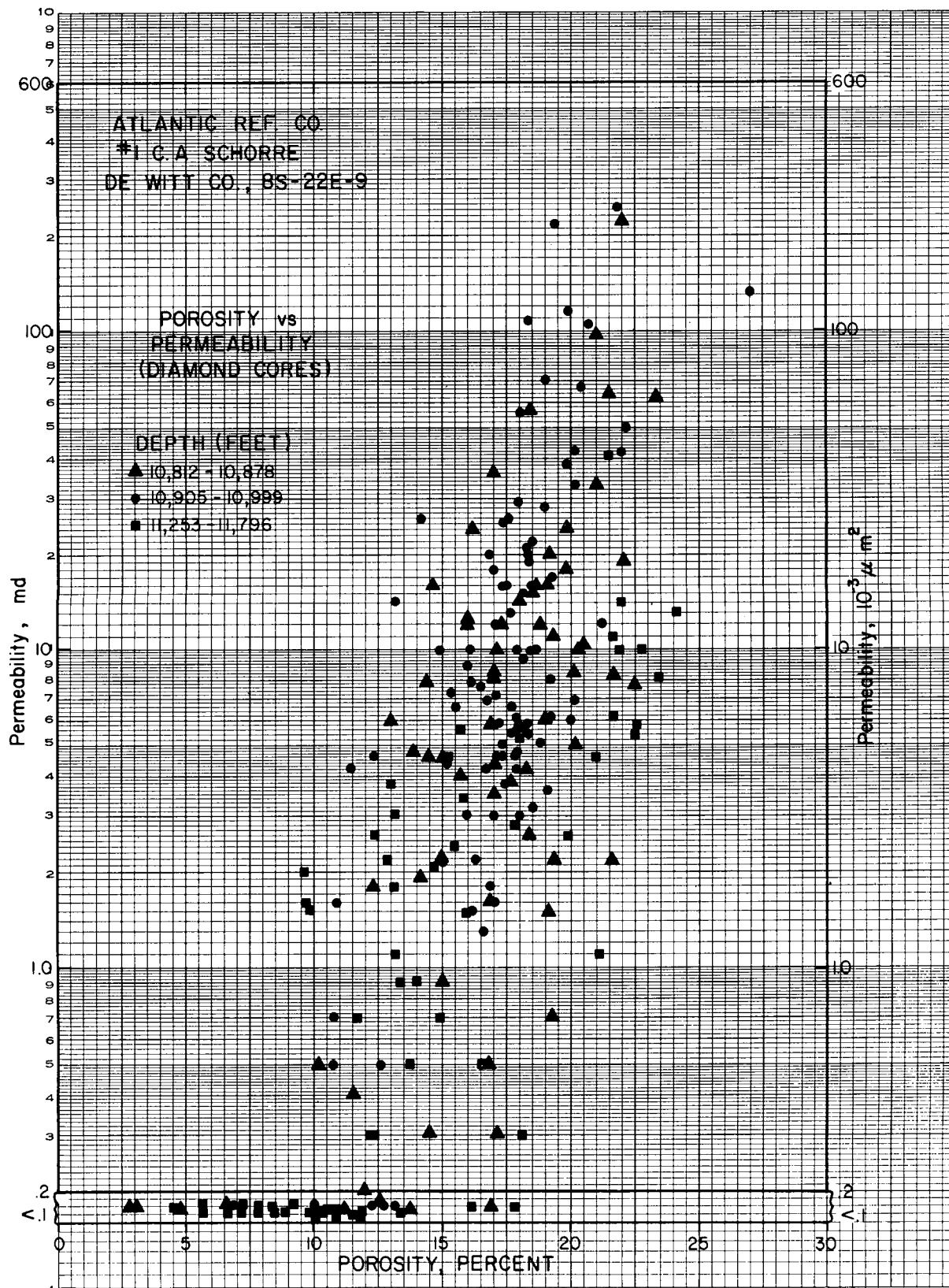


Figure 95. Porosity versus permeability for Atlantic No. 1 Schorre well on cross section D-D', De Witt County.

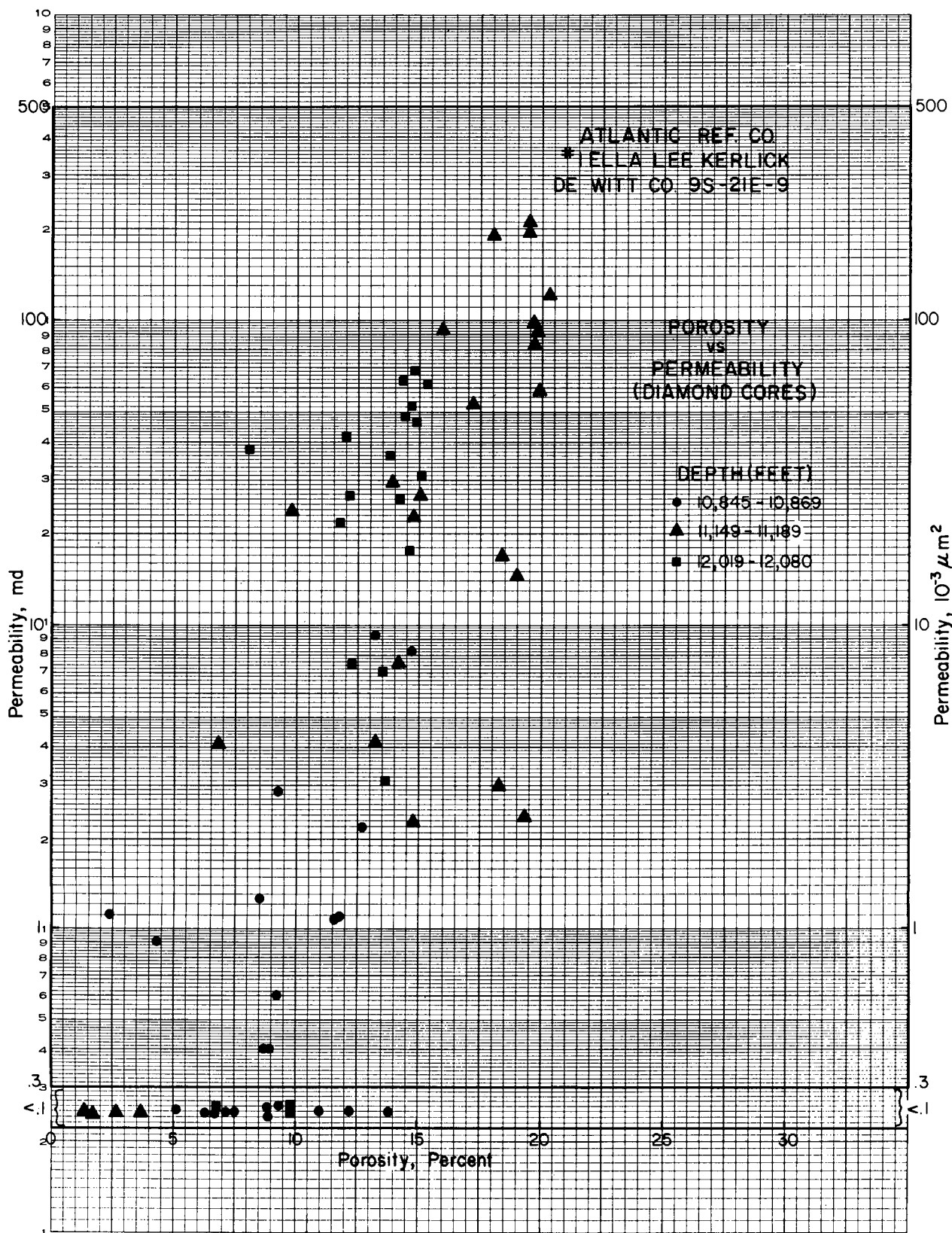


Figure 96. Porosity versus permeability for Atlantic No. 1 Kerlick well on cross section B-B', De Witt County.

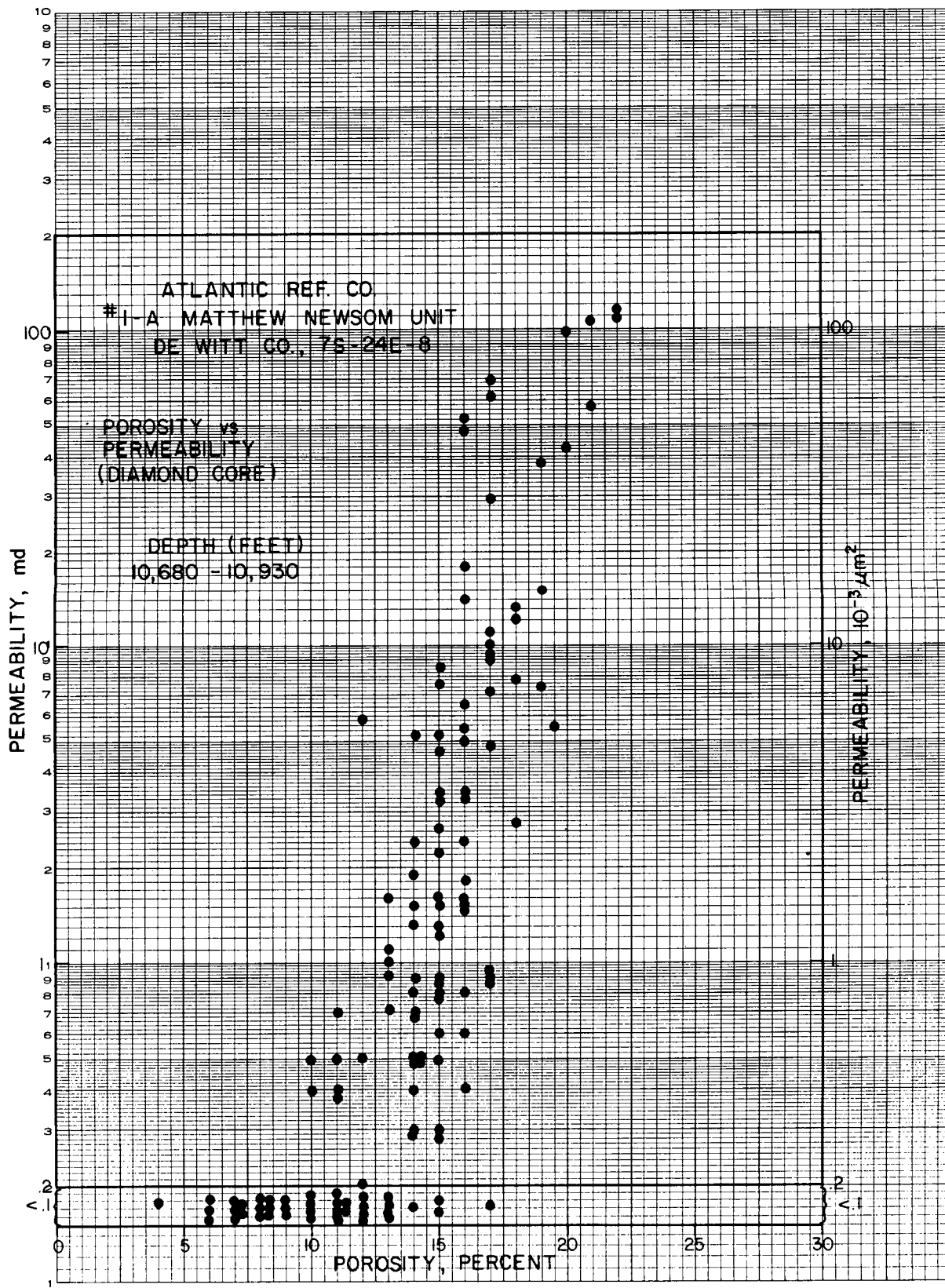


Figure 97. Porosity versus permeability for Atlantic No. 1-A Newsom well in De Witt County.

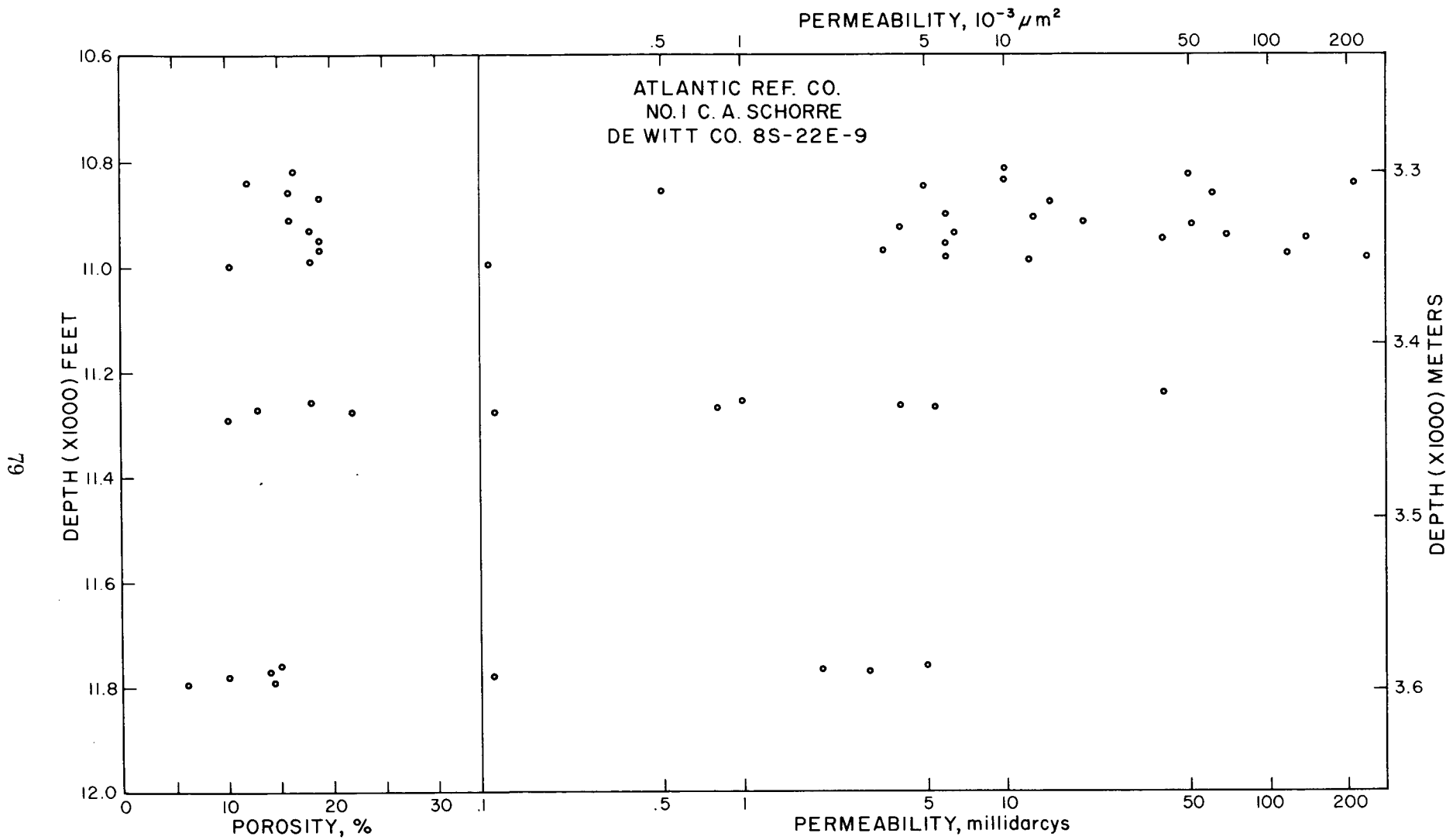
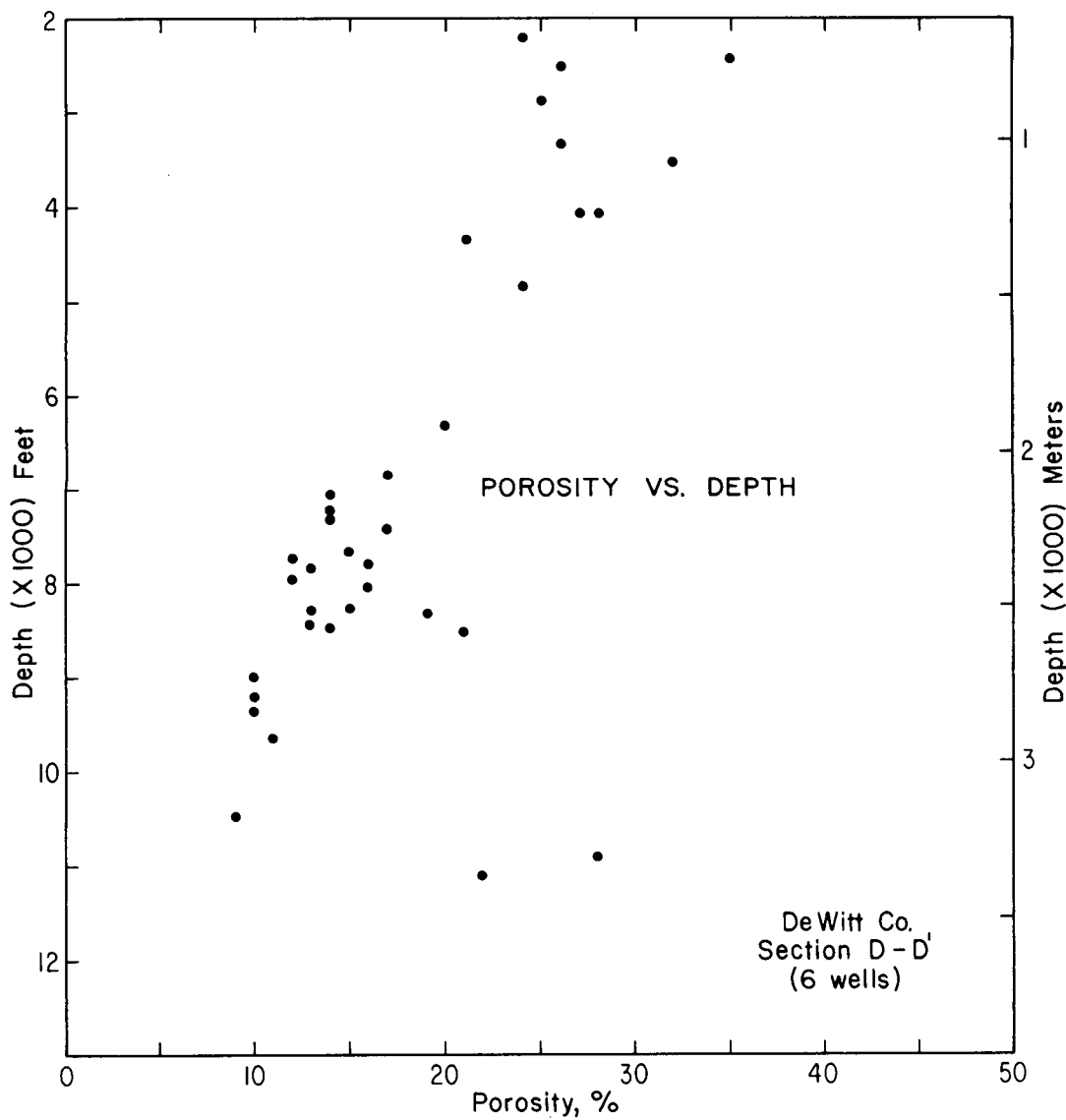


Figure 98. Porosity and permeability versus depth for Atlantic No. 1 Schorre well on section D-D', De Witt County.



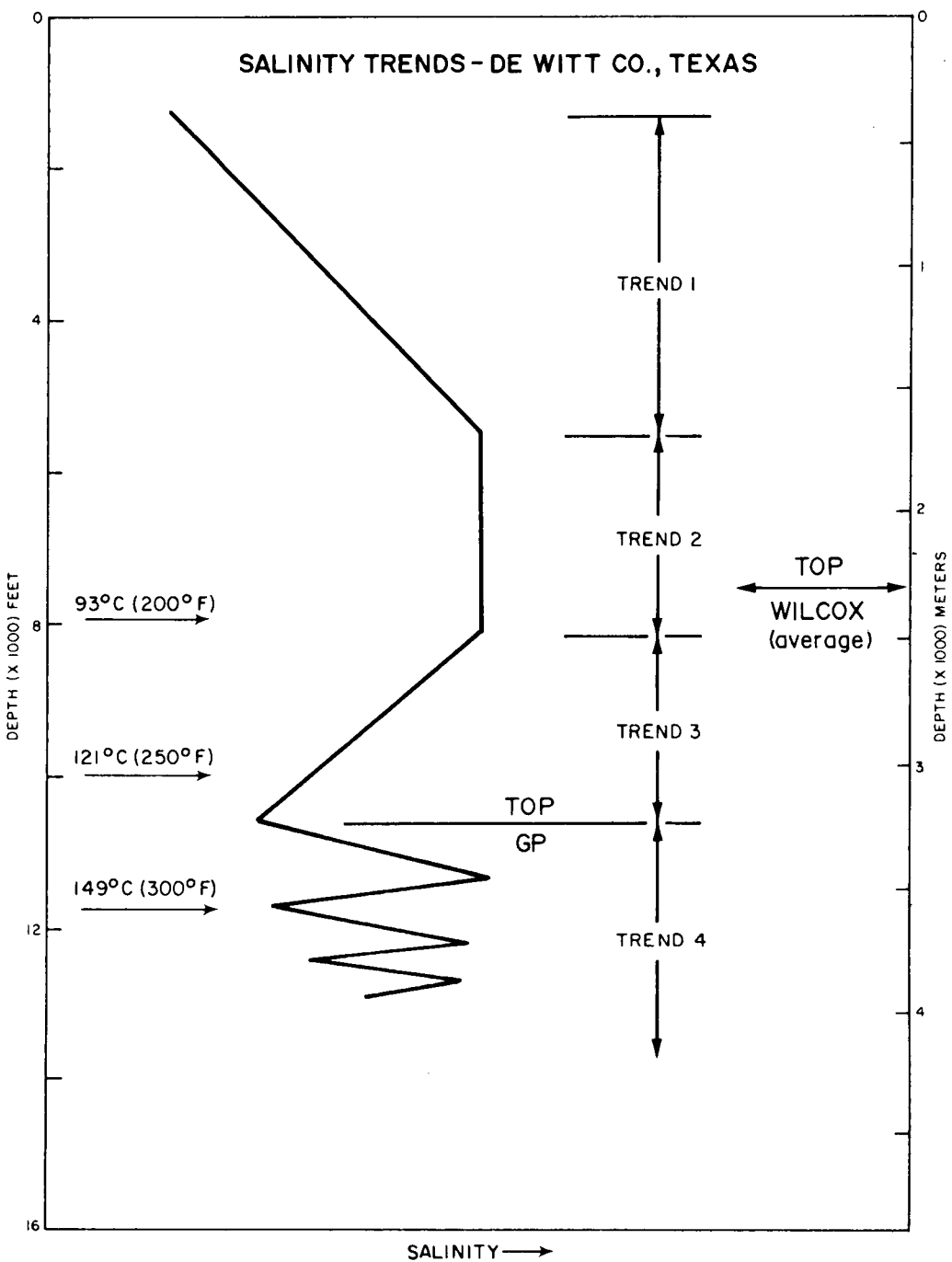


Figure 100. Generalized salinity trends as a function of depth in De Witt County.

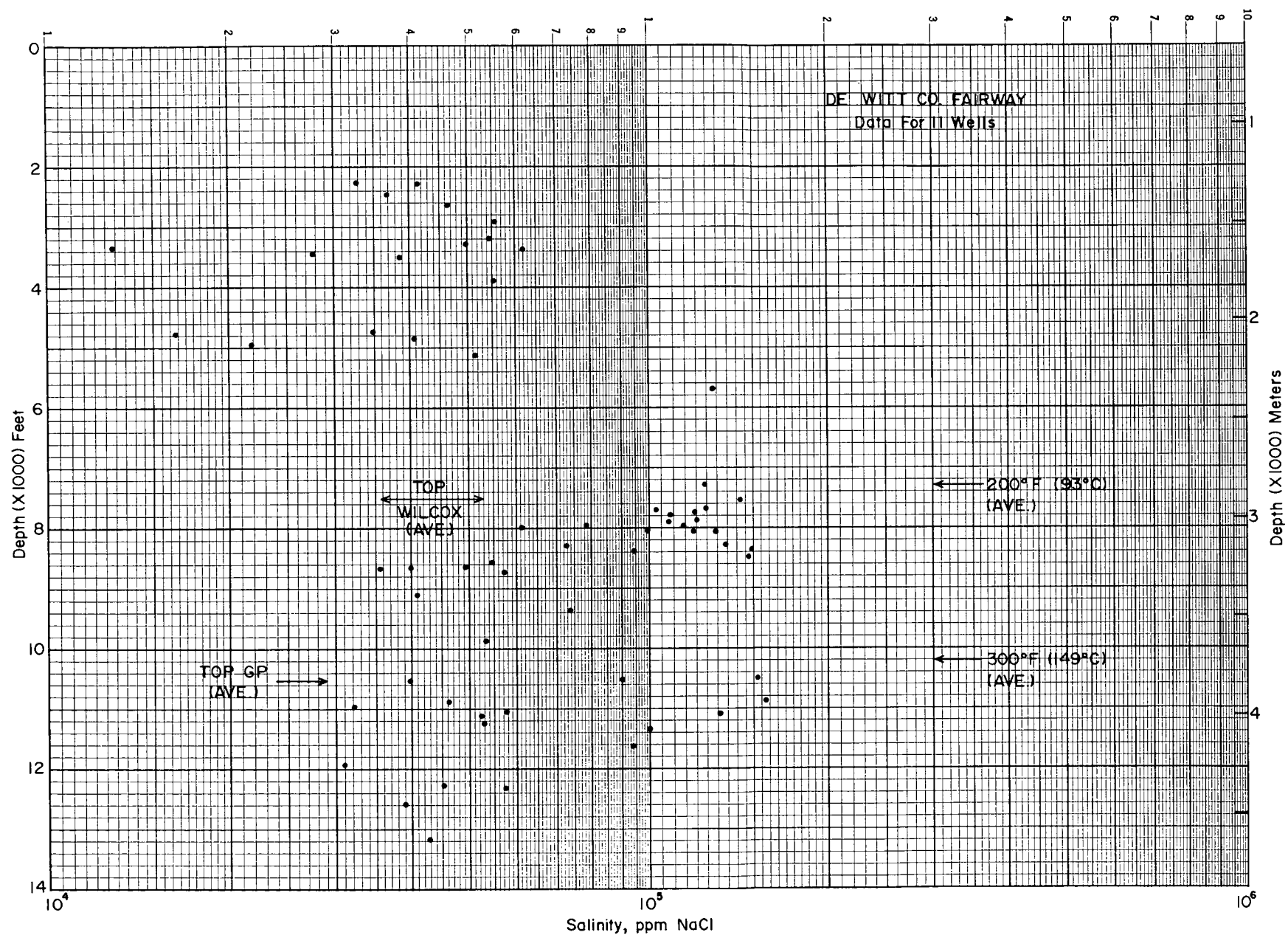


Figure 101. Salinity versus depth calculated from electric logs of 11 wells in De Witt County.

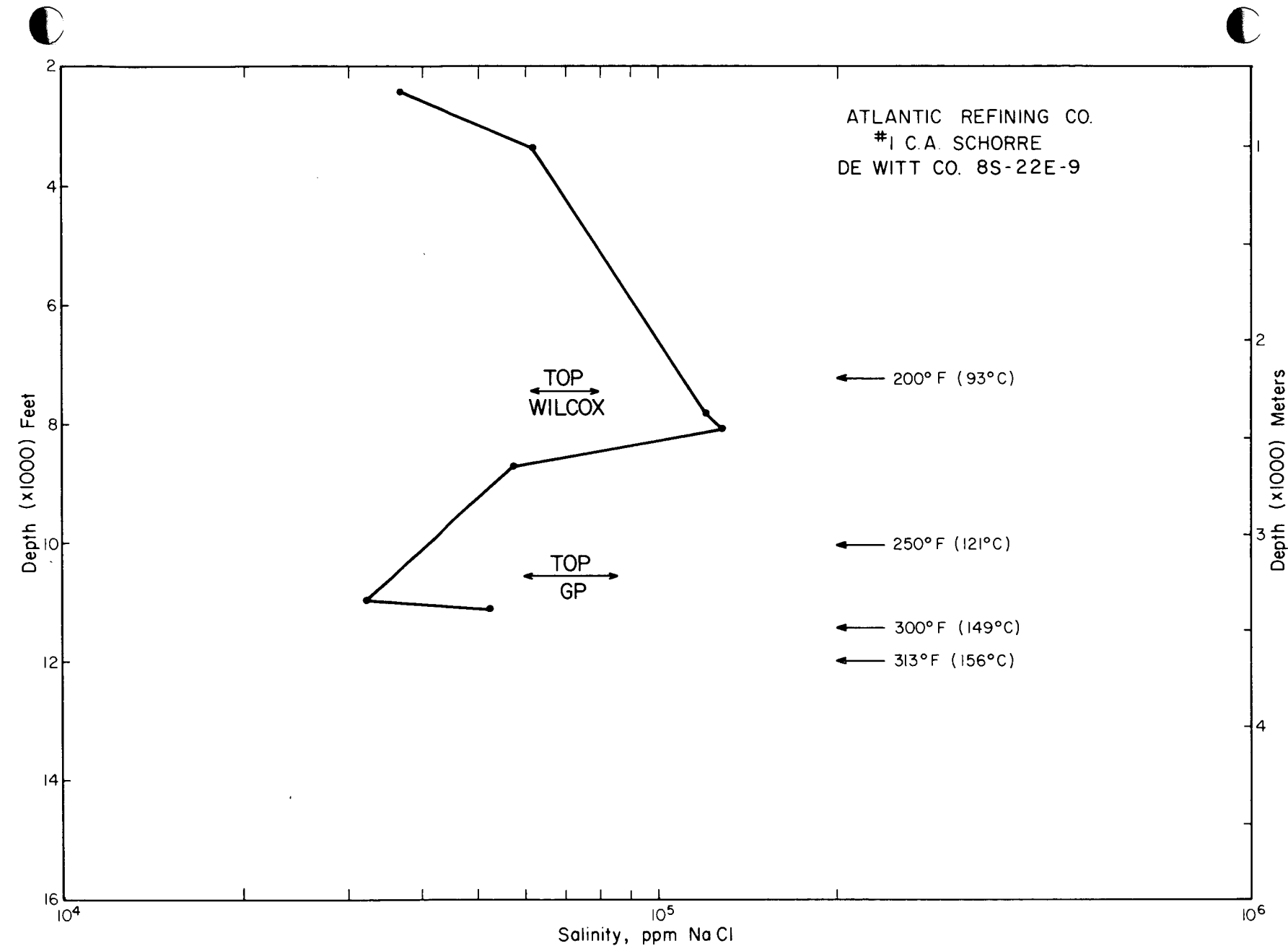


Figure 102. Calculated salinity profile for Atlantic No. 1 Schorre well on section D-D', De Witt County.

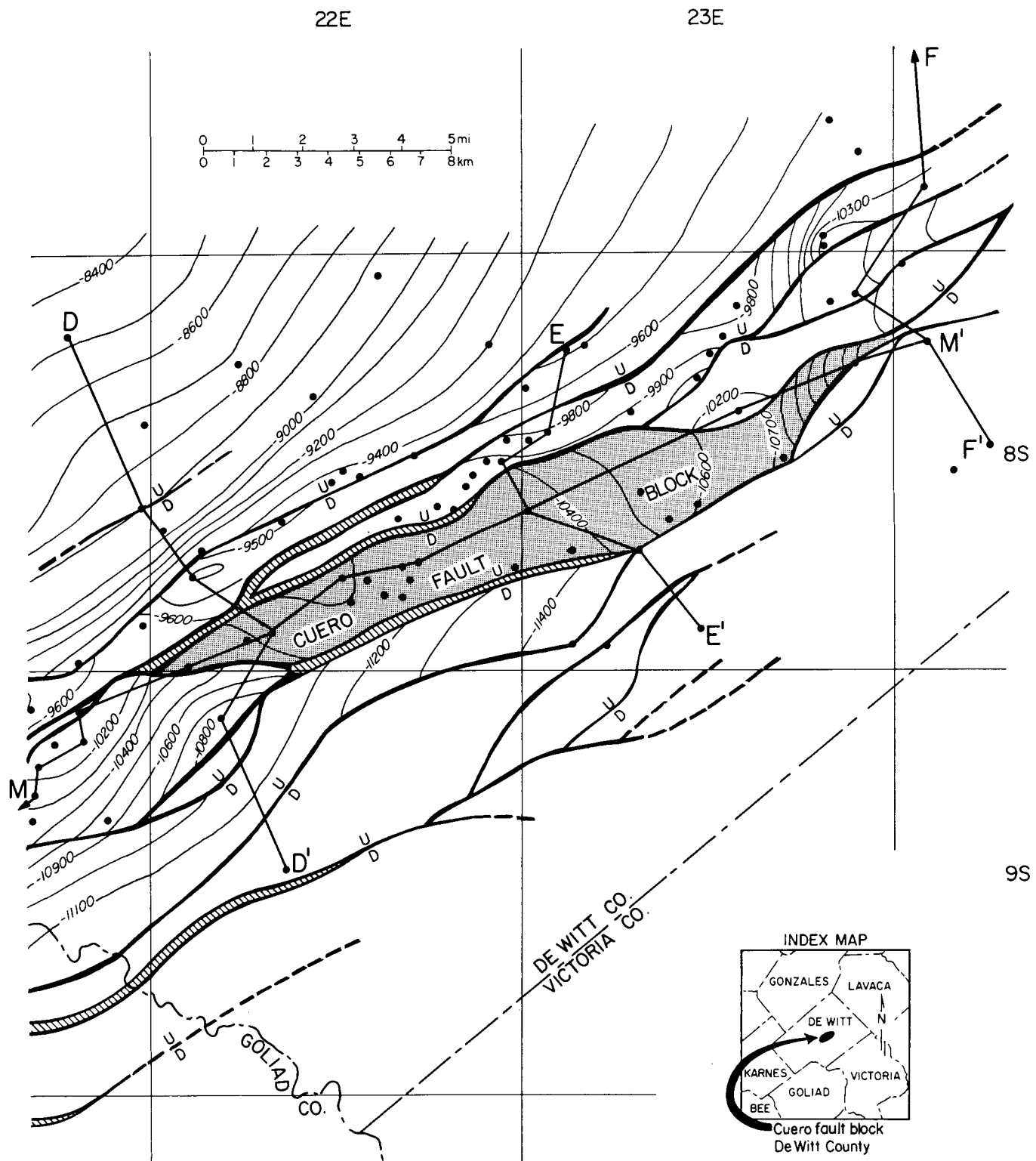


Figure 103. Structure, well control, lines of section, and location of the Cuero fault block.

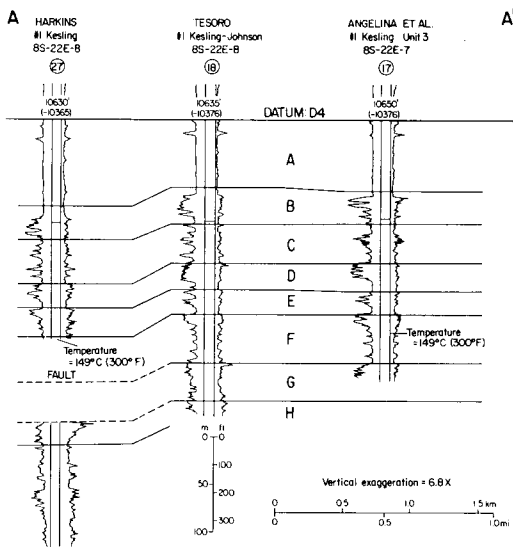


Figure 104. Stratigraphic dip section A-A', Cuero fault block.

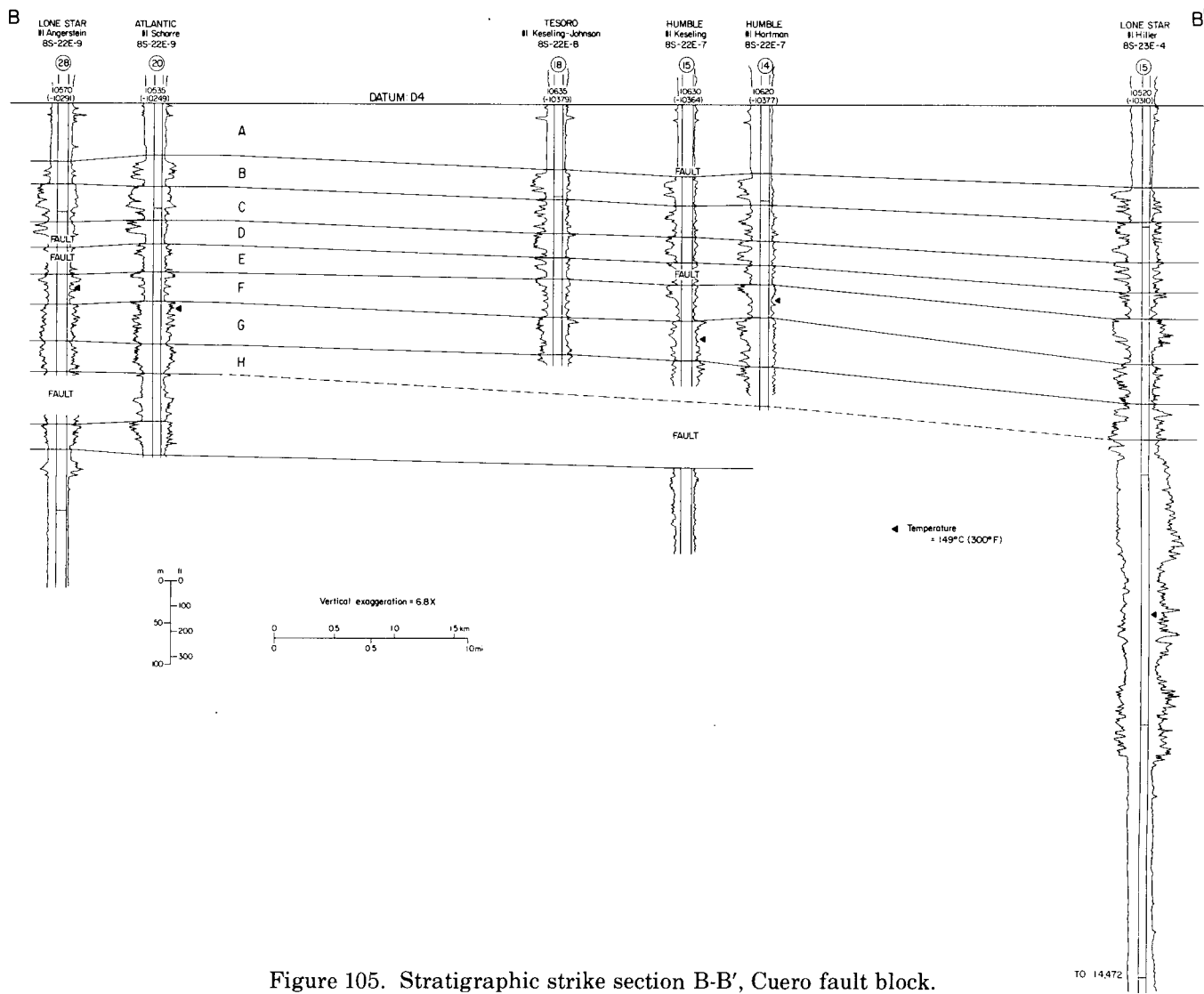


Figure 105. Stratigraphic strike section B-B', Cuero fault block.

TO 14,472

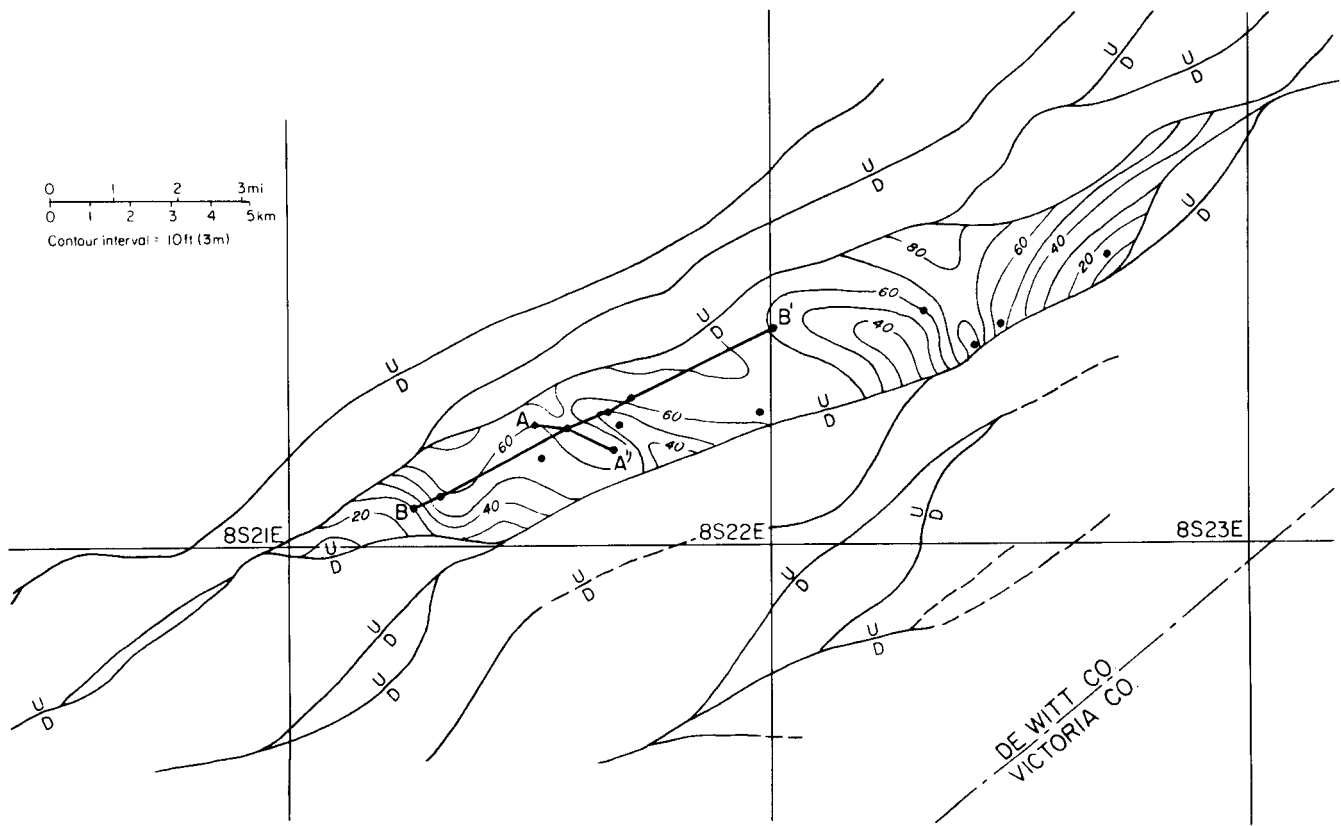


Figure 106. Net sandstone in correlation unit B, Cuero fault block.

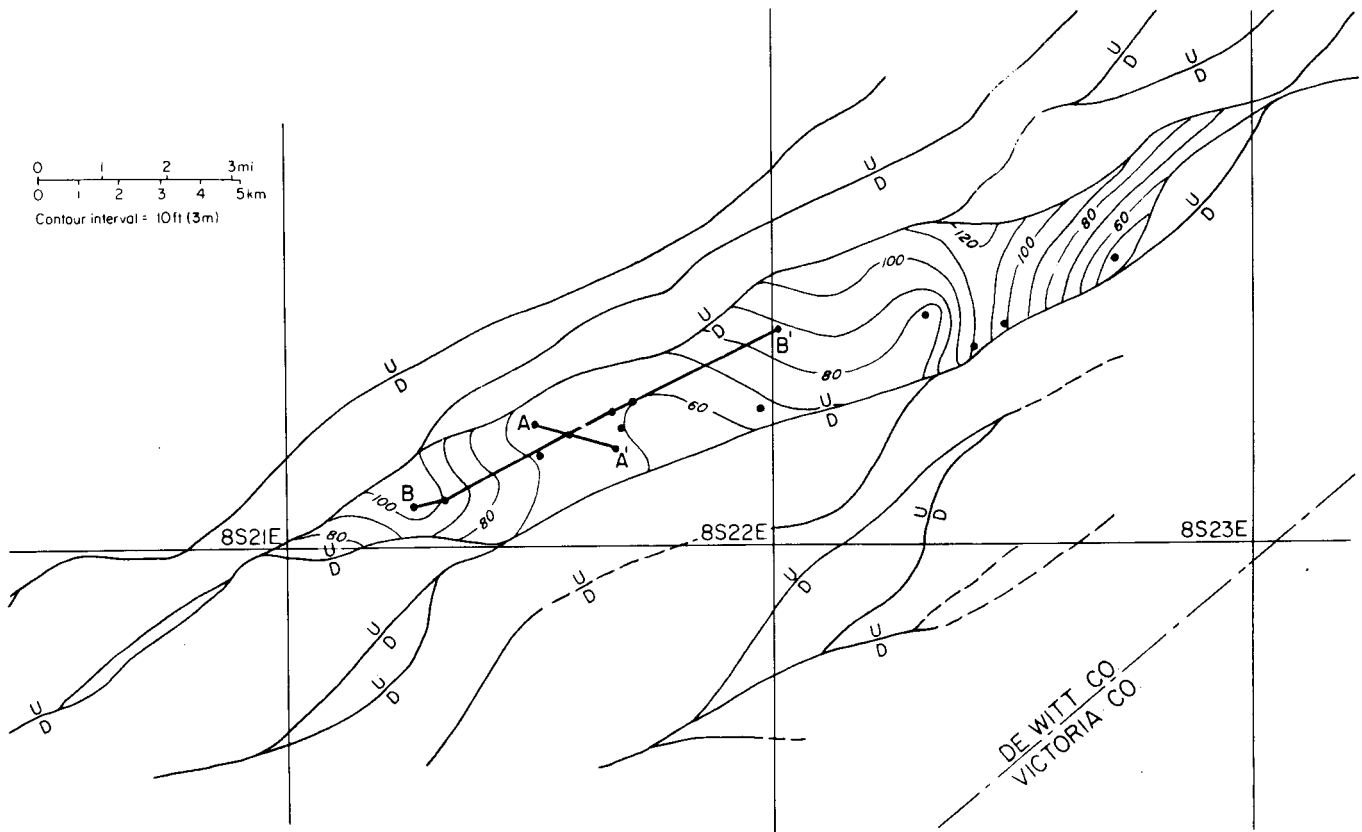


Figure 107. Net sandstone in correlation unit C, Cuero fault block.

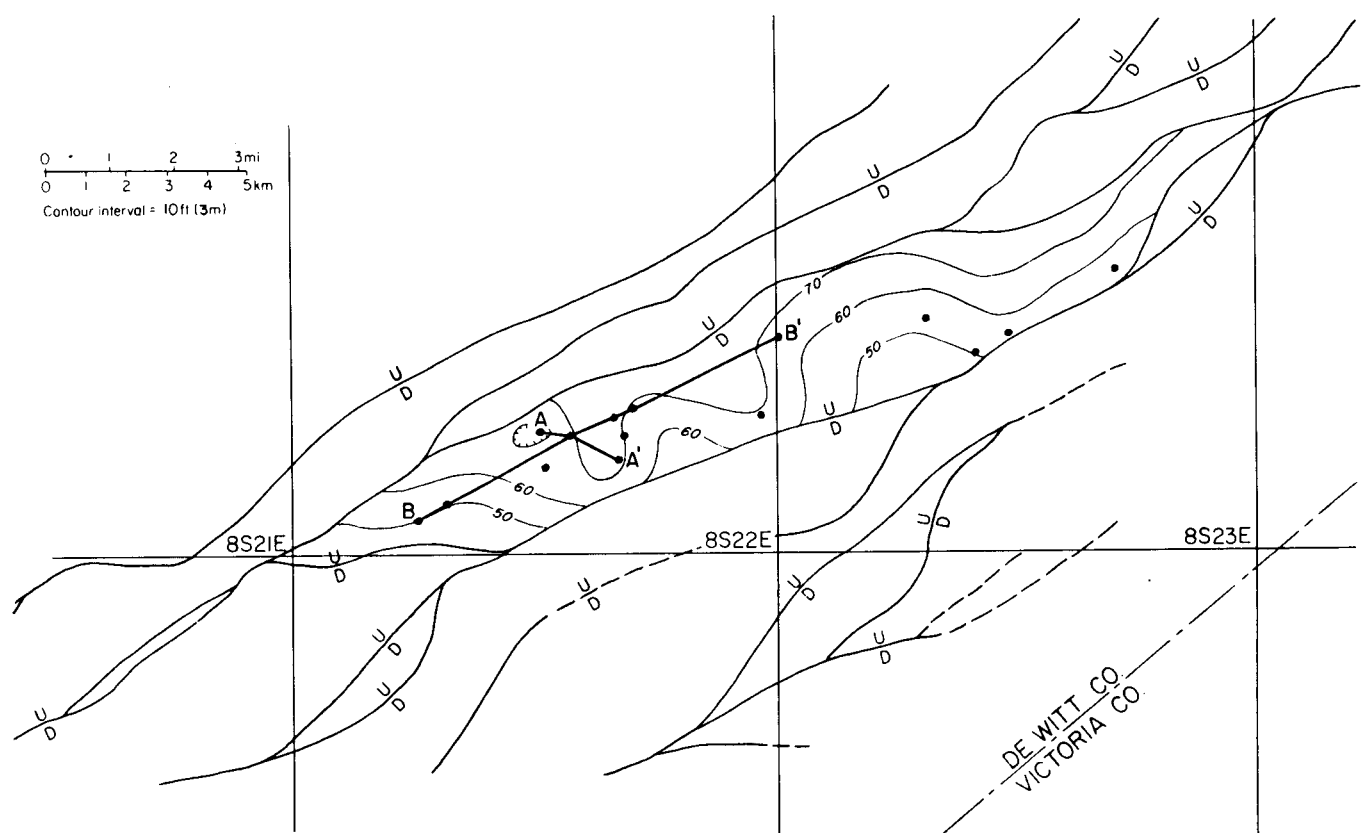


Figure 108. Net sandstone in correlation unit D, Cuero fault block.

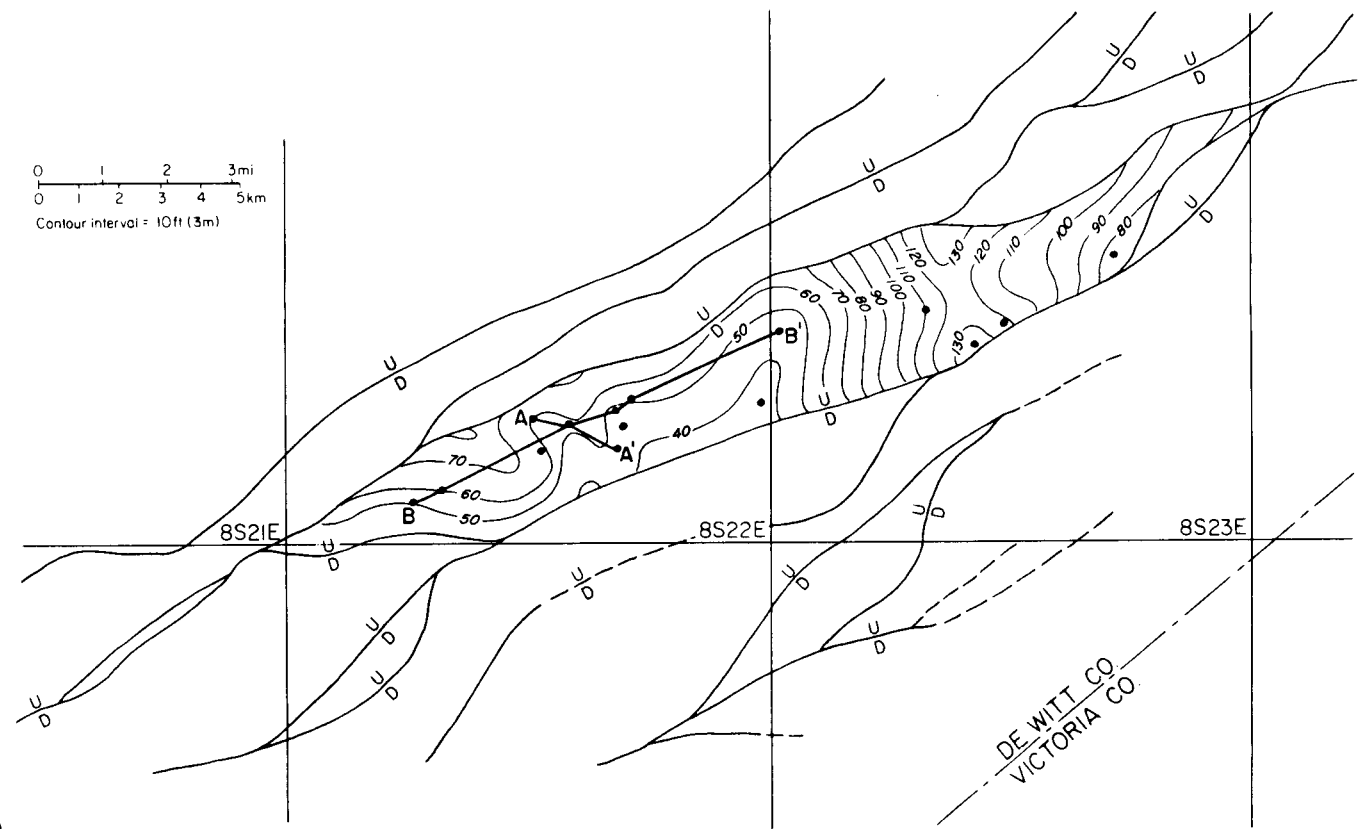


Figure 109. Net sandstone in correlation unit E, Cuero fault block.

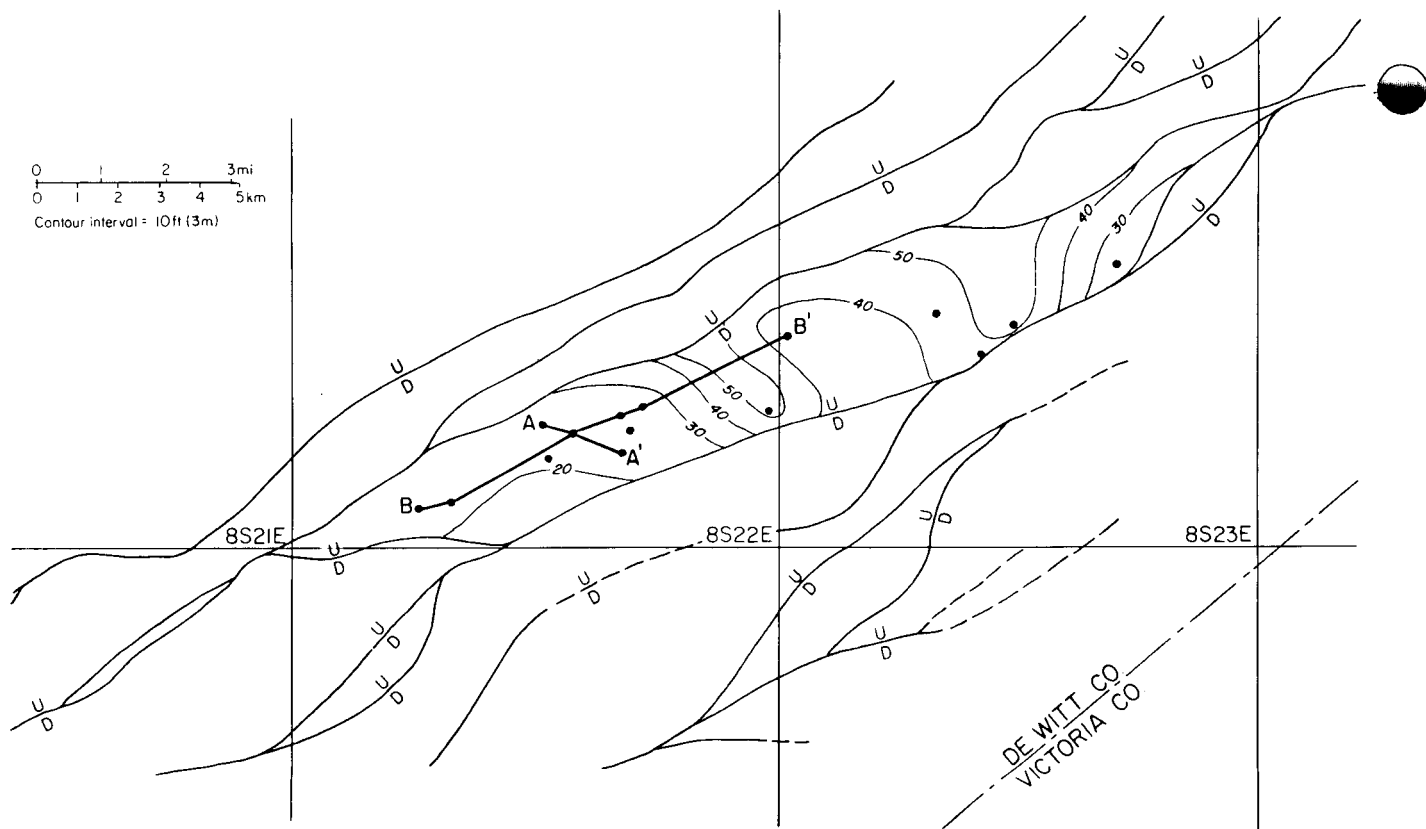


Figure 110. Net sandstone in correlation unit F, Cuero fault block.

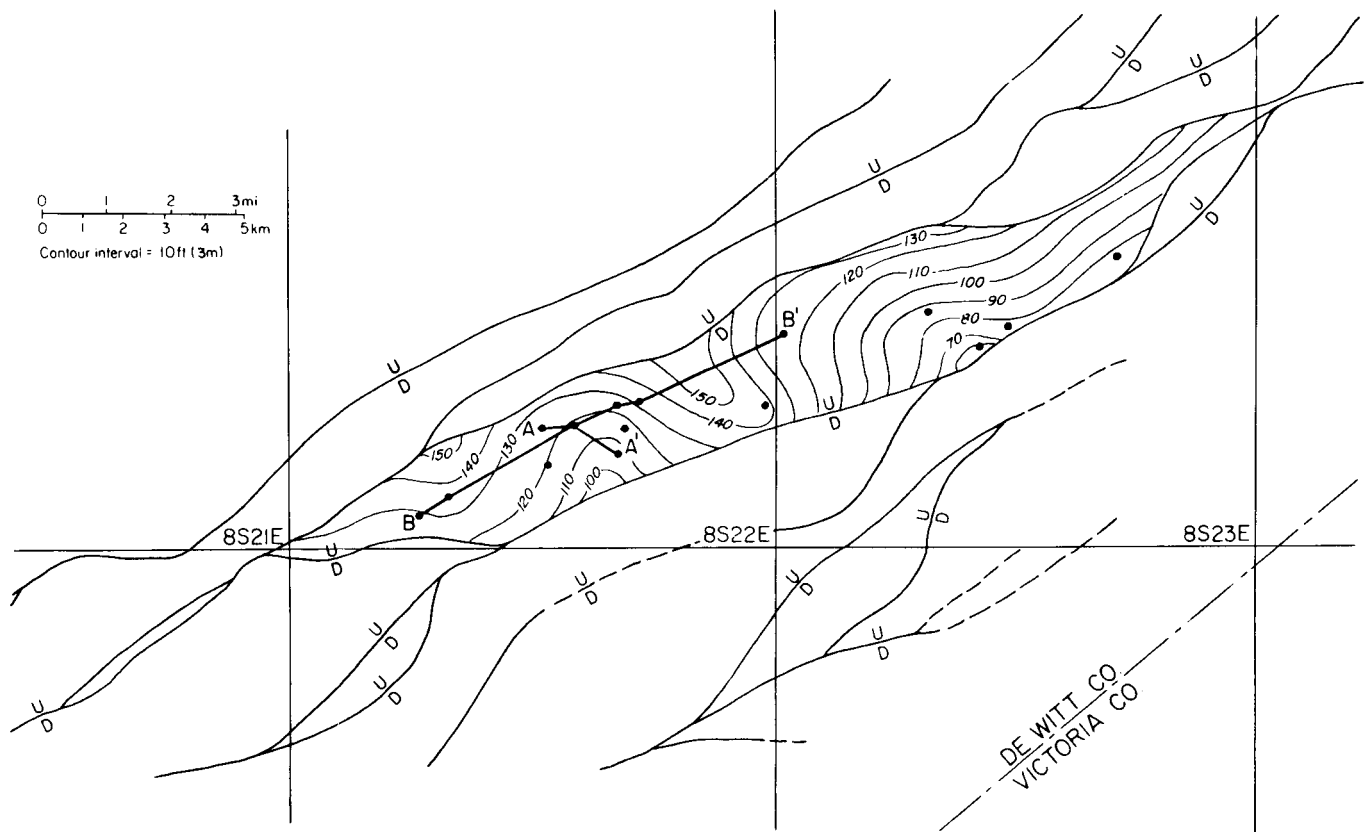


Figure 111. Net sandstone in correlation unit G, Cuero fault block.

## COLORADO FAIRWAY

### Formation and Fluid Properties

#### *Depositional and Structural Style*

The Colorado Fairway extends over approximately 440 mi<sup>2</sup> in parts of Colorado, Austin, and Wharton Counties (fig. 112). The area was recognized as a geopressured geothermal fairway in an earlier study by Bebout and others (1978a). A thick section of sandstones, having net-sandstone values of 1,200 to 1,600 ft, occurs in the lower Wilcox in parts of the fairway (fig. 34). Although most of the wells in the area do not penetrate the geopressured zone, certain wells show that the deepest sandstones of the lower Wilcox are geopressured and have fluid temperatures greater than 300°F.

The Wilcox section in the Colorado Fairway is similar to that of the De Witt Fairway; the upper and lower Wilcox contain thick sandstones and are separated by the more shaly section of the middle part of the Wilcox (fig. 113). A correlation marker, C1, occurs at the base of the upper Wilcox and can be extended into other fairways. This is the "regional marker" shown on regional cross sections (figs. 11 through 33, in pocket) and is equivalent to D1 in the De Witt Fairway and H1 in the Harris Fairway. Three other Wilcox stratigraphic markers, C2, C3, and C4, were used for local correlation within the Colorado Fairway (fig. 113); the C3 marker, equivalent to the H3 marker in the Harris Fairway, was the only one of these three markers to be traced outside the Colorado Fairway.

The C4 marker occurs at depths of 160 to 250 ft above the top of the lower Wilcox, shown on regional cross sections 13 and 14 (figs. 23 and 24). Throughout most of the Colorado Fairway, the lower Wilcox contains massive sandstones. Rapid facies changes, however, in addition to faults and sparse deep well control, make the lower Wilcox section difficult to correlate. Only within the Eagle Lake fault block was the lower Wilcox subdivided.

Down-to-the-coast faults are common in the Colorado Fairway, as shown by the structure map of the C4 marker (figs. 114a and b) and cross sections A-A', B-B', and C-C' (figs. 115 through 117). However, no large upper Wilcox growth faults that are characteristic of the fairways of the Lower Texas Gulf Coast occur in the Colorado Fairway. Growth faults affecting the lower Wilcox probably exist but are not detected because of the sparse deep well control.

Many wells in Colorado County do not reach highly geopressured zones. Some wells have pressure gradients only slightly greater than hydrostatic, probably because they were not drilled deep enough to penetrate formations with higher pressures. The shale resistivity versus depth plot for the Union No. A-1 Thomas well is typical of wells in the Colorado Fairway (fig. 118). The Union No. A-1 Thomas, located on cross section M-M' (fig. 119), was a dry hole drilled to a total depth of 11,901 ft. Details of core-analysis data and fluid properties are given for this well in the next section.

An equilibrium temperature of 300°F occurs at an average depth of 12,470 ft in Colorado County (fig. 120). Geothermal gradients average 1.40°F per 100 ft down to a depth of 8,000 ft. Below 8,000 ft, the gradient is 2.67°F per 100 ft.

Average porosity and permeability in the depth interval of 9,840 to 9,854 ft in the Shell No. 1 Engstrom (5S-29E-9), 17 mi to the southwest of the fault block, were 15.9 percent and 16.8 md, respectively. Sidewall-core measurements from several wells indicate porosities of 20 to 30 percent and permeabilities up to 450 md in sandstone intervals occurring between depths of 8,000 and 11,000 ft.

#### *Eagle Lake Fault Block*

The Eagle Lake fault block extends over an elongate area of approximately 17.4 mi<sup>2</sup> within the Colorado Fairway in eastern Colorado County (fig. 121). The block is bounded on the northwest and southeast by major faults.

The top of the lower Wilcox sandstone section below marker C4 in the Union No. A-1 Thomas well (fig. 119) occurs at a depth of 11,180 ft. Within the fault block, the top of the sandstone interval ranges in depth from 10,960 to 11,400 ft. Although none of the existing wells in the fault block penetrated the entire sandstone interval, wells along strike but several miles from the fault block indicate that the entire sandstone section is at least 1,600 ft thick. Trends of the lower Wilcox sandstone are projected to thicken into the syncline in the fault block, as shown by detailed correlation units A through F (fig. 122). The base of the sandstone interval in the fault block should be at depths ranging from about 12,600 to 13,300 ft. The sandstone beds range in thickness from 8 to 70 ft, and the intervening shale beds are from 5 to 40 ft thick.

Diamond-core analyses from the sandstone interval below marker C4 in the Union No. A-1 Thomas well show that porosity ranges from 4 to 19 percent and averages 13 percent. Most of the sandstone section is characterized by permeabilities of less than 5 md (fig. 123). However, permeabilities range from 89 to 545 md and average 275 md in the thin sandstone interval between depths of 11,620 and 11,624 ft. Several other isolated thin sandstones have permeabilities ranging from 10 to 100 md.

In the Union No. A-1 Thomas well, fluid temperatures of 200° and 300°F occur at depths of 7,100 and 11,780 ft, respectively. Temperatures in the sandstone section of this well range from 275°F, calculated for the top of the sandstone

interval at 11,180 ft, to 302°F, recorded at the total depth of 11,826 ft.

As determined from mud weights, the highest pressure gradient in the Union No. A-1 Thomas well is 0.634 psi per foot, which was reached at a depth of 11,300 ft. Bottom-hole pressure was calculated to be 7,164 psi on the basis of that gradient (fig. 118).

Salinities were computed only for this well (fig. 124). In shallow formations, values of salinity increase from about 60,000 ppm to a maximum of 119,000 ppm NaCl at a depth of 6,665 ft, where the temperature approaches 200°F. Below 6,665 ft, salinities decline to a minimum value of 59,000 ppm NaCl at a depth of 10,910 ft and then increase again to 113,000 ppm NaCl at a depth of 11,760 ft, where the temperature is about 300°F.

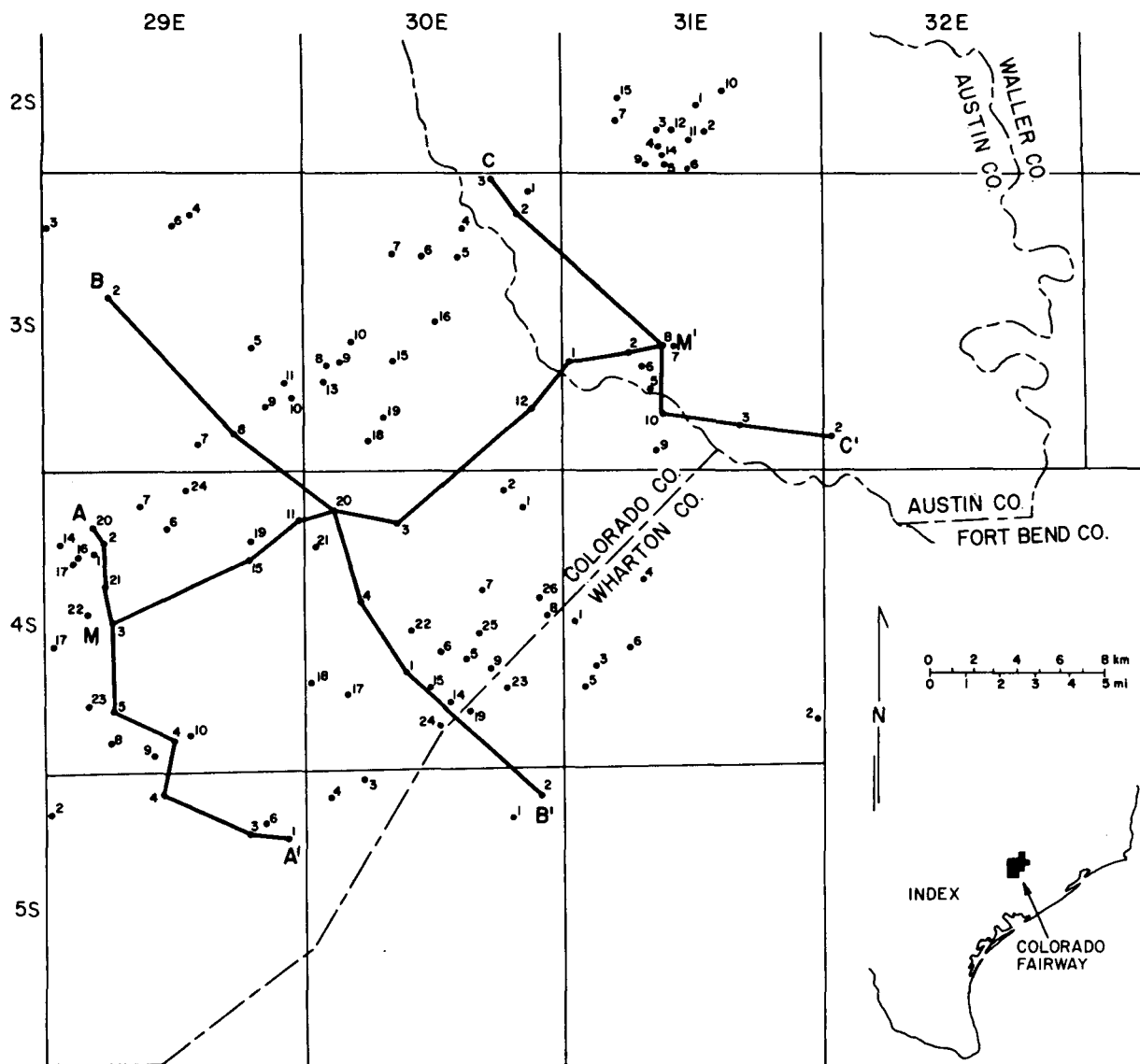


Figure 112. Location of wells and lines of section, Colorado Fairway.

C

C

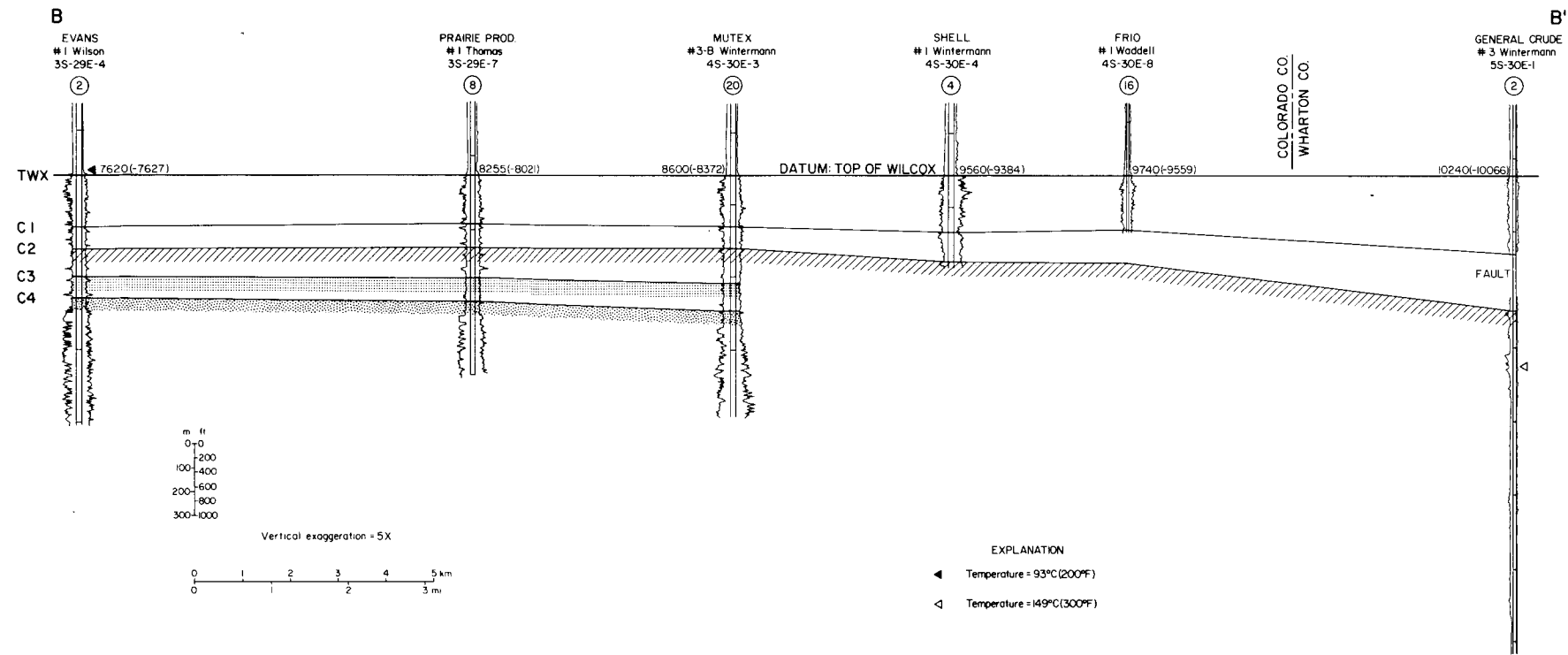


Figure 113. Stratigraphic dip section B-B', Colorado Fairway.

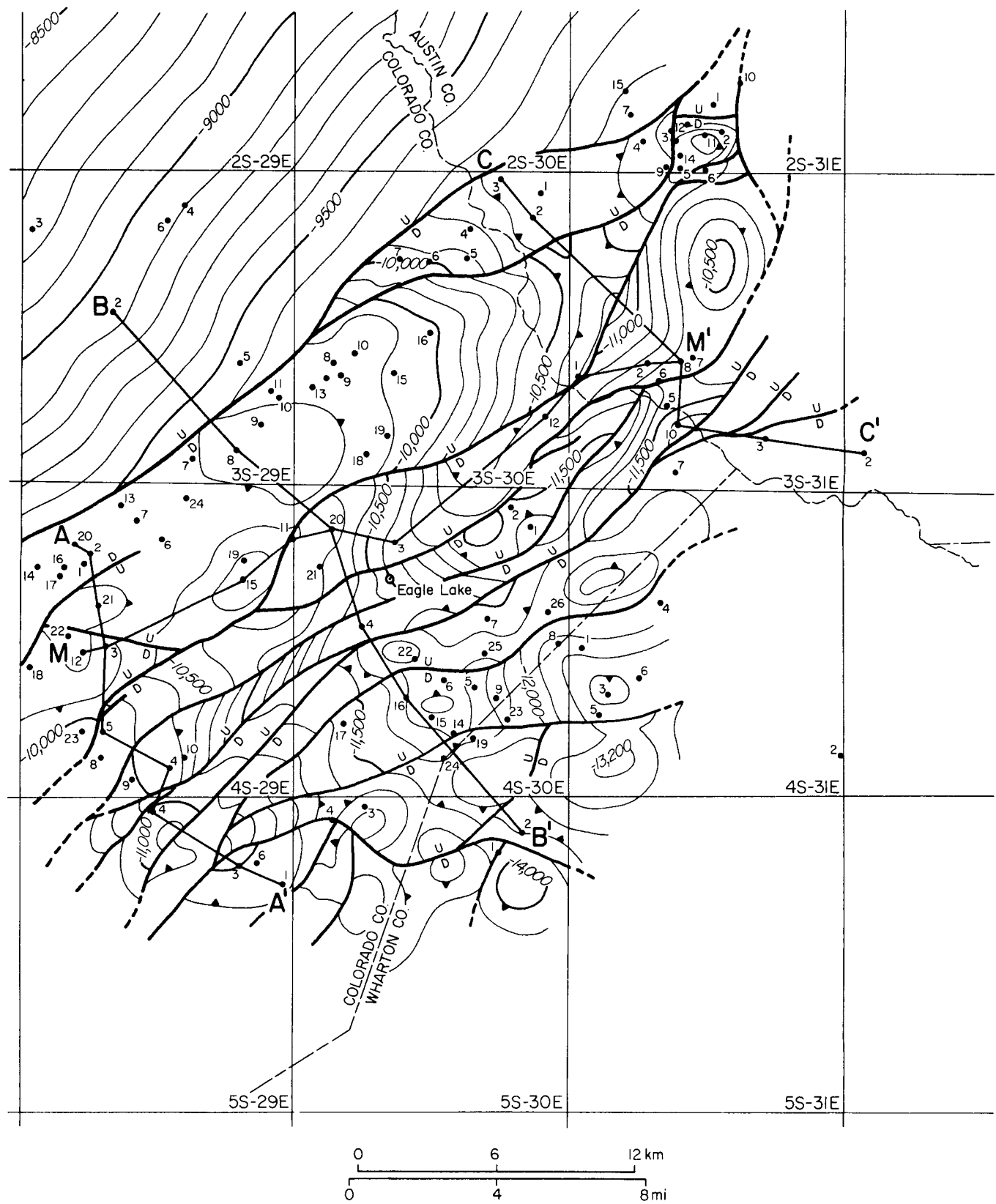


Figure 114a. Structural map, Colorado Fairway.

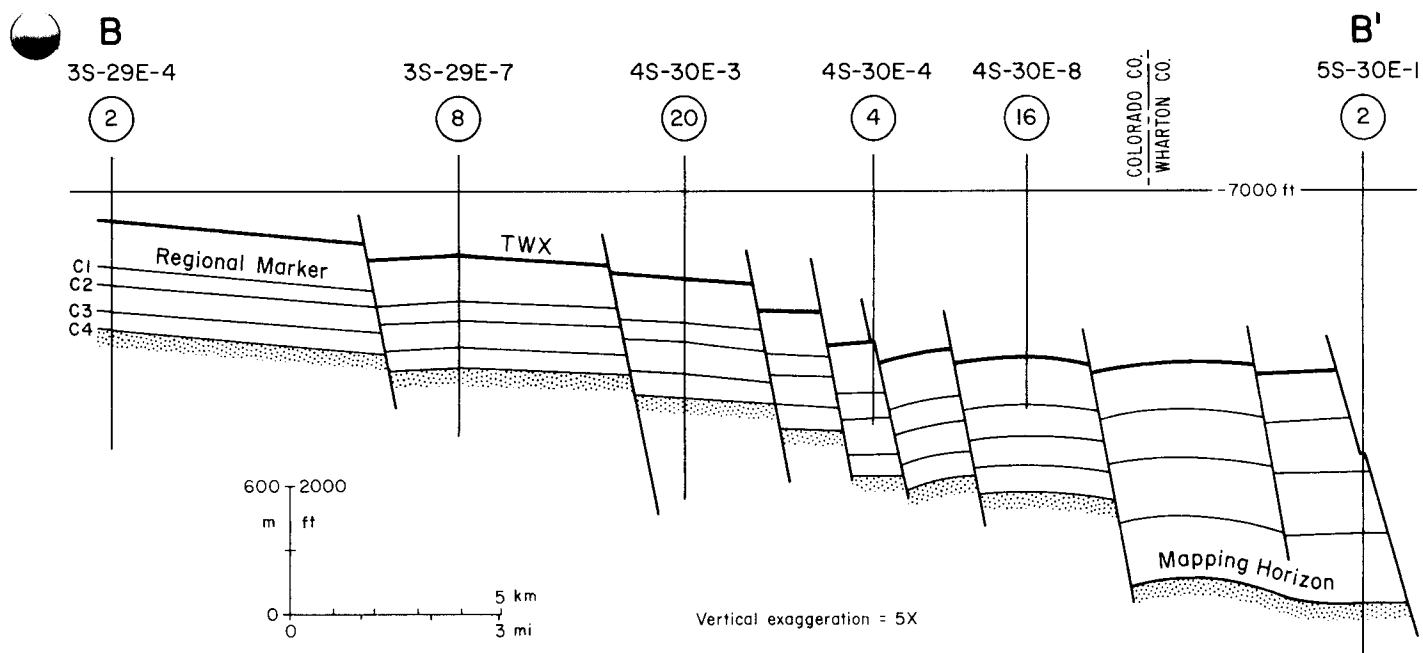


Figure 114b. Index section, Colorado Fairway. Mapping horizon is the C4 marker, which occurs slightly above the top of the lower Wilcox.

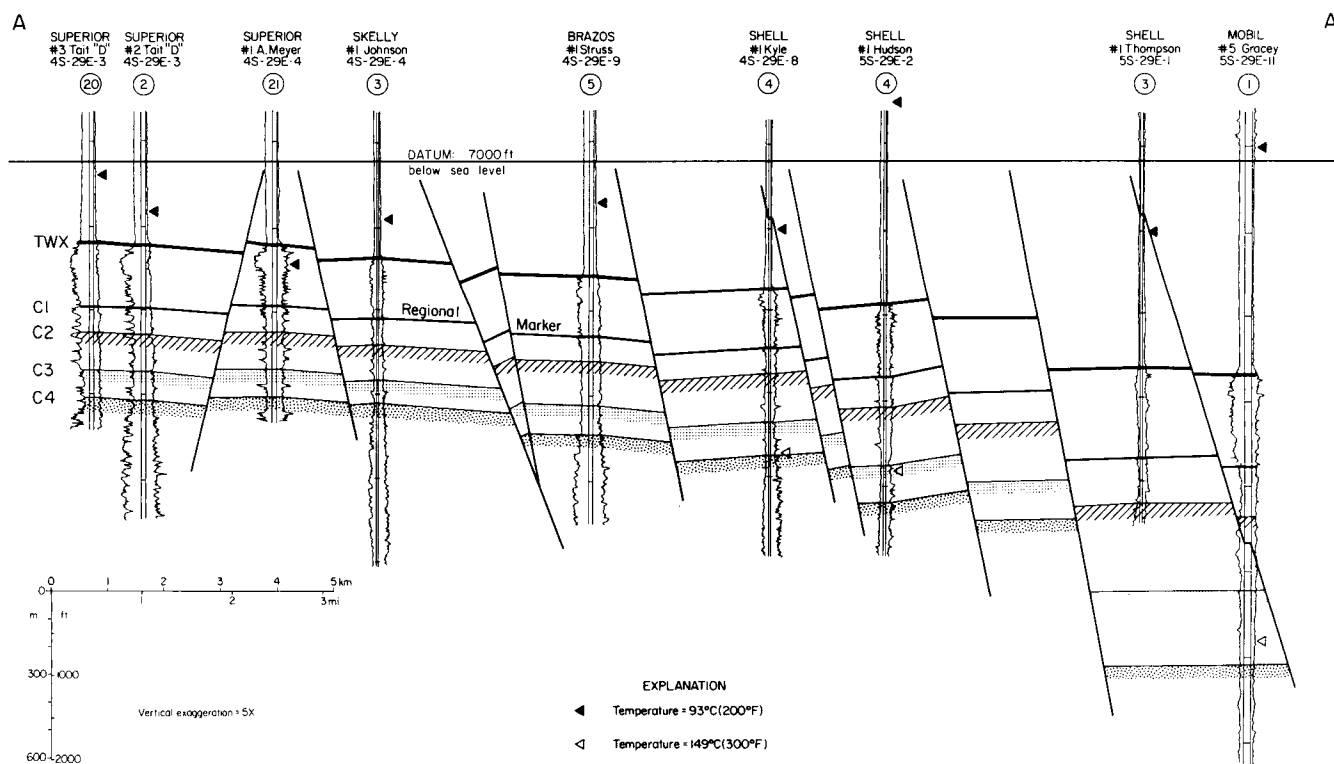


Figure 115. Structural dip section A-A', Colorado Fairway.

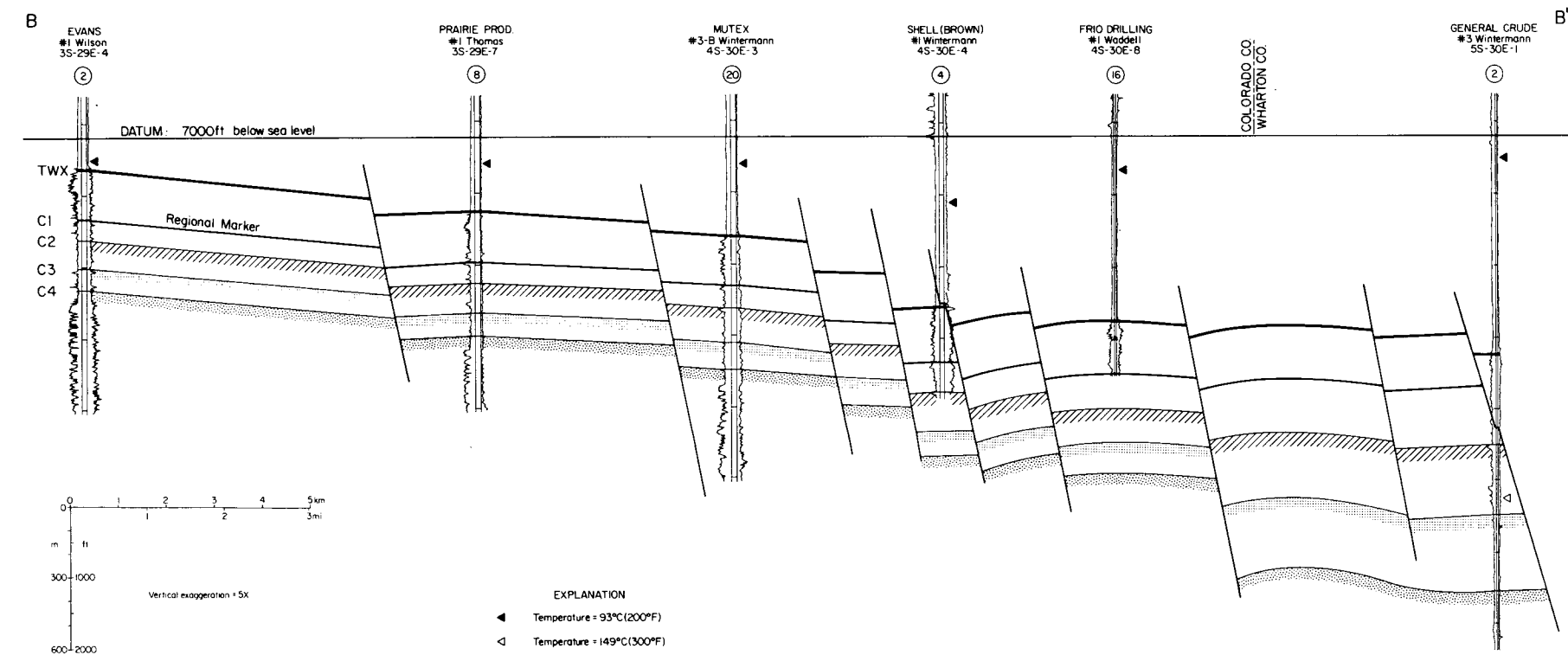


Figure 116. Structural dip section B-B', Colorado Fairway.

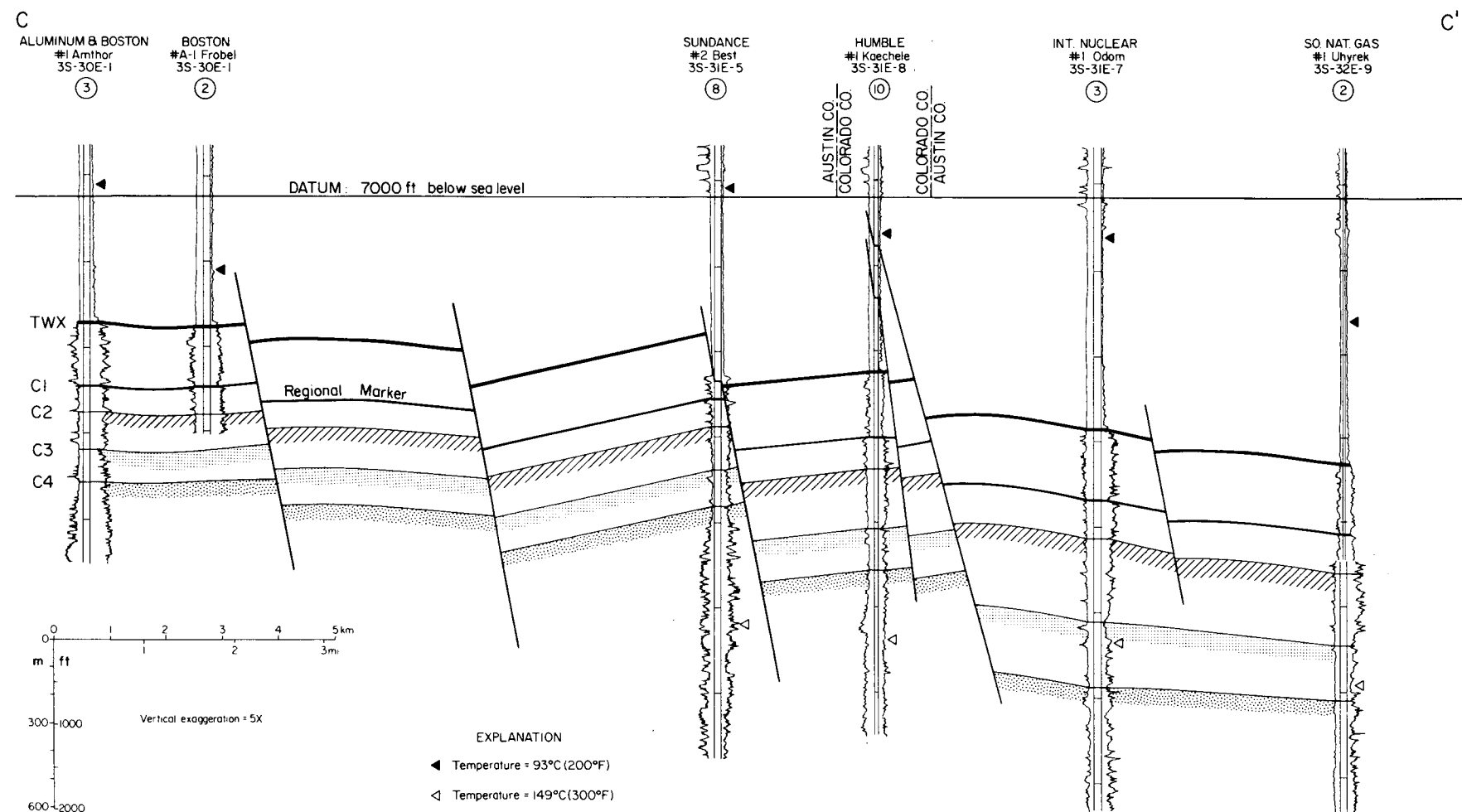


Figure 117. Structural dip section C-C', Colorado Fairway.

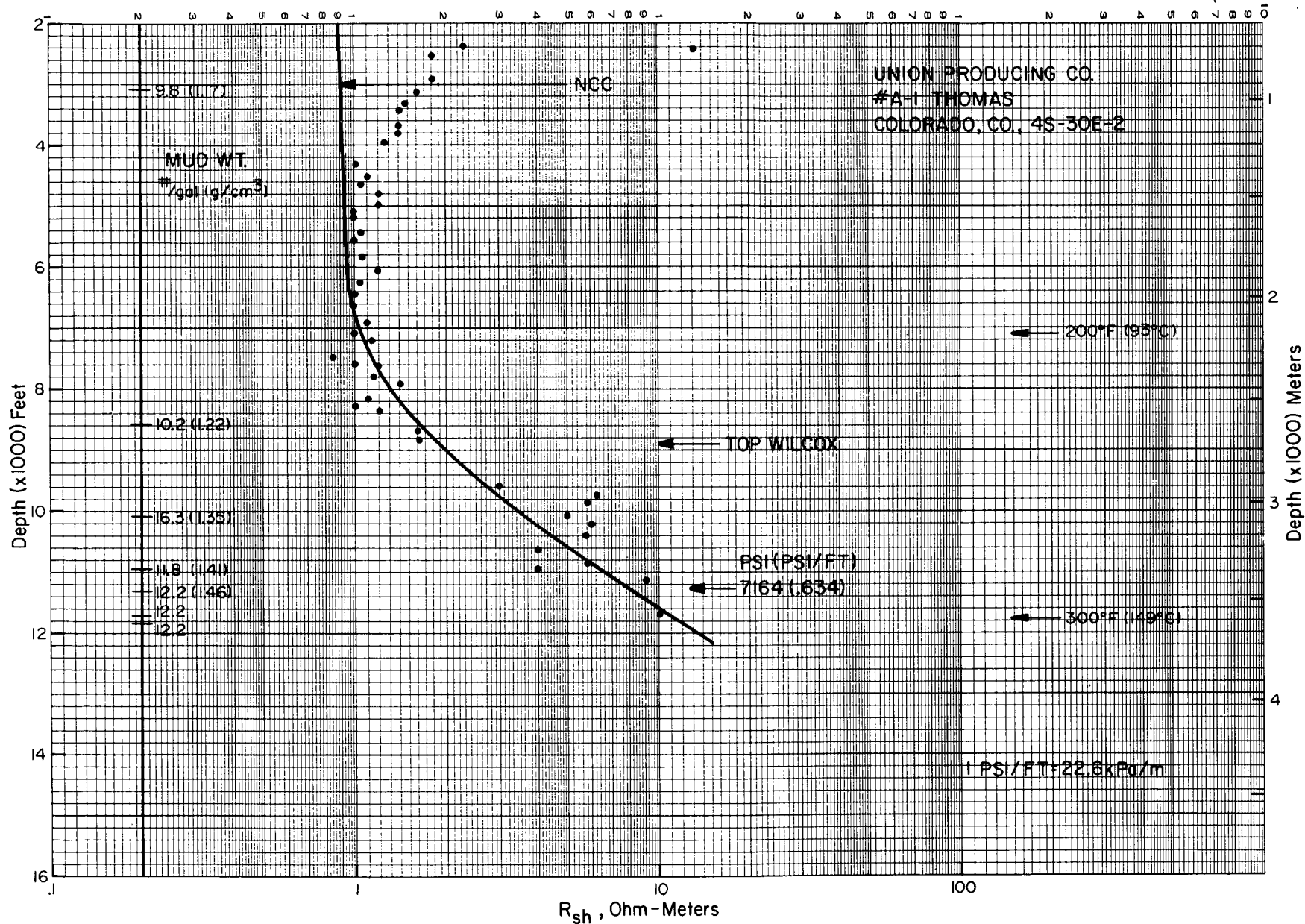


Figure 118. Shale resistivity versus depth for the Union No. A-1 Thomas well on cross section M-M', Colorado County.

M

M'

SKELLY  
#1 Johnson  
4S-29E-4

KIRKWOOD &  
ANDERSON  
#1 Johnson  
4S-29E-4

MUTEX  
#3-B Wintermann  
4S-30E-3

HUMBLE  
#1 Lange  
4S-29E-1

SKELLY  
#1 Wintermann  
4S-29E-1

UNION  
#A-1 Thomas  
4S-30E-2

COLORADO CO. AUSTIN CO.

HUMBLE  
#1-B Kaechele  
3S-31E-4

SUNDANCE  
#2 Best  
3S-31E-5

(2) (3)

(15)

(11)

(20)

(3)

(12)

(1)

(2)

(8)

DATUM: 7000 ft.  
below sea level

TWX

C1

C2

C3

C4

C5

Regional Marker

m  
0 0

200  
400

Vertical exaggeration=10X

0 2 4 6 8 10 km  
0 2 4 6 8 mi

EXPLANATION

- ◀ Temperature = 93°C (200°F)
- △ Temperature = 149°C (300°F)

Figure 119. Structural strike section M-M', Colorado Fairway.

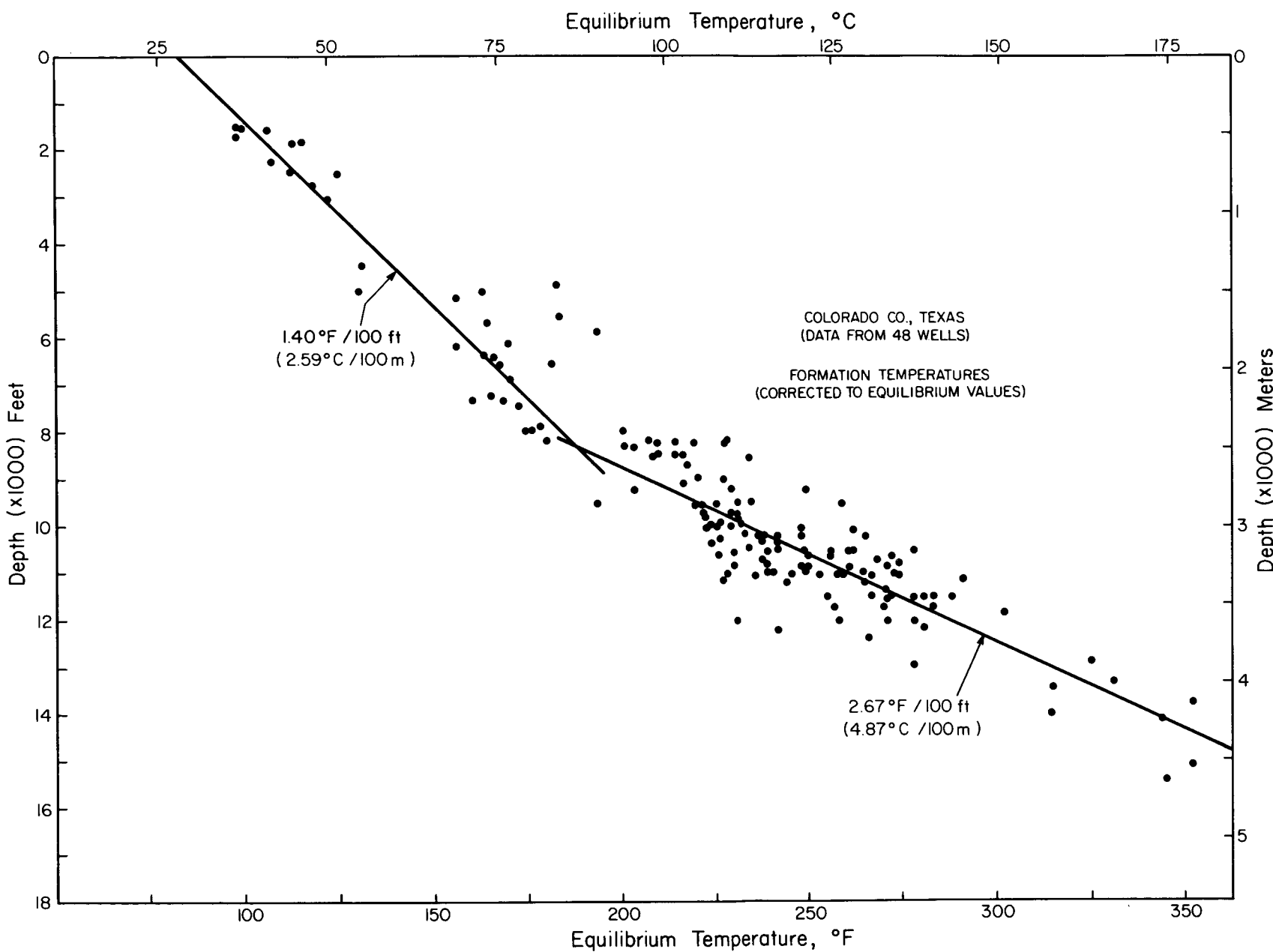


Figure 120. Temperatures and geothermal gradients for 48 wells in Colorado County.

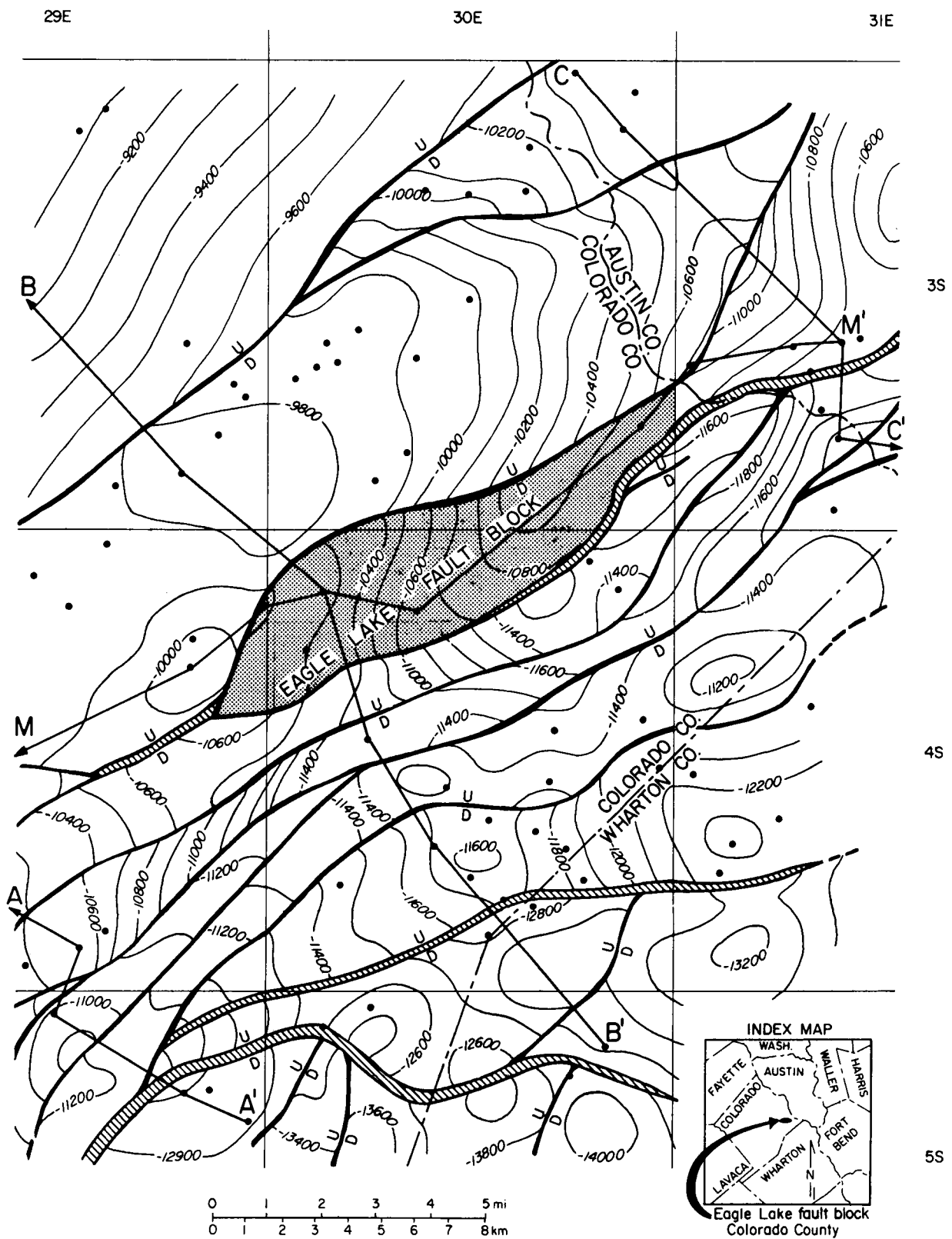


Figure 121. Eagle Lake fault block, Colorado Fairway. Mapping horizon is the C4 marker, which occurs slightly above the top of the lower Wilcox. Contour interval is 100 ft.

001

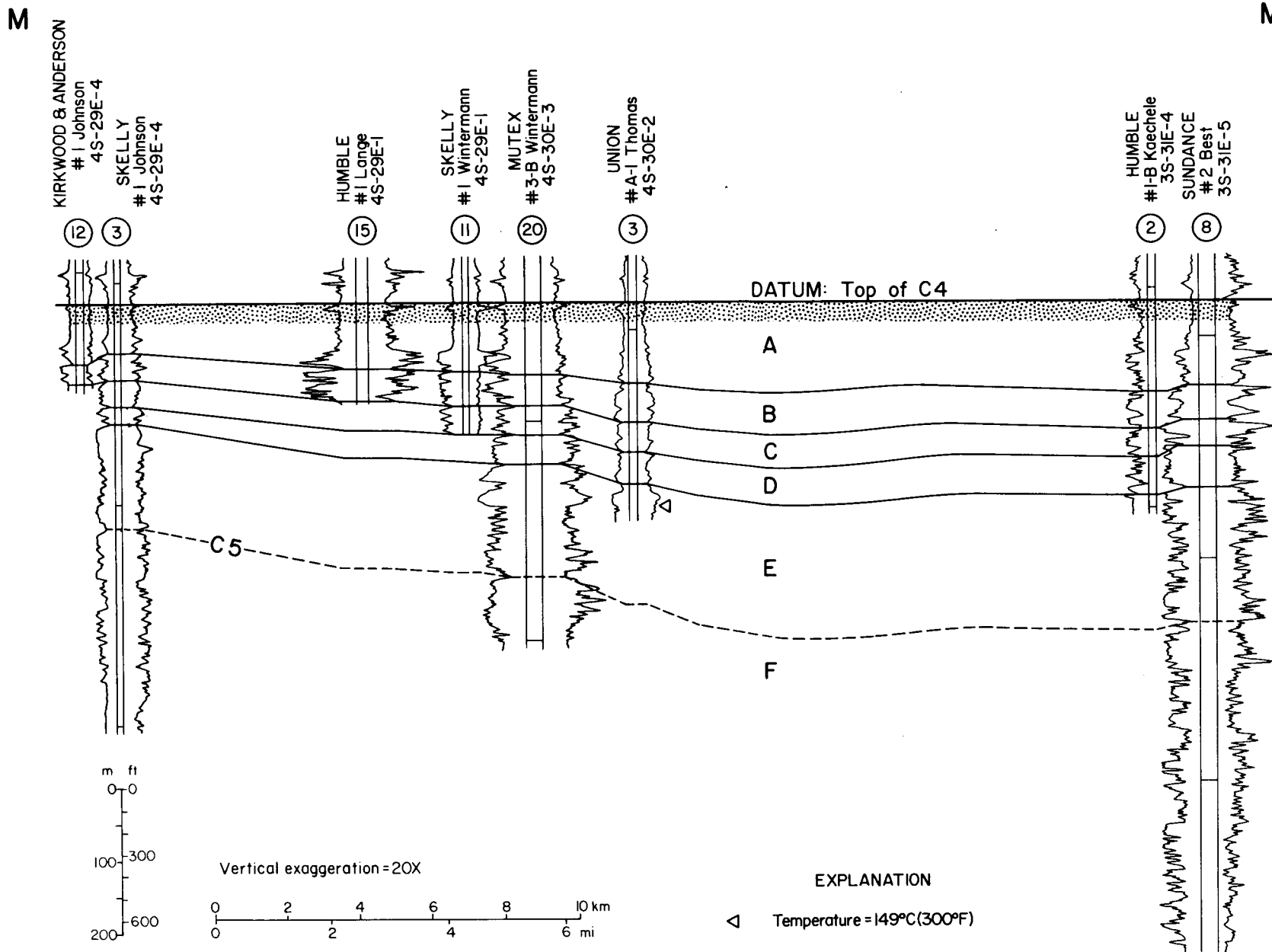


Figure 122. Stratigraphic strike section M-M', Colorado Fairway. Datum is the C4 marker. The reservoir section below the C4 marker is correlated in detail (units A through F).

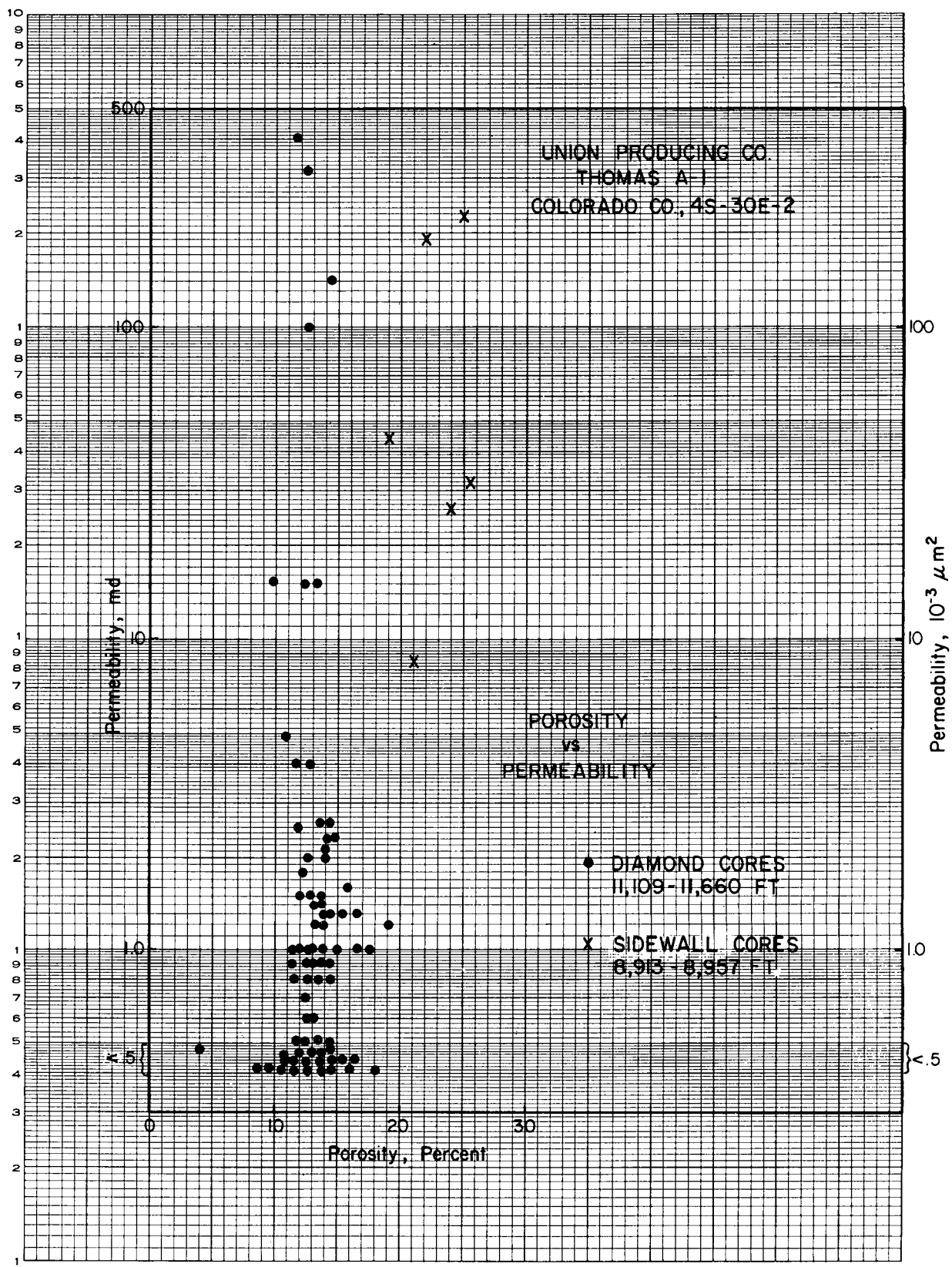
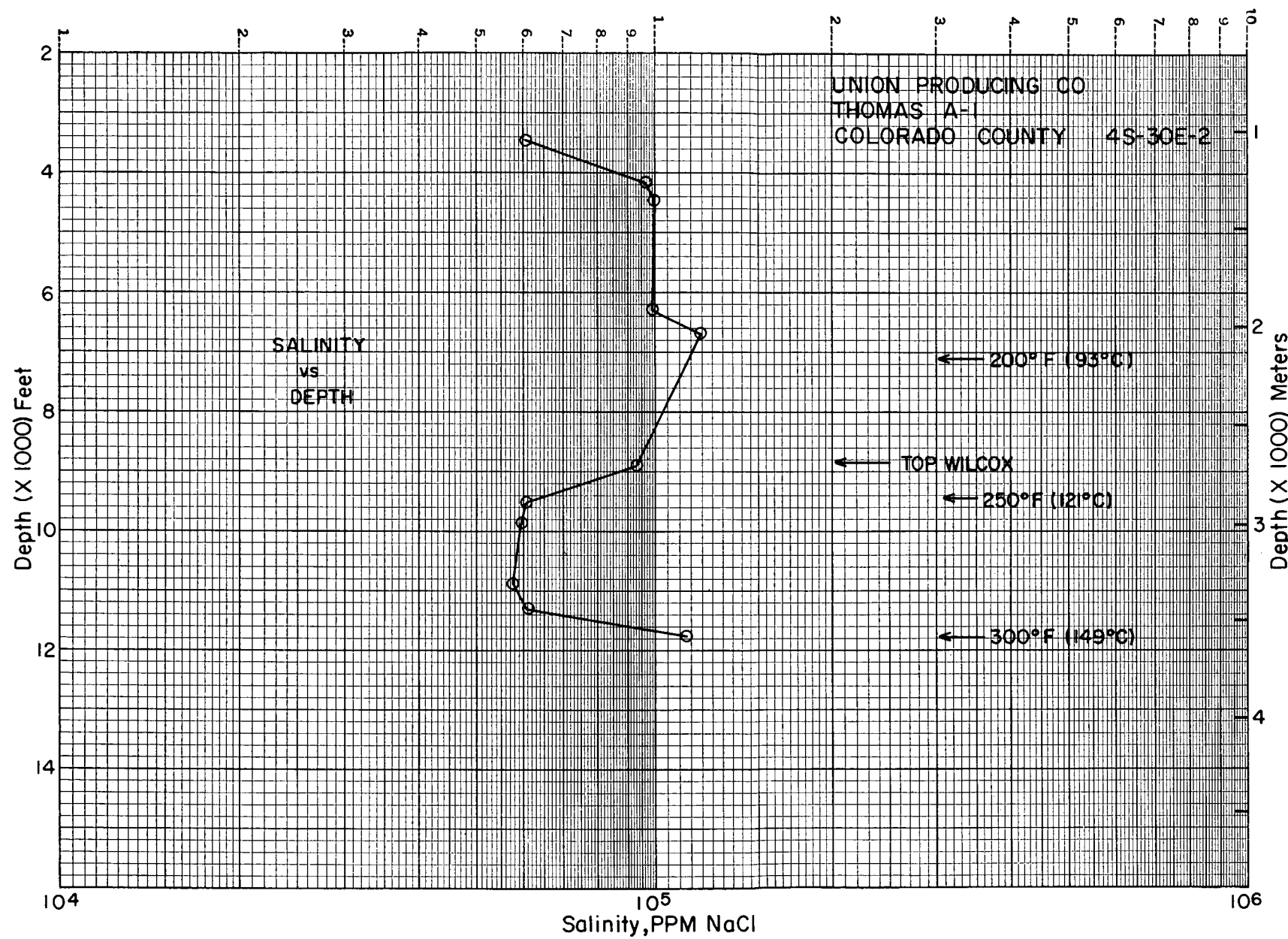


Figure 123. Porosity versus permeability for the Union No. A-1 Thomas well on cross section M-M', Colorado County.



## HARRIS FAIRWAY

The Harris Fairway trends northeast and extends over parts of Waller, Fort Bend, Harris, Grimes, Montgomery, Liberty, and San Jacinto Counties (fig. 125). The fairway study area is approximately 77 mi long and 34 mi wide. This fairway was delineated as an area of potential geopressured geothermal reservoirs in an earlier study (Bebout and others, 1978a). This area was selected for continued study because very thick, massive sandstones are present in the lower Wilcox. Maximum net-sandstone values

(thicknesses of more than 2,000 ft) for the lower Wilcox of Texas occur within the Harris Fairway (fig. 34). Much of the lower Wilcox sandstone in the downdip parts of this area is geopressured and has fluid temperatures greater than 300°F.

The Harris study area extends farther updip than do the Colorado or De Witt study areas. The Wilcox in these updip parts of the Harris Fairway is sandy throughout, as shown by the logs of wells farthest updip on stratigraphic section D-D' (fig. 126). Downdip in this fairway, however, the Wilcox section is similar to that of the Colorado and De Witt Fairways; the middle Wilcox is shaly, and the

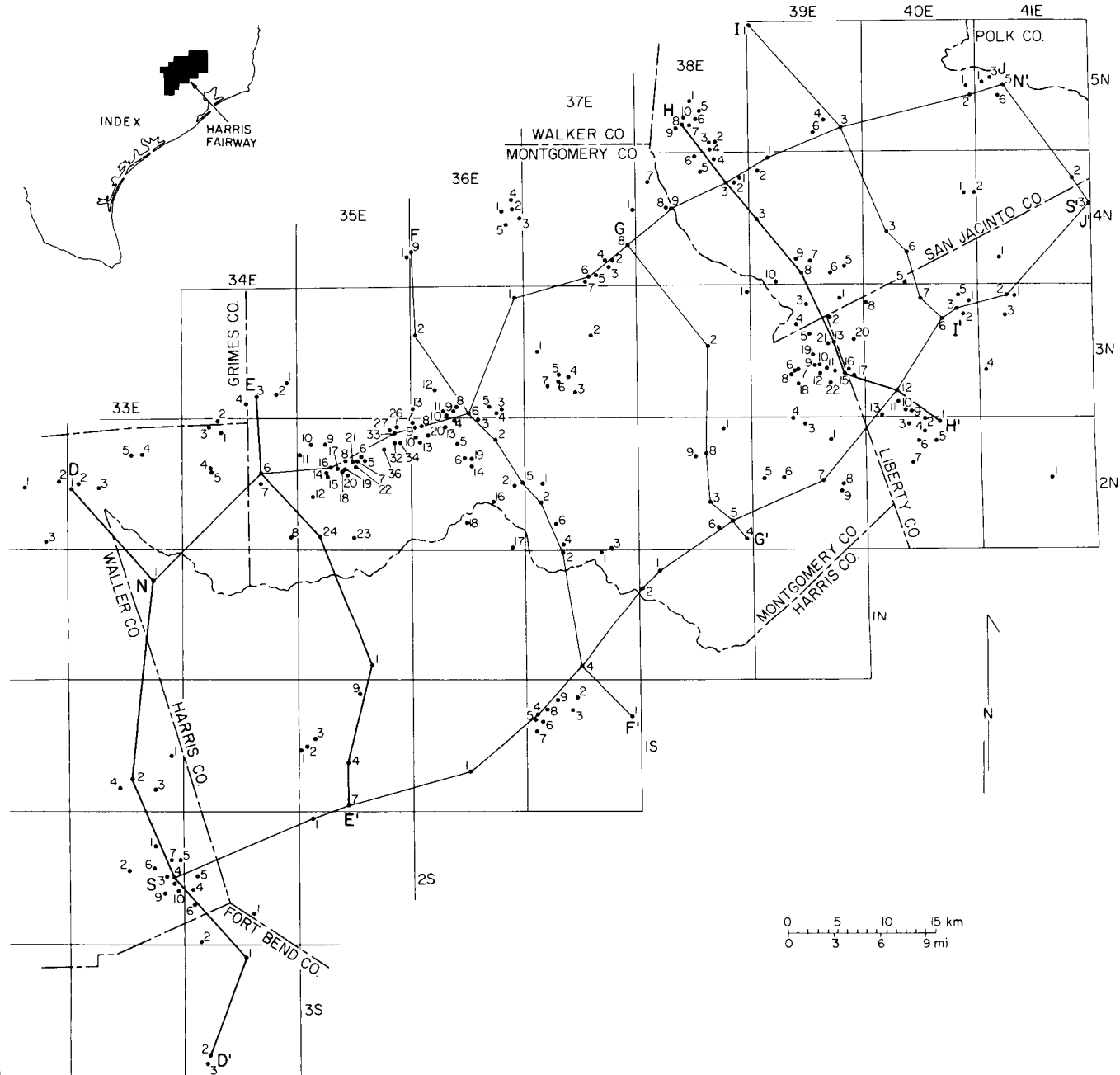


Figure 125. Location of wells and lines of section, Harris Fairway.

upper and lower Wilcox sandy intervals are much more distinct.

The upper Wilcox contains massive sandstone units over the entire Harris Fairway. The H1 marker occurs at the base of the upper Wilcox (fig. 126) and can be correlated into other fairways. This marker is the "regional marker" shown on the regional cross sections (figs. 11 through 33, in pocket) and is equivalent to C1 in the Colorado Fairway and D1 in the De Witt Fairway. Three other markers, H2, H3, and H4, are recognized locally within the Harris Fairway (fig. 126); H3 is the only marker to be traced outside the Harris Fairway and is equivalent to the C3 marker in the Colorado Fairway (fig. 113).

The H4 marker occurs at depths of 40 to 360 ft below the top of the lower Wilcox, shown on regional cross sections 15 through 19 (figs. 25 through 29). Throughout most of the Harris Fairway, the lower Wilcox contains massive sandstones. As in the De Witt and Colorado

Fairways, however, rapid facies changes, faults, and sparse deep well control make the lower Wilcox section difficult to correlate. Thus, the thick section having potential for geopressured geothermal reservoirs could not be subdivided for more detailed study and construction of meaningful net-sandstone maps. Cross sections, however, indicate areas of maximum sandstone. Lower Wilcox intervals of thick net sandstone, all or much of it geopressured and having fluid temperatures greater than 300°F, are shown on the Humble No. 31 Katy Gas Field well log (cross section D-D', fig. 127) and the Texaco No. 1 Mergele and Texaco No. 1 Sweeney Estate logs (section E-E', fig. 128).

The Harris Fairway is an area of salt domes and salt withdrawal basins. Parts of the middle and upper Wilcox thin over a few of the domes. The thinning is probably due to a lack of deposition, rather than the result of erosion. Therefore, some of the domes began to grow

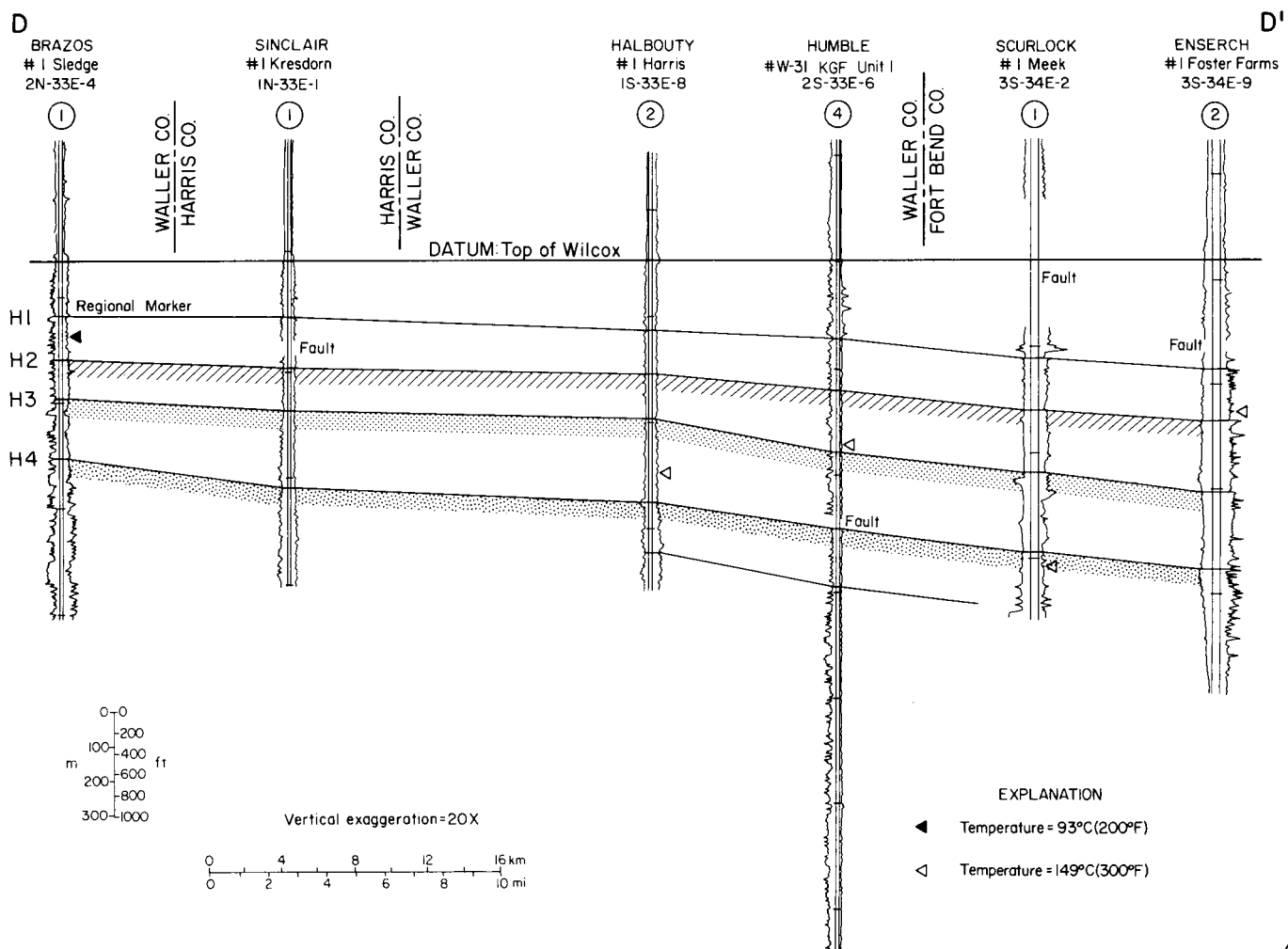


Figure 126. Stratigraphic dip section D-D', Harris Fairway.

during or before Wilcox deposition, whereas others did not affect Wilcox structure until after deposition and burial.

Down-to-the-coast faults are common in the Harris Fairway, but Wilcox growth faults with large displacements are rarer here than in most of the other fairways to the southwest. The upper and middle Wilcox show no differential growth caused by fault movement except in the areas farthest downdip (southeastward). Stratigraphic section D-D' (fig. 126) illustrates the gradual downdip

thickening of the intervals defined by the various correlation markers. Examples of growth faults occurring in the most basinward part of the fairway are shown on the Scurlock No. 1 Meek well log on structural cross section D-D' (fig. 127) and on the Superior No. 1 Hightower well log on section H-H' (fig. 129). Growth faults affecting the lower Wilcox within the fairway may be more numerous and of greater magnitude but are much more difficult to characterize because of the sparse deep well control.

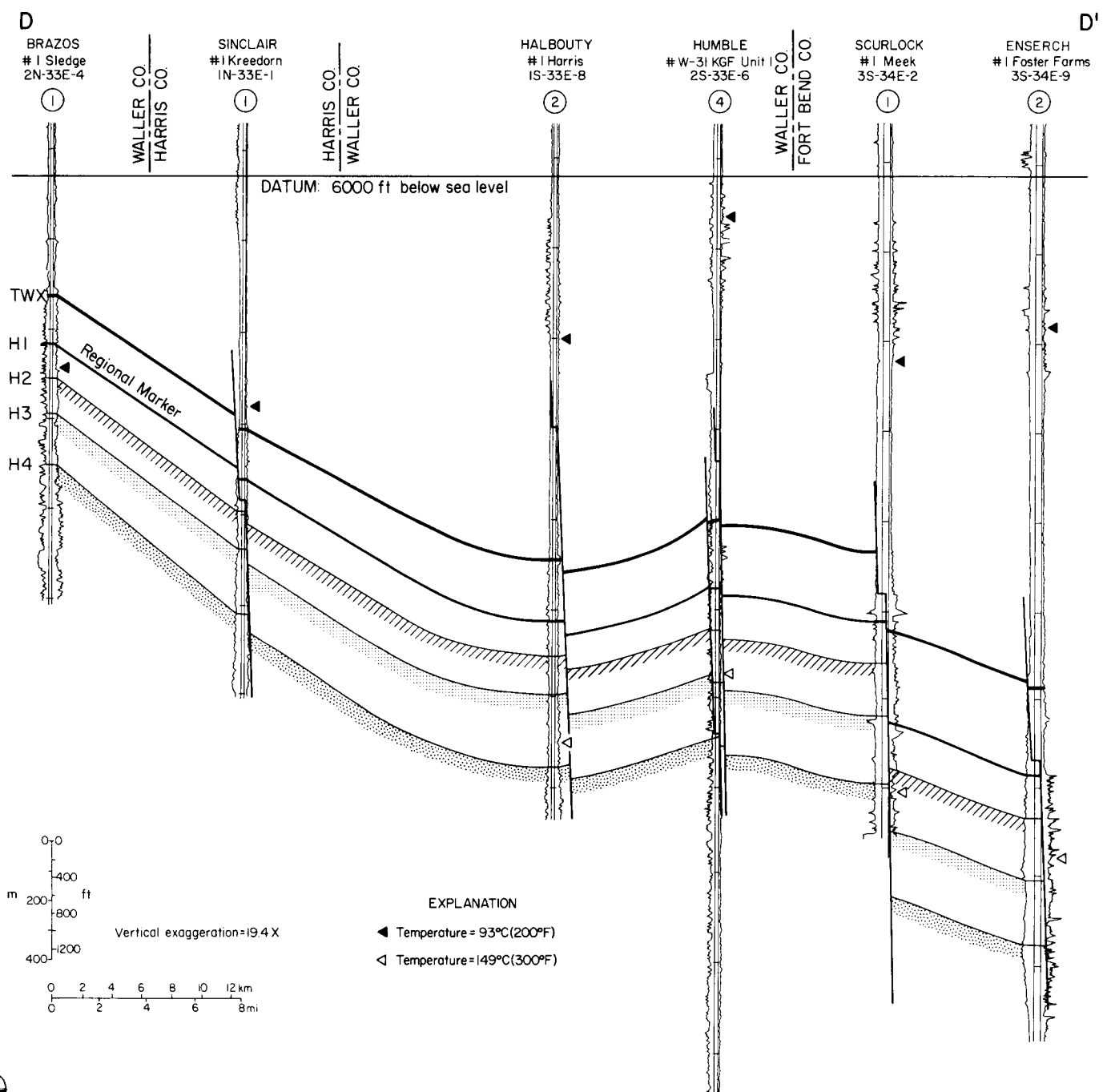


Figure 127. Structural dip section D-D', Harris Fairway.

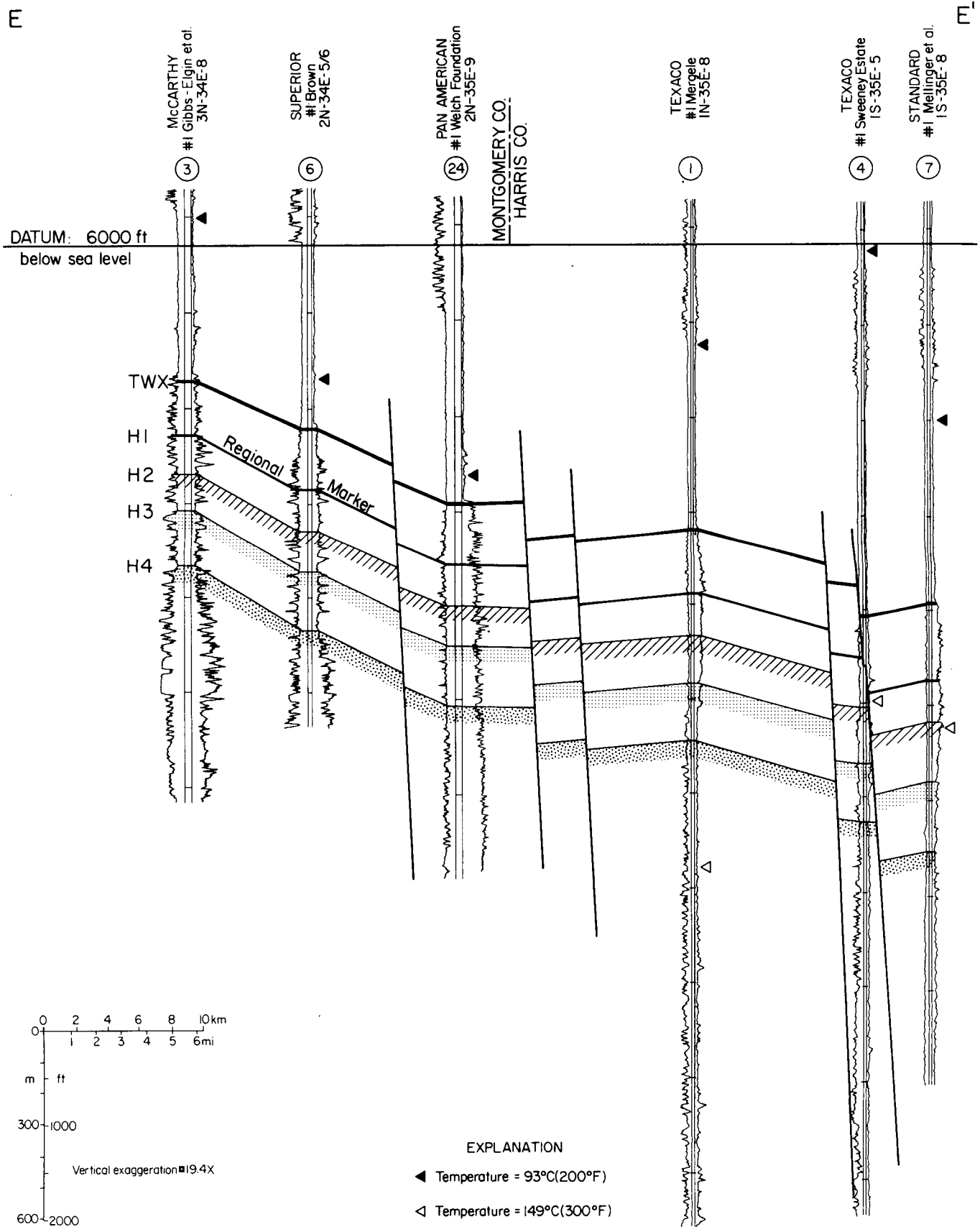


Figure 128. Structural dip section E-E', Harris Fairway.

H

H'

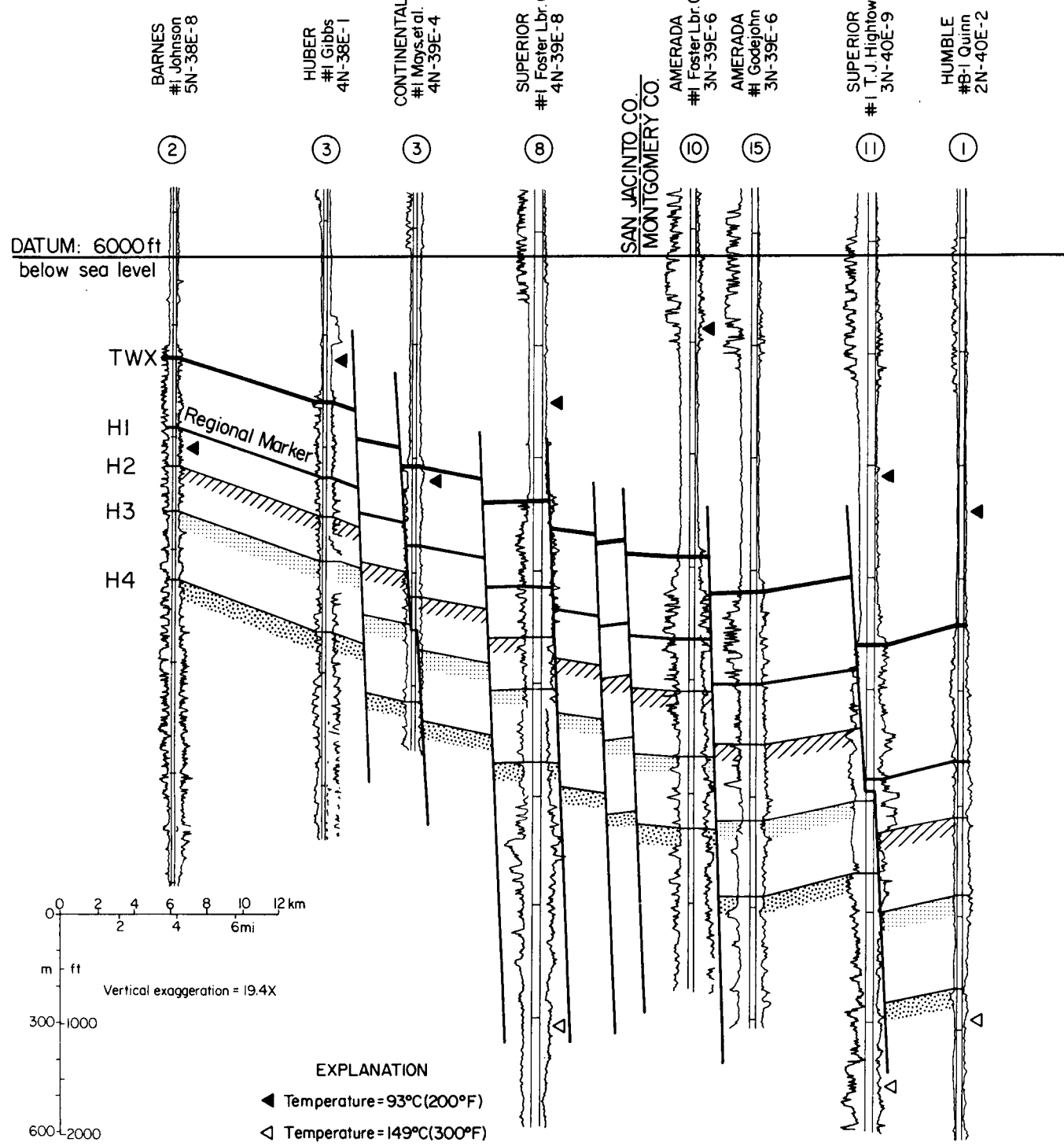


Figure 129. Structural dip section H-H', Harris Fairway.

Average depths to the top of geopressure gradients of 0.465 and 0.70 psi per foot are 9,150 and 11,550 ft, respectively (fig. 130); these calculations are based on bottom-hole shut-in pressure measured in 23 wells in Harris County. Pressure gradients increase with depth to a maximum of 0.84 psi per foot at a depth of 13,350 ft. Operational top of geopressure was picked from shale resistivity plots for selected wells on the geological cross sections. Wells with shale resistivities that fall on or to the right of the normal compaction curve (NCC) were not considered to be geopressured in this report (fig. 131). Geopressure profiles were computed for wells with shale resistivity values that were less than normal. An example of a well with highly geopressured formations is the Humble No. W-21 Katy Gas Field, Unit No. 1 (fig. 132).

Equilibrium temperatures and geothermal gradients have been calculated for an area that includes parts of Harris, Liberty, Austin, Colorado, and adjacent counties (fig. 133). The geothermal gradient in the upper Wilcox is about 2.10°F per 100 ft in the depth interval of 8,300 to 14,000 ft. The lower Wilcox from a depth of 14,000 to 18,000 ft has a gradient of about 1.20°F per 100 ft. Formations above the Wilcox at depths of 0 to 10,000 ft have a geothermal gradient of about 1.40°F per

100 ft. A subsurface temperature of 300°F occurs at 13,050 ft below sea level.

Plots of temperature versus depth (fig. 134) for wells on geological cross sections D-D', E-E', and H-H' show a geothermal gradient of 1.58°F per 100 ft above a 12,000-ft depth. A gradient of 2.16°F per 100 ft is present in deeper formations down to a 17,500-ft depth. A temperature of 300°F occurs at depths of about 12,990 ft.

As observed in 14 Harris Fairway wells, salinity decreases between depths of 7,600 and 13,000 ft (fig. 135). Maximum salinity of 197,000 ppm NaCl occurs at 8,500 ft, and minimum values of 11,500 to 20,000 ppm NaCl occur at depths between 10,600 and 14,450 ft. Few salinity values were calculated for shallow sandstones, but the normal trend is one of increasing salinity between depths of 2,000 and 8,200 ft.

Available diamond-core data for several wells in Harris County show that most permeabilities of sandstones in the deep subsurface are less than 1 md. Moderately good permeabilities of 1.5 to 19 md occur in a few thin sandstone intervals at depths exceeding 13,120 ft. Porosities in these thin sandstones average about 15 percent. Sidewall cores from the same wells have measured average permeabilities and porosities of 241 md and 32 percent, respectively, in the depth interval of 6,420 to 6,800 ft.

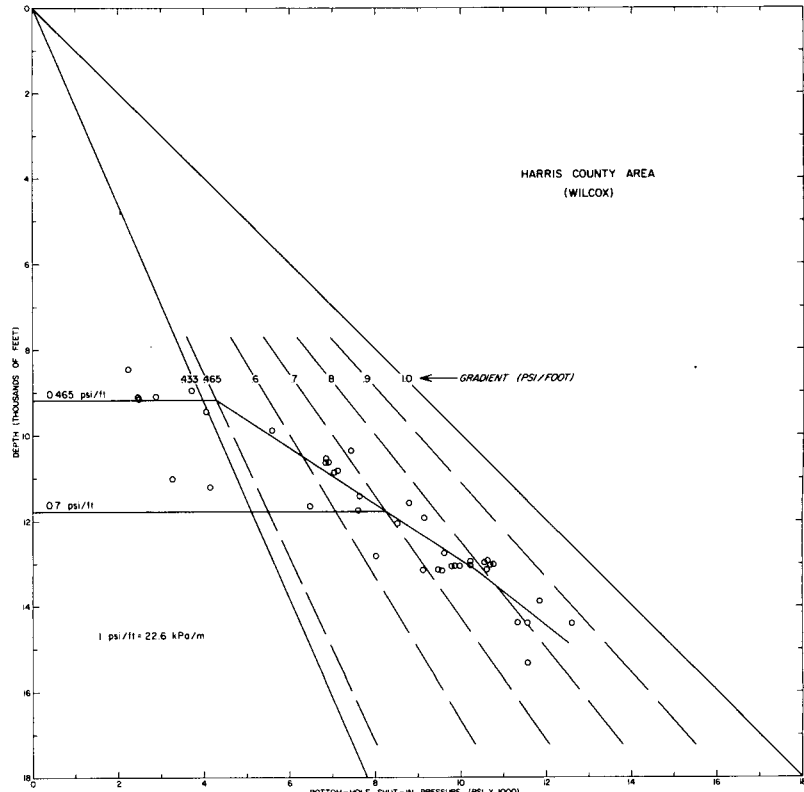


Figure 130. Bottom-hole shut-in pressures plotted as a function of depth for 23 wells in Harris County area.

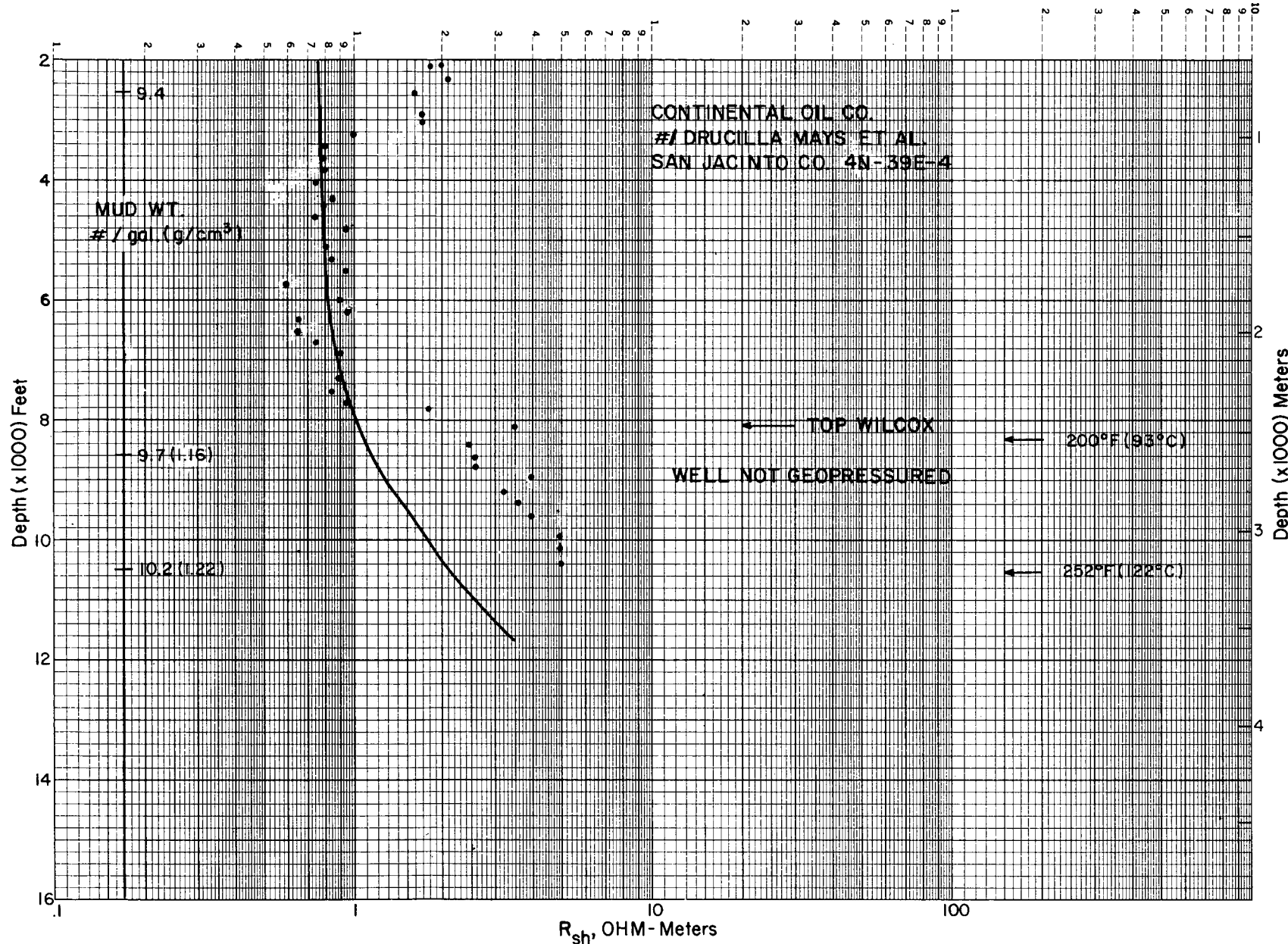


Figure 131. Shale resistivity versus depth for a nongeopressured well on cross section H-H', San Jacinto County.

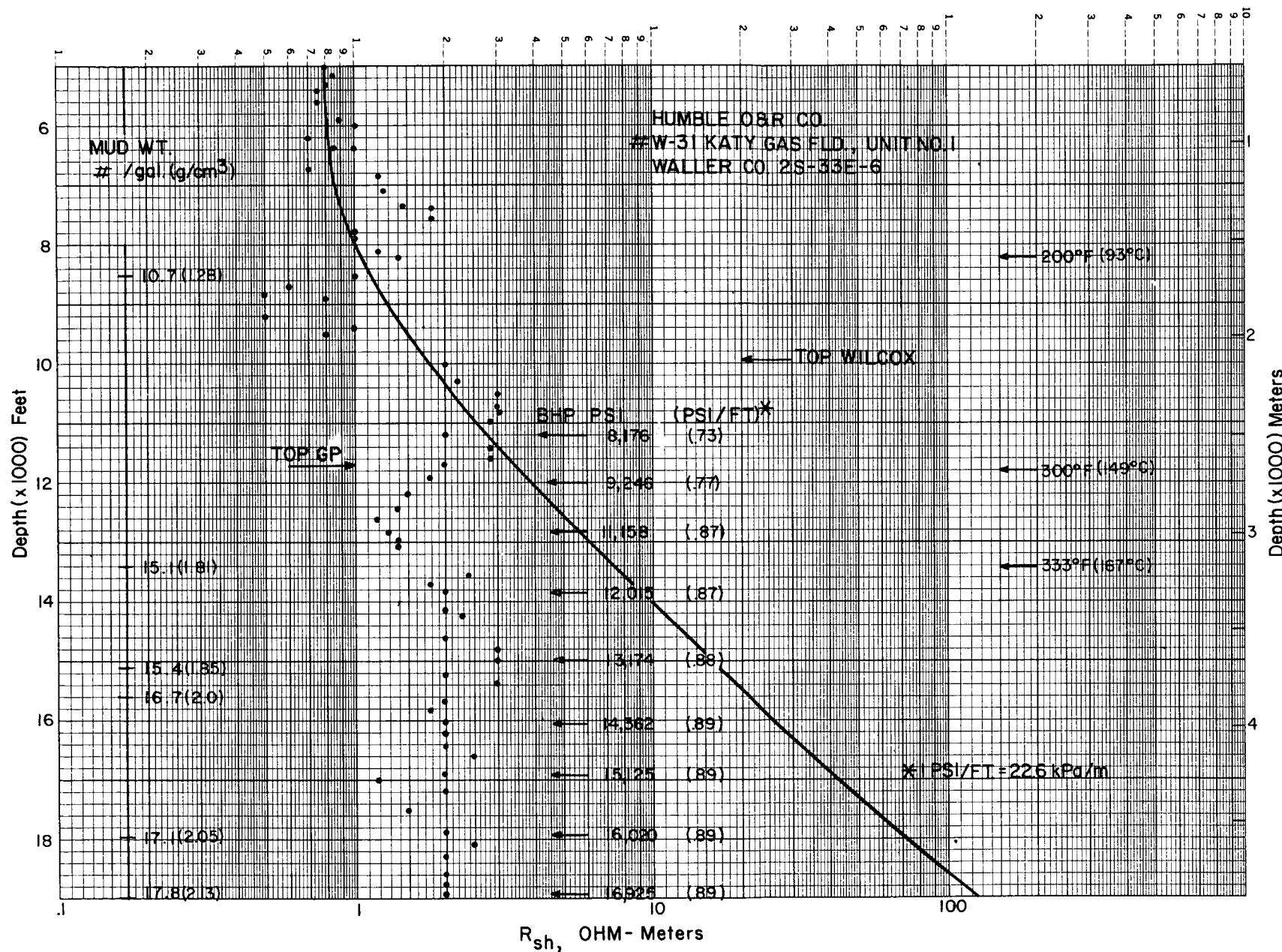


Figure 132. Operational top of geopressure and geopressure gradients from shale resistivity data for a well on cross section D-D', Waller County.

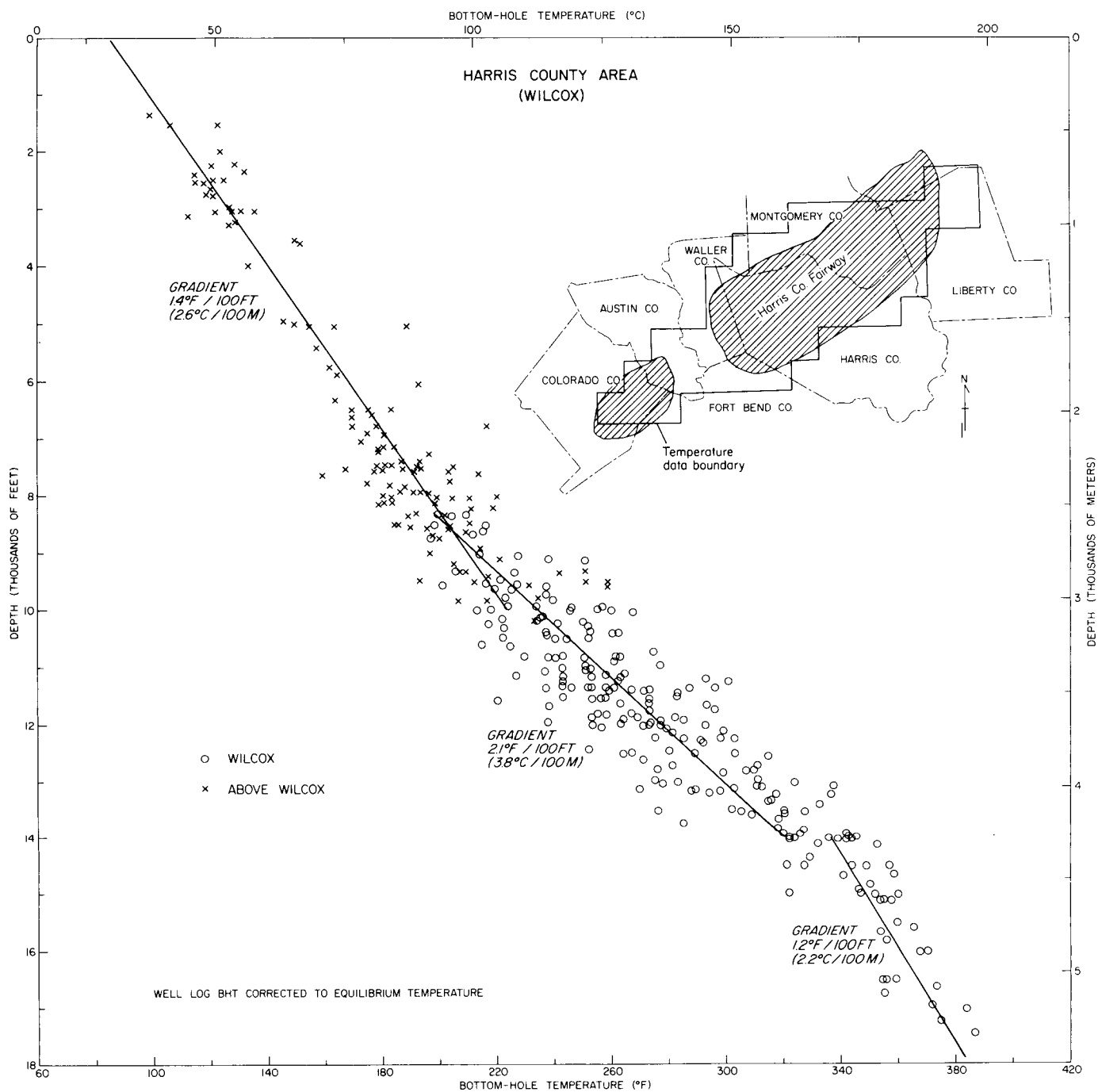


Figure 133. Temperatures and geothermal gradients for Harris Fairway.

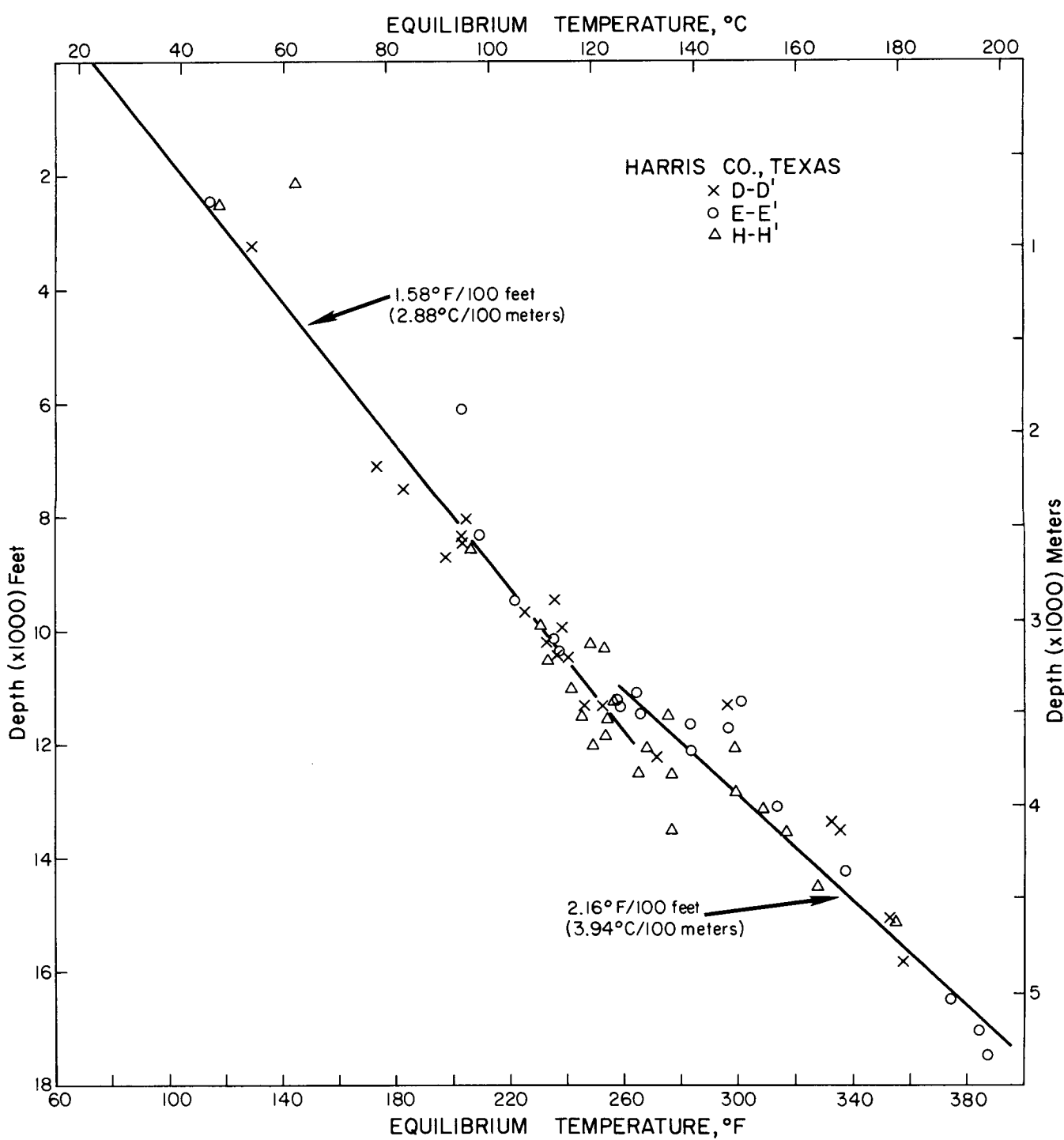


Figure 134. Temperatures and geothermal gradients for wells on three fairway cross sections, Harris County.

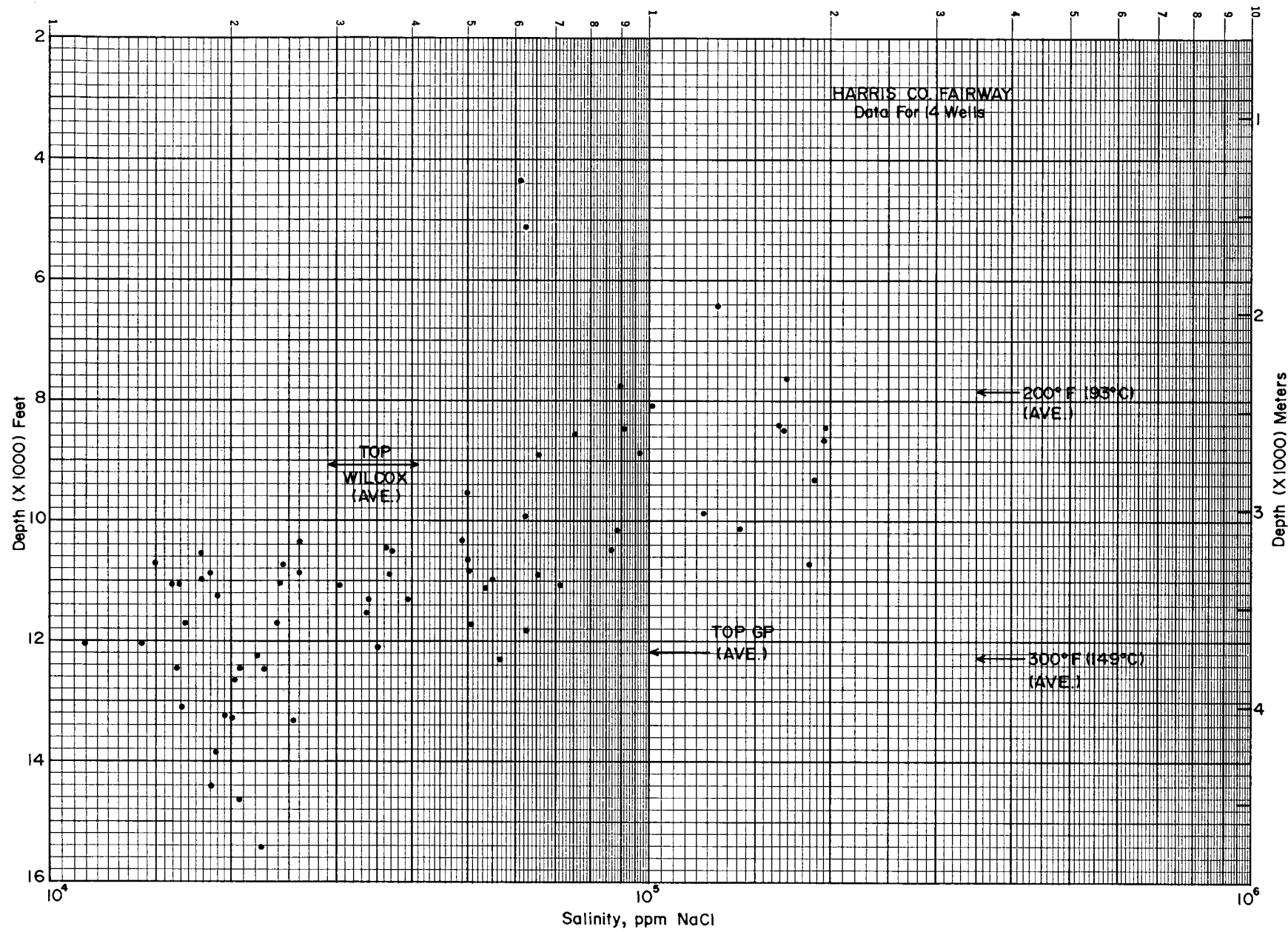


Figure 135. Salinity versus depth calculated from electric logs of 14 wells in Harris Fairway.

## SUMMARY AND CONCLUSIONS

Areas in Texas having the greatest potential for containing geopressured geothermal fluids in economic quantities in the Wilcox Group occur where the gulfward-dipping sandstone/shale wedge thickens abruptly across a complex growth-fault system. As a result of faulting occurring contemporaneously with deposition, the Wilcox thickens from less than 2,000 ft up dip near the outcrop belt to more than 8,000 ft down dip at depths greater than 10,000 ft. The Wilcox is divided into three parts—the sandstone-rich upper and lower parts, which represent two major progradational cycles, and the shale-rich middle part, which in part represents a major transgression. In the lower Wilcox, thick sandstone and shale sequences occur in deltaic lobate patterns along the Middle and Upper Texas Gulf Coast; in the upper Wilcox, on the other hand, similar thick deltaic sandstones and shales occur along the Lower and Middle Texas Gulf Coast.

The objective of this study was to identify areas along the Wilcox trend favorable for testing the feasibility of producing large quantities of hot water from the geopressured zone. Methane would then be separated from solution, and the hot water would be used to produce electric energy from heat.

Criteria used to identify geopressured geothermal reservoirs with resources suitable for electric power generation were a sandstone reservoir of 3 mi<sup>3</sup>, fluid temperature greater than 300°F, pressure gradient of at least 0.7 psi per foot, and permeability of more than 20 md (Bebout and others, 1976a).

The top of geopressure (0.465 psi per foot) occurs at depths of 8,000 to 10,000 ft in those areas where shale is dominant and 11,000 to 13,000 ft where sandstone is dominant. Formation temperatures also vary within the Wilcox according to the position along dip, the lithology, the location of growth faults, and the location along the Texas Gulf Coast. Temperatures higher than 300°F occur at depths ranging from 10,800 to 13,100 ft.

Six geothermal fairways in the Wilcox—Zapata, Duval, Live Oak, De Witt, Colorado, and Harris—have been delineated along the Texas Gulf Coast by combining information from the sandstone-distribution and isotherm maps (fig. 4). Sandstone-rich sections that have formation fluid temperatures of greater than 300°F occur in these fairway areas.

The Zapata, Duval, and Live Oak Fairways (table 4) contain thick, laterally extensive

Table 4. Summary of the physical characteristics of the six Wilcox geopressured geothermal fairways.

PART OF WILCOX	ZAPATA	DUVAL	LIVE OAK	DE WITT	COLORADO	HARRIS
DEPTH TO TOP OF PROSPECTIVE SANDSTONE (ft)	Upper	Upper	Upper	Lower	Lower	Lower
THICKNESS OF PROSPECTIVE SANDSTONE (ft)	9,600 to 10,500	11,000 to 12,000	9,200 to 11,000	10,490 to 10,660	10,960 to 11,400	12,500 to 13,300
TOP OF GEOPRESSURE (0.7 psi/ft)	280 to 620	> 600	> 600	550	1,600	> 2,000
TEMPERATURE	10,700 ft 300° F at 11,400 ft	10,000 ft 300° F at 10,750 ft	9,950 ft 300° F at 11,000 ft	10,000 ft 300° F at 10,850 ft	12,000 ft 300° F at 11,780 ft	11,550 ft 300° F at 12,990 ft
POROSITY (%)	17 to 22	7 to 14	16 to 24	6 to 25	4 to 19	Average: 15
PERMEABILITY (in millidarcys)	0 to 19 *SWC	0.1 to 44 **DC	5 to 40 SWC + DC	0.01 to 242 DC	Most < 5; locally up to 545 DC	Most < 1 DC

\*SWC = Sidewall core

\*\*DC = Diamond core.

sandstone units in the upper Wilcox. The sections in which these sandstones occur are extremely thick as a result of contemporaneous subsidence along large growth faults. Fluid temperatures are greater than 300°F in the Zapata and Duval Fairways but are lower in the Live Oak Fairway. Core analyses indicate that porosity and permeability are low in these deep sandstone units, and, for this reason, these sandstones are not considered favorable for geopressured geothermal energy production.

The De Witt Fairway is located in a complex growth-faulted part of the lower Wilcox trend just downdip of the underlying Lower Cretaceous Stuart City trend (fig. 7). The Cuero fault block, within the De Witt Fairway, contains more than 550 ft of geopressured sandstone. These sandstones, deposited in a variety of deltaic environments, occur at the tops of at least eight upward-coarsening cycles. Overall, the sequence is regressive; progressively shallower cycles contain sandstones deposited in more proximal deltaic environments. Fluid temperatures of 300°F have been recorded within the reservoir section. Core analyses from the De Witt Fairway indicate that permeabilities range from less than 2.1 to more than 100 md. The highest permeability is at

the top of the sandstone-bearing interval in thick, well-sorted channel sandstones occurring in the most proximal deltaic facies. Sandstones in this fairway have a high potential for geopressured geothermal energy production.

In the Colorado Fairway, 1,200 to 1,600 ft of sandstone with fluid temperatures of greater than 300°F occur in the lower Wilcox Group. Few growth faults have been recognized in the fairway area, perhaps in part because of lack of adequate deep well control. The lower Wilcox contains as much as 1,600 ft of net sandstone within the Eagle Lake fault block. Pressure gradients in the Colorado Fairway are generally low, and many wells in the area do not penetrate the top of geopressure. Most permeabilities are lower than 5 md, but some range up to 545 md in thin, isolated sandstones.

The Harris Fairway contains a massive sandstone section with more than 2,000 ft of net sandstone in the lower Wilcox. Most of the lower Wilcox in the downdip part of the fairway is geopressured and has fluid temperatures greater than 300°F. However, most permeabilities are less than 5 md, and many are less than 1 md. The Colorado and Harris Fairways are considered to have poor potential for geopressured geothermal energy production.

## ACKNOWLEDGMENTS

Funding for geopressured geothermal regional assessment and site selection studies in the Wilcox Group was provided by the U.S. Department of Energy under Contract No. DE-AS05-76ET28461 (formerly EY-76-S-05-4891). However, many companies have contributed a variety of subsurface data essential to the success of this project. These companies are gratefully acknowledged:

*Amoco Production Company  
Atlantic Richfield Company  
Cities Service Company  
Exxon Company, U.S.A.  
Gulf Oil Company, U.S.A.  
Mobil Oil Corporation  
Phillips Petroleum Company  
Shell Oil Company  
Tenneco Oil Company  
Texaco, Inc.*

We thank Robert G. Loucks, Kinji Magara, Mark W. Presley, Susan J. Tewalt, Robert A. Morton, L. F. Brown, Jr., and W. R. Kaiser for reviewing the manuscript and providing many helpful suggestions. Victor J. Gavenda prepared the regional cross sections.

This report was edited by Michelle C. Pemberton-Gilson. Typesetting was by Charlotte J. Frere and Fannie M. Sellingsloh, under the direction of Lucille C. Harrell. Drafting of text and plate figures was by Greg Miller, Richard L. Dillon, David M. Ridner, Margaret R. Day, Paula Kirtley, Margaret L. Evans, Richard P. Flores, Thomas M. Byrd, and France Davis. Text illustration photography was by James A. Morgan. Micheline R. Davis designed the publication and cover.

## REFERENCES

Archie, G. E., 1942, The electrical resistivity log as an aid in determining some reservoir characteristics: American Institute of Mining Engineers Transactions, v. 146, p. 54-67.

Bateman, R. M., and Konen, C. E., 1977, The log analyst and the programmable pocket calculator: The Log Analyst, v. 18, no. 5, p. 3-11.

Bebout, D. G., Agagu, O. K., and Dorfman, M. H., 1975a, Geothermal resources, Frio Formation, Middle Texas Gulf Coast: The University of Texas at Austin, Bureau of Economic Geology Geological Circular 75-8, 43 p.

Bebout, D. G., Dorfman, M. H., and Agagu, O. K., 1975b, Geothermal resources—Frio Formation, South Texas: The University of Texas at Austin, Bureau of Economic Geology Geological Circular 75-1, 36 p.

Bebout, D. G., Gavenda, V. J., and Gregory, A. R., 1978a, Geothermal resources, Wilcox Group, Texas Gulf Coast: The University of Texas at Austin, Bureau of Economic Geology, Report to U.S. Department of Energy, Division of Geothermal Energy, Contract No. AT-E(40-1)-4891 (EY-76-S-05-4891), 82 p.

Bebout, D. G., Loucks, R. G., Bosch, S. C., and Dorfman, M. H., 1976a, Geothermal resources—Frio Formation, Upper Texas Gulf Coast: The University of Texas at Austin, Bureau of Economic Geology Geological Circular 76-3, 47 p.

Bebout, D. G., Loucks, R. G., and Gregory, A. R., 1978b, Frio sandstone reservoirs in the deep subsurface along the Texas Gulf Coast—their potential for the production of geopressured geothermal energy: The University of Texas at Austin, Bureau of Economic Geology Report of Investigations No. 91, 92 p.

Bebout, D. G., Luttrell, P. E., and Seo, J. H., 1976b, Regional Tertiary cross sections—Texas Gulf Coast: The University of Texas at Austin, Bureau of Economic Geology Geological Circular 76-5, 10 p.

Burst, J. F., 1959, Post-diagenetic clay mineral environmental relationships in the Gulf Coast Eocene, in Swineford, A., ed., Clays and clay minerals: Sixth National Clays and Clay Minerals Conference Proceedings, Pergamon Press, 411 p.

\_\_\_\_\_, 1969, Diagenesis of Gulf Coast clayey sediments and its possible relation to petroleum migration: American Association of Petroleum Geologists Bulletin, v. 53, no. 1, p. 73-93.

Culbertson, J. A., 1940, Downdip Wilcox (Eocene) of coastal Texas and Louisiana: American Association of Petroleum Geologists Bulletin, v. 24, no. 11, p. 1891-1922.

Dorfman, M. H., and Deller, R. W., eds., 1975, First geopressured geothermal energy conference proceedings: The University of Texas at Austin, Center for Energy Studies, 369 p.

\_\_\_\_\_, 1976, Second geopressured geothermal energy conference proceedings: The University of Texas at Austin, Center for Energy Studies, 5 v.

Dow, W. G., 1978, Petroleum source beds on continental slopes and rises: American Association of Petroleum Geologists Bulletin, v. 62, no. 9, p. 1584-1606.

Echols, D. J., and Malkin, D. S., 1948, Wilcox (Eocene) stratigraphy, a key to production: American Association of Petroleum Geologists Bulletin, v. 32, no. 1, p. 11-33.

Edwards, M. B., 1980a, A look at the upper Wilcox Rosita Delta System of South Texas: Oil and Gas Journal, v. 78, no. 19, p. 197-205.

\_\_\_\_\_, 1980b, The Live Oak Delta Complex: an unstable, shelf-edge delta in the deep Wilcox trend of South Texas: Gulf Coast Association of Geological Societies Transactions, v. 30, p. 71-79.

\_\_\_\_\_, 1981, The upper Wilcox Rosita Delta System of South Texas: record of growth-faulted shelf-edge deltas: American Association of Petroleum Geologists Bulletin, v. 65, no. 1, p. 54-73.

Fisher, W. L., 1969, Facies characterization of Gulf Coast Basin delta systems, with some Holocene analogues: Gulf Coast Association of Geological Societies Transactions, v. 19, p. 239-261.

Fisher, W. L., and McGowen, J. H., 1967, Depositional systems in the Wilcox Group of Texas and their relationship to occurrence of oil and gas: Gulf Coast Association of Geological Societies Transactions, v. 17, p. 105-125.

Hardin, F. R., and Hardin, G. C., Jr., 1961, Contemporaneous normal faults of Gulf Coast and their relation to flexures: American Association of Petroleum Geologists Bulletin, v. 45, no. 2, p. 238-248.

Hargis, R. N., 1962, Stratigraphy of the Carrizo-Wilcox of a portion of South Texas and its relationship to production: Gulf Coast Association of Geological Societies Transactions, v. 12, p. 9-25.

Hottmann, C. E., and Johnson, R. K., 1965, Estimation of formation pressures from log-derived shale properties: Journal of Petroleum Technology, v. 17, no. 6, p. 717-723.

Hoyt, W. V., 1959, Erosional channel in the middle Wilcox near Yoakum, Lavaca County, Texas: Gulf Coast Association of Geological Societies Transactions, v. 9, p. 41-50.

Johnston, J. E., 1977, Depositional systems in the Wilcox Group and the Carrizo Formation (Eocene) of Central and South Texas and their relationship to the occurrence of lignite: The University of Texas at Austin, Master's thesis, 113 p.

Kehle, R. O., 1971, Geothermal survey of North America, 1971 Annual Progress Report: Research Committee, American Association of Petroleum Geologists (unpub.), 31 p.

Loucks, R. G., 1978, Geothermal resources, Vicksburg Formation, Texas Gulf Coast: The University of Texas at Austin, Bureau of Economic Geology, Report to U.S. Department of Energy, Division of Geothermal Energy, Contract No. EY-76-S-05-4891, 52 p.

Murray, G. E., 1955, Midway Stage, Sabine Stage, and Wilcox Group: American Association of Petroleum Geologists Bulletin, v. 39, no. 5, p. 671-689.

Townsend, J. V., Jr., 1954, The generalized geology of the Wilcox Group of northeast Texas: Gulf Coast Association of Geological Societies Transactions, v. 4, p. 69-74.

## APPENDICES

### APPENDIX A

#### METRIC CONVERSION FACTORS

Standard Unit	x	Conversion Factor	=	Metric Unit
ft	x	0.3048	=	m
ft/mi	x	0.189394	=	m/km
lb/gal	x	119.8264	=	kg/m <sup>3</sup>
md	x	0.00098692	=	μm <sup>2</sup>
mi	x	1.609344	=	km
mi <sup>2</sup>	x	2.589988	=	km <sup>2</sup>
mi <sup>3</sup>	x	4.168182	=	km <sup>3</sup>
psi	x	6.894757	=	kPa
psi/ft	x	22.62059	=	kPa/m
°F/100 ft	x	1.825	=	°C/100 m
°F	x	(°F - 32)/1.8	=	°C

### APPENDIX B

#### WELL NAMES AND LOCATIONS

##### ZAPATA FAIRWAY

##### ZAPATA FAIRWAY (cont.)

Township Range	Well No.	Well Name	Township Range	Well No.	Well Name
23S-8E-5	1	Belco #1 Frost National Bank	25S-7E-6	3	General Crude (Gulf) #1 Romero
23S-8E-2	2	Killam and Hurd #1 Fulbright et al. Fee	25S-7E-3	4	Killam and Hurd et al. #1 Flores Heirs
23S-8E-6	4	Atlantic #1 Lopez Estate	25S-7E-6	5	Samedan #1 Matles Unit
23S-8E-7	5	Union #1 De Cuellar	25S-7E-4	6	Coastal States #1 Flores
23S-8E-9	6	Hughes & Hughes and Pennzoil #1 Martinez	25S-7E-6	7	Rutter et al. #1 Volpe
23S-8E-6	7	Hughes & Hughes #1 Fulbright	25S-7E-8	9	Gulf #1 De Pena
23S-8E-5	8	Hughes & Hughes #A-1 De Uribe Estate	25S-7E-8	10	Alaska Steamship et al. #1 Cuellar
23S-8E-1	9	Killam and Hurd #1-16 Killam Fee	25S-7E-8	11	Osage #1 Uribe
23S-8E-8	10	Hughes & Hughes and Pennzoil #1-B Cuellar Estate	25S-7E-8	12	MacDonald #1 Uribe
23S-8E-1	11	Killam and Hurd #1 Uribe	25S-7E-9	13	Rio Grande Valley #1 Dodier
23S-8E-1	12	Atlantic #1 Hinnant	25S-8E-4	14	Miller and Fox #1 Dodier
23S-9E-1	1	Atlantic Richfield #4-C Marrs McLean	25S-8E-4	15	Coastal States #4 Dodier
23S-9E-1	2	Atlantic Richfield #2-C Marrs McLean Trust	25S-8E-5	16	KRM #1 Volpe
23S-9E-1	4	Standard #2 Holbein	25S-8E-5	17	McAll #3 Singer
23S-9E-2	5	Hamon #2 Holbein	25S-7E-5	18	McDaniel #1 Singer
23S-9E-3	6	Atlantic #1-B Hinnant	25S-7E-5	19	Bateman #1 Gutierrez
23S-9E-1	7	Atlantic Richfield #2-C McLean Trust	25S-7E-5	20	Miles #1 Ramirez
24S-7E-1	1	Blanco #1 Jennings	25S-7E-5	21	McAll #1 Gutierrez
24S-8E-7	1	Halbouy and Jonnell #1 Garza "C"	25S-7E-5	22	Rowe #1 Flores
24S-8E-7	2	Lively and Fountain #1 Trevino et al.	25S-7E-9	23	Alaska Steamship et al. #1 Vasquez
24S-8E-7	3	Halbouy and Jonnell #1 Trevino	25S-7E-9	24	Solo #1 N. Singer
24S-8E-7	4	Halbouy and Jonnell #D-1 Garza	25S-7E-9	25	Solo #1 Singer
24S-8E-6	5	Gulf #1 Trevino	25S-8E-1	26	Halbouy and Jonnell #1-E Garza
24S-9E-1	1	Standard of Texas #1 Frost National Bank et al. "3"	25S-8E-1	1	Blanco and Dougherty #1 Benavides
24S-9E-3	2	Gulf #1 H. Vela	25S-8E-4	4	Pennzoil #4 Haynes
24S-9E-3	3	Union #18 Jennings	25S-8E-4	5	Pennzoil and Patrick #2 Haynes Estate
24S-9E-3	4	Gulf #1 Garza et al.	25S-8E-5	6	Pennzoil and Patrick #1 Haynes Estate
24S-9E-8	5	Standard of Texas #1 Rancho Blanco	25S-8E-5	8	Humble #1 Haynes Estate
25S-7E-2	1	Gulf #1 Flores	25S-8E-6	9	Gulf #1 Security National Bank of L.A. et al. Fee
25S-7E-3	2	Gulf #1 Ramirez	25S-8E-7	10	Gulf #1 Trevino
			25S-8E-8	11	Crescent #1 Haynes
			25S-8E-9	12	Pennzoil #1 A. Vela
			25S-8E-9	13	Gulf #1 Volpe
			25S-8E-8	15	Bright & Schiff #1 Vela
			25S-8E-8	16	Pennzoil #1 L. Vela et al.
			25S-9E-9	2	Hamon #1 Campbell
			26S-7E-8	1	Texas #1-M Guerra
			26S-7E-8	2	Pan Am (Stanolind) #1 Vela
			26S-7E-8	3	Texas #1 Guerra "I"
			26S-7E-8	4	Hamon #1 Alexander
			26S-8E-1	1	Suburban #1 Sanchez
			26S-8E-2	5	Katz #1 Vela
			26S-8E-3	6	Standard of Texas #1 Garcia "2"
			26S-8E-5	8	Trahan #1 Garcia
			26S-8E-5	9	Crescent and Wynn #1 Morales
			26S-8E-5	10	Tenneco (Delhi-Taylor et al.) #1 Garcia
			26S-8E-8	11	Crescent #1 Foss
			26S-8E-8	12	Gulf #1 Benavides
			26S-8E-8	13	Crescent #2 Benavides
			26S-8E-8	14	Jonnell #3 Benavides
			26S-8E-9	15	Frankfort #1 Benavides
			26S-8E-8	17	Clinton #1 Benavides
			26S-8E-5	18	Trahan #1 Whittier
			26S-8E-5	19	Crescent #1 Vela
			26S-8E-8	20	Jonnell #1 Zamora
			27S-7E-7	1	Standard of Texas #1 Ramirez
			27S-7E-1	2	Fullerton #1 Vela
			27S-7E-3	4	National #1 Barberio
			27S-8E-3	1	Hudson #1 Zamora

ZAPATA FAIRWAY (cont.)

Township Range	Well No.	Well Name
27S-8E-3	2	Frankfort #1 Sanchez
27S-8E-3	3	Frankfort #1 Garcia
27S-8E-3	4	Jonnell #1 Lopez Heirs
27S-8E-4	6	Cosden and Mid America #1 Ramirez
27S-8E-8	7	Union #1 McDermott
27S-8E-9	8	Jonnell #1 Yzaguirre
27S-8E-9	9	Jonnell #1 Ramos
27S-8E-9	10	Jonnell #1-A Guerra
27S-8E-9	11	Jonnell #2 Ramos
27S-8E-4	13	Ashland #1 Munoz
27S-8E-9	14	Standard of Texas #1 Ramirez "2"
27S-8E-4	17	Katz #1 Ramirez
27S-8E-4	18	Jonnell & Sohio #2 Ramirez
27S-8E-4	19	Delhi #2 Ramirez
27S-8E-9	20	Jonnell #2 M. Ramirez
27S-8E-9	21	Jonnell #2 B. Ramirez
27S-8E-9	22	Jonnell #1 Guerra
27S-8E-2	24	Frankfort #2 Sanchez
27S-9E-4	1	Sun #1 Guerra Gas Unit
28S-7E-1	1	Hamon and Colorado #1 Guerra
28S-7E-1	2	Hamon #1 Yzaguirre
28S-7E-1	3	Hamon #1 Ramirez "A"
28S-8E-2	2	Humble #1 Humble-Martinez Fee
28S-9E-4	1	Austral and Tidewater #1 Sanchez

DUVAL FAIRWAY

Township Range	Well No.	Well Name
14S-13E-7	1	Archer #1 Wheeler
15S-13E-1	1	Delange & Neatherly #B-1 Brown
15S-13E-3	2	Davenport #1-A Dolph
15S-13E-7	3	Argo #V-1 Edrington
15S-13E-2	5	Pace & Vreeland #1 La Jolla
15S-13E-5	6	Southland, Delange and Ellis #1 Caron
15S-13E-5	7	Olson #1 Whitfield
15S-13E-5	8	Texaco #1 Rhode
15S-13E-8	9	Argo #R-1 Edrington Estate
16S-12E-1	1	Cox #1 Atkinson
16S-12E-9	2	Atlantic #1 Hagist Ranch
16S-12E-4	3	Hawkins & Ranger #1 Hagist Ranch
16S-12E-8	4	Marion #1 Welder Heirs
16S-12E-8	5	Humble #26 Dowdy Fee
16S-12E-1	6	Atlantic #1 Atkinson
16S-12E-6	7	Rutherford #1 Pursch
16S-13E-3	1	Argo #1 Roos
16S-13E-4	2	Harkins #1-112 Murphy Estate
16S-13E-4	3	Coastal States #1 Ragsdale
16S-13E-6	4	Humble #1 Yeager
16S-13E-6	5	Sun-DX #4 Penn
16S-13E-6	6	Sunray #1 American National Insurance
16S-13E-6	7	Seaboard of Delaware #1 Lowe
16S-13E-7	8	Siegfried #1 Lowe
16S-13E-7	9	Petro-Lewis #1 Bindewald
16S-13E-8	10	Mobil #1 Labbe Ranch
16S-13E-9	11	Harkins & Humble #1 Ragsdale
16S-13E-6	12	Texaco #2 Gouger Gas Unit #3
16S-13E-2	13	Argo #Q-1 Edrington
16S-13E-1	14	Sunray #1 Penn
		Trans Texas #1 Hahl-Burch
	2	Mavin #1 Hahl-Wiederkehr
	3	Magnolia #9 D.C.R.C.
	4	Horizon #1 Lundell
	5	Fair & Woodward #1 Luptack
	2	Argo & Haring #1 Gorman
	3	Texaco #1 Marshall
	4	Humble #B-1 Welder Heirs
	5	Ramada #1-B Welder Heirs
	6	Ramada et al. #1 Welder Heirs
	7	Atlantic-Richfield #1 Arco et al. Humble Fee
	8	Atlantic-Richfield #B-7 Welder
	9	Humble #2 Welder Heirs "F"
	10	Cherryville #1 Gorman
	12	Atlantic-Richfield #F-1 Welder Heirs
	1	Stanolind #1-D Farmers Life Insurance
	1	Shell #1 Duval County Ranch
	1	Humble #98 White "B"
	2	Waggoner Estate #1 Arnstein et al.
	1	Huber et al. #1 Hubberd
	2	Shell #1 Penwell
	4	Shell #1 Hubberd "B"
	5	Shell #A-3 Weatherby
	6	Shell #1 L. C. Weatherby "A"
	7	Shell #1 Stegall "A"
	10	Shell #A-2 Weatherby
	11	Huber and Shell #1 Stegall
	13	Socony Mobil and Lacy #1 Weatherby
	15	Hamm et al. #15 Duval-Hoffman
	16	Huber #1 Hoffman et al.
	1	Sundance #1 Frost
	1	Atlantic #1-A Billings Ranch
	2	Mayfair #1 Kirkpatrick et al.
	3	Houston Oil & Minerals #1 Billings
	4	Rowe #1 Pearl Estate
	5	Harrell et al. #1 Lopez
	6	Humble #100 Kohler "A"
	1	Eason-Harper #1-160 Peters Estate
	2	Eason #1 Peters Estate
	4	Monterey #1 Peters
	1	Frost et al. #1 Walker
	2	Sunray #1 Walker
	2	Shell #1 El Paso - Benavides Ranch
	3	Hamon #1 Perez et al.
	4	Hamon (Hawkins & Hawkins) #1 Leal
	5	Houston Oil & Minerals #1 Dinn
	7	Morgan #3-B Richardson
	8	Mobil #1 Dinn
	3	Gulf #1 Gulf-Peters
	2	Texaco #28 Da Camara
	3	Skelly #6 Martin
	4	Skelly #1 Martin
	5	Gulf #1 Villareal
	1	Brown et al. #1 Laurel Heirs
	2	Atlantic #1 Garcia Estate "A"
	3	Pauley #1 Laurel Fee
	4	Amistad #1 White "A"
	1	Hamon #1 de Benavides
	2	McCulloch and Venus #1 Cuellar
	3	Getty #1 de Benavides

## DUVAL FAIRWAY (cont.)

## LIVE OAK FAIRWAY (cont.)

Township Range	Well No.	Well Name	Township Range	Well No.	Well Name
21S-10E-7	4	Union #1 Brennan-Benavides	13S-16E-6	8	Blanco #1 Gillette Unit
21S-10E-3	5	Standard of Texas #1-B de Benavides	13S-16E-1	9	Texas Oil & Gas #1 Maguglin
21S-10E-3	6	Morgan #2-B de Benavides	13S-16E-2	10	Venus #1 Goebel
22S-8E-8	1	Shell #1 Bruni Trust & Killam Trust	13S-16E-2	11	Service Contracting & Longhorn #1 Goebel
22S-9E-2	1	Atlantic #1 Garcia Estate	13S-16E-6	13	Ryan et al. #1 Gillette
22S-9E-2	3	Coastal States #2 Puig	13S-16E-6	14	Stanolind #1 Coquat
22S-9E-3	4	Atlantic #1 Puig Gas Unit	13S-16E-6	15	Davis #1 Dunn
22S-9E-4	6	Hamon #1 Ramirez	13S-16E-6	16	Texaco #1 Cochran
22S-9E-4	8	Pickens #1 Bruni	13S-16E-6	17	Abercrombie et al. #1 Dunn
22S-9E-7	10	Atlantic #2 Bruni Gas Unit #1	13S-16E-6	19	Coastal States #1 Morrison
22S-9E-7	11	Atlantic and Austral #1 Stroman-Armstrong	13S-16E-8	2	Hughes et al. #1 MacDon-Holzmark
22S-9E-7	12	Atlantic #2 Stroman-Armstrong	13S-17E-1	3	Hughes et al. #1-A Pouloit
22S-9E-7	13	Austral #1 Marrs McLean Trust	13S-17E-6	5	Carl #1 Gillette
22S-9E-7	15	Atlantic-Richfield #3 Marrs McLean "C"	13S-17E-6	6	Carl #1 Turnbow
22S-9E-7	17	Austral #2 Marrs McLean	13S-17E-6	8	Dow #1 McCollum
22S-9E-7	18	Coastal States #1 Yeager-Armstrong	13S-17E-7	9	North Central et al. #1 Bomar
22S-9E-9	20	Atlantic #A-1 Hinnant	13S-17E-8	10	Coastal States #1 McCord
22S-9E-2	21	4-B Trust #1 Laredo National Bank	13S-17E-9	11	Argo #1 Huegler
22S-9E-4	22	Atlantic #1-A Puig	13S-17E-9	13	Colorado #1 Choate
			13S-17E-2	14	Quintana #1 Vickers
			13S-17E-1	15	Atlantic #1 Coward
			13S-17E-3	17	Hamon #1 Ragsdale
			13S-17E-2	18	Viking and Delange #1 Williams
			13S-17E-2	20	Warren #1 Dove
			13S-17E-2	21	Bright and Schiff #1 Schoolfield
			13S-17E-2	22	Stanolind #1 McCollum
			13S-18E-4	6	White Shield #1 Martin Unit
			13S-18E-4	9	Tidewater #1 Taylor
11S-18E-9	2	Cox and Haring #1 Copeland	13S-18E-8	10	Tamarack #1 Humberson
11S-18E-5	3	Union #2 Burnell Unit Spielhagen	13S-18E-4	11	Halbouty #1 Gillette et al.
11S-18E-8	5	Pennzoil #79 Ray	14S-14E-4	1	Texam #1 Hayes-Ezzell
11S-18E-2	6	Sohio et al. #1 Nichols Estate	14S-14E-6	4	Magnolia #1 Means
11S-18E-5	7	Pennzoil #10 N. P. U-Ray	14S-14E-9	5	Jones #1 Shiner
11S-18E-7	8	Union #6 N. P. U-Ray	14S-14E-1	6	Kilroy #1 Herring
12S-17E-9	1	Northern Pump and Hunt #A-1 Hall	14S-14E-6	7	Tenneco #1 Stephens
12S-17E-2	5	Forest #1 Borroun "B-C" Unit	14S-14E-6	8	Scoggins & Troporo #1 Schmid
12S-17E-2	6	Southland #1 Barber et al.	14S-14E-8	9	Magnolia #1 Jones
12S-17E-1	7	Stanolind #1 Dugat Estate	14S-14E-9	10	Jones #C-2 Ezzell
12S-17E-3	8	Shell #1 Gordon	14S-14E-9	11	Jones #C-4 Ezzell
12S-17E-9	10	Dyco #1 Ballard	14S-14E-8	12	Meeker #1 Lebman
12S-17E-4	12	Texas #A-1 Knight	14S-14E-5	13	Magnolia #1 Block 86
12S-17E-5	13	Texas #1 Rodriguez Gas Unit	14S-15E-6	1	Humble #1 Coker
12S-17E-2	14	Carrl Oil et al. #1 Copeland	14S-15E-6	2	Mosbacher (Hughes & Hughes) #1 Kendall
12S-17E-6	16	Clover #1 South Texas Children's Home	14S-15E-6	3	Hanson #1 Prosen et al.
12S-17E-6	17	Arkansas Fuel et al. #1 Booth	14S-15E-6	4	Mosbacher #1 Garza Unit 1
12S-17E-7	18	Gasoline #A-1 Bast	14S-15E-8	5	Continental #2 Burns
12S-18E-2	10	Frankfort (Texas Pacific) #10 Walton	14S-15E-8	7	Atlantic #8 Lyne
12S-18E-1	17	Texas #A-1 McKinney	14S-15E-7	8	Getty #1 Christenson
12S-18E-2	25	Texas Pacific (Rowan & Tong) #9 Freeland	14S-15E-8	13	La Gloria et al. #1 Bush Unit
12S-19E-3	1	MPS #1 McKinney	14S-15E-8	14	Kilroy and Southland (Fountain) #1 Bierwirth et al.
12S-19E-4	3	Hewit et al. #1 Weiss	14S-15E-9	16	Atlantic-Richfield #12 Lyne
12S-19E-4	5	Martin (Miller) #1 Farish	14S-15E-9	17	Atlantic #9 Lyne
12S-19E-8	7	Coastal States #1 Farish	14S-15E-2	18	Jones #1 West Estate
13S-16E-1	1	Sinclair #3 Dilworth	14S-15E-2	19	Texas Eastern #1 Schreiner
13S-16E-6	2	Newman Bros. #1 Edwards et al.	14S-15E-3	20	Argo #1 Schreiner
13S-16E-7	3	Jones et al. #1 Dunn	14S-15E-3	21	Kilroy of Texas #A-1 Herring
13S-16E-7	4	National Exploration #1 McKinney et al.	14S-15E-3	22	Interamerican Funds #2 Herring
13S-16E-1	6	Hanson & MacDonald #1 Maguglin	14S-15E-3	23	Venus #1 Schreiner
			14S-15E-9	24	Argo et al. #1 Houdman

## LIVE OAK FAIRWAY (cont.)

Township Range	Well No.	Well Name
14S-15E-9	25	Warren #1 Whitley-Johnson
14S-15E-9	26	Atlantic #11 Lyne
14S-15E-9	27	Mesa #1 Johnson
14S-15E-8	28	Gulf Coast (Fischer) #1 Korczinsky-Wojtasczyk
14S-16E-1	1	Cherryville #1 Williams
14S-16E-3	3	Gulf #1 Lee
14S-16E-4	4	Pan American #B-1 West
14S-16E-6	5	Brown #1 Hayes
14S-16E-8	8	Atlantic #1 Riser
14S-16E-8	9	Pan American #1 Randall
14S-16E-8	10	Union of California #1 Riser
14S-16E-9	11	Abercrombie #1 West & Perkins
14S-16E-9	12	Patrick #1 Abbey
14S-16E-4	13	Hanson #1 Perkins
14S-16E-4	17	Hughes & Hughes #2 Kendall Gas Unit
14S-16E-4	18	American Petrofina #1 Perkins
15S-14E-1	1	Davis #2 Lyne
15S-14E-1	3	El Chorro & Lawley #1 Paul et al.
15S-14E-5	4	Atlantic #1 Morris
15S-14E-6	5	Davis #1 Sanger Heirs
15S-14E-6	6	Atlantic-Richfield #1 El Paso "300"
15S-14E-7	7	Continental #4 Somerset Land and Cattle
15S-14E-7	8	Continental #5 Somerset Land and Cattle
15S-14E-7	9	Coastal States et al. #1 Lehmberg
15S-14E-7	10	Southland #1 El Paso
15S-14E-8	11	Argo #1 Baker
15S-14E-8	12	Rutherford #2-A Baker et al.
15S-15E-2	1	Coastal States and King #2-A Lennox
15S-15E-2	2	Atlantic #1 Burns
15S-15E-2	4	Pace #1 Burns
15S-15E-2	5	Continental #A-1 Burns
15S-15E-2	6	Cox #1 Sparkman
15S-15E-2	7	Hanson and Hurt #1 Sparkman
15S-15E-3	10	Hanson #1 National Bank of Commerce
15S-15E-3	11	Austral #1 Lyne
15S-15E-3	12	Standard of Texas #1 Lyne et al. "1"
15S-15E-3	13	Midwest #1 Lyne
15S-15E-3	14	S.R.G. #1 Lyne
15S-15E-4	15	Atlantic #2 Lyne
15S-15E-4	16	Katz #1-B Slick
15S-15E-4	17	Sands #1 Dolan
15S-15E-4	19	Cherryville #1 Lyne
15S-15E-4	20	Coastal States #1 Ferrell
15S-15E-5	22	Tidewater #1 Burns
15S-15E-6	23	Huber #1 Tullis
15S-15E-6	24	Tidewater #1 Tullis Unit
15S-15E-6	25	Cherryville #1 Tullis
15S-15E-6	26	Cities Service #1 Bailey "C"
15S-15E-8	27	Tenneco #1 Jones Gas Unit
15S-15E-8	28	Placid #1 Patteson
15S-15E-9	29	Cities Service #1 Hendrick "B"
15S-15E-9	30	Hamill #1 McClure
15S-15E-9	31	Continental #3 Somerset
15S-15E-9	32	Katz #C-1 Slick
15S-15E-9	33	Coastal States #1 Slick
15S-16E-2	1	Lone Star #1 Watson
15S-16E-3	2	Hanson and McCormick #1 Johnson
15S-16E-4	3	Tidewater #1-A Hall Estate

## LIVE OAK FAIRWAY (cont.)

Township Range	Well No.	Well Name
15S-16E-4	4	Highland #1 Crocker Transfer & Storage
15S-16E-8	5	Austral #1 Hinnant "A"
16S-14E-1	1	Skelly #1 "A" Weil
16S-14E-3	3	Atlantic-Richfield #4 Baker
16S-14E-3	4	Argo #1 De Arman
16S-14E-4	5	Argo #2 De Arman
16S-14E-6	6	Humble #1 Brookshire
16S-14E-9	7	Austral #1 Baker
16S-15E-3	2	Hamon #1 Hefner
DE WITT FAIRWAY		
Township Range	Well No.	Well Name
7S-23E-5	1	Avalanche Journal #1 Palmer et al.
7S-23E-7	2	Rowe #2 Parker
7S-23E-7	3	Apache and N. Central #1 Daniels
7S-23E-7	4	Patrick #1 Daniels
7S-23E-7	5	Weaver #1 Bolton
7S-24E-3	2	Mobil #1 Hagen
7S-24E-7	5	Shell #1 Carroll
7S-24E-8	6	Argo et al. #1 Granberry
7S-24E-9	7	Humble #1 Kunetka
7S-24E-5	8	Lone Star #1 McManus
7S-24E-8	9	Lone Star #1 Garrett
7S-24E-7	10	Humble #1 Matthews
8S-21E-1	1	Gulf #1 Mueller
8S-21E-4	3	Shell #1 Brown
8S-21E-4	4	Lone Star #1 Alex
8S-21E-5	5	Atlantic #1 Smith
8S-21E-6	6	International Nuclear #1 Weber et al.
8S-21E-7	7	Commonwealth #1 Richards
8S-21E-7	8	Scurlock #1 Murray
8S-21E-8	9	Highland #1 Wood
8S-21E-8	11	McCulloch #1 Domann
8S-21E-8	12	Brown #1 Jablonski
8S-21E-9	14	Shell & Mobil #1 Roehl
8S-21E-6	15	Superior #1 Blackwell
8S-21E-4	16	Esperanza #1 Sheppard
8S-22E-3	1	Sterling & Fox #1 Hamilton
8S-22E-9	2	Humble #1 Cook
8S-22E-5	4	Argo #1 Keseling
8S-22E-5	5	Coastal States #1 Lackey
8S-22E-6	6	Viking #1 Ward
8S-22E-6	7	Venus #1 Hartman
8S-22E-6	8	Gas Producing Enterprises #1 Musselman Gas Unit
8S-22E-6	9	Texaco #1 Jernigan
8S-22E-6	10	Harkins #1 Jernigan
8S-22E-6	11	Harkins & Cox #1 Henneke Unit
8S-22E-6	12	Sun #1 Henneke Gas Unit
8S-22E-7	13	Lone Star #1 Mueller
8S-22E-7	14	Humble #1 Hartman
8S-22E-7	15	Humble #1 Keseling
8S-22E-7	16	Edwards #1 Keseling
8S-22E-7	17	Angelina, Owen and Smith #1 Keseling (Unit #3)
8S-22E-8	18	Tesoro #1 Keseling-Johnson
8S-22E-8	19	Humble #1 Schorlemer

## DE WITT FAIRWAY (cont.)

## DE WITT FAIRWAY (cont.)

Township Range	Well No.	Well Name	Township Range	Well No.	Well Name
8S-22E-9	21	Tana #1 White	9S-20E-5	11	Tidewater #1 Korth
8S-22E-5	22	Scheig #1 Brown	9S-20E-6	12	Harkins #1 Korth
8S-22E-5	23	Abercrombie #1 Williams	9S-20E-6	13	Holmes and Union Texas #1 Mann
8S-22E-8	25	Braman #1 Keseling	9S-20E-6	14	Mortimer #1 Butler Gas Unit
8S-22E-8	27	Harkins and Humble #1 Keseling Gas Unit #2	9S-20E-7	15	McCulloch #1 Hurst & Poehlmann
8S-22E-9	28	Lone Star #1 Angerstein	9S-20E-7	16	Monsanto #1 Estrella
8S-22E-9	29	Atlantic #1 Schorre	9S-20E-7	17	Humble #1 Guaranty Title & Trust
8S-22E-5	30	Catlett & Ferguson #1 Thomas	9S-20E-7	18	McCulloch #1 Franke
8S-22E-5	31	Monsanto #1 Ley	9S-20E-7	19	Monsanto and Bridger #1 Green
8S-22E-1	32	Bridewell #1 Burns Estate	9S-20E-8	20	Cox #1 Clark
8S-22E-6	33	Hanover #1 Sager	9S-20E-8	21	Colorado #1 Clark
8S-22E-2	34	Tesoro #1 Kirkham et al.	9S-20E-8	22	Monsanto #1 Hilgartner
8S-23E-1	1	Arco #1 Daniels	9S-20E-8	23	Cox and Hewitt #1 Kleine
8S-23E-1	2	Zinn et al. #1 Daniels "A"	9S-20E-8	24	Coloma #1 Buesing
8S-23E-1	3	Seeligson #1 Friar	9S-20E-8	25	Hanson et al. #1 Waskow
8S-23E-2	4	Apache and North Central #1 Friar	9S-20E-8	26	Hanson and Cox #1 Buesing
8S-23E-2	6	Coastal States #1 Friar	9S-20E-8	27	Hanson et al. #1 Altman
8S-23E-2	7	Sinclair and Coastal States #1 Stiles	9S-20E-8	28	Hanson et al. #1 Kolodzey
8S-23E-2	8	Brown #1-A Friar	9S-20E-8	29	M.K. #1 Dean Trust
8S-23E-3	9	Texas Gas #1 Adams	9S-20E-8	30	Hanson et al. #1 Rau
8S-23E-3	10	Viking #1 Schultz	9S-20E-9	31	Hanson et al. #1 Matejek
8S-23E-3	11	Osborn #1 Wesley	9S-20E-9	32	Hanson #1 Schlosser
8S-23E-4	12	Tidewater #1 Adams	9S-21E-1	1	Brown #1 Leister
8S-23E-4	13	Argo #1 McDougal	9S-21E-1	2	Austral #1 Schroeter
8S-23E-4	15	Lone Star #1 Hiller	9S-21E-1	3	Argo #1 Schroeter
8S-23E-4	16	Viking #1 Reuss	9S-21E-1	4	Harkins et al. #1 Duderstadt
8S-23E-5	17	Texaco #1 Probst	9S-21E-2	9	Harkins et al. #2 Duderstadt
8S-23E-5	18	Texaco #1 Cheatham	9S-21E-2	10	Houston Natural Gas #3 Boldt
8S-23E-5	19	Coastal States #1 Legalley and Harwood	9S-21E-2	11	Quintana #1 Jochen
8S-23E-6	20	Whiffen Estate #1 Legalley	9S-21E-3	12	Monsanto et al. #1 Boldt
8S-23E-8	21	Atlantic #1 Hartman	9S-21E-3	15	Commonwealth et al. #1 Machost
8S-23E-9	22	Humble #1 Goebel	9S-21E-3	16	Mobil #1 Berck
8S-23E-9	23	Mitchell #1 Koenig	9S-21E-3	17	Harkins and Musselman #1 Sauermilch
8S-23E-9	24	Zachry #1 Rath	9S-21E-3	18	Musselman #1 Danysh et al. Gas Unit
8S-23E-9	25	Bright & Schiff #1 Brown	9S-21E-4	20	Brown #1 Henze Gas Unit
8S-23E-4	26	Hunt #1 Garza	9S-21E-4	21	Amarillo #1 Gips
8S-24E-2	1	Avalanche Journal #1 Boothe	9S-21E-4	22	Lone Star and Musselman #1 Gips
8S-24E-3	2	Lone Star #1 Means	9S-21E-4	23	Hanson #1 Gips Gas Unit
8S-24E-3	3	Lone Star #1-A Friar	9S-21E-4	24	Lone Star #1 Felter
8S-24E-4	4	Humble #1 Pridgen	9S-21E-4	25	Monsanto and Hughes & Hughes #1 Norris
8S-24E-4	5	Shell #1 Blackwell	9S-21E-4	26	Greenbrier #1 Alves
8S-24E-6	8	Shell #1 Collum	9S-21E-5	27	Skelly #1 Menn
9S-18E-6	1	Occidental #1 Osterloh et al.	9S-21E-5	28	Monsanto #1 Witte
9S-19E-6	2	Hunt Trust #1 Schuenemann	9S-21E-5	29	Monsanto #2 Houchins
9S-19E-6	3	Texas Eastern #2 Voelkel Gas Unit #1	9S-21E-5	31	Monsanto #1 Fromme
9S-19E-6	4	Texas Eastern #1 Mugge	9S-21E-6	32	Monsanto #3 Kulawik
9S-19E-6	5	Standard of Texas #1 Mugge	9S-21E-8	33	Brazos #1 Sievers et al.
9S-19E-8	6	Hunt #1 Flenniken	9S-21E-9	35	Alcoa #1 Casper
9S-19E-8	7	Standard of Texas #1 Tipton	9S-21E-9	36	Atlantic #1 Ladner
9S-19E-2	9	Union Texas et al. #1 Musselman Band Unit	9S-21E-9	38	Lone Star #1 Gips
9S-19E-7	11	Stone #1 Waskow Unit	9S-21E-5	41	Atlantic #2 Kerlick
9S-20E-1	1	Harper-Smith #1 Gips	9S-21E-2	42	Monsanto #2 Kulawik
9S-20E-1	3	Southland & Auld #1 Gips	9S-21E-6	43	Texaco #2 Broughton
9S-20E-1	4	Haxwell #1 Gips	9S-21E-4	44	Pace #1 Coleman
9S-20E-2	6	Magnolia #1 Kleberg Eckhart	9S-21E-3	45	Monsanto #1 Alves
9S-20E-2	7	Hamon and Ehman #1 Kleberg	9S-22E-3	2	Ada #1 Jendrzey
9S-20E-3	8	Dixel #1 Roeder	9S-22E-3	3	Kilroy of Texas #1 Mueller
9S-20E-3	9	Union Texas #1 Warwas	9S-22E-3	4	La Gloria #1 Ferguson
9S-20E-3	10	Monsanto and Ada #1 Roberts	9S-22E-5	4	Austral and Crown Central #1 Ferguson
				5	Texaco #1 Angerstein

## DE WITT FAIRWAY (cont.)

Township Range	Well No.	Well Name
10S-17E-7	1	General Crude #1 Grunwald
10S-18E-6	3	General Crude #1 Wessendorff
10S-18E-7	4	Atlantic #1 Pullin et al.
10S-18E-5	5	Hunt #1 Huckman
10S-18E-9	8	General Crude #1 McDowell
10S-19E-1	1	Cities Service #1 Stanchos "A"
10S-19E-2	2	Argo #1-A Dittmer Estate
10S-19E-2	3	Mobil #1 Speary
10S-19E-6	4	Cities Service #1-A Janssen
10S-19E-7	5	National Exploration #1 Effenberger
10S-19E-9	6	Shell #1 Atkinson
10S-19E-9	7	Shell #1-R Atkinson
10S-19E-1	8	Cities Service #1-A Gaus
10S-19E-1	9	Kirk and Need #1 Mueller Estate
10S-19E-2	10	Mobil #1 Meyer Unit
10S-19E-4	11	Cities Service #1 Wood "B"
10S-19E-8	13	Hunt #1 Zavesky
10S-20E-2	1	Atlantic #1 Skinner
10S-20E-3	2	Humble #1 Nordheim Gas Unit
10S-20E-3	3	Getty #13 Nordheim
10S-20E-3	4	Getty #11 Nordheim
10S-20E-6	5	Lone Star #1 Jank
10S-20E-3	6	Southland #1 Fuhrken
10S-20E-2	7	Cox #1 Riedel
10S-21E-2	2	Humble #1 Meyer
10S-21E-3	3	Humble #2 McMillan
10S-21E-3	5	Lone Star #1 Haynes Estate
10S-22E-9	3	Chevron #1 Jacobs
11S-19E-1	1	Samedan #1 Berkenhoff
11S-19E-1	4	Haring et al. #1 Powell
11S-20E-6	2	Humble #1 Neese
11S-21E-1	4	Associated and Halbouy #1 Von Dohlen
11S-22E-4	1	Shell #1 Friedrichs

## COLORADO FAIRWAY

Township Range	Well No.	Well Name
2S-31E-8	1	Mound #1 Newsome
2S-31E-8	2	Delhi-Taylor #1 Hillboldt
2S-31E-8	3	Shell #1 Hintz
2S-31E-8	4	Shell #2 Hillboldt
2S-31E-8	5	Shell #1 Cole
2S-31E-8	6	Mound #1 Hillboldt
2S-31E-9	7	Delhi-Taylor #1 Findeisen
2S-31E-9	9	Shell #1 Sealy Gas Unit
2S-31E-8	10	Mound #1 Konescheck
2S-31E-8	11	Ranger #3 Hintz Estate "A"
2S-31E-8	12	Ranger #1 Finke
2S-31E-8	14	Shell #5 Hillboldt
2S-31E-9	15	Scurlock #1 Kulow-Bielefeld Unit
3S-29E-4	2	Evans #1 Wilson
3S-29E-3	3	House and American Republics #1 Tolbirt
3S-29E-2	4	Cummins and Walker #1 Nelson
3S-29E-6	5	Skelly #1 Stringer
3S-29E-2	6	Texas #1 Coddou
3S-29E-8	7	King Resources #1 Lyle
3S-29E-7	8	Prairie #1 Thomas

## COLORADO FAIRWAY (cont.)

Township Range	Well No.	Well Name
3S-29E-7	9	Cities Service #B-2 Stephens
3S-29E-7	10	Cities Service #1 Pode
3S-29E-7	11	Cities Service #A-2 Pode
3S-30E-1	1	Carthay #1 Ludwig
3S-30E-1	2	Boston #A-1 Frobel
3S-30E-1	3	Alcoa and Boston #1 Amthor
3S-30E-2	4	Intercoastal #1 Krueger
3S-30E-2	5	Hanson and McCormick #1 Krueger
3S-30E-2	6	International Nuclear #1 Weishun
3S-30E-2	7	Union #1 Glueck
3S-30E-4	8	King Resources #1 Wintermann
3S-30E-4	9	Natural Resources #2 Wintermann
3S-30E-4	10	King Resources #1 Herder
3S-30E-7	12	Gray #1 Vineyard and Foster
3S-30E-9	13	National Resources #1 Birdwell
3S-30E-5	15	Newmont and Tidewater #1 Everett
3S-30E-5	16	Apexco #1 Meir
3S-30E-9	18	Cico #2-A Wintermann
3S-31E-4	19	Hanson #1 Wintermann
3S-31E-4	1	Gray #1 Bonnette
3S-31E-7	3	International Nuclear #1 Odom
3S-31E-8	5	Humble #1 Hillboldt
3S-31E-4	6	Hillard #1 Hillboldt
3S-31E-5	7	Sundance and Stuarco #3-A Best
3S-31E-5	8	Sundance et al. #2 Best
3S-31E-8	9	Texas #1 Kaechele
3S-31E-8	10	Humble #1 Kaechele
3S-32E-9	2	Southern #1 Unyrek
4S-29E-3	1	Superior #D-1 Tait
4S-29E-3	2	Superior #D-2 Tait
4S-29E-4	3	Skelly #1 Johnson
4S-29E-8	4	Shell #1 Kyle Estate
4S-29E-5	5	Brazos #1 Struss
4S-29E-2	6	Tidewater et al. #1 Brandon
4S-29E-2	7	Skelly #1 Walker
4S-29E-9	8	Bright and Schiff #1 Struss
4S-29E-8	9	Texas #1 Johnson "E"
4S-29E-8	10	Texas #1 Bunge
4S-29E-1	11	Skelly #1 Wintermann
4S-29E-7	12	Rain and Buck #1 Duncan
4S-29E-3	14	British-American #1 Wells
4S-29E-2	15	Continental #1 Tait
4S-29E-3	16	Superior #1 Tait
4S-29E-3	17	Superior #1 Tait
4S-29E-4	18	Fidelity #1 Dodson
4S-29E-1	19	Dow #1 Lange
4S-29E-3	20	Superior #D-3 Tait
4S-29E-4	21	Superior #1 Meyer
4S-29E-4	22	Parker Brothers #1 Parker Brothers Fee
4S-29E-9	23	Fidelity #1 Struss
4S-29E-2	24	Mosbacher #1 Tait
4S-30E-1	1	Shell #2 Hayes-Stephens
4S-30E-1	2	Clark-Sherwood (Stanolind) #1 Stephens Gas Unit
4S-30E-2	3	Union #A-1 Thomas
4S-30E-4	4	Brown #1 Wintermann
4S-30E-5	5	Tex-Star and Harkins #1 Haley Trust
4S-30E-5	6	Mosbacher and Harkins #1 Foster
4S-30E-6	7	Shell #1 Martin
4S-30E-6	8	Fidelity #1 Hoyo
4S-30E-7	9	Midwest #1 Haley

COLORADO FAIRWAY (cont.)

HARRIS FAIRWAY (cont.)

Township Range	Well No.	Well Name	Township Range	Well No.	Well Name
4S-30E-8	14	Mosbacher #1 Duncan	4N-36E-9	4	Cities Service #1 Madeley
4S-30E-8	15	Starr #1 Wintermann	4N-36E-6	5	Sunset International #1 Shaver
4S-30E-8	16	Frio #1 Waddell	4N-37E-6	1	Oil Reserves #1 Foster Estate
4S-30E-9	17	Fidelity #1 Duncan	4N-37E-7	2	Moran #3-A Hutchins-Sealy
4S-30E-9	18	Cherry #1 Wintermann Estate	4N-37E-7		National Bank
4S-30E-8	19	Sun #1 Duncan et al.	4N-37E-7	3	Moran #3 Hutchins-Sealy
4S-30E-3	20	Mutex #3-B Wintermann	4N-37E-7	4	Moran #2-A Hutchins-Sealy
4S-30E-3	21	Chicago and Skelly #1 Dennis	4N-37E-7		National Bank
4S-30E-5	22	Flaitz #1 Hoyo	4N-37E-8	5	Texmo #1 Hutchins-Sealy
4S-30E-7	23	Clover and Hanover #1 Harrison et al.	4N-37E-8		National Bank
4S-30E-8	24	Scurlock #1 Duncan-Wintermann Unit	4N-37E-8	6	Texmo-Brown #1 Gas Unit #2
4S-30E-6	25	Barnwell #1 Colorado Rose	4N-37E-8	7	Kirby (McKay & Donkin et al.)
4S-30E-6	26	Fidelity #1 Briggs	4N-37E-7		#1 Rawson
4S-31E-4	1	Crosby #1 Poole	4N-37E-7	8	Glen Rose #1 Champion
4S-31E-7	2	Getty #1 Leveridge	4N-37E-7	9	Moran #1-B Hutchins-Sealy
4S-31E-9	3	Newmont #1 Poole	4N-38E-1		National Bank
4S-31E-4	4	Humble #1 Thomas et al.	4N-38E-1	1	Continental #1 Gibbs
4S-31E-9	5	Magnolia #1 Poole	4N-38E-1	2	Continental #2 Gibbs
4S-31E-4	6	Humble #1 Isenhower	4N-38E-1	3	Huber Co. #1 Gibbs
5S-29E-1	1	Socony-Mobil #5 Gracey	4N-38E-1	4	Texas City #1 Foster Estate
5S-29E-3	2	Halbouyt #1 Lehrer	4N-38E-2	5	Cities Service #1 Frazier & Campbell
5S-29E-1	3	Shell #1 Thompson	4N-38E-2	6	Dominion #1 Campbell
5S-29E-2	4	Shell #1 Hudson	4N-38E-3	7	Continental #1 Frazier
5S-29E-3	6	Mosbacher et al. #1 Lehrer	4N-38E-4	8	Donkin & Smith #1 Browder
5S-30E-1	1	General Crude #1 Wintermann	4N-38E-4	9	Moran #1 Browder
5S-30E-1	2	General Crude #3 Wintermann	4N-39E-3	1	Prairie & Convest #1 Gibbs et al.
5S-30E-3	3	Brazos #1 Matthews et al.	4N-39E-3	2	Impact #1 Mays
5S-30E-3	4	Magnolia #1 Gracey-Wegenhoff	4N-39E-4	3	Continental #1 Mays et al.
			4N-39E-7	5	Amerada & Mid-States
					#1 Central Coal & Coke

HARRIS FAIRWAY

Township Range	Well No.	Well Name	Township Range	Well No.	Well Name
5N-38E-5	1	Cities Service #B-1 Browder	4N-39E-8	7	Shell #11 Central Coal & Coke
5N-38E-7	2	Texas City #1 Elmore	4N-39E-8	8	Superior #1 Foster
5N-38E-8	3	Dominion #2 Elmore et al.	4N-39E-8	9	Manning #1 Central Coal & Coke
5N-38E-8	4	Dominion #1 Elmore	4N-39E-9	10	Fain #1 Baldwin
5N-38E-8	5	Houston #1 Lewis Unit	4N-40E-1	1	Texas Gas Exploration #1 Ogletree
5N-38E-8	6	Cities Service #1 Ellisor	4N-40E-1	2	Magnolia #2 Dixon-Falvey
5N-38E-8	7	Triton #1 Roche-Ellisor	4N-40E-4	3	Magnolia #1 Hinchliff-Sims
5N-38E-8	8	Barnes #1 Johnson	4N-40E-8	4	Magnolia & Abercrombie #1 Brewer
5N-38E-8	9	Cities Service #1 Melvin Unit	4N-40E-8	5	Davis #1 Sims
5N-38E-8	10	Cities Service #1 Browder	4N-41E-9	1	Oil Reserves #1 Jefferson
5N-39E-3	1	Glen Rose #1 Cary Heirs	4N-41E-1	2	Continental & Speed #1 Frost
5N-39E-7	3	Standard of Texas #1 Foster	4N-41E-6	3	Pan American #1 Moore Estate
5N-39E-7	4	Shell #1 Coline	3N-33E-8	1	Gulf #2 Gardner
5N-39E-8	6	Reserve #2 Richards	3N-33E-8	2	Millican #1 Gardner
5N-40E-6	1	Sun #1 McGowan Unit 1	3N-34E-7	3	Gulf #1 Gardner
5N-40E-6	2	Viking and De Lange #1 Langham	3N-34E-7	4	Atlantic #1 Sanders
		Gas Unit	3N-34E-8	5	Millican #1 Baner
5N-41E-4	1	Amoco #A-3 Langham	3N-34E-8	1	Colorado #1 Rice University
5N-41E-4	3	Pan American #B-2 Langham	3N-36E-1	2	Callery #1 Thompson
5N-41E-4	5	Stanolind #B-1 Langham	3N-36E-4	3	McCarthy #1 Gibbs-Elgin et al.
5N-41E-4	6	Stanolind #C-1 Langham	3N-36E-8	4	Standard of Texas #2 Sanders et al.
5N-42E-9	2	Sunray #1 Bell	3N-36E-7	1	Feldman #1 Teas Nursery
4N-35E-7	1	Capital #1 Alliance Trust	3N-36E-7	2	Socony-Mobil
4N-36E-6	1	Superior & Speed #1 Elam	3N-36E-7		#1 Sealy-Smith Foundation
4N-36E-6	2	Superior & Speed #1 Sykes	3N-36E-7	3	Prairie & Convest #1 Madeley et al.
4N-36E-6	3	Moran #1 Sykes	3N-36E-7	4	Delhi-Taylor
					#2 Sealy-Smith Foundation
				5	Delhi-Taylor
					#1 Sealy-Smith Foundation

HARRIS FAIRWAY (cont.)

Township Range	Well No.	Well Name
3N-36E-8	6	McCulloch & Venus #1 Frost
3N-36E-8	7	Prairie #1 Frost et al.
3N-36E-8	8	Superior #3 Frost
3N-36E-8	9	Superior #1 Frost
3N-36E-8	10	Mecom & Cockrell #1 Bertrand
3N-36E-9	11	Stanolind #1 William
3N-36E-9	12	Sinclair #1 Grogan
3N-36E-9	13	Mitchell #1 Asche et al.
3N-37E-4	1	Moran #1 Cartwright
3N-37E-5	2	Hagen & Litchfield #1 Harris & Freeman
3N-37E-8	3	Skelly #1 Tipton
3N-37E-8	4	Humble #1 Grande Lake Gas Unit #2
3N-37E-9	5	Humble #1 Grande Lake Gas Unit #1
3N-37E-9	6	Humble #2 Grande Lake Gas Unit #1
3N-37E-9	7	Humble #1 Council
3N-38E-1	1	Sands #1 San Jacinto Trust
3N-38E-5	2	Texaco #1 Griffin
3N-39E-1	1	Atlantic #1 White
3N-39E-1	2	Trice #1 Foster
3N-39E-2	3	Cauble #1 Combe Heirs
3N-39E-2	4	Gulf #1-A Foster
3N-39E-5	5	Rowan #1 Dunnam
3N-39E-5	6	Atlantic #1 Foster
3N-39E-5	7	Halbouyt #1 Foster-Gulf
3N-39E-8	8	Pure Oil #1 Foster
3N-39E-5	9	Halbouyt #1-B Foster
3N-39E-5	10	Halbouyt #2 Foster
3N-39E-5	11	Halbouyt #1-A Foster
3N-39E-8	12	Union & Halbouyt #E-1 Foster
3N-39E-6	13	Amerada #1 Foster
3N-39E-6	14	Halbouyt #1 Godejohn
3N-39E-6	15	Amerada #1 Godejohn
3N-39E-6	16	Halbouyt #1 Burkett
3N-39E-7	17	Halbouyt #1 Leggett
3N-39E-8	18	Halbouyt #1 Southland Paper
3N-39E-5	19	Sohio & Leben #1 Kingswood et al.
3N-39E-6	20	Sanchez-O'Brien #1 Friendswood
3N-39E-6	21	Sanchez-O'Brien #1 Friendswood
3N-39E-7	22	Halbouyt #1 Todd
3N-40E-1	1	Sun #1 Quinn
3N-40E-1	2	Karsten #5-A Quinn
3N-40E-1	3	Houston Mineral #1 Ott Gas Unit
3N-40E-1	4	Pan American #1 Howard
3N-40E-1	5	Ohio #1 Quinn
3N-40E-1	6	Pan American #A-1 Kirby
3N-40E-2	7	Sundance #1 Davis
3N-40E-3	8	Mitchell #1 Cherry
3N-40E-8	9	Superior #1 Bosworth
3N-40E-8	10	Hunt #1 Grogan
3N-40E-9	11	Superior #1 Hightower
3N-40E-9	12	Superior #1 Hightower
3N-40E-9	13	Humble #1 McDonald
3N-41E-3	1	Humble #1 Smith
3N-41E-3	2	Cherryville #1 Jackson
3N-41E-3	3	Brazos #1 Ballard
3N-41E-4	4	Porter & Phillips #1 Champion
2N-32E-5	1	Continental Thomas & Scardino
2N-32E-6	2	Harrison #1 Gaines
2N-32E-7	3	Sinclair #1 McDade
2N-33E-4	1	Brazos #1 Sledge
2N-33E-4	2	Sun #1 Von Blucher

HARRIS FAIRWAY (cont.)

Township Range	Well No.	Well Name
2N-33E-4	3	Mana #1 Smith
2N-33E-2	4	Brazos #1-A Connell
2N-33E-2	5	Sun-Indiola #1 Connell
2N-34E-3	1	Strake #1 Humphries
2N-34E-3	2	Speed #1 Sauerbrunn et al.
2N-34E-3	3	Texas #1 Humphries
2N-34E-4	4	Associated et al. #1-A Rice University
2N-34E-4	5	Texas #1 Rice University
2N-34E-5	6	Superior #1 Harry Brown
2N-34E-5	7	McCarthy #1 Tucker
2N-34E-7	8	Enterprises #1 Welch Foundation
2N-34E-7	9	Ashland #1 Welch Foundation
2N-35E-2	5	Gray Wolfe #4 Pan Am
2N-35E-2	6	Gray Wolfe #3 Pan Am
2N-35E-2	7	Pan Am #1 Posey
2N-35E-2	8	La Gloria #2 Cochran
2N-35E-3	9	Hawkins & Hawkins #1 Von Streety
2N-35E-3	10	Christie et al. #1 Von Streety
2N-35E-3	11	Standard of Texas #1 Dean et al.
2N-35E-4	12	Humble #1 Lewis et al.
2N-35E-4	14	Superior #1 Kramer
2N-35E-4	15	Gose #1 Kramer
2N-35E-4	16	Mitchell #1 Hagen
2N-35E-5	17	Superior #3-A Dean
2N-35E-5	18	Superior #A-1 Dean
2N-35E-4	19	Gray Wolfe #6 Pinehurst
2N-35E-5	20	Superior #2-A Dean
2N-35E-5	21	Gray Wolfe #3 Pinehurst
2N-35E-5	22	Gray Wolfe #4 Pinehurst
2N-35E-8	23	Commercial #1 Pills & Leyle
2N-35E-9	24	Pan Am #1 Welch Foundation
2N-35E-1	26	Superior #A-5 McWhorter
2N-35E-1	27	Superior #2-C McWhorter
2N-35E-1	31	Superior #1-C McWhorter
2N-35E-1	32	Superior #1-D McWhorter
2N-35E-1	34	Superior #4-A McWhorter
2N-35E-1	36	Progress #1 Winslow
2N-36E-1	1	Superior #1 McMahon
2N-36E-1	2	Texaco #1 Winslow
2N-36E-2	3	International Nuclear & Prairie #1 M & M
2N-36E-2	4	Stanolind #1 McMahon
2N-36E-2	5	Royal #1 M & M
2N-36E-2	6	Magnolia #1 Chase National Bank
2N-36E-3	7	Superior #A-7 McWhorter
2N-36E-3	8	Stanolind #A-1 South Texas
2N-36E-3	9	Superior #1 Homer Brown
2N-36E-3	10	Superior #30 Lake Creek
2N-36E-3	11	Superior #1 South Texas
2N-36E-3	12	Superior #1 M & M
2N-36E-3	13	Del Mar #1 South Texas
2N-36E-5	14	Moran #1 M & M
2N-36E-6	15	Superior #1 Foley
2N-36E-6	16	Sohio et al. #1 1936 Development
2N-36E-7	17	Shell #1 Peden
2N-36E-8	18	Shell #1 Holderreith
2N-36E-2	19	Vaquero #B-1 M & M
2N-36E-3	20	Superior #3 South Texas
2N-36E-3	21	Superior #2 South Texas
2N-37E-4	1	Sinclair #1 Grogan-Cockran
2N-37E-4	2	Sinclair #1 Porter

HARRIS FAIRWAY (cont.)

HARRIS FAIRWAY (cont.)

Township Range	Well No.	Well Name	Township Range	Well No.	Well Name
2N-37E-7	3	Texaco #1 Bender	1S -35E-4	2	Standard of Texas #1 Josey et al.
2N-37E-9	4	Shenandoah #1 Evans	1S -35E-4	3	Scurlock #1 Josey
2N-37E-9	6	McDaniel #1 Baldwin	1S -35E-5	4	Texaco #1 Sweeney Estate
2N-38E-1	1	Atlantic #1 South Texas	1S -35E-8	7	Standard of Texas #1 Millinger et al. #4
2N-38E-5	3	Standard of Texas #1 Anderson et al.	1S -35E-2	9	Roeser & Pendleton #1 Townes
2N-38E-7	4	Winwell #1 Schwing	1S -36E-8	1	Pan American #1 Brown
2N-38E-7	5	Lacal #1 Schwing	1S -37E-1	1	Meredith et al. #1 Ross et al.
2N-38E-7	6	Humble #1 Wickizer	1S -37E-2	2	Ginther & Warren
2N-38E-2	8	Humble #1 Hines	1S -37E-3		#1 Taub-Dwyer-McCall Unit #1
2N-38E-2	9	Goodale Bertman #1 Maynard	1S -37E-3	3	Sunset #1 Hamill
2N-39E-1	1	Samedan #1 Coleman	1S -37E-2	4	Houston Natural Gas #1 Hamill Gas Unit #1
2N-39E-2	3	Humble #B-1 Long Leaf	1S -37E-4		Texaco #1 Sweeney Gas Unit #1
2N-39E-2	4	Kurth Trustee #4 Southland Paper	1S -37E-4	6	Texaco #1 Sharman Gas Unit #1
2N-39E-4	5	Humble #1 Ovalline	1S -37E-3	7	Texaco #1 Rodgers
2N-39E-4	6	Sinclair #1 Foster	1S -37E-5	8	Houston Natural Gas #1 Hamill Gas Unit #1
2N-39E-5	7	Humble #1 Patton	2S -33E-1	1	Exxon #W-45 K.G.F.U.
2N-39E-6	8	Union #1 Foster	2S -33E-5	2	Houston Natural Gas & Halbouy #1 Ainsworth
2N-39E-6	9	Atlantic #1 Foster	2S -33E-6	3	Stanolind #1 Freeman (#8 K.G.F.U. Unit 1)
2N-40E-2	1	Humble #B-1 Quinn	2S -33E-6	4	Humble #W-31 K.G.F.U.
2N-40E-2	2	Sun #2 Quinn	2S -33E-6	5	Humble #W-32 K.G.F.U.
2N-40E-2	3	Sundance #1 Quinn	2S -33E-6	6	Exxon #W-44 K.G.F.U.
2N-40E-2	4	Sun #1 Quinn	2S -33E-6	7	Exxon #W-38 K.G.F.U.
2N-40E-2	5	Gulf #C-1 Quinn	2S -33E-8	8	Humble #W-34 K.G.F.U.
2N-40E-2	6	Allday & Hammax #1 Quinn	2S -33E-8	9	Exxon #W-41 K.G.F.U.
2N-40E-5	7	Sun #1 Friendswood	2S -33E-8	10	Humble #33 K.G.F.U. #1
1N-30E-5	1	Holmes & Mosbacher #1 Wright	2S -33E-6		Scurlock #1 Arnold
1N-31E-1	1	Karsten #1 Menke	2S -34E-9	2	Scurlock #1 McMillian
1N-31E-9	2	Skelly #1 Sander	2S -34E-4	3	Exxon #W-43 K.G.F.U.
1N-33E-1	1	Sinclair #1 Krezdorn	2S -34E-4	4	Exxon #W-35 K.G.F.U.
1N-35E-8	1	Texaco #1 Mergele	2S -34E-4	5	Exxon #W-42 K.G.F.U.
1N-37E-1	1	Humble #1 Bender	2S -34E-9	6	Exxon #W-36 K.G.F.U.
1N-37E-2	2	Humble #1 Baldwin	2S -33E-8	1	Conroe #1 Addicks
1N-37E-8	4	Houston Natural Gas #1 Tanneberger	3S -33E-3	1	Mound #1 England et al.
1N-38E-3	1	Mobil #1 Bender Estate	3S -34E-2	1	Scurlock #1 Meek
1N-38E-3	2	Continental #1 Bender Estate	3S -34E-9	2	Enserch #1 Foster Farms
1N-38E-3	3	Texaco #1 Bender	3S -34E-9	3	Mobil #1 Foster Farms
1S -32E-3	1	Humble #17-B Hardy "B"			
1S -33E-6	1	Humble #1 Sparks			
1S -33E-8	2	Halbouy #1 Harris et al.			
1S -33E-7	3	Exxon HW-46 K.G.F.U. #2			
1S -33E-8	4	Pet-Tex #1 Harris			
1S -35E-4	1	Standard of Texas #1-1 Logenbaugh			



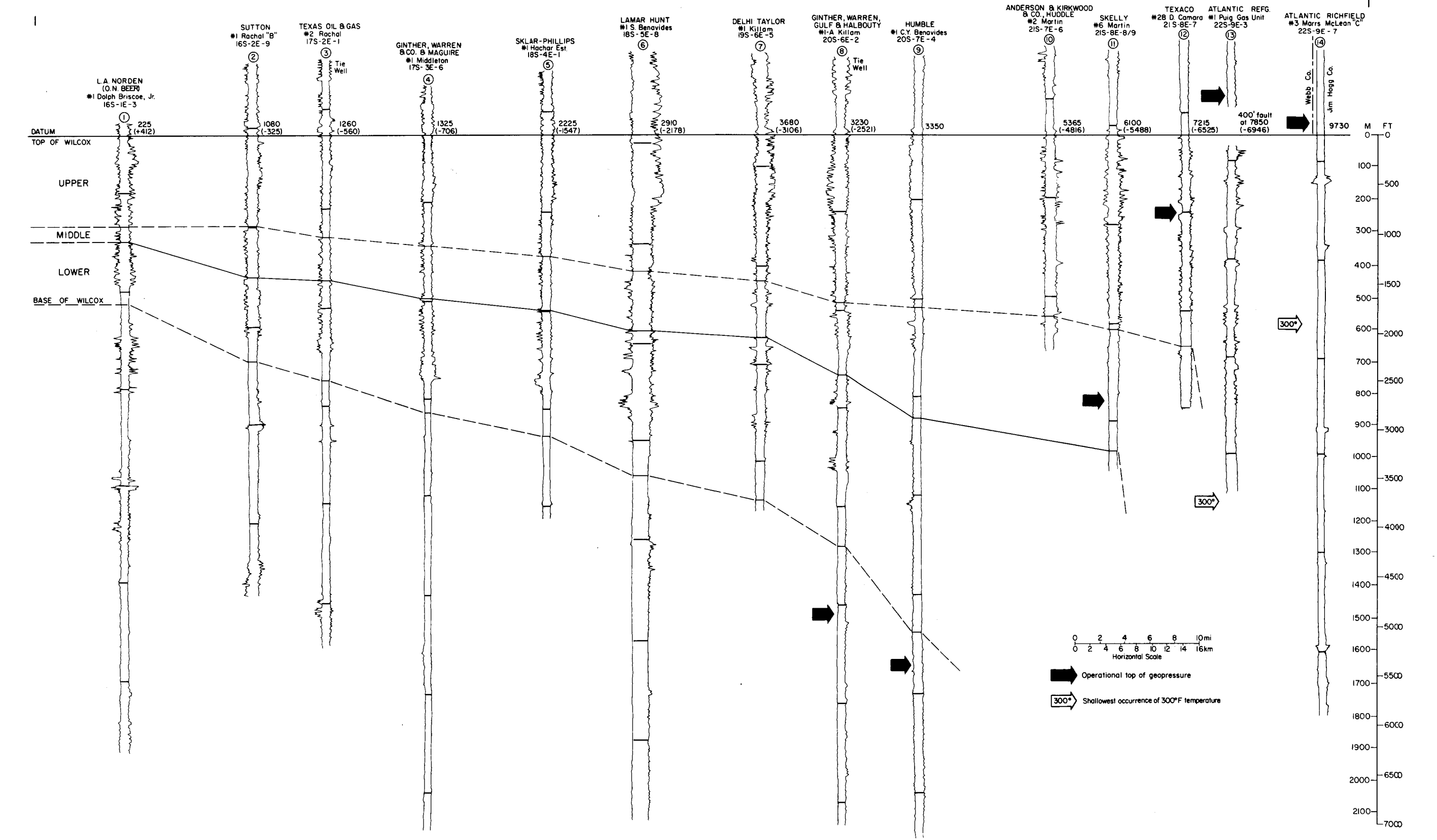


Figure 11. Stratigraphic dip section 1.

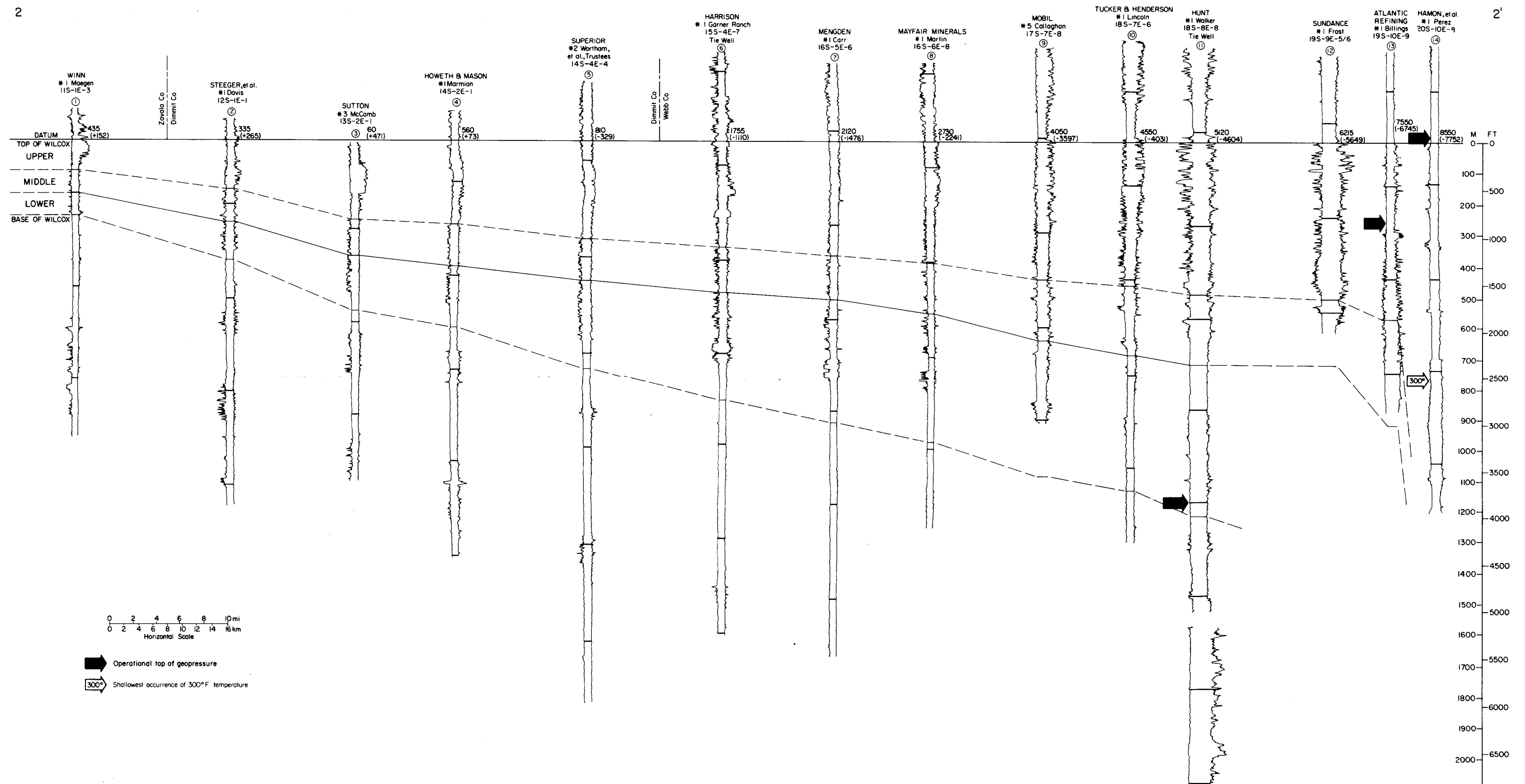


Figure 12. Stratigraphic dip section 2.

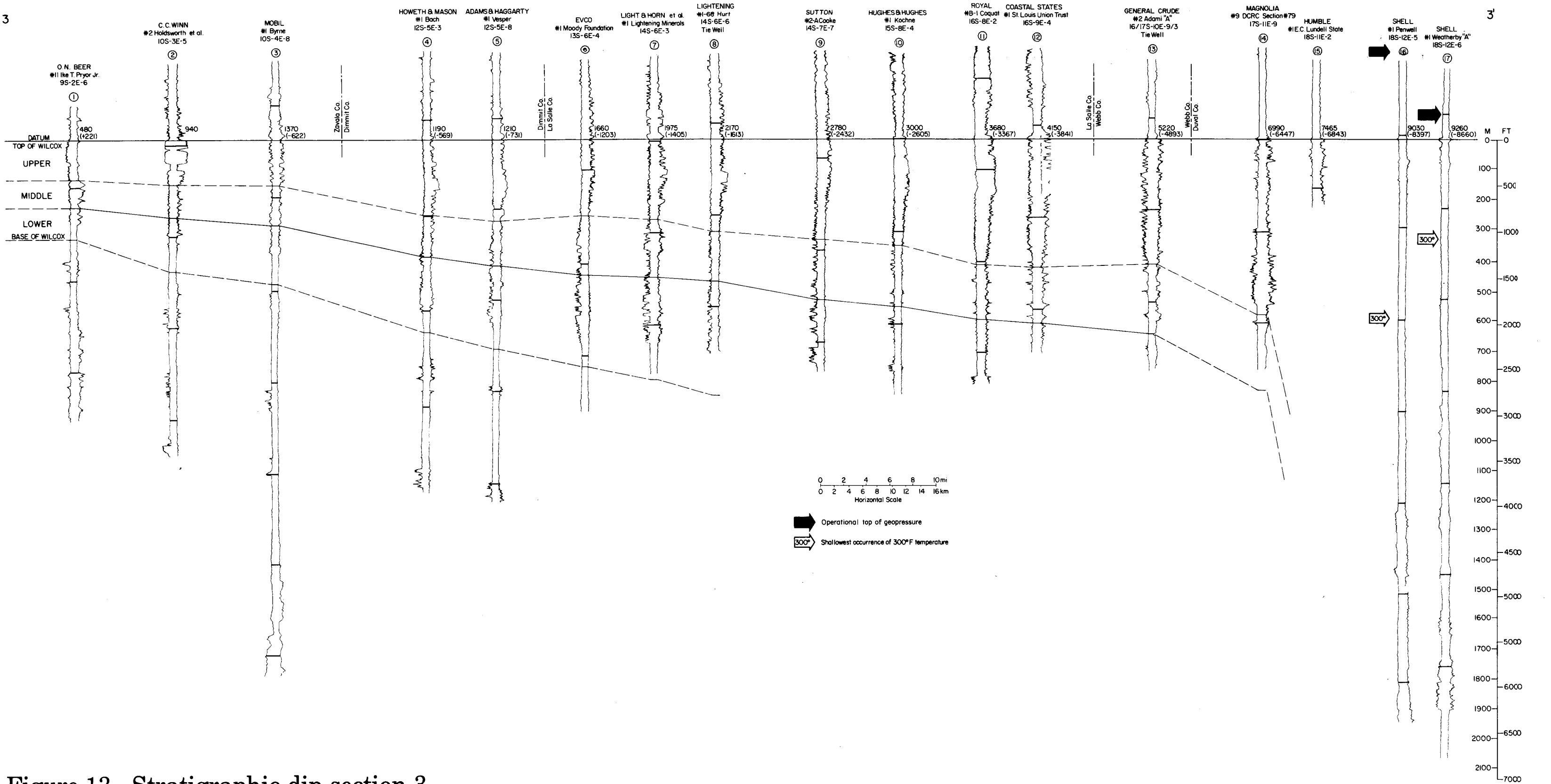


Figure 13. Stratigraphic dip section 3.

The locations of these sections are shown in figure 9 (in text). The datum for each section is the top of the Wilcox Group, and the transition between the Wilcox and the underlying Midway is shown by the dashed line. A pressure gradient of 0.7 psi per foot is shown by the black arrows; the approximate points at which a temperature of 300°F occurs are shown by the arrows so labeled.

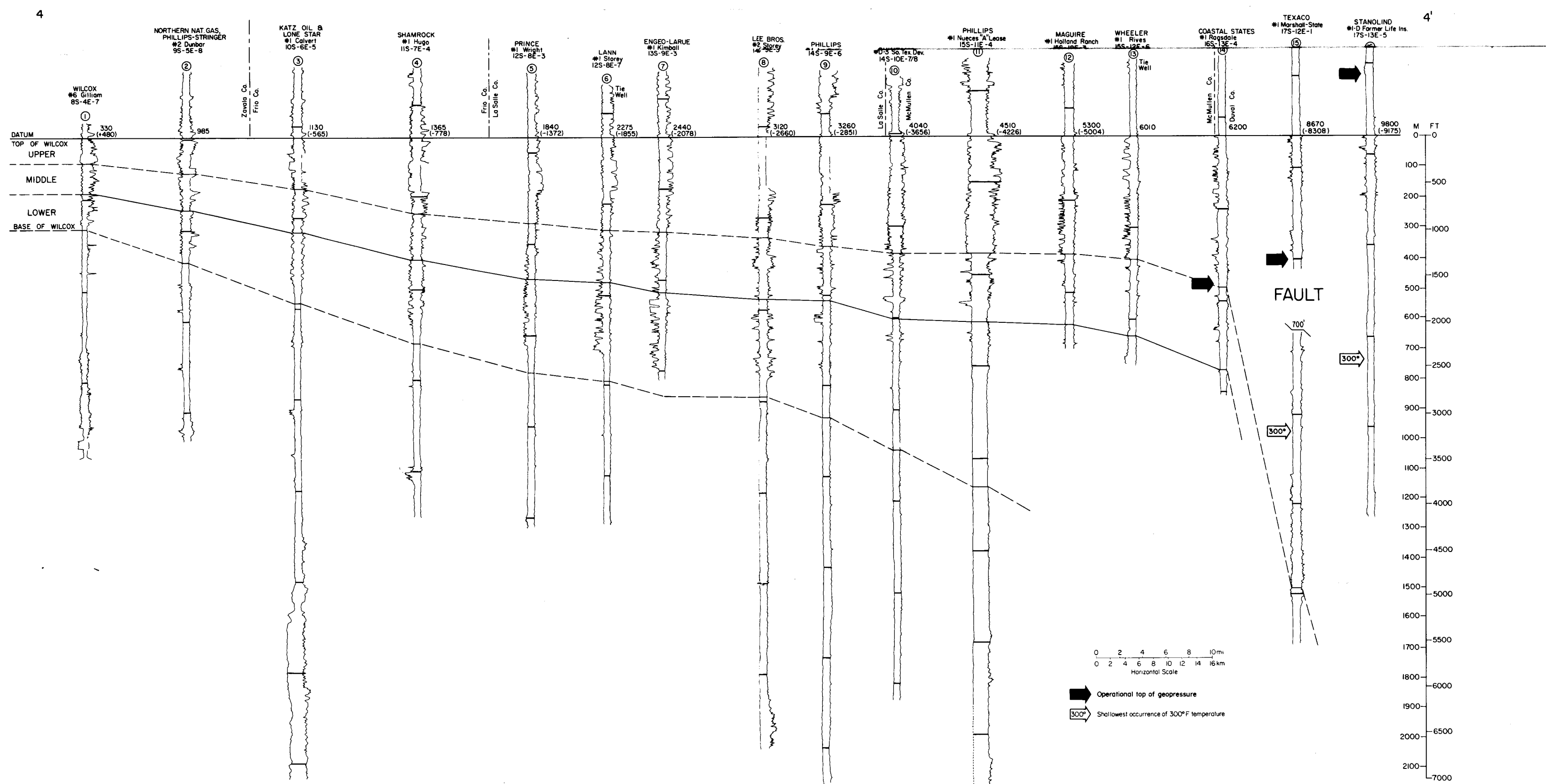


Figure 14. Stratigraphic dip section 4.

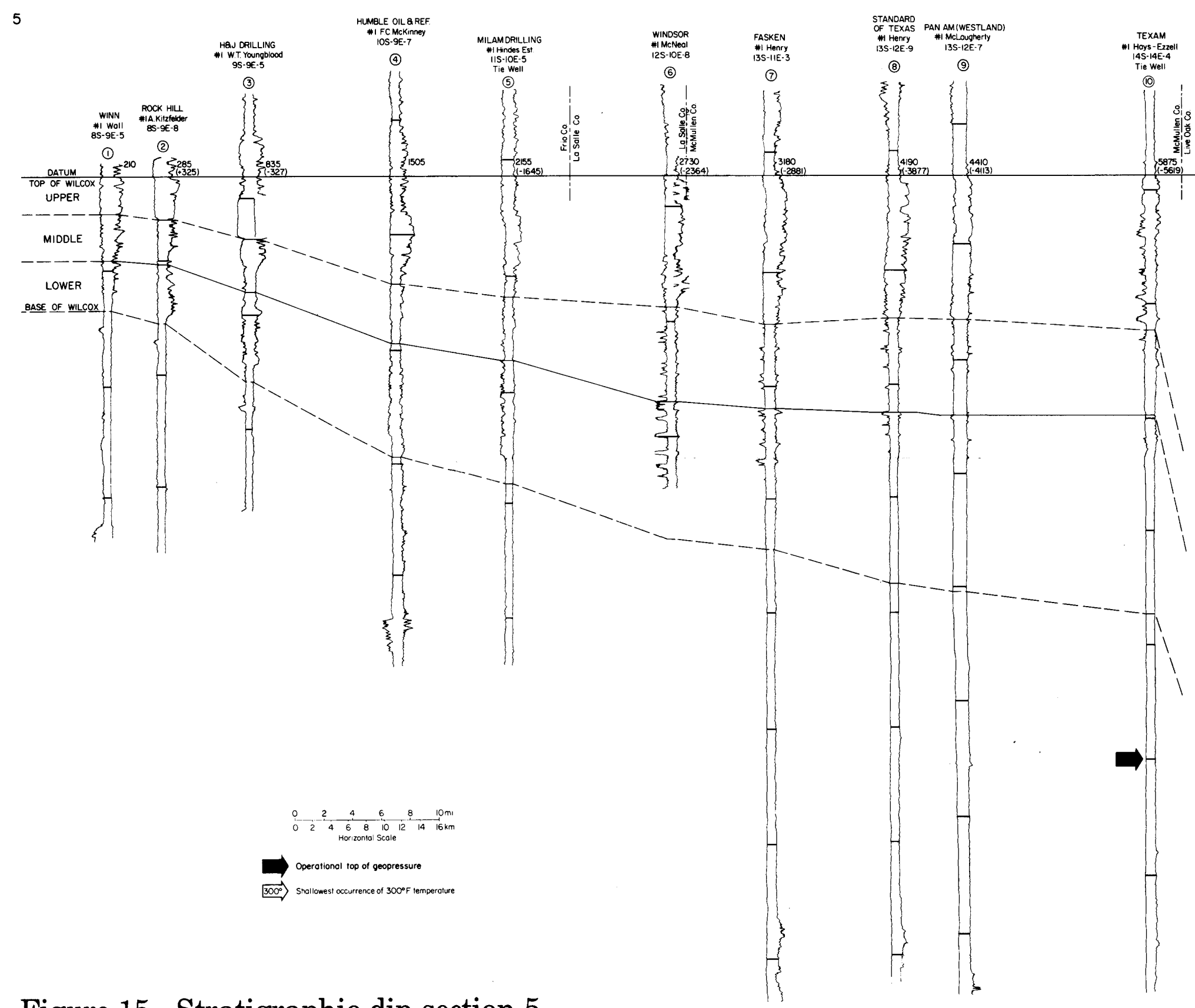


Figure 15. Stratigraphic dip section 5.

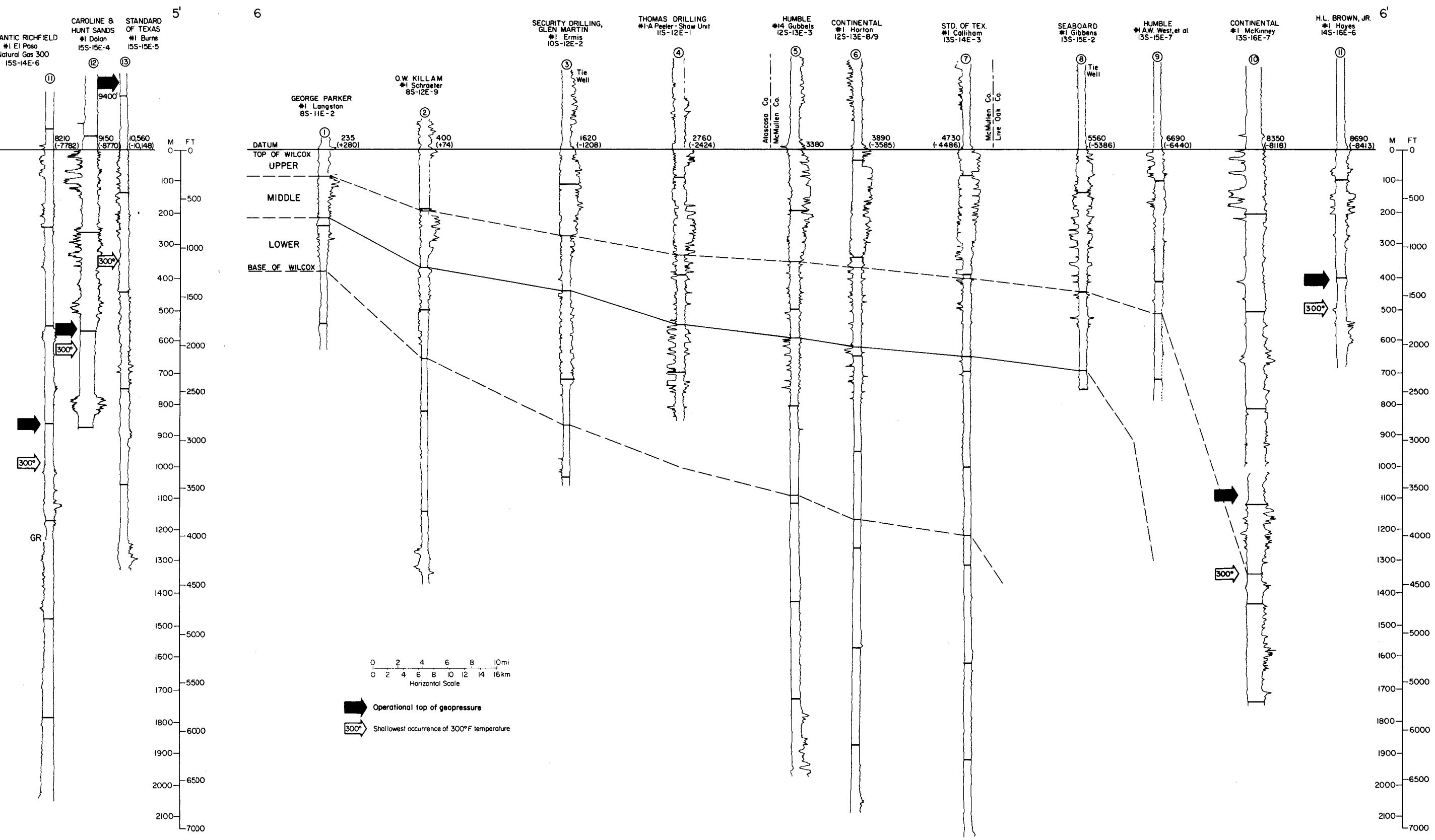


Figure 16. Stratigraphic dip section 6.

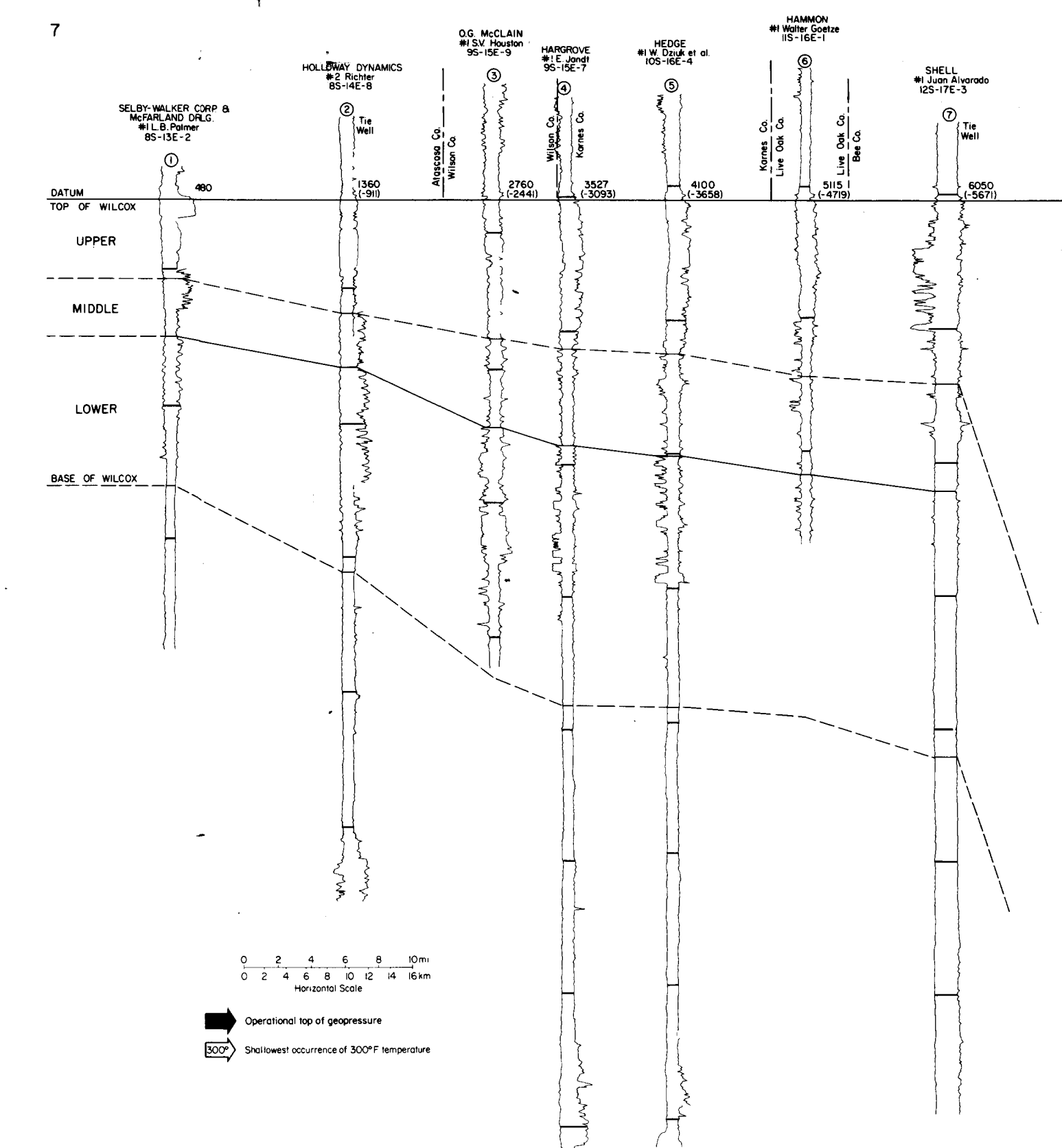


Figure 17. Stratigraphic dip section 7.

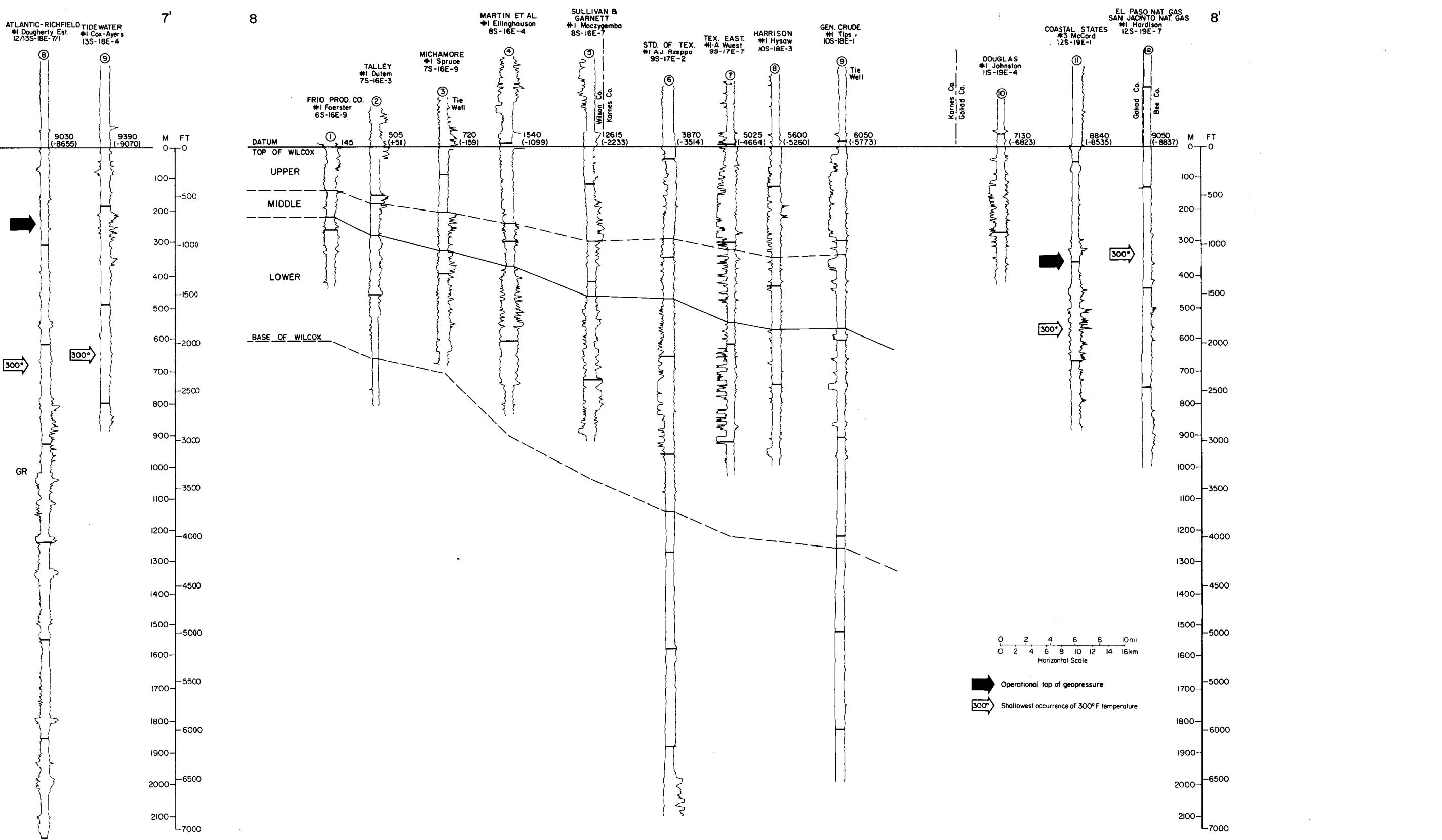


Figure 18. Stratigraphic dip section 8.

The locations of these sections are shown in figure 9 (in text). The datum for each section is the top of the Wilcox Group, and the transition between the Wilcox and the underlying Midway is shown by the dashed line. A pressure gradient of 0.7 psi per foot is shown by the black arrows; the approximate points at which a temperature of 300°F occurs are shown by the arrows so labeled.

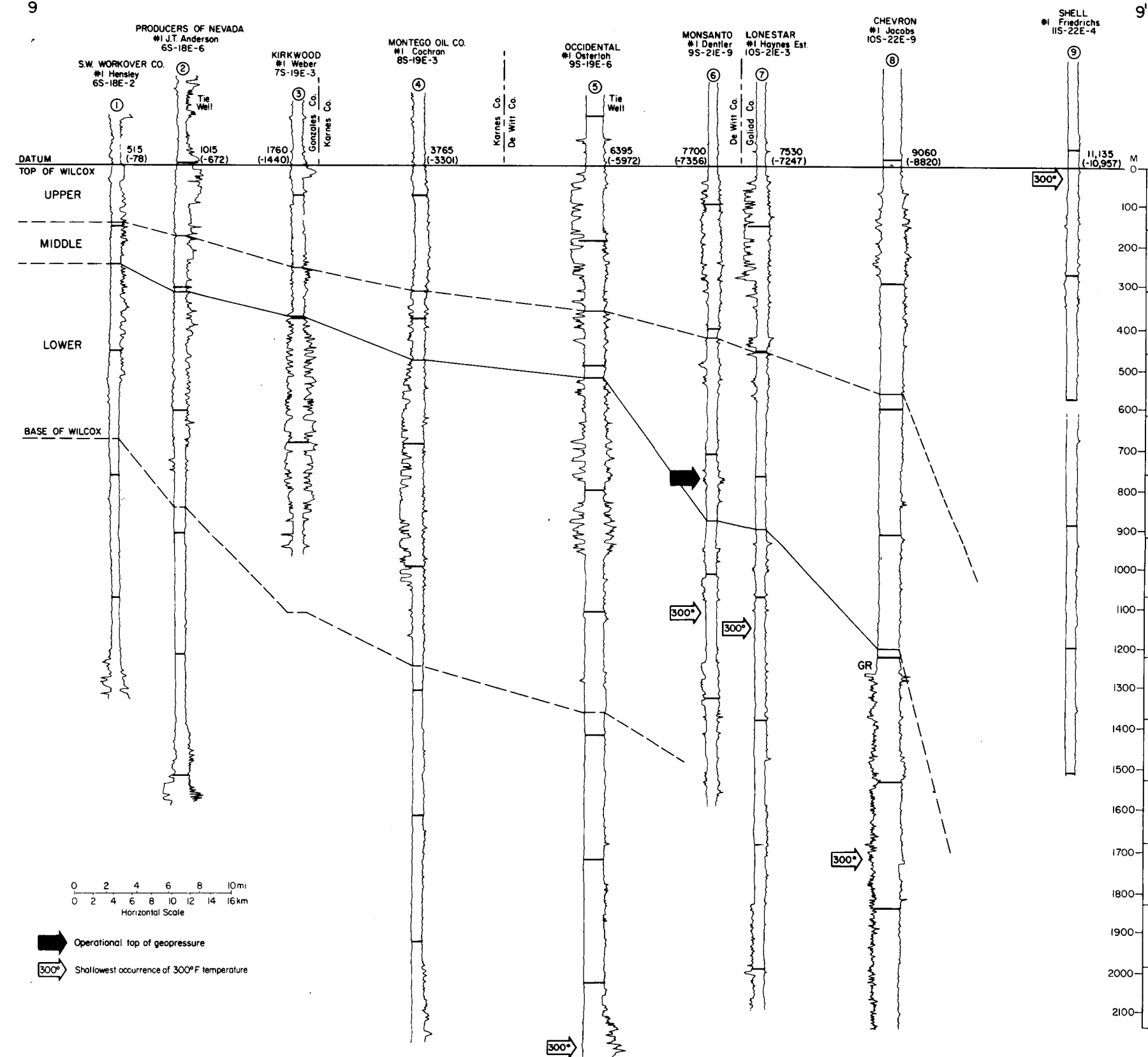


Figure 19. Stratigraphic dip section 9.

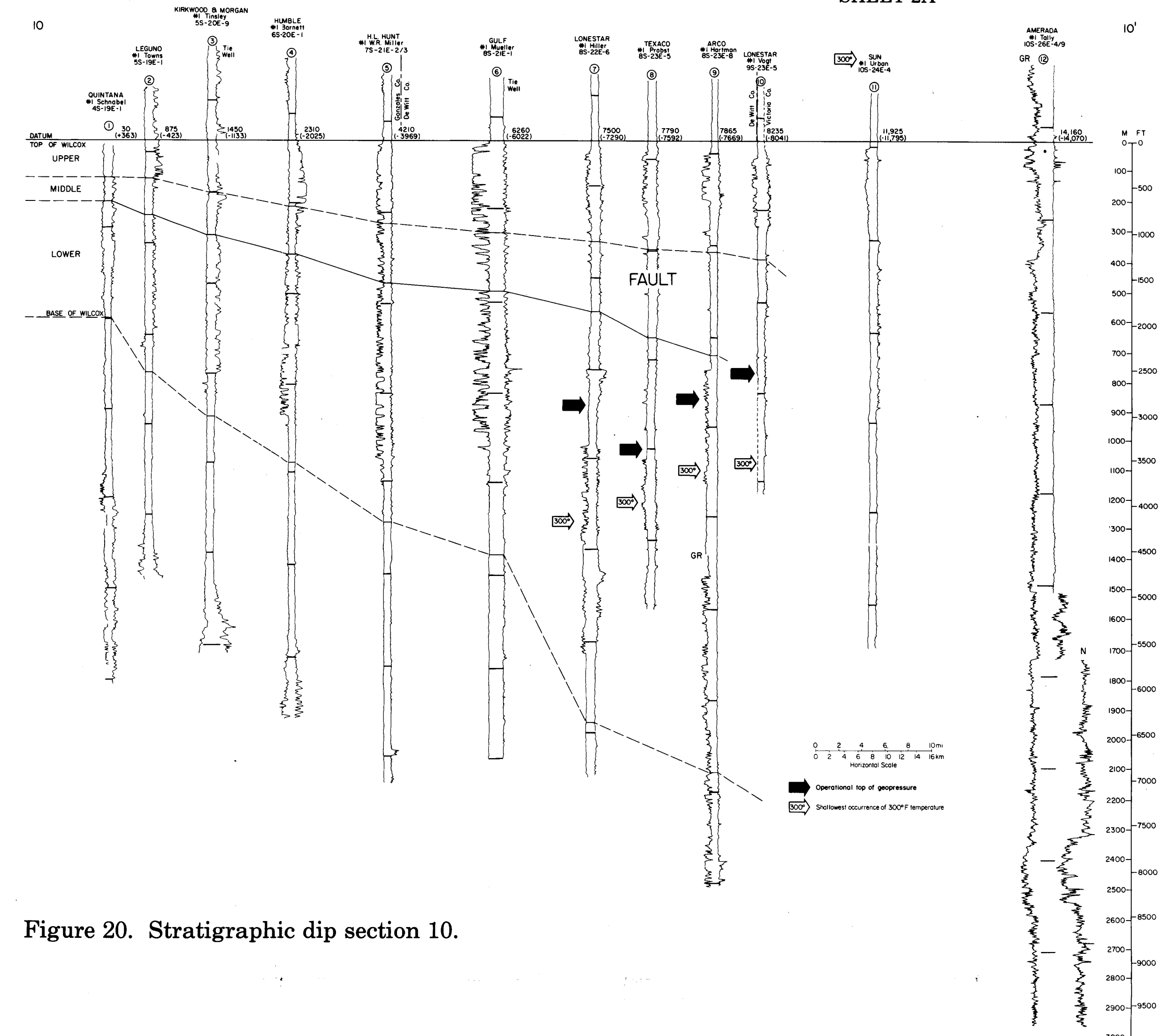


Figure 20. Stratigraphic dip section 10.

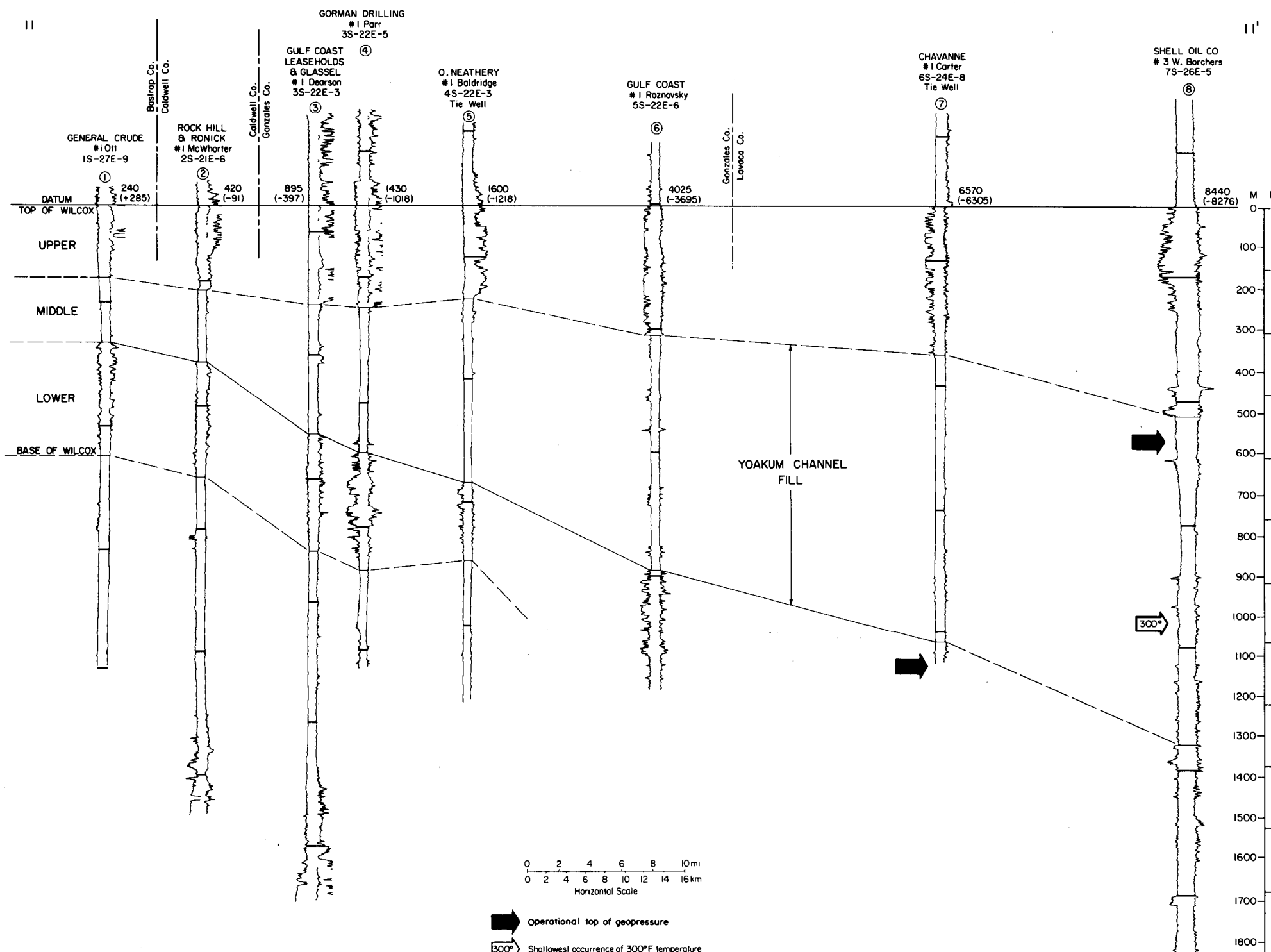


Figure 21. Stratigraphic dip section 11.

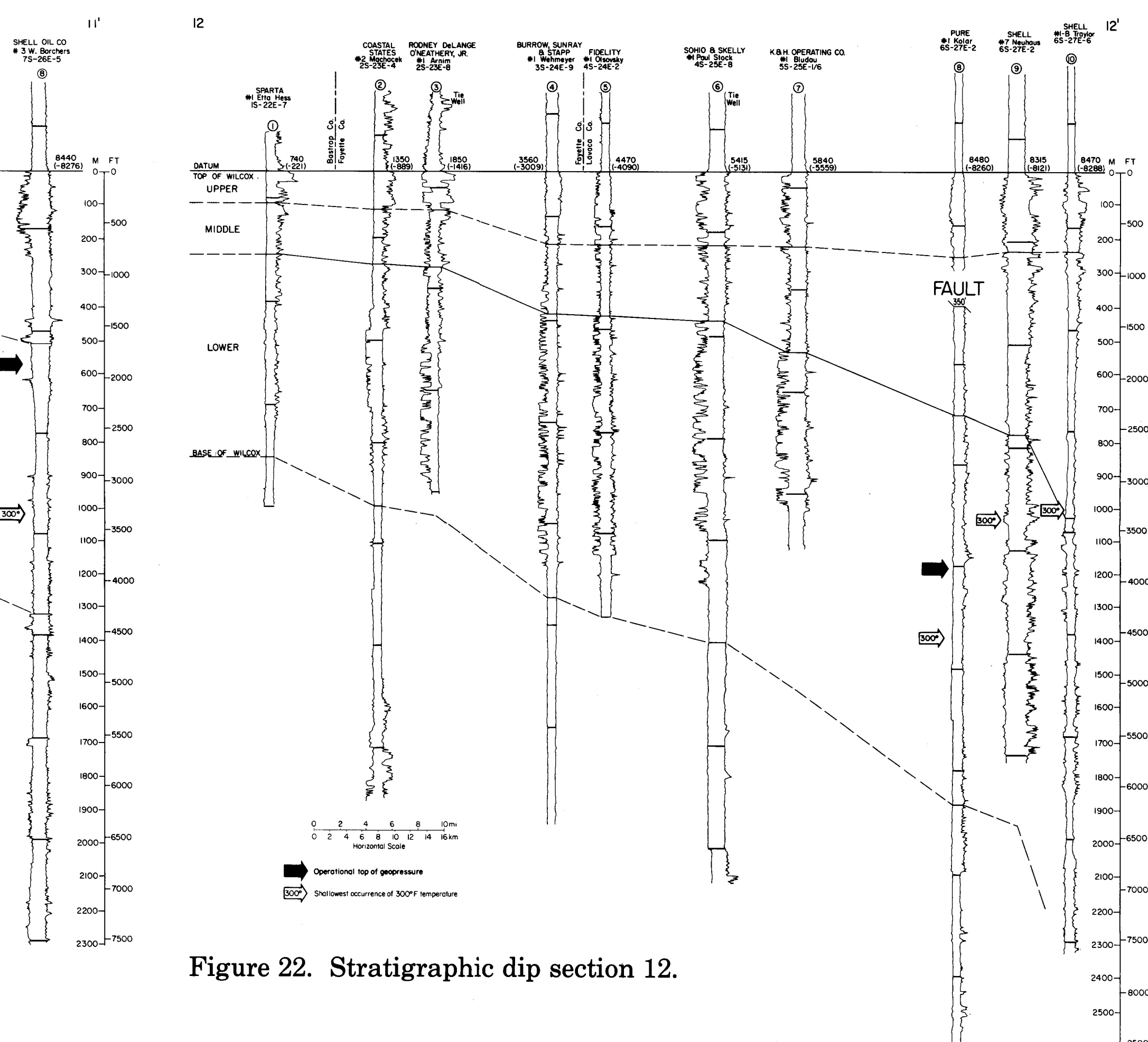


Figure 22. Stratigraphic dip section 12.

The locations of these sections are shown in figure 9 (in text). The datum for each section is the top of the Wilcox Group, and the transition between the Wilcox and the underlying Midway is shown by the dashed line. A pressure gradient of 0.7 psi per foot is shown by the black arrows; the approximate points at which a temperature of 300°F occurs are shown by the arrows so labeled.

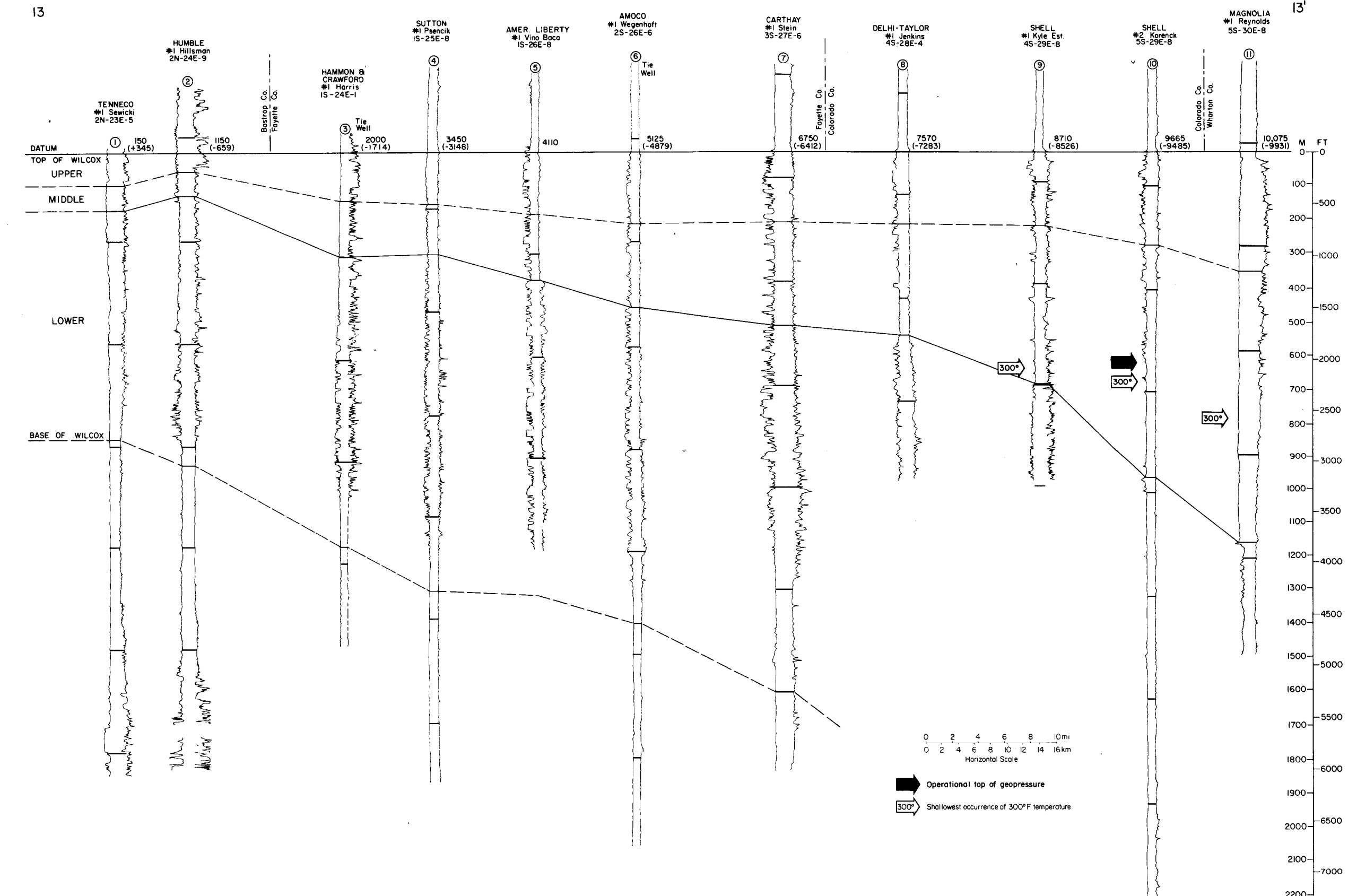


Figure 23. Stratigraphic dip section 13.

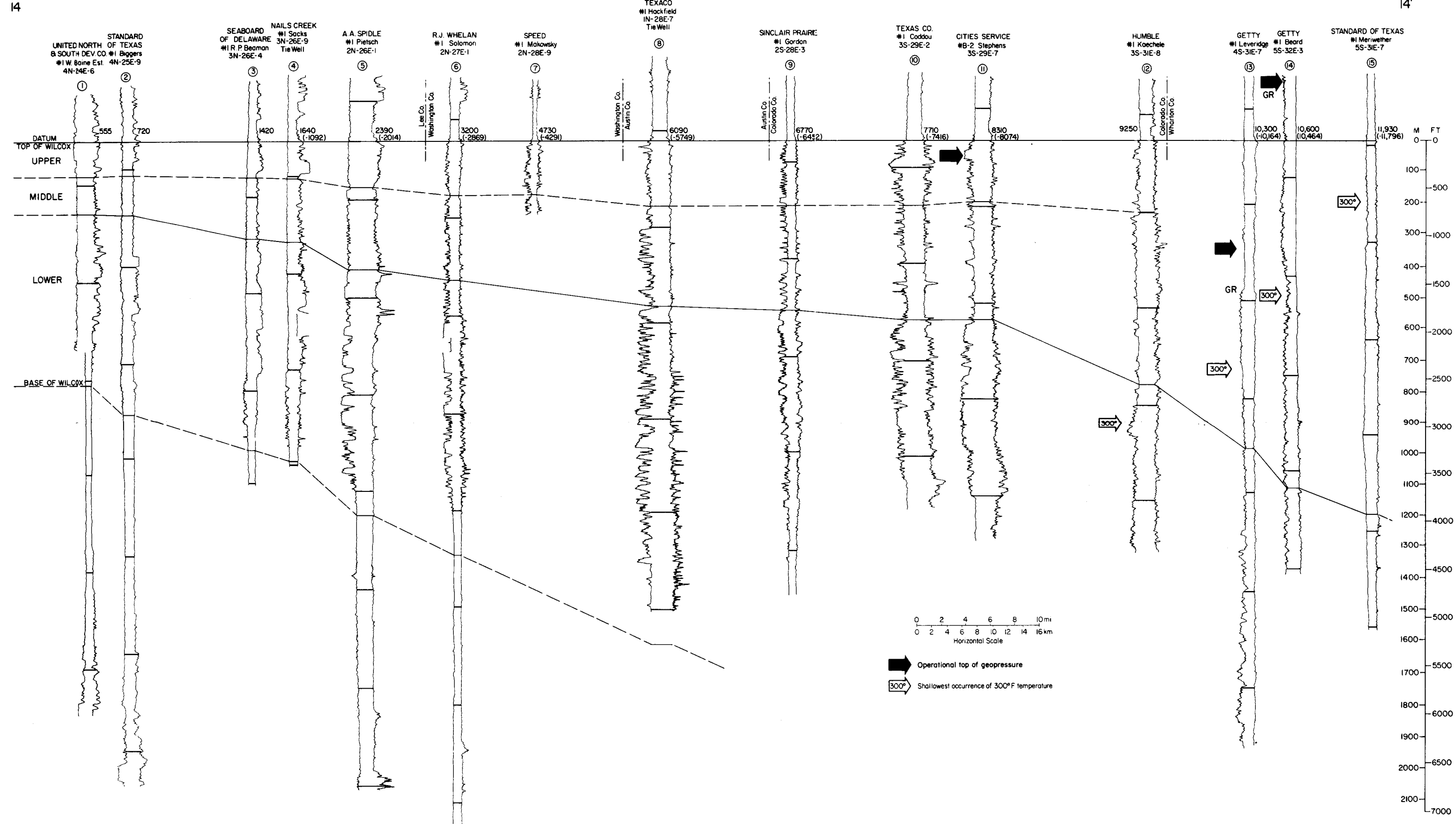


Figure 24. Stratigraphic dip section 14.

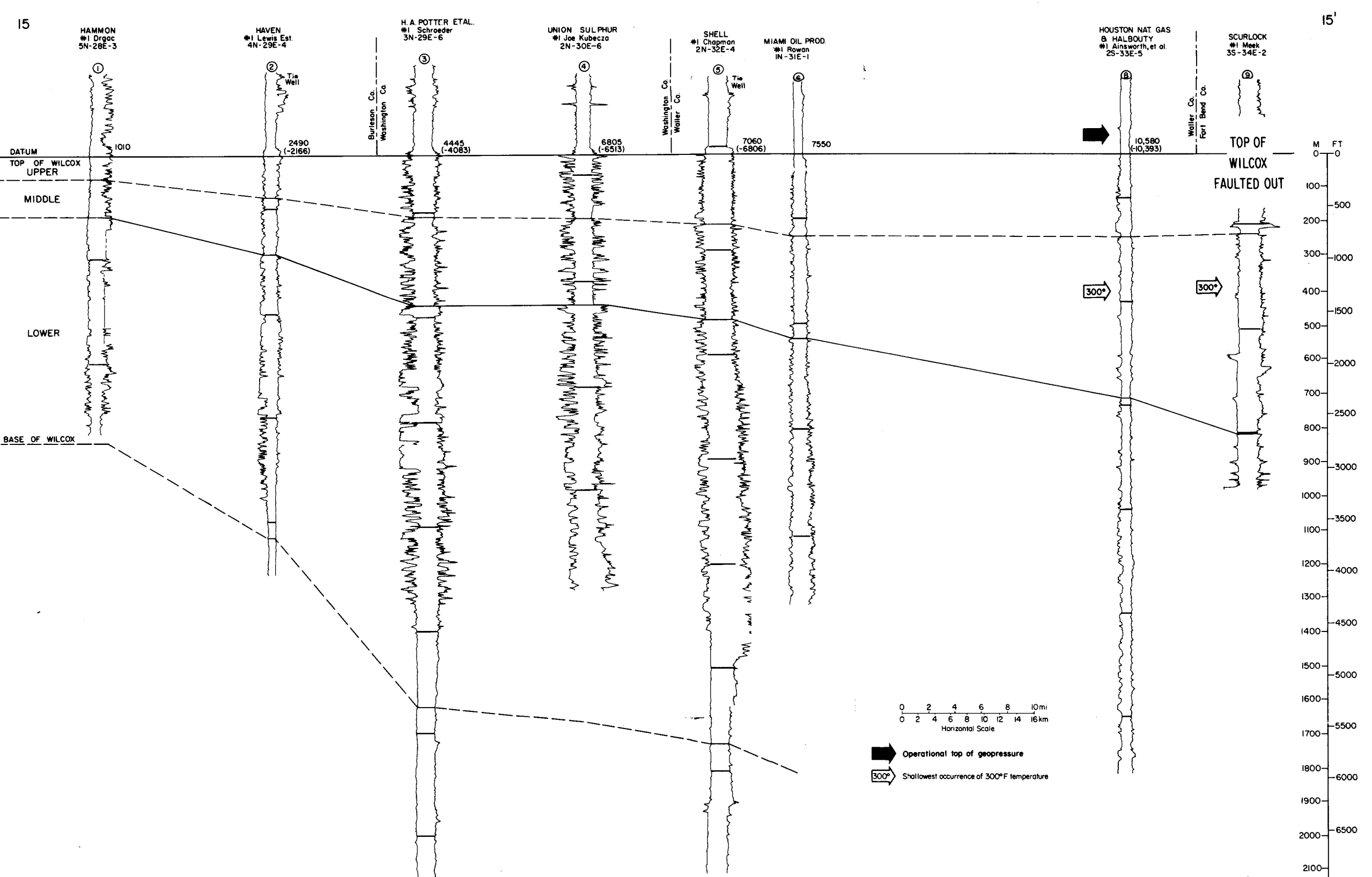


Figure 25. Stratigraphic dip section 15.

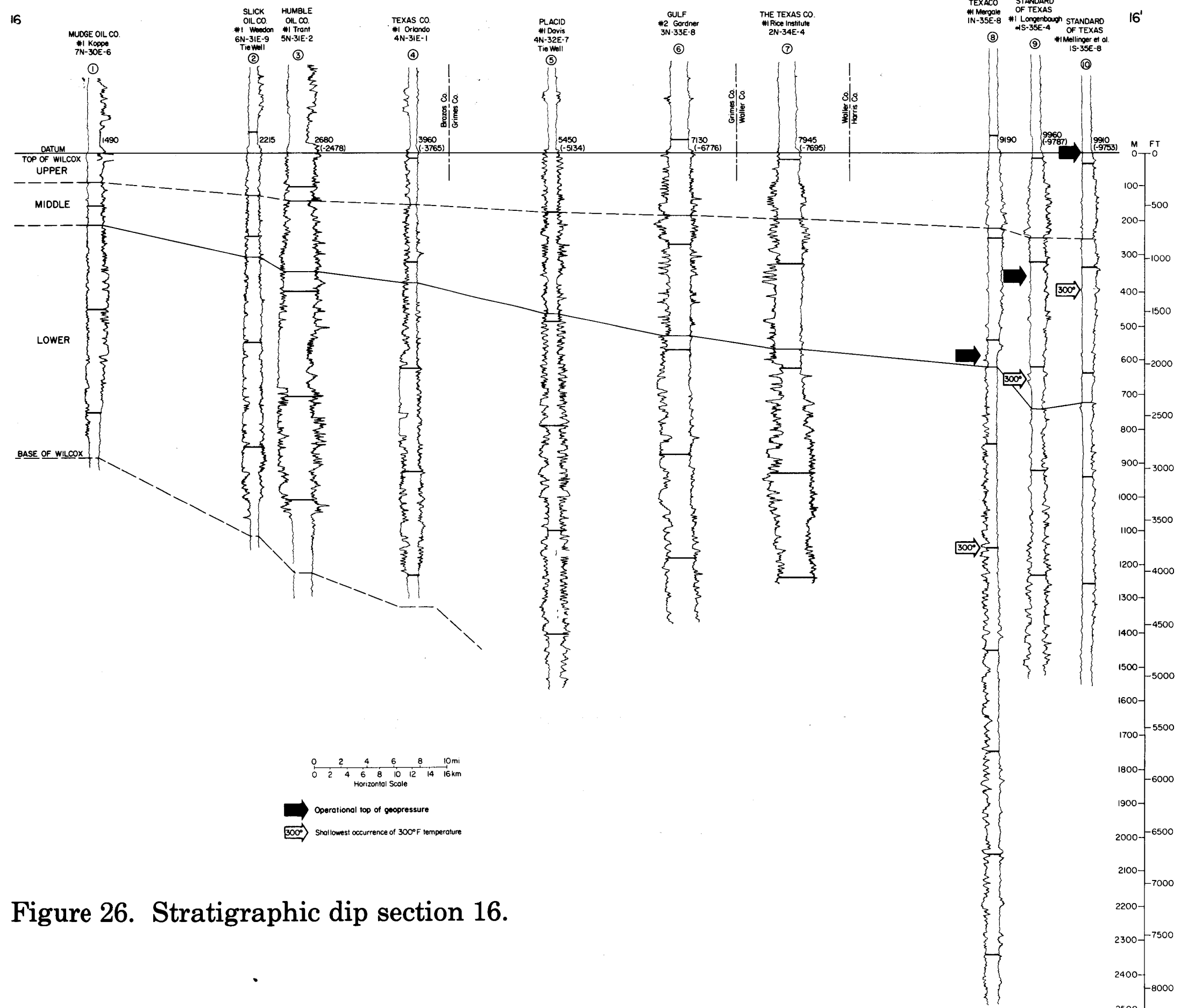


Figure 26. Stratigraphic dip section 16.

The locations of these sections are shown in figure 9 (in text). The datum for each section is the top of the Wilcox Group, and the transition between the Wilcox and the underlying Midway is shown by the dashed line. A pressure gradient of 0.7 psi per foot is shown by the black arrows; the approximate points at which a temperature of 300°F occurs are shown by the arrows so labeled.

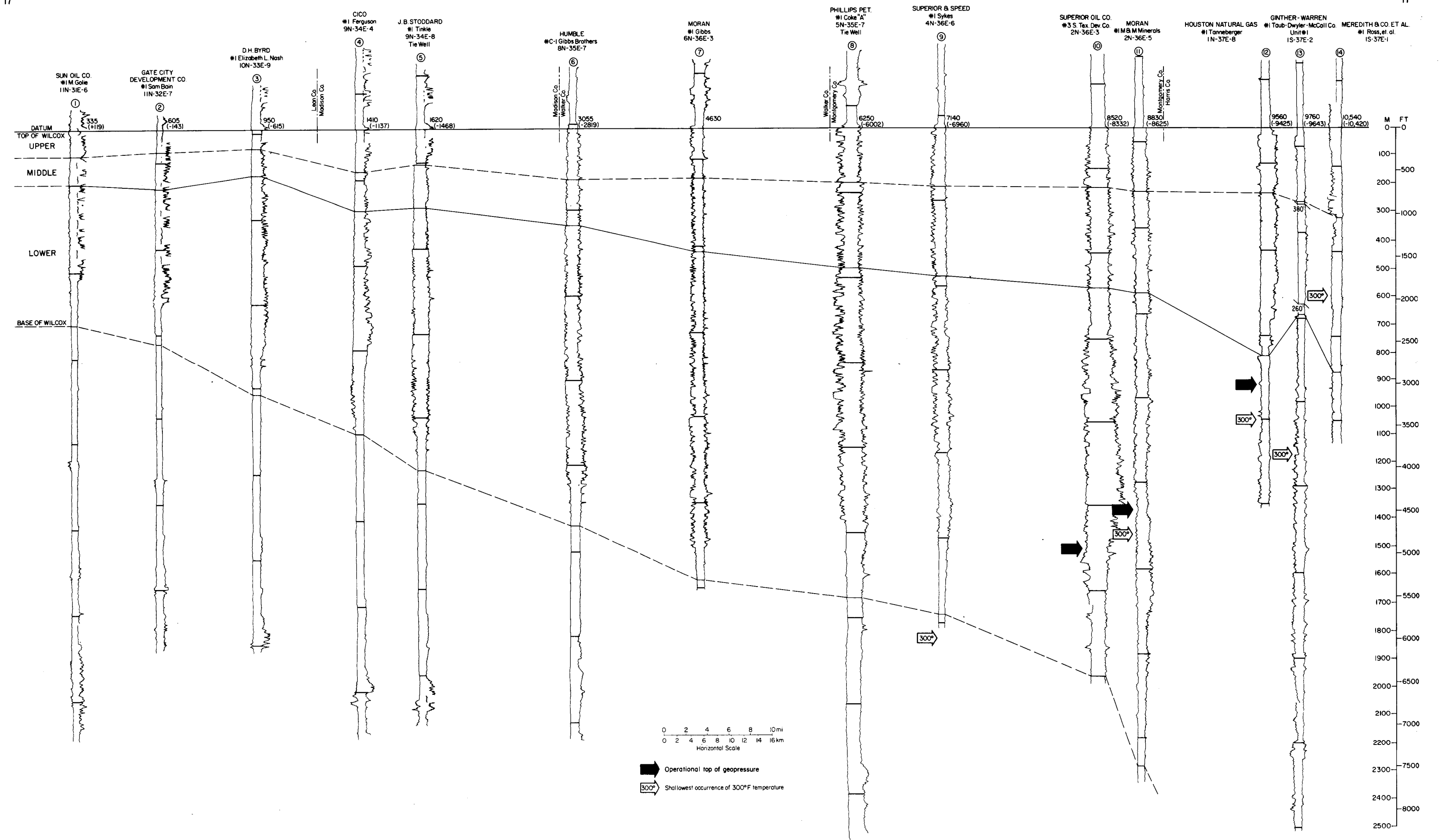


Figure 27. Stratigraphic dip section 17.

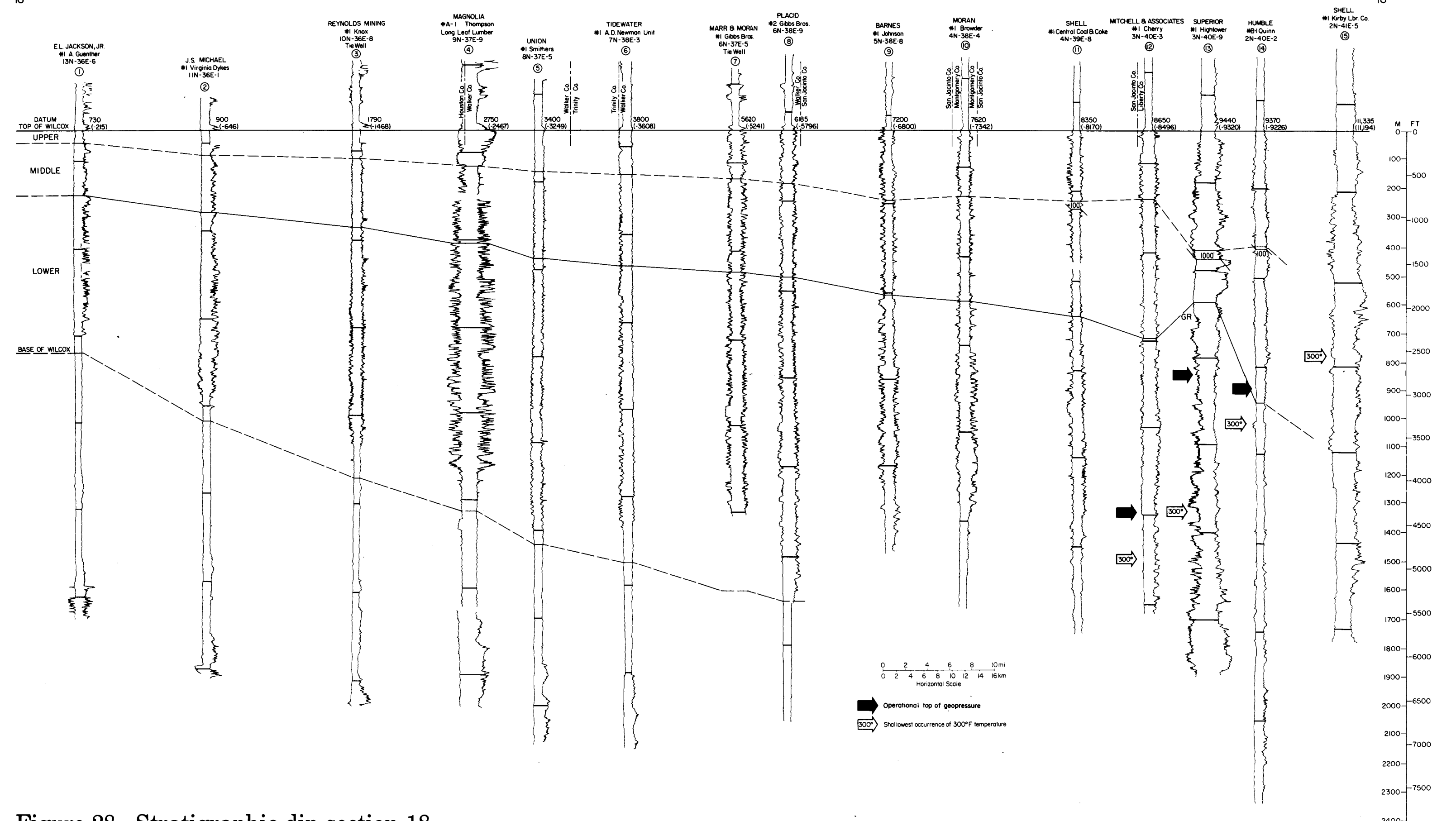


Figure 28. Stratigraphic dip section 18.

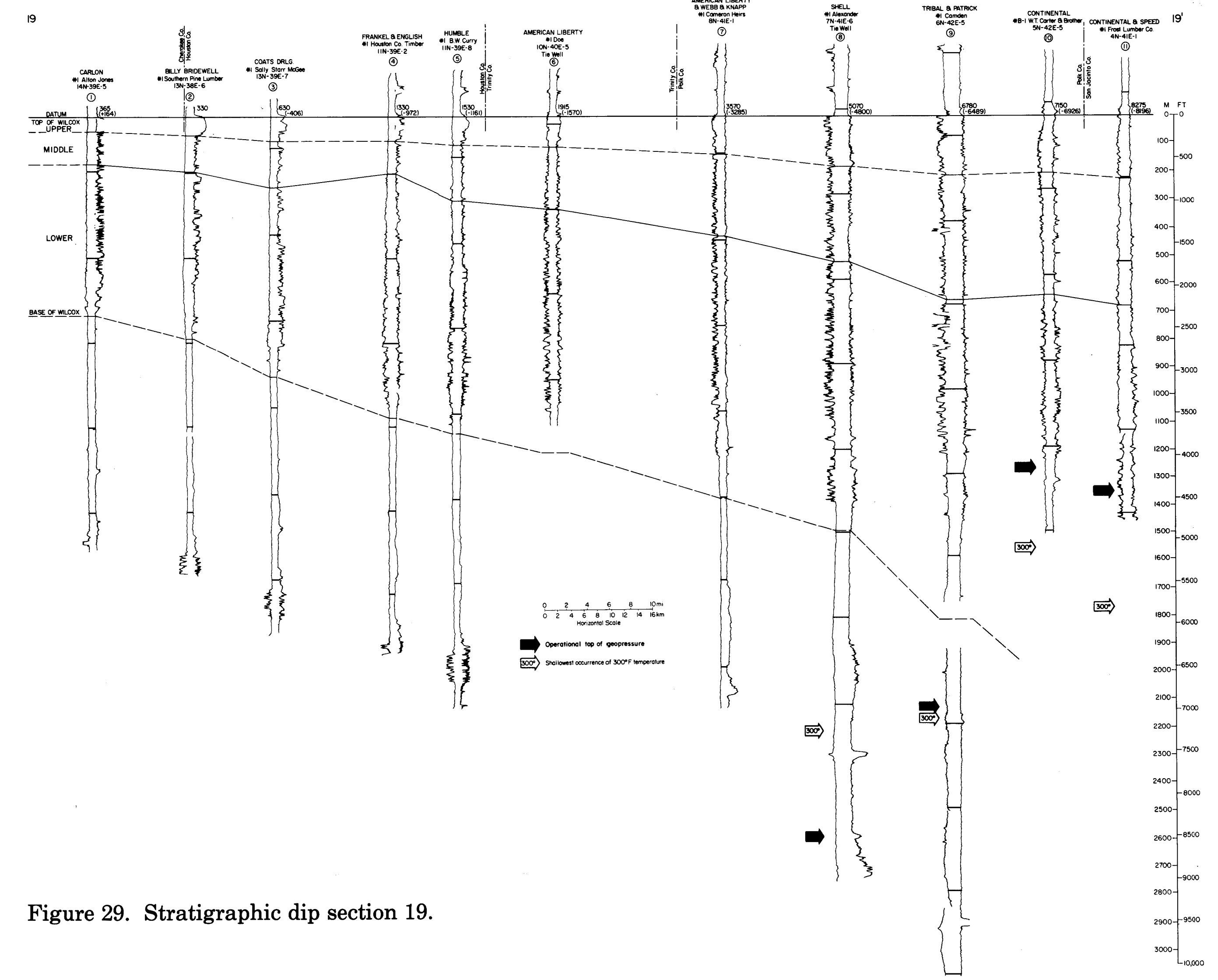


Figure 29. Stratigraphic dip section 19.

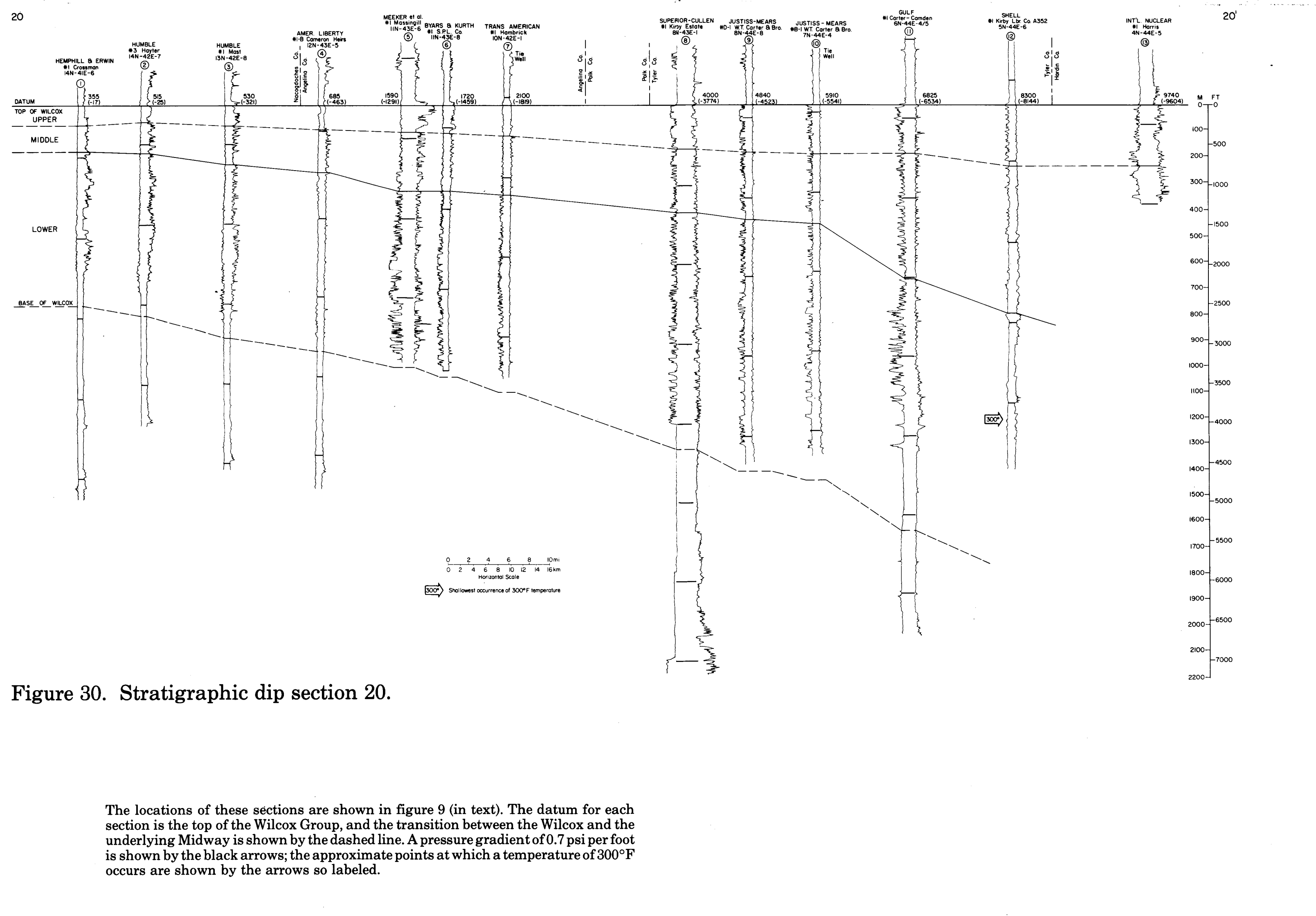
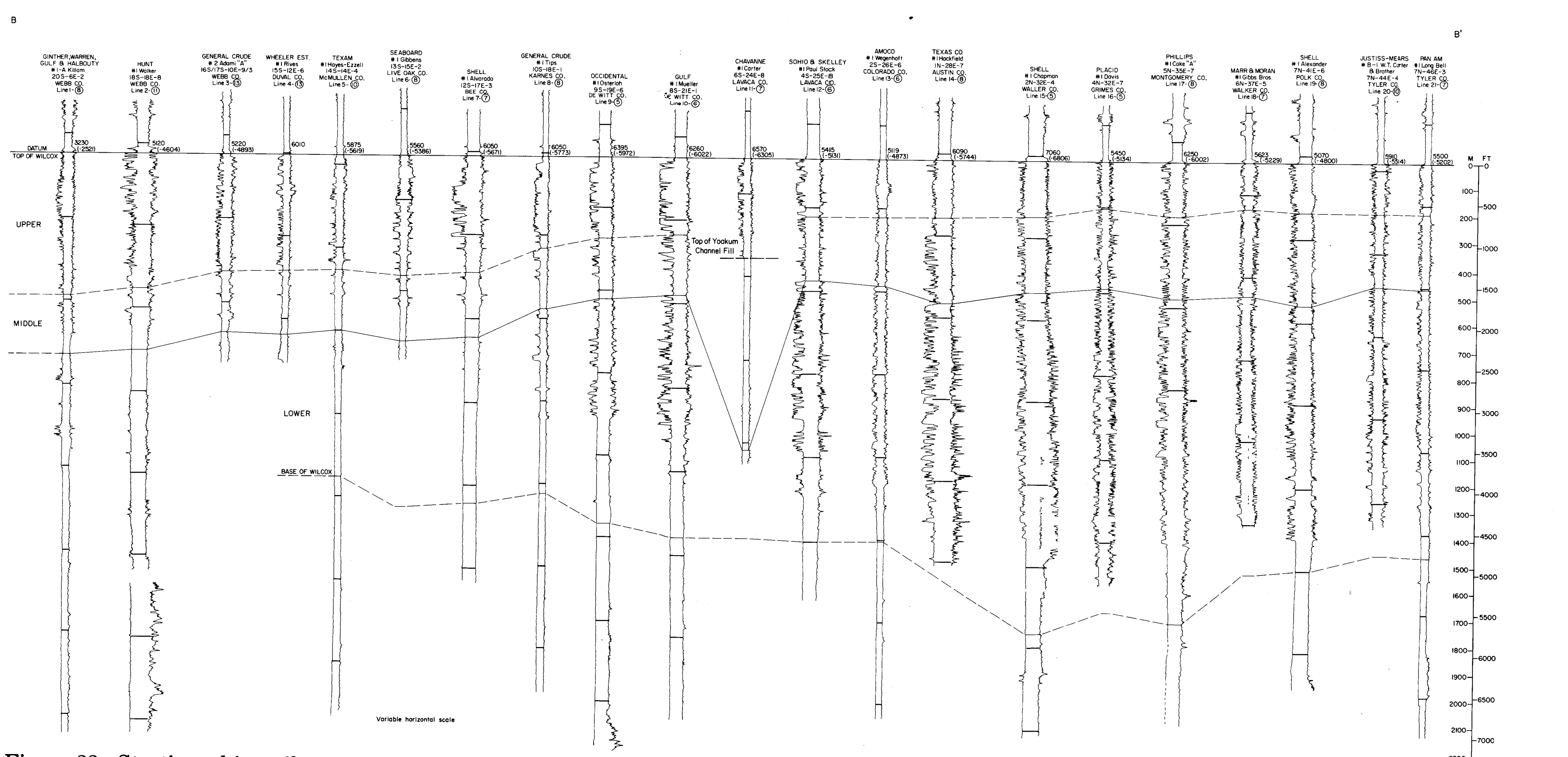
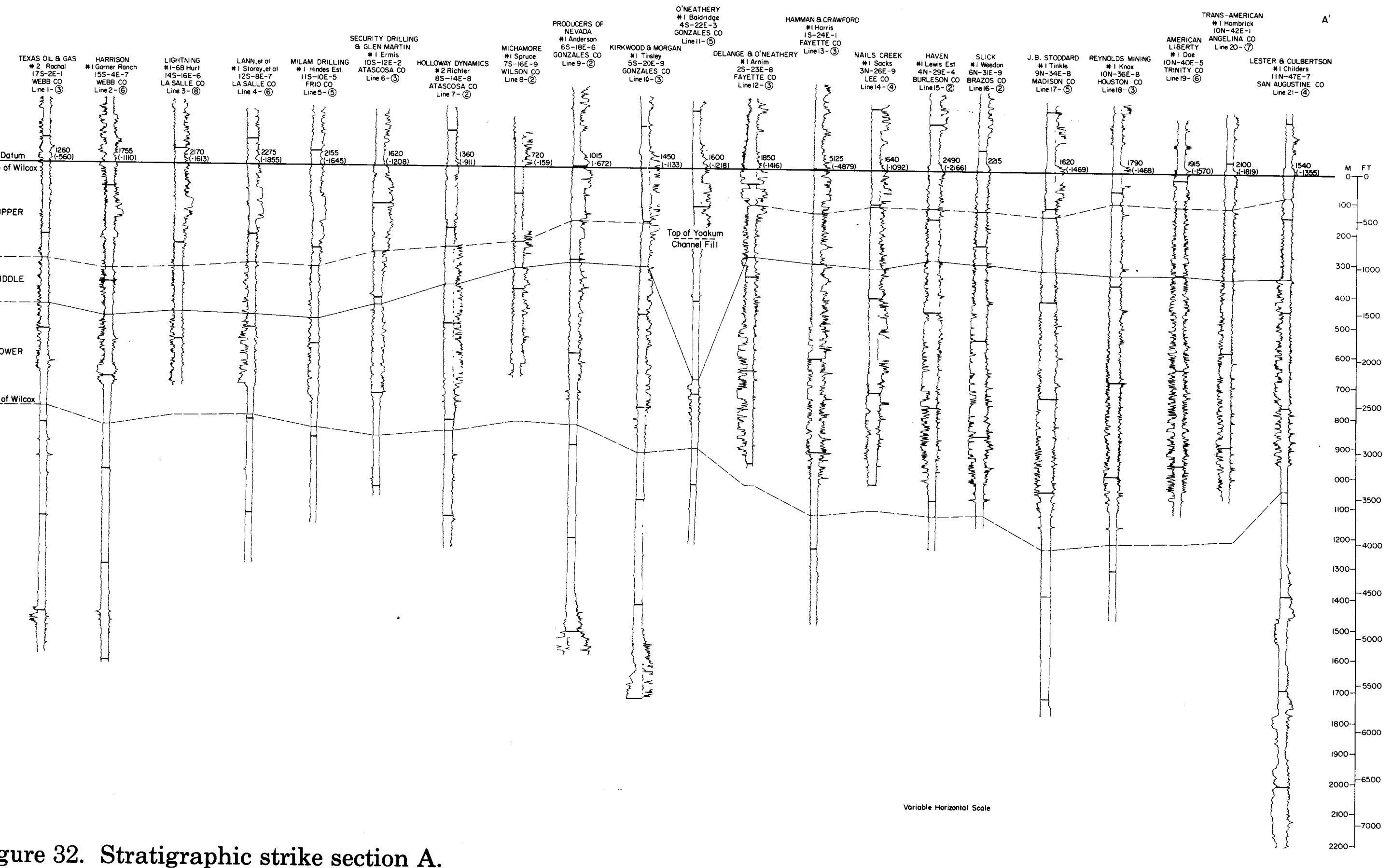
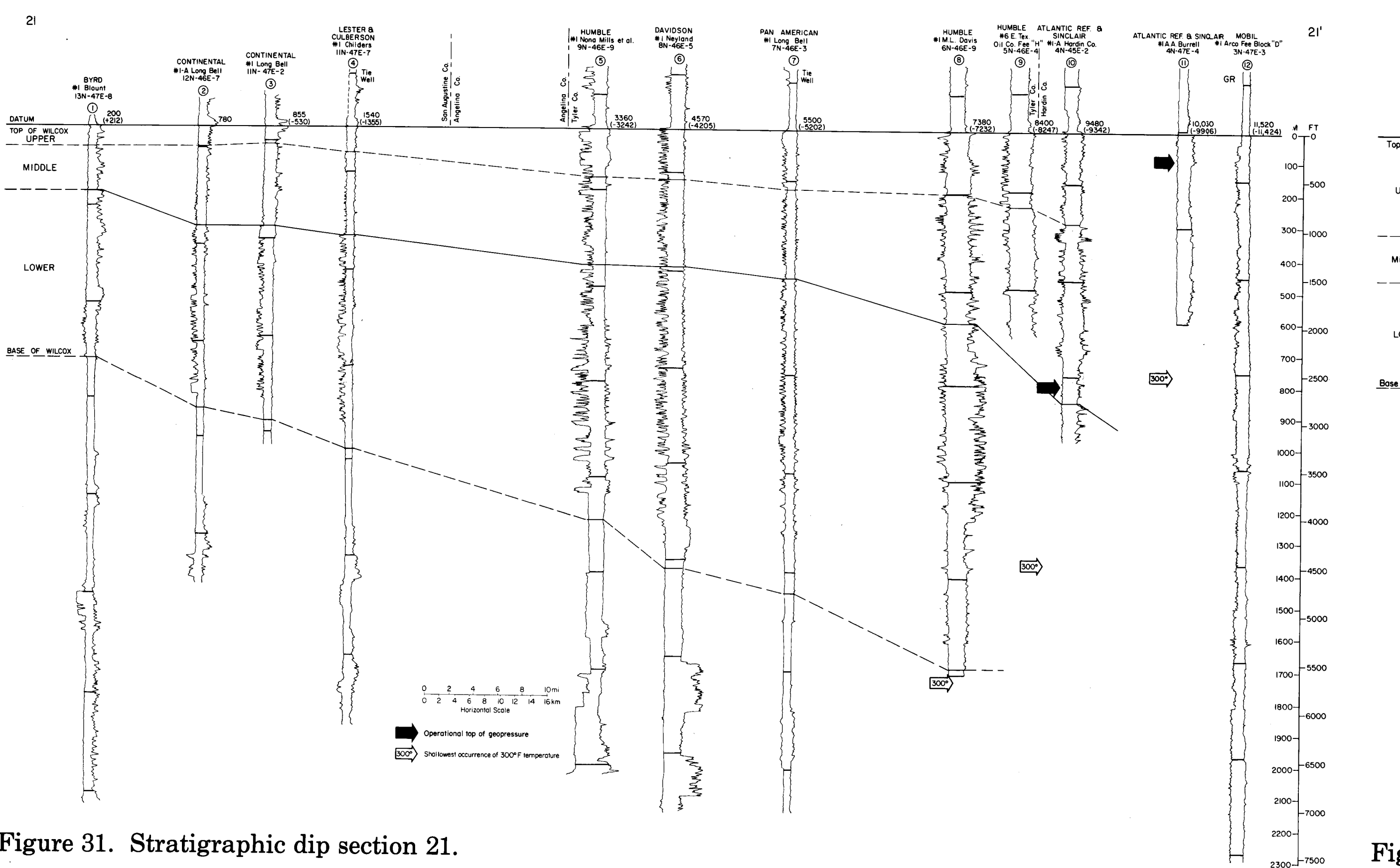


Figure 30. Stratigraphic dip section 20.

The locations of these sections are shown in figure 9 (in text). The datum for each section is the top of the Wilcox Group, and the transition between the Wilcox and the underlying Midway is shown by the dashed line. A pressure gradient of 0.7 psi per foot is shown by the black arrows; the approximate points at which a temperature of 300°F occurs are shown by the arrows so labeled.



The locations of these sections are shown in figure 9 (in text). The datum for each section is the top of the Wilcox Group, and the transition between the Wilcox and the underlying Midway is shown by the dashed line. A pressure gradient of 0.7 psi per foot is shown by the black arrows; the approximate points at which a temperature of 300°F occurs are shown by the arrows so labeled.